Submarine landforms and past ice flow in the Krossfjorden system, northwest Svalbard

David Burton

Queens' College

13th June 2013

Supervisor: Professor Julian Dowdeswell

Scott Polar Research Institute

Department of Geography

University of Cambridge

Lensfield Road

Cambridge CB2 1ER

England

This dissertation is submitted for the degree of Master of Philosophy

Acknowledgements

Firstly, I would like to thank my supervisor Professor Julian Dowdeswell for his excellent guidance over the course of the thesis. Dr. Kelly Hogan is also thanked for her assistance throughout the project; for assistance with the visualisation programmes and for the helpful discussions whilst she was on her way to tea. I thank both of you for sharing your knowledge and for being so patient with me.

The Norwegian Hydrographic Service and Dr. Riko Noormets at the University Centre in Svalbard (UNIS) are also acknowledged for collecting and providing the bathymetric data to the Scott Polar Research Institute (SPRI). I must thank Arnstein Osvik at the Norwegian Hydrographic Service, Anders Skoglund at the Norsk Polarinstitutt and Dr. Endre Før Gjermundsen and PhD student Heidi Sevestre at UNIS for their help, providing me with further information and data.

I would also like to take this opportunity to thank all the staff at SPRI for an enjoyable year, particularly my classmates TJ Young, Mia Bennett, Grant Macdonald, Jonathan Ryan and Edward Pope. I thank TJ Young and Grant Macdonald for thier company on the late nights and TJ's assistance with all things GIS.

Special thanks is given to all my friends and family who listened to me discuss my project and proof-read drafts, namely being Robert Headland at SPRI, Olivia De Beukelaer, Samuel Lay and fellow Queens' members Samantha Bates and William Thanhouser.

Contents

Chapter 1 – Introduction 1

1.1 Location: northwest Spitsbergen 2

1.1.1 Study area 2

1.1.2 Glaciers draining into the fjord system 3

1.1.3 Local Geology 8

1.1.4 Oceanography 9

1.2 Glacial history: last glacial-interglacial cycle 12

1.3 Regional bathymetry 16

1.4 Structure of thesis 18

Chapter 2 - Methods 19

2.1 Multi-beam swath bathymetry 19

2.2 Acoustic, seismic and sediment core datasets 24

2.3 Background mosaic of land areas 25

Chapter 3 - Submarine landforms in Lilliehöökfjorden 28

3.1: Inner Lilliehöökfjorden 28

3.1.1 Large transverse ridges: terminal and overridden moraines 28

3.1.2 Fjord-perpendicular ridge: medial moraine 32

3.1.3 Streamlined bedforms: glacial lineations 33

3.1.4 Small transverse ridges: recessional moraines 35

3.2 Outer Lilliehöökfjorden 36

3.2 .1 Smooth outer fjord: sediment-filled basin 36

3.2.2 Drumlinised bedrock outcrop 37

3.2.3 Depositional and erosional features: debris lobes and gullies 39

3.3 Distribution and timing of submarine landforms in Lilliehöökfjorden 42

3.3.1 Geographical distribution 42

3.3.2 Timing 44

4. Submarine landforms in the Möllerfjorden system 46
4.1 Möllerfjorden 48
4.1.1 Smooth outer: sediment-filled basin 48
4.1.2 Large transverse ridge: palaeo-stillstand 48
4.1.3 Small transverse ridges: recessional moraines 49
4.1.4 Curvilinear incisions and seabed depressions: iceberg ploughmarks and pitting 52
4.1.5 Erosional and depositional features: mass wasting and gullies 55
4.1.6: Sculpted mounds: modified bedrock 57
4.2 Mayerbukta 58
4.2.1 Large transverse ridges: terminal moraines 58
4.2.2 Small transverse ridges: recessional moraines 61
4.2.3 Streamlined features: glacial lineations 62
4.2.4 Large mounds: glacially sculpted bedrock 64
4.2.5 Medium sized transverse ridge and lobe: large recessional moraine 66
4.2.6 Lobe associated with transverse ridge: ice-contact fan 66
4.2.7 Erosional and depositional features: mass wasting and gullies 67
4.3 Kollerfjorden 68
4.3.1 Outer Kollerfjorden 69
4.3.2 Inner Kollerfjorden 73
4.4 Tinayrebukta 78
4.5 Distribution and timing of submarine landforms in Möllerfjorden 83
4.5.1 Geographical Distribution 83
4.5.2 Timing 87
Chapter 5 – Krossfjorden and Fjortende Julibukta 89
5.1 Krossfjorden 89
5.1.1 Transverse morphologies: bedrock outcrops 90
5.1.2 Transverse ridges: recessional moraine 92
5.1.3 Distribution and timing of submarine landforms in Krossfjorden 93
5.2 Fjortende Julibukta 94

5.2.1 Geographical distribution 95
Chapter 6 – Acoustic, sediment cores and historical data from the Krossfjorden system 97
6.1 Acoustics and sediment cores 97
6.1.1 Acoustic data 98
6.1.2 Gravity Cores 104
6.2 Ice front positions 105
Chapter 7 – Discussion and Conclusions 110
7.1 Submarine landsystems in Krossfjorden 110
7.2 Past ice flow behaviour in the Krossfjorden system 111
7.2.1 Implications for the ice sheet over Svalbard since the LGM 111
7.2.2 Implications for Little Ice Age advance 113
7.3 Concluding summary 116
7.4 Further research 117
8. Bibliography 118

List of figures

Figure	Description	Page
1.1	**A:** Overview of the Svalbard archipelago. **B:** Map of the Kongsfjorden-Krossfjorden complex. The Krossfjorden study area is marked by a black rectangle (from Svendsen *et al.*, 2002).	2
1.2	Drainage basins of glaciers in the Krossfjorden basin.	6
1.3	Tinayrebukta and Tinayrebreen's ice extent in 1906 and 2011. **A:** Painting from1906. Provided courtesy of Professor Julian Dowdeswell. **B:** A photograph taken in August 2011 of Tinayrebreen. Provided courtesy of Dr. Endre Før Gjermundsen.	7
1.4	Simplified local geology of the Krossfjorden system from the Norsk Polarinstitutt's ArcGIS geodatabase.	8
1.5	**A:** Map of the north Atlantic giving an overview of the currents operating within it (from Rasmussen *et al.*, 2007). **B:** Greater detail of the currents around Svalbard (from Svendsen *et al.*, 2002).	9
1.6	**A:** Overview of locations of the hydrographic sampling stations. **B: S**pring, summer and autumn hydrographic conditions from the continental slope into inner Kongsfjorden in 2002 (from Walkusz *et al.*, 2009).	11
1.7	Suspended particulate matter (SPM) flux from Kronebreen and Kongsvegen, Kongsfjorden (from Zajączkowski, 2008).	12
1.8	The mapped extent of LGM. The Svalbard archipelago is marked with a red box (from Svendsen *et al.*, 2004).	14
1.9	Postglacial re-emergence curves from key sites across Svalbard. The two curves near Krossfjorden are indicated by red circles and the red box (modified from Forman *et al.*, 2004).	15
1.10	**A:** Regional bathymetry shown in IBCAO 3. **B:** bathymetry of Kongsfjordrenna. **C:** Detail of GZW. **D:** Acoustic profile of the GZW. **B – D** from Ottesen *et al.* (2007).	17
1.11	Overview of the Svalbard archipelago with ice-streams marked with arrows in the direction of ice flow. The Kongsfjorden-Krossfjorden ice-stream is marked by the black box (modified from Ottesen *et al.*, 2007).	18
2.1	The principles of a multi-beam swath bathymetric system (from Alfred-Wegener-Institut, 2013).	20
2.2	**A:** Map of the study area showing the two cruises (from the Norwegian Hydrographic Service). **B:** Ship's tracks for the Sjoemaaleren-4100 cruise and the survey area of Hydrograf-2010-113 cruise.	21
2.3	Demonstrating the processing procedure. **A:** Section of Kollerfjorden with unrealistic points in DMagic.	23

	B: View in 3D Editor which demonstrates that these mounds represent unrealistic points. **C:** The same area, now processed and in ArcGIS.	
2.4	Comparison between the coastline provided by the Norsk Polarinstitutt (NPI) and the customised coastline based on their aerial photography.	25
2.5	Background mosaic of the Krossfjorden system.	27
3.1	Overview map of Lilliehöökfjorden; the outer and inner fjord are labelled as well as the tidewater margin of Lilliehöökbreen. The water depth bar has been hypsometrically optimised for the range within each area. The background map derived from Landsat imagery and aerial photographs shows the adjacent glaciers and snow-free land.	29
3.2	**A:** Inner Lilliehöökfjorden. SL denotes small lobe-like features. The white labelled boxes indicate the locations of Figures 3.3 and 3.4. **B:** The three large transverse ridges described are evident in this long profile as well as a few of the smaller transverse ridges. TR1, 2 and 3 denote the three large transverse ridges.	30
3.3	**A:** Western flank of inner Lilliehöökfjorden showing greater detail of the lineations, hooked lineations and the sets of small transverse ridges. **B:** Cross-sectional profile across a set of glacial lineations. **C:** Surface long-profile demonstrating the morphology of small transverse ridges (marked with black arrows).	34
3.4	**A:** The C-shaped transverse ridge is highlighted by a dashed white circle. The black arrows indicate the medium sized transverse ridge. **B:** Long-profile of the C-shaped transverse ridge.	34
3.5	**A:** Seabed topography of outer Lilliehöökfjorden. **B:** Possible relict drumlins. **C:** Modified bedrock feature at the sill of outer Lilliehöökfjorden and the entrance to Krossfjorden. **D:** Cross-profile across the prominent bedrock outcrop. One of the drumlinised landforms imposed upon the bedrock is marked with a black arrow.	38
3.6	**A:** Lobe-shaped deposits at the base of the western side-wall of outer Lilliehöökfjorden. **B:** Gullies on the eastern side-wall. Streams are indicated by blue lines. **C:** Photograph looking down Kong Haakon Halvøy, exemplifying how steep the terrain is. Photo courtesy of Endre Før Gjermundsen.	41
3.7	**A:** Landform map for Lilliehöökfjorden indicating the submarine landforms described and their geographical distribution. **B:** More detailed landform map for the area closest to the tidewater margin.	43
3.8	An analysis of spatial and temporal variations for individual submarine landforms, which make up the landsystem within inner Lilliehöökfjorden.	45
4.1	Overview map and bathymetric extent of Möllerfjorden, with the locations of Kollerfjorden, Mayerbukta and Tinayrebukta labelled.	46

4.2	**A:** Overview map of Möllerfjorden. **B:** Long-profile demonstrating the morphology of the large transverse ridge at the fjord mouth.	47
4.2.1	Detailed view of the transverse ridge at the sill of Möllerfjorden.	49
4.2.2	**A:** Basin leading to Mayerbukta, inner Möllerfjorden, demonstrating the small transverse ridges present. **B** and **C**: Fjord long-profiles showing the morphology of transverse ridges on the lateral margins of this basin.	51
4.2.3	Small transverse ridges located on the western side of Möllerfjorden, leading towards Kollerfjorden.	51
4.2.4	**A:** Topographic highs at the northern extent of data coverage in Möllerfjorden, which are covered in indentations and small curvilinear features. **B:** Cross-profile demonstrating the morphology of the small curvilinear features. **C:** Detailed view of the indented seabed. **D:** Cross-profile demonstrating the morphology of one of these indentations.	54
4.2.5	**A:** Bathymetry of Möllerfjorden which demonstrates the interplay between the steep slopes and the side-wall of the fjord. **B:** Cross-profile of one of the sets of gullies leading down the slope into the basin.	56
4.2.6	MTDs on the southern side-wall near the entrance to Möllerfjorden.	57
4.3	**A:** The seabed topography of Mayerbukta. **B:** Long profile across the four transverse ridges labelled.	59
4.3.1	Large transverse ridge found at the mouth of Mayerbukta. At the base small lobe-like features are visible and on the ice-distal side of the slope gullies are also evident.	60
4.3.2	**A:** Small transverse ridges found within Mayerbukta, indicated by black arrows. **B:** Long profile demonstrating the morphology of small transverse ridges, indicated with black arrows within Mayerbukta.	61
4.3.3	**A:** Hooked lineations within central Mayerbukta, highlighted by the dashed white oval and marked with black arrows. Sets of small recessional moraines are also observed. **B:** Cross-profile demonstrating the morphology of the hooked lineations, marked with black arrows.	63
4.3.4	**A:** Inner Mayerbukta, proximal to the glacier terminus. **B:** Long profile across lobe shape feature. **C:** Cross profile of the lineations on the lee side of the large mound.	65
4.3.5	Gullies on the side-wall near the entrance to Mayerbukta.	67
4.4	Overview map of Kollerfjorden,	68
4.4.1	Features observed in outer Kollerfjorden. **A:** Glacially sculpted feature with the appearance of whalebacks. Transverse ridges are also visible leading away from the feature. **B:** Long profile of the features, demonstrating their drumlinised appearance. **C:** Elongated streamlined features, with similar appearances of drumlins.	69

	D and E: Long profile of features demonstrating their drumlin-like appearance.	
4.4.2	**A**: Topographic highs and the shallow side of outer Kollerfjorden with the described scouring and depressions on the seabed.	71
	B: Cross-section of depressions and curvilinear incisions, demonstrating their morphology, with berms on the sides of many.	
4.4.3	Possible MTD, with gullies super-imposed on it, from a fluvial stream leading into outer Kollerfjorden.	72
4.5	Inner Kollerfjorden and the features observed within it.	73
4.5.1	**A:** Lobe shapes at the margin between inner and outer Kollerfjorden.	75
	B: Long profile across a lobe.	
4.5.2	**A:** Small transverse ridges observed within inner Kollerfjorden. Small hooked lineations are highlighted with a dashed white oval.	77
	B: Long profile across the transverse ridges, demonstrating their morphology.	
4.6	Map of Tinayrebukta, showing the bathymetry of the fjord.	78
4.6.1	**A:** The large transverse ridge in Tinayrebukta, demarcating inner and outer fjord. SL denotes the small-lobes observed at the base of this large ridge.	79
	B: Long profile across the large transverse ridge demonstrating its morphology.	
4.6.2	**A:** The large mound with transverse ridges imposed on it, within inner Tinayrebukta.	81
	B: Long profile across this mound and other smaller recessional moraines. **C:** Cross-section of the area with the large mound, demonstrating the raised northern side of the fjord and deeper southern side. The large mound separates the two.	
4.6.3	Area with an interpreted faster retreat, with fewer transverse ridges, is indicated, leading back to a ridge demonstrating a brief stillstand. The bedrock outcrop, associated with lineations and hooked lineations is also labelled.	82
4.7	**A:** Landform map of Möllerfjorden	84
	B: More detailed map for the area closest to the present ice-front of Kollerbreen (inner Kollerfjorden).	85
	C: More detailed map for the area closest to the present ice-front of Mayerbreen (Mayerbukta).	84
	D: More detailed map for the area closest to the present ice-front of Tinayrebreen (Tinayrebukta).	86
4.8	An analysis of spatial and temporal variations for individual submarine landforms, which make up the landsystem within the inner fjord and bays of Möllerfjorden.	88
5.1	Map of the outer Krossfjorden system, comprising bathymetric data of Krossfjorden proper, Fjortende Julibukta and a part of Kongsfjordrenna	89
5.1.1	**A:** The lengthy complex of hummocky morphology.	91
	B: Part of a detailed geological map for Krossfjorden (Ohta *et al.*, 2008). A number of faults (marked as black lines and indicated by black arrows) are visible on the northern coast of Krossfjorden.	

5.1.2	**A:** The two transverse ridges (TR1 and 2), with their associated bedrock outcrop (denoted by Bed). The elongated bedforms are also visible on the ice-proximal side of the ridges. Bathymetric data gridded at 8 m cell sizes, with illumination of 45° and sun angle of 50°. **B:** long profile across both transverse ridges within Krossfjorden, demonstrating their morphology.	92
5.2.1	**A:** Detailed view of Fjortende Julibukta's mouth. **B:** Demonstrates the limited extent of data coverage in Fjortende Julibukta, 2 km from the ice front of Fjortende Julibreen. **C:** Long profile across data cover, demonstrating small transverse ridges, marked with black arrows.	95
5.2.2	Landform map for Fjortende Julibukta indicating the submarine landforms described and their geographical distribution.	96
6.1	Map showing the extent of the acoustic surveys (transects **1-6**) conducted by Sexton *et al.* (1992) and the locations of gravity cores (indicated by black triangles).	97
6.1.1	Acoustic profiles of sedimentary architecture in Lilliehöökfjorden (modified from Cromack, 1991). **A:** Sparker record. **B:** 3.5 kHz PDR record. **C:** Acoustic units interpreted by Sexton *et al.* (1992). The positions of the subsequent transects in Lilliehöökfjorden are given.	98
6.1.2	**A:** Sparker profile showing the sedimentary architecture of transect 2 (modified from Sexton et al., 1992). **B:** Bathymetric image of inner Lilliehöökfjorden, demonstrating the location of the three transverse ridges.	99
6.1.3	**A:** 3.5 kHz PDR record showing the sediment-filled basin. **B:** Unit boundaries, units are labelled on the figure. Dashed black ellipses indicate the position of the small-lobe like features (from Sexton *et al.*, 1992).	100
6.1.4	**A:** Sedimentary architecture from the cliff at the mouth of Lilliehöökfjorden. From 3.5 kHz PDR record (modified from Sexton *et al.*, 1992). **B:** Bathymetric data of the area covered by transect 4	101
6.1.5	**A:** Acoustic transect 5 of Mayerbukta (modified from Sexton *et al.*, 1992). **B:** Appearance of these features in the bathymetric data.	102
6.1.6.	**A:** Acoustic transect 6 of Tinayrebukta (modified from Sexton *et al.*, 1992). **B:** Appearance of these features in the bathymetric data.	103
6.2	Sediment logs of two gravity cores, one from inner **(A)** and one from outer **(B)** Tinayrebukta (from Sexton *et al.*, 1992).	104
6.3	**A:** Part of a map from the Prince of Monaco's expedition to northwest Spitsbergen in 1906 to 1907, showing Lilliehöökbreen's ice front (from Cromack, 1991). **B:** Part of a map from Gunnar Isachsen's Norvégienne expedition in 1909 to 1910 with positions of all the tidewater margins within Krossfjorden.	105

6.4	Norsk Polarinstitutt aerial photography from 1966. The ice fronts are labelled in each.	106
	A: Shows the north-western most section of the Krossfjorden system.	
	B: Tinayrebukta and the ice front of Tinayrebreen are visible.	
	C: Fjortende Julibreen and its ice front.	
6.5	**A:** Map of study area with dated positions of the tidewater margins, where available.	107
	B: Detailed view of Kollerfjorden.	108
	C: Detailed view of Mayerbukta.	108
	D: Detailed view of Tinayrebukta.	109
7.1	Models for inter-ice-stream (**A**) or ice-stream (**B**) landform assemblages (from Ottesen and Dowdeswell, 2009).	112
7.2	The two models put forward for surge-type tidewater glaciers on Svalbard.	115
	A: Model from Ottesen and Dowdeswell (2006)	
	B: Model from Ottesen *et al.* (2008b).	

List of tables

Table	Description	Page
1.1	List of glaciers within the study area, including whether they are currently land or tidewater terminating, known surge-type and their approximate area.	4
2.1	Details of the two cruises conducted by the NHS and the type of bathymetric system.	20
2.2	Outline of the processing procedure.	22
2.3	The type, sources and method of the data previously presented for Krossfjorden that are useful to consider applying with the bathymetric data in this thesis.	24
2.4	The type, sources, identification codes and the acquisition date of the data are included in the table for all the datasets from which the background mosaic was constructed.	26
6.1	Calculated retreat rates for the three tidewater glaciers located within Möllerfjorden.	109

Abstract

Very high-resolution swath-bathymetric data, acquired by the Norwegian Hydrographic Service, have been analysed to investigate submarine landforms and their implications for the dynamics and extent of past ice flow in the whole of the Krossfjorden system, northwest Svalbard.

The results from this study confirm that ice extended out of the Krossfjorden system (to the shelf edge west of Svalbard) during the Late Weichselian glacial maximum. They also improve the understanding of the relative chronology of retreat through Krossfjorden, which represents the outer part of the fjord system under study. Two transverse ridges were the only ice-marginal features present within Krossfjorden proper, indicating a relatively rapid ice retreat from the continental shelf to the shallower inner fjords of the Krossfjorden system. This retreat was part of the Late Weichselian deglaciation of the northwestern part of the Svalbard-Barents Sea ice sheet.

The bathymetric data from the innermost fjords and bays represent the advance and subsequent retreat of ice during the period known as the Little Ice Age, when ice on Svalbard reached a recent maximum about 100 years ago. These advances of the five tidewater glaciers in the Krossfjorden system varied from 2.3 to 5 km, with retreat rates of about 30 to 40 m a^{-1} from 1910 to 1966 and 10 to 45 m a^{-1} from 1966 to the present. This variation in retreat rate is attributed to local differences in glacier drainage-basin size, fjord depth and the presence of bedrock outcrops that provided pinning-points during retreat. The very recent deposition of these submarine landforms and the detail in the swath-bathymetric data (including small transverse ridges that in some cases represent annual glacier-terminus positions) have made it possible to produce descriptions and interpretations of the landforms, and to infer the dynamics and retreat rate of ice, at a higher resolution than elsewhere in the Svalbard archipelago.

Chapter 1 – Introduction

This thesis investigates the glacial history of the Krossfjorden system, northwest Spitsbergen, Svalbard. The project primarily utilises high-resolution multi-beam swath bathymetric data from the seabed, which have been collected during scientific cruises over the study area in 2000 and 2010 by the Norwegian Hydrographic Service (NHS). There are three overall aims of this investigation: first, to further the understanding of ice flow dynamics within the Krossfjorden system by providing new information on the landform assemblages that have been linked to the period known as the Little Ice Age (LIA); next, to improve the understanding of the dynamics and retreat within Krossfjorden during the Last Glacial Maximum (LGM), by revising previous interpretations of the last glaciation within the fjord system; and finally to link these findings to the overall ice-sheet history of the entire northwest Spitsbergen region.

These aims will be accomplished by analysing bathymetric datasets collected by the NHS, together with data from previous marine geological and geophysical investigations. The assemblage of landforms present will enable an understanding of the past sedimentary processes within the fjord, from which inferences of changes in glacial activity and climate will be assessed. Past ice extent and flow will be reconstructed along with the pattern of retreat to the present position of the tidewater glaciers entering the Krossfjorden system.

Work from Sexton *et al.* (1992), Howe *et al.* (2003) and Maclachlan *et al.* (2010), who have previously investigated the submarine geomorphology and geophysics of the study area, will be re-examined in light of the much higher resolution swath-bathymetry being analysed within this report. Previous seismic surveys conducted by the above authors, aerial-photographic images (from the Norsk Polarinstitutt) and satellite imagery (Landsat) will also be used with the bathymetric data to gain a greater understanding of the various influences on the marine geology within the study area. Therefore, this project will provide a comprehensive understanding of past glacial activity across the whole Krossfjorden system, with particular reference to areas not previously studied. The most important of these are the areas proximal to the current termini of the tidewater glaciers.

1.1 Location: northwest Spitsbergen

1.1.1 Study area

Krossfjorden is part of the Kongsfjorden-Krossfjorden complex and is located on the northwest coast of Spitsbergen, the main island of the Svalbard Archipelago (Fig.1.1A). Krossfjorden is located between 79°06’ and 79°22’ N and 11°13’ and 12°17’ E with an orientation of northeast to southwest (Fig. 1.1B).

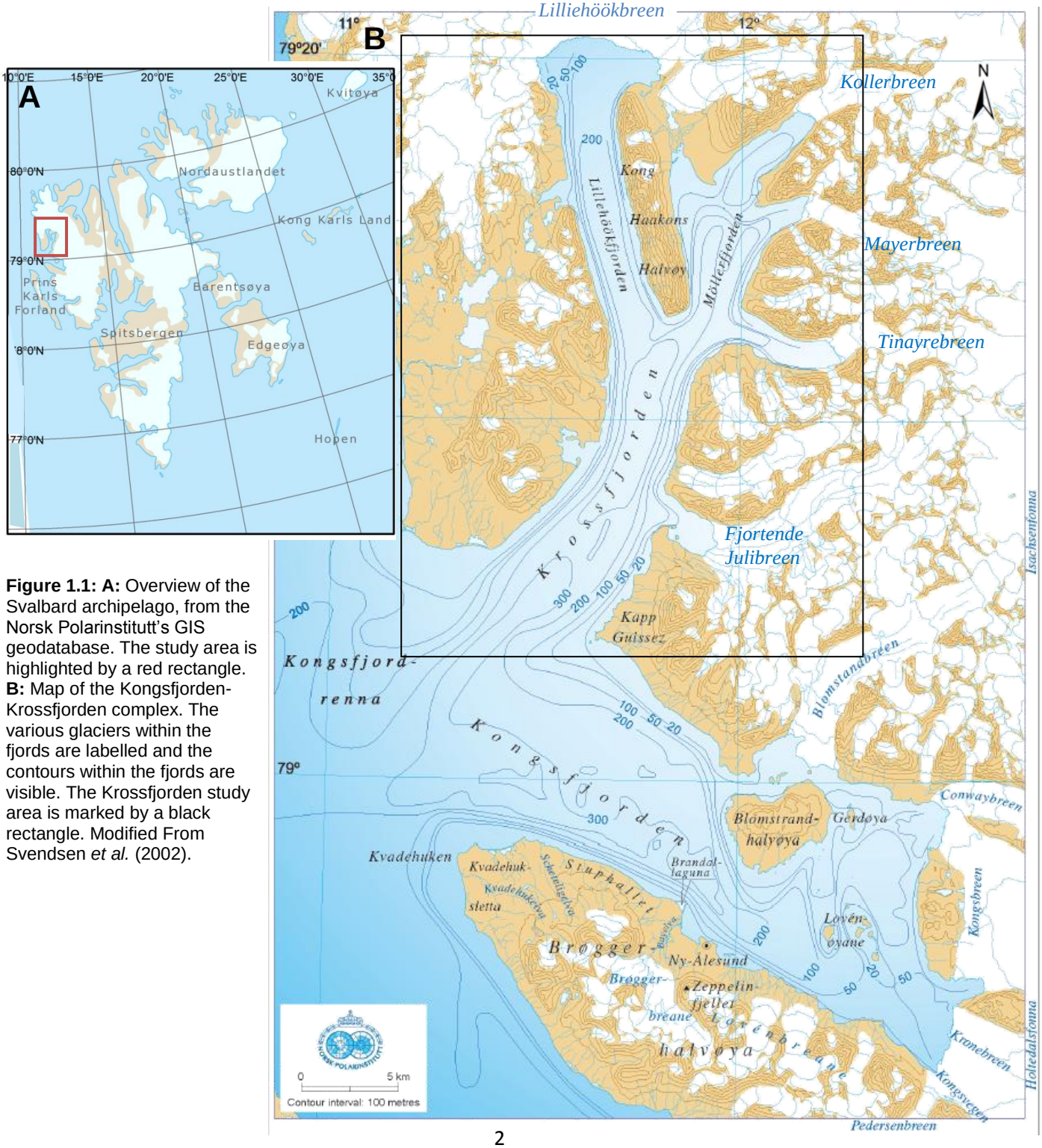

Figure 1.1: A: Overview of the Svalbard archipelago, from the Norsk Polarinstitutt’s GIS geodatabase. The study area is highlighted by a red rectangle. **B:** Map of the Kongsfjorden-Krossfjorden complex. The various glaciers within the fjords are labelled and the contours within the fjords are visible. The Krossfjorden study area is marked by a black rectangle. Modified From Svendsen *et al.* (2002).

The larger fjord of the Kongsfjorden-Krossfjorden system, Kongsfjorden, is approximately 20 km long and at its distal margin it widens to 10 km before merging with Krossfjorden to form a single fjord mouth that opens onto the continental shelf west of Spitsbergen known as Kongsfjordrenna, with a width of approximately 15 km.

The area of study with the fjord system is Krossfjorden. The contours for the study fjord derived from the bathymetric data (Fig. 1.1B) show the general topography of Krossfjorden. The fjord has a maximum depth of 373 m with an estimated volume of 25 km³ (Svendsen *et al.*, 2002). The Krossfjorden system is approximately 30 km long and the inner part splits into two relatively shallow fjords and a number of bays which drain extensive mountainous ice fields (Lilliehöökbreen, with its tributary glaciers, and Isachsenfonna). Lilliehöökfjorden continues to the north and Möllerfjorden to the northeast. Lilliehöökfjorden terminates at the major tidewater glacier of Lilliehöökbreen, whereas Möllerfjorden splits further, into Möllerhamma, Kollerfjorden, Mayerbukta and Tinayrebukta. The three inner parts of Kollerfjorden, Mayerbukta and Tinayrebukta end with the tidewater glaciers of Kollerbreen, Mayerbreen and Tinayrebreen, respectively (Fig 1.1B). In addition, a further tidewater glacier, Fjortende Julibreen, feeds into central Krossfjorden on its eastern side.

1.1.2 Glaciers draining into the fjord system

The total area of the Kongsfjorden-Krossfjorden drainage basin is calculated to have been sizeable during the Last Glacial Maximum (LGM), between 3074 km² (Svendsen *et al.*, 2002) and 2735 km² (Ottesen and Dowdeswell, 2009). The Kongsfjorden-Krossfjorden system has clearly played a substantial, but highly variable, role in past and present glacial activity of northwest Spitsbergen (Landvik *et al.*, 1998; Ottesen *et al.*, 2005; 2007; Sarkar *et al.*, 2011). A list of the glaciers within the study area is given in Table 1.1. This table also indicates whether the glaciers are thought to be of surge-type.

Surge-type glaciers are relatively common on Svalbard (Hagen, 1988; Dowdeswell *et al.* 1991; Liestøl, 1993; Hagen *et al.* 1993; Jiskoot *et al.* 2000; Błaszczyk *et al.*, 2009) with some well documented surges, such as Perseibreen (Dowdeswell and Benham, 2003) and Paulabreen (Kristensen and Benn, 2012), but their overall distribution is still undetermined. Błaszczyk *et al.* (2009) used a number of sources, including aerial photographs and satellite imagery of the glaciers indicating any evidence of folded foliation and looped medial moraines, to suggest that up to 43% of tidewater glaciers on Svalbard could be classified as

surge-type, compared to the 13% estimated by Jiskoot *et al.* (1998). Surging of glaciers has implications for the formation of the submarine geomorphology within the fjords.

Table 1.1: List of glaciers within the study area, including whether they are currently land or tidewater terminating, known surge-type (including dates, if known) and their approximate area.

Glacier	Known surge-type?	Surge onset and termination (If known surge-type)	Area (km^2)
	Tidewater Glaciers		
Lilliehöökbreen	No		246
Forbesbreen	No		10
Kollerbreen	No		28
Mayerbreen	Possibly[1]		38
Tinayrebreen	No		50
Fjortende Julibreen	Yes	2002-2005	76
	Major land-terminating Glaciers (over 2 km^2)		
Slørbreen	No		3
Øyenbreen	No		2.5
Supanbreen	No		17
Sagtindbreen	No		3
Snødombreen	No		2.5
Unnamed	No		2.5
Flankebreen	No		2
Kambreen	No		5
Flakbreen	No		15
D'Arodesbreen			
Estimated modern drainage basin of Krossfjorden (km^2)			**500.5**

Source: The area of the various drainage basins has been obtained from the Randolph Glacier Inventory for all of the glaciers over 2 km^2 within the Krossfjorden system. Whether the glaciers are surge-type and when this occurred are from: Liestøl, 1993; Mansell *et al.*, 2012; Sevestre *et al.* (unpublished).[1]= Blaszczyk *et al.* (2009); area is from the Randolph Glacier Inventory 2.0

Surging glaciers have a cyclical occurrence (Meier and Post, 1969; Benn and Evans, 2010). In the slow flow period, known as the quiescent phase, ice accumulates in the higher regions of the glacier. When the surge phase begins there is a large and rapid ice flux to the lower regions of the glacier, with velocities usually at least one order of magnitude greater than in the quiescent phase (Hagen, 1988; Błaszczyk *et al.*, 2009; Benn and Evans, 2010). The surge often causes frontal advances and, although not initially (Mansell *et al.*, 2012), produces severe crevassing and calving at the snout of the glacier (Błaszczyk *et al.*, 2009; Kristensen and Benn, 2012). Post-surge, the glaciers tend to stagnate, re-entering the quiescent phase, until the next surge which is often decades to centuries later (Dowdeswell *et al.*, 1991).

During the quiescent phase, retreat is expected to be observed (Błaszczyk *et al.*, 2009), with a peak in calving rates (Mansell *et al.*, 2012).

A number of glaciers are known to surge within Kongsfjorden (Liestøl, 1993; Sevestre et al, unpublished), particular the large tide-water glacier Kronebreen. However, Fjortende Julibreen is the only tidewater glacier in Krossfjorden which is known to be of surge-type (Mansell *et al.*, 2012), and this has been observed only recently. Mayerbreen has apparent indications that it could possibly be of surge-type (Błaszczyk *et al.*, 2009) but this is not yet confirmed.

Fjortende Julibreen has been recorded to have had a three year active surge phase, during 2002 – 2005, and has demonstrated similar characteristics to other surge-type glaciers on Svalbard (Mansell *et al.*, 2012). Interferometric synthetic aperture radar showed that Fjortende Julibreen had a pre-surge maximum velocity of ~0.07 m d^{-1} near the equilibrium line and this increased by approximately five times during the surge (Mansell *et al.*, 2012). During Fjortende Julibreen's surge, flow peaked in 2002 and the glacier reached its maximum extent in 2004, when it still had a relatively low calving rate (Mansell *et al.*, 2012) indicating a 'slow' surge (Kristensen and Benn, 2012).

All the tidewater glaciers in the fjord system (Table 1.1, Fig. 1.2) have been recorded to be receding (with the exception of Fjortende Julibreen's surge). There are a number of new and still unnamed islands which have been revealed near the heads of fjords from the regression of the tidewater margins. Figure 1.3 shows a painting of Tinayrebreen, Krossfjorden, by an artist on one of Prince Albert I of Monaco's expeditions to northwest Spitsbergen in 1906 and a photograph from 2011; the retreat of the glacier over the last century is striking.

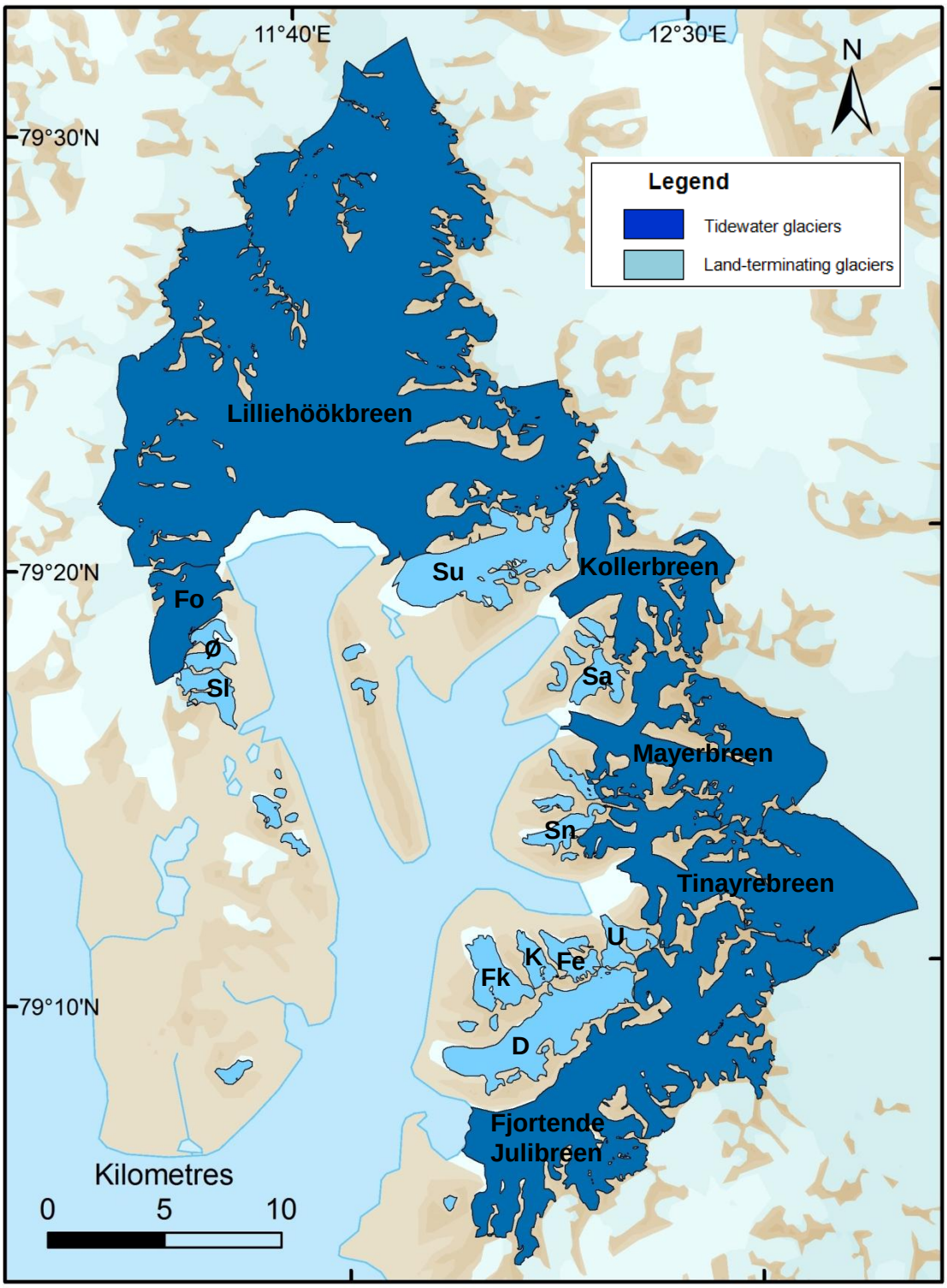

Figure 1.2: Drainage basins of glaciers in the Krossfjorden basin. The two colours symbolise the tidewater and land-terminating basins. Names are shown or denoted for all the glaciers in Table 1.1, as follows: Sl = Slørbreen, Ø = Øyenbreen, Fo = Forbesbreen, Su = Supanbreen, Sa = Sagtindbreen, Sn = Snødombreen, U = Unnamed, Fe = Flankebreen, K= Kambreen, Fk= Flakbreen, D = D'Arodesbreen. The base map is from the topographic map of Svalbard from the Norsk Polarinstitutt's ArcGIS database and the glaciers were delineated with the RGI 2.0.

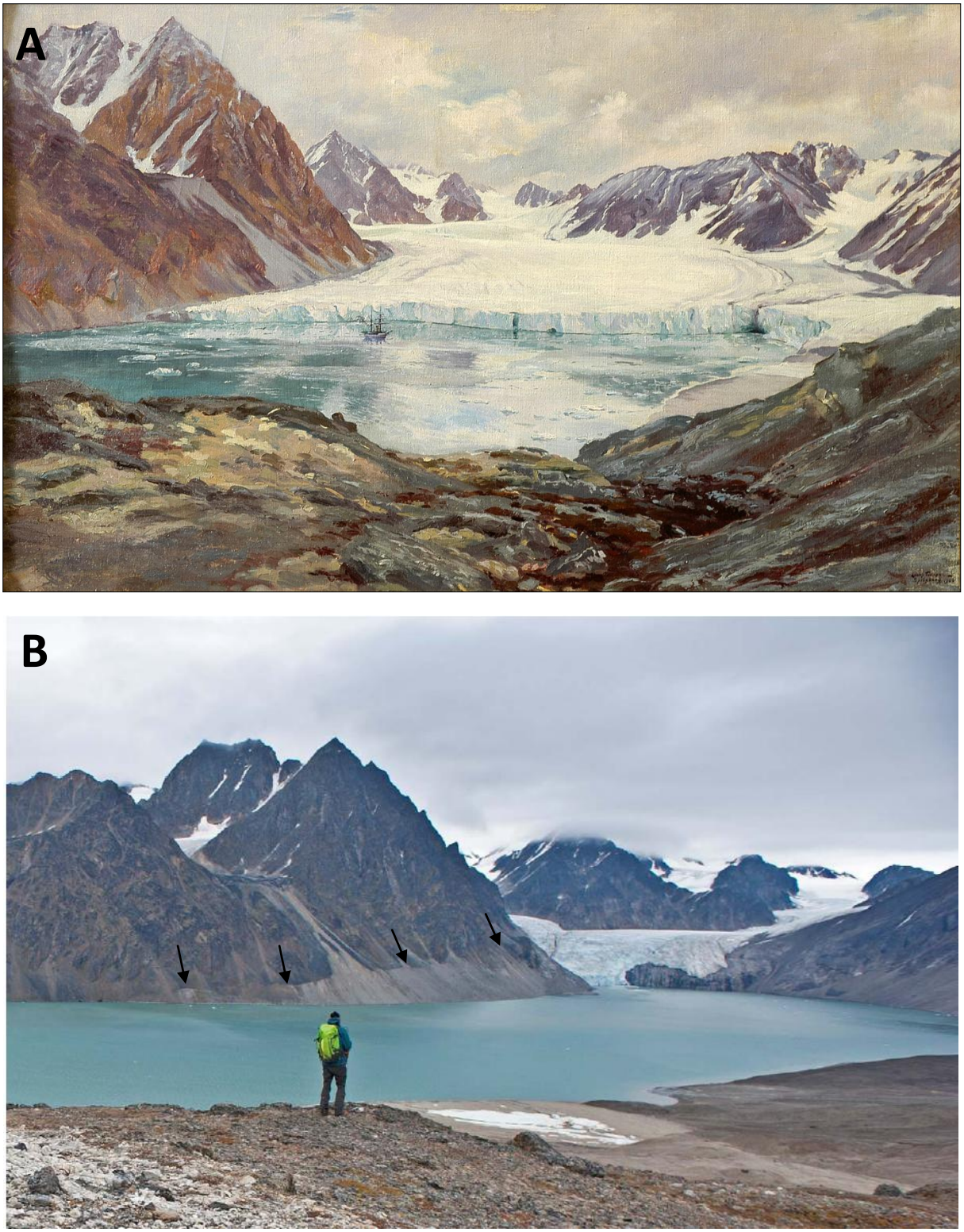

Figure 1.3: Tinayrebukta and Tinayrebreen's ice extent in 1906 and 2011. **A:** Oil on canvas painting by Jean Paul Louis Tinayre of the bay during Prince Albert I of Monaco's expedition to northwest Svalbard in 1906. Provided courtesy of Professor Julian Dowdeswell. **B:** A photograph taken in August 2011 showing the significant retreat of Tinayrebreen. A lateral moraine making the former extent of the glacier is marked with black arrows. Provided courtesy of Dr. Endre Før Gjermundsen.

1.1.3 Local Geology

Krossfjorden lies north of a major tectonic boundary found in Kongsfjorden, between the Tertiary fold-thrust belt of western Spitsbergen and the north-western Basement Province (Bergh *et al.*, 2000). Figure 1.4 shows that there has been tectonic activity around Krossfjorden, with a large number of faults evident. Lilliehöökfjorden drains an area of acidic metamorphic basement rocks (Cromack, 1991), which includes the Hornemantoppen formation of granites at the northern extent of Lilliehöökbreen's catchment. However, at its northern extent the glacier also drains areas with high grade metamorphic rocks (Fig. 1.4). In contrast, Möllerfjorden and the east of Krossfjorden are fed by glaciers eroding younger, lower grade metamorphic rocks of Middle Proterzoic age (Fig. 1.4), with the majority of rocks being marbles, mica schist and quartzites in the Signehamma and Generalfjella formations and the Smeerenburgfjorden complex (Cromack, 1991; Svendsen *et al.*, 2002).

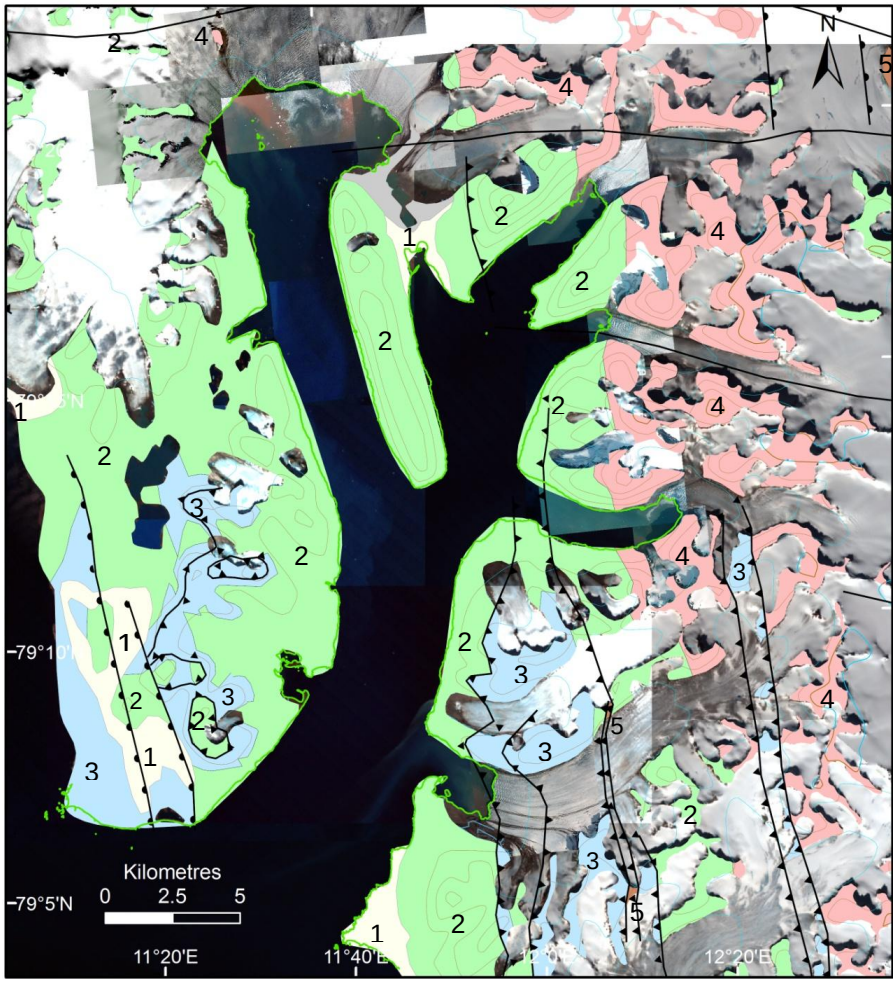

Figure 1.4: Simplified local geology of the Krossfjorden system from the Norsk Polarinstitutt's ArcGIS geodatabase. The numbers denote the various formations found surrounding Krossfjorden as follows: 1 = Marine and fluvial deposits, 2 = Signehamna, 3 = Generalfjella, 4 = Migmatites of Smeerenburgfjorden complex, 5 = Nissenfjella. Major faults are marked with black lines.

1.1.4 Oceanography

The Svalbard archipelago is uniquely situated, with the warm West Spitsbergen Current (WSC) circulating around the island (Ebbesen *et al.*, 2007). The WSC flows from south to north along the continental slope off the west coast of Spitsbergen before entering the Arctic Ocean (Fig. 1.5; Gammelsrød and Rudels, 1983; Saloranta and Svendsen, 2001). The cold current from the east, derived from the Arctic Ocean, is known as the East Spitsbergen Current (ESC) and circulates cold Arctic water along the west coast of Spitsbergen (Fig 1.5), where it is known as the Coastal Current (CC) (Skogseth *et al.*, 2005; Rasmussen *et al.*, 2007).

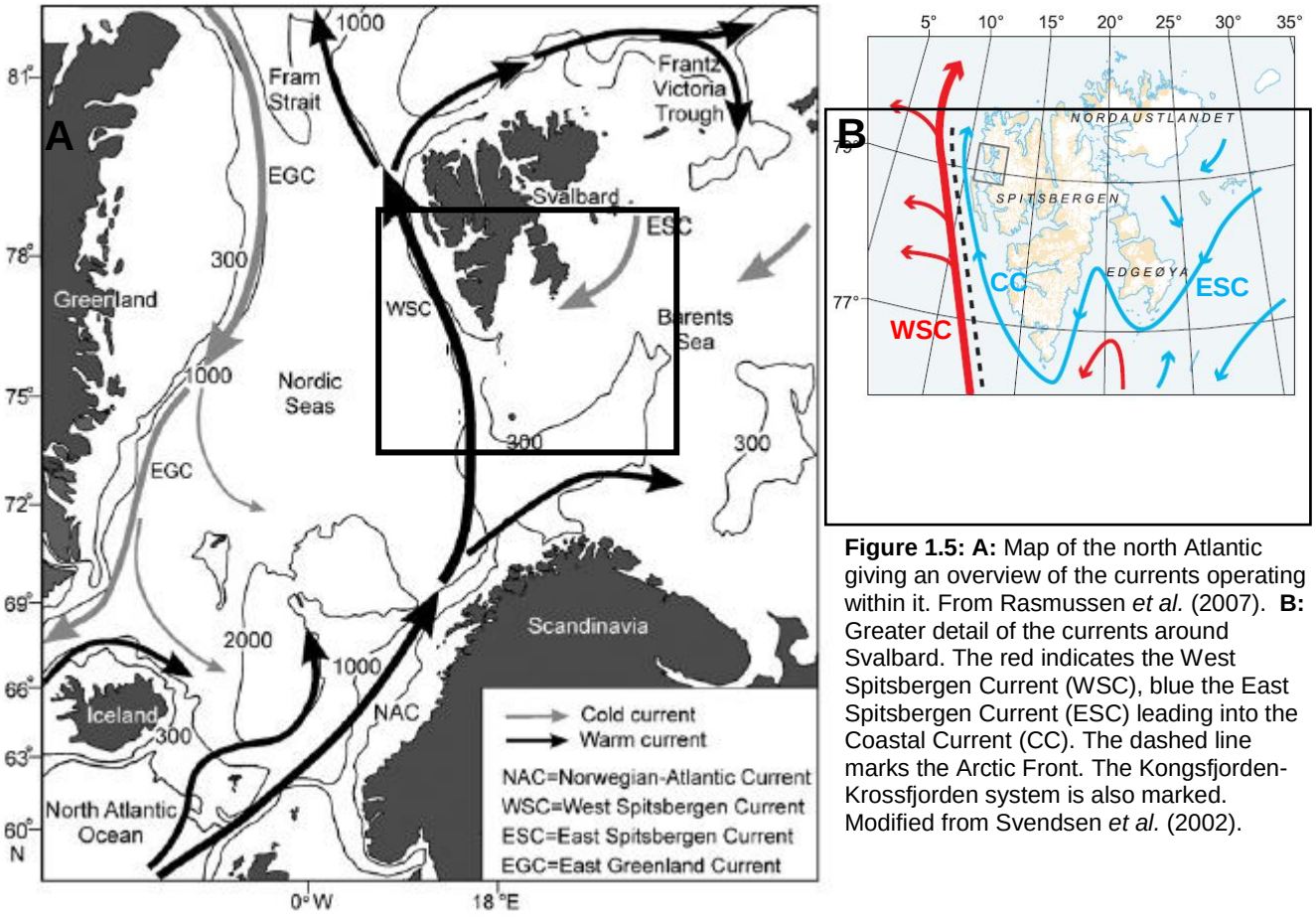

Figure 1.5: A: Map of the north Atlantic giving an overview of the currents operating within it. From Rasmussen *et al.* (2007). **B:** Greater detail of the currents around Svalbard. The red indicates the West Spitsbergen Current (WSC), blue the East Spitsbergen Current (ESC) leading into the Coastal Current (CC). The dashed line marks the Arctic Front. The Kongsfjorden-Krossfjorden system is also marked. Modified from Svendsen *et al.* (2002).

The Atlantic water (AW) in the WSC is relatively warm and saline (Nilsen *et al.*, 2008), at >3°C and a salinity of >35 ppt (Klekowski *et al.*, 1990; Ebbesen *et al.*, 2007). Whereas the cold mixture of Arctic and Polar waters associated with the ESC have temperatures around -1°C to 3°C and salinity of 34.6-34.9 ppt (Skogseth *et al.*, 2005; Ebbesen *et al.*, 2007). It has been demonstrated that these currents have persisted over the whole of the Holocene and that

it has been only variations in their strength and stratification which have resulted in changes in oceanographic conditions (Israelson *et al.*, 1994; Rhamstorf, 2002; Ślubowska-Woldengen *et al.*, 2007).

The north-western and northern margins of Svalbard are highly susceptible to changes in inter-annual inflow of AW from the WSC (Cottier *et al.*, 2007; Forwick *et al.*, 2010; Skarðhamar and Svendsen, 2010), which has significant implications to the hydrography of the fjords (Nilsen *et al.*, 2008). Fluctuations in the dominance of the warm WSC and the cold ESC have been shown to cause variations in sea surface temperatures (SST) and to change the position of the Arctic Front significantly (Dokken and Hald, 1996; Ślubowska-Woldengen *et al.*, 2007). The position of the Arctic Front has direct effects on the water entering the fjords along the west coast (Saloranta and Svendsen, 2001). It has even been noted that the AW has been warming during the previous century, with particularly high temperatures recorded in the 21st century (Pavlov *et al.*, 2013).

The Kongsfjorden-Krossfjorden system has been examined by Svendsen *et al.* (2002), Cottier *et al.* (2005) and Harms *et al.* (2007). It has been estimated that 90% of the total freshwater input into Kongsfjorden enters during the summer months of June to August due to the inflow of meltwater (Svendsen *et al.*, 2002) and it is likely that this would be similar in Krossfjorden. In April the water masses have been demonstrated to be relatively homogenous, being dominated by cold local water and with some winter cooled water (Fig.1.6; Cottier *et al.*, 2005). Intrusions of AW from the Polar Front lead to inflow of transformed Arctic water (TAW) into the fjord. This process is controlled by a horizontal pressure gradient between the coastal waters and the fjord system and is topographically directed across the shelf in Kongsfjordrenna (Cottier et al, 2005; Harms *et al.*, 2007). This inflow of TAW water with large heat content seems to begin in May (Harms *et al.*, 2007). By September AW and TAW become dominant within the fjord, with cool fresh surface water and intermediate water confined to the upper few metres (Fig.1.6), thus the fjord is clearly stratified (Svendsen *et al.*, 2002; Cottier *et al.*, 2005).

The general circulation of a fjord depends on a number of external variables; these include the amount of freshwater inflow, the strength of the winds and tides, the bathymetry of the fjord and the Coriolis Effect (Skogseth *et al.*, 2005; Harms *et al.*, 2007; Skarðhamar and Svendsen, 2010). It is the Coriolis Effect which causes inflow along the right side of the fjords in west Spitsbergen (Syvitski *et al.*, 1989; Harms *et al.*, 2007) and therefore there is

often an additional variable stratification across the fjord (Svendsen *et al.*, 2002; Cottier *et al.*, 2005; 2010; Skarðhamar and Svendsen, 2010).

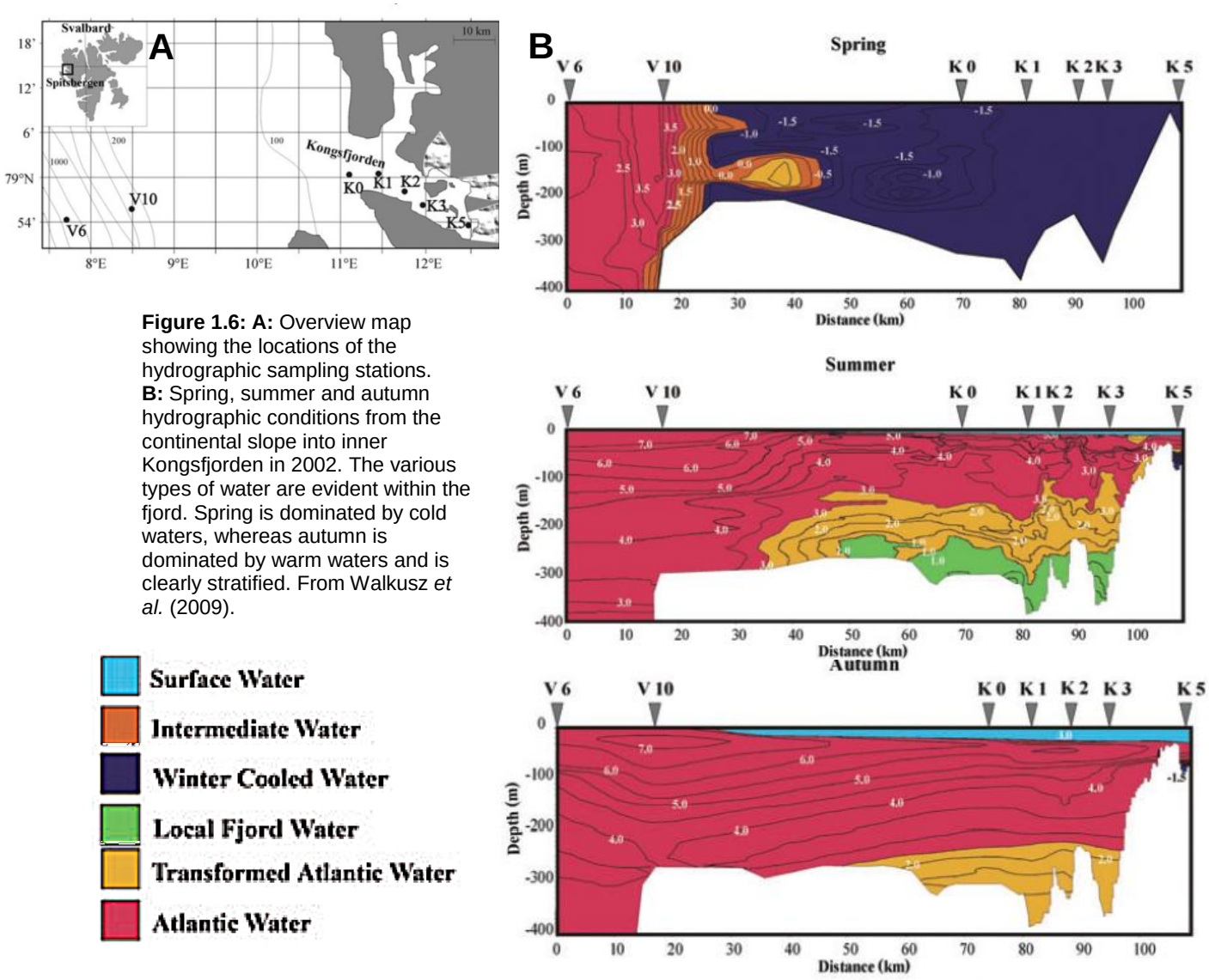

Figure 1.6: A: Overview map showing the locations of the hydrographic sampling stations. **B:** Spring, summer and autumn hydrographic conditions from the continental slope into inner Kongsfjorden in 2002. The various types of water are evident within the fjord. Spring is dominated by cold waters, whereas autumn is dominated by warm waters and is clearly stratified. From Walkusz *et al.* (2009).

The variables that control circulation have implications for the depositional processes occurring within the fjords (Skarðhamar and Svendsen, 2010) and how the waters may affect tidewater glaciers (Cottier *et al.*, 2010). Zajączkowski (2008) describes how the buoyant hypopycnal water layer combined with the turbid overflow plume is important in sediment transport within Kongsfjorden. Flux of suspended particulate matter (SPM) declines substantially along the fjord away from the tidewater margins (Fig. 1.7); within 1 km 23% of suspended particulate matter has settled and 71% is deposited within 5 km of the margins (Zajączkowski, 2008). Sediment accumulation rates within Krossfjorden have been calculated to be in the region of 0.7 to 4 mm a^{-1}, with the greatest sedimentation rates near the termini of the glaciers (Cromack, 1991).

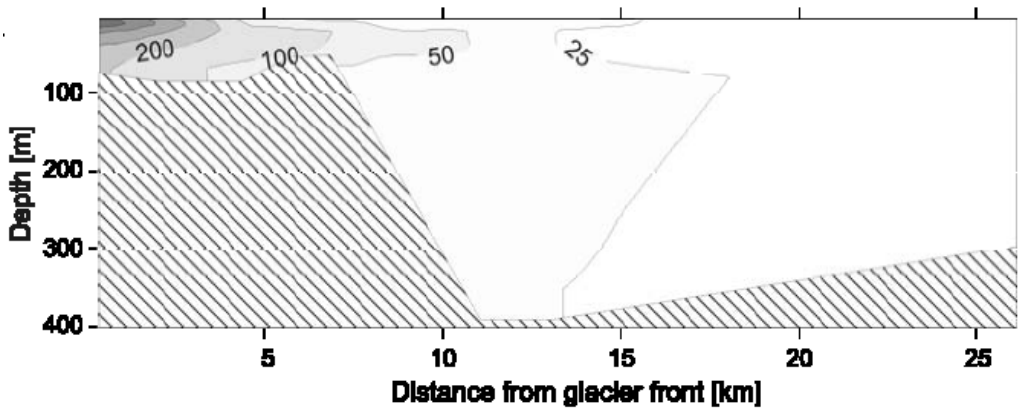

Figure 1.7: Suspended particulate matter (SPM) flux from Kronebreen and Kongsvegen, Kongsfjorden. SPM is given in g m^{-2} $24h^{-1}$. From Zajączkowski (2008).

1.2 Glacial history: last glacial-interglacial cycle

Ice was grounded over the entire Barents Sea region, including the Svalbard archipelago and its continental shelf, during the Last Glacial Maximum (LGM) of the Late Weichselian (Fig. 1.8; Mangerud *et al.*, 1998; Forman *et al.*, 2004; Landvik *et al.*, 2005; Ottesen *et al.*, 2007). Therefore the glaciers on Svalbard formed part of what can be termed as the Svalbard-Barents Sea Ice Sheet (SBSIS; Gjermundsen *et al.*, 2013); thus the entire study area would have been subjected to ice flow and glacial processes (Landvik *et al.*, 1987; 1998; Mangerud *et al.*, 1992; Svendsen *et al.*, 1992; Elverhøi *et al.*, 1998; Ottesen and Dowdeswell, 2009; Gjermundsen *et al.*, 2013). There has been at least one ice re-advance since the LGM. This was documented within the inner fjords of the archipelago, including the Krossfjorden system during the turn of the 20th Century and is attributed to the period known as the LIA (Liestøl, 1988; Sexton *et al.*, 1992; Werner, 1993).

It has been suggested that at about 30 ka BP glaciers were similar in size and extent to those at present on Svalbard, which indicates that it was an interstadial period. Therefore this indicates that the SBSIS had not yet formed (Mangerud and Svendsen, 1992). Models show that a decrease in sea level, combined with an increase in precipitation, led to the growth of the SBSIS (Siegert and Dowdeswell, 1995).

Reductions of rate of sedimentation and IRD delivery over the last 30,000 years or so have been suggested to be the result of a change in ice-flow dynamics. This change occurred when ice reached the shelf edge, around 22.5 – 18 ka BP (Andersen *et al.*, 1996; Dowdeswell and Elverhøi, 2002; Jessen *et al.*, 2010). This led to the development of inter-fan areas with minor

sediment accumulation, due to lesser basal meltwater and fewer icebergs calved within these areas of slow moving ice (Siegert and Dowdeswell, 2002), as well as the development of cross-shelf troughs and trough mouth fan areas, where flow and sediment outflow became concentrated into high velocity ice-streams (Dowdeswell and Siegert, 1999; Bennett, 2003; Ottesen *et al.*, 2008a).

Terrestrial evidence for reconstructions has relied largely on the mapping of post-glacial emergence rates tied to radiocarbon dated raised beaches across the Svalbard archipelago (Fig. 1.9; Forman *et al.*, 2004). Post-glacial emergence curves represent the amount of isostatic rebound following deglaciation and demonstrate the geographical variations. They can therefore be used to indicate approximately where greater glacial loading occurred. Eastern Svalbard has raised beaches largely in the range of 60 – 130 m a.s.l., whereas those in the Krossfjorden-Kongsfjorden region did not exceed 45 m a.s.l. (Fig. 1.8; Forman *et al.*, 2004; Salvigsen and Høgvard, 2005). This demonstrates that northwest Spitsbergen had a smaller ice load and therefore a more marginal location within the SBSIS. Northwest Svalbard thus probably had later glaciation and earlier deglaciation dates, with brief ice cover of a few thousand years.

The deglaciation is radiocarbon dated to have occurred between 13 – 12 ka BP (Forman, 1990; Lehman and Forman, 1992; Svendsen *et al.*, 1992; Elverhøi *et al.*, 1995; Landvik *et al.*, 1998; Forman *et al.*, 2004). This is supported by cosmogenic radionuclide (CRN) dating on islands in northwest Svalbard which revealed that there were some ice-free peaks present (Landvik *et al.*, 2003). Therefore, for nunataks to occur the ice cover must have been thin. However, results of new CRN dating in northwest Spitsbergen have revealed that cold-based ice was present during the Late Weichselian. Additionally, areas previously perceived as possibly ice free during the last glaciation, due to the presence of ancient raised beaches, such as Reinsdyrflya, north Spitsbergen, were covered by cold-based ice which allowed the preservation of these older features (Gjermundsen, submitted-A).

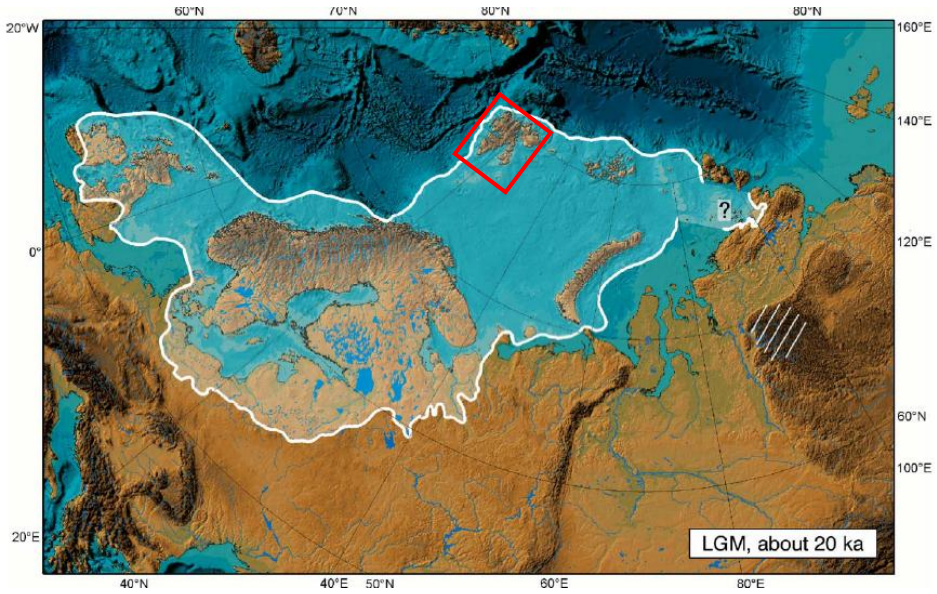

Figure 1.8: The mapped extent of LGM. The Svalbard archipelago is marked with a red box. From Svendsen *et al.* (2004).

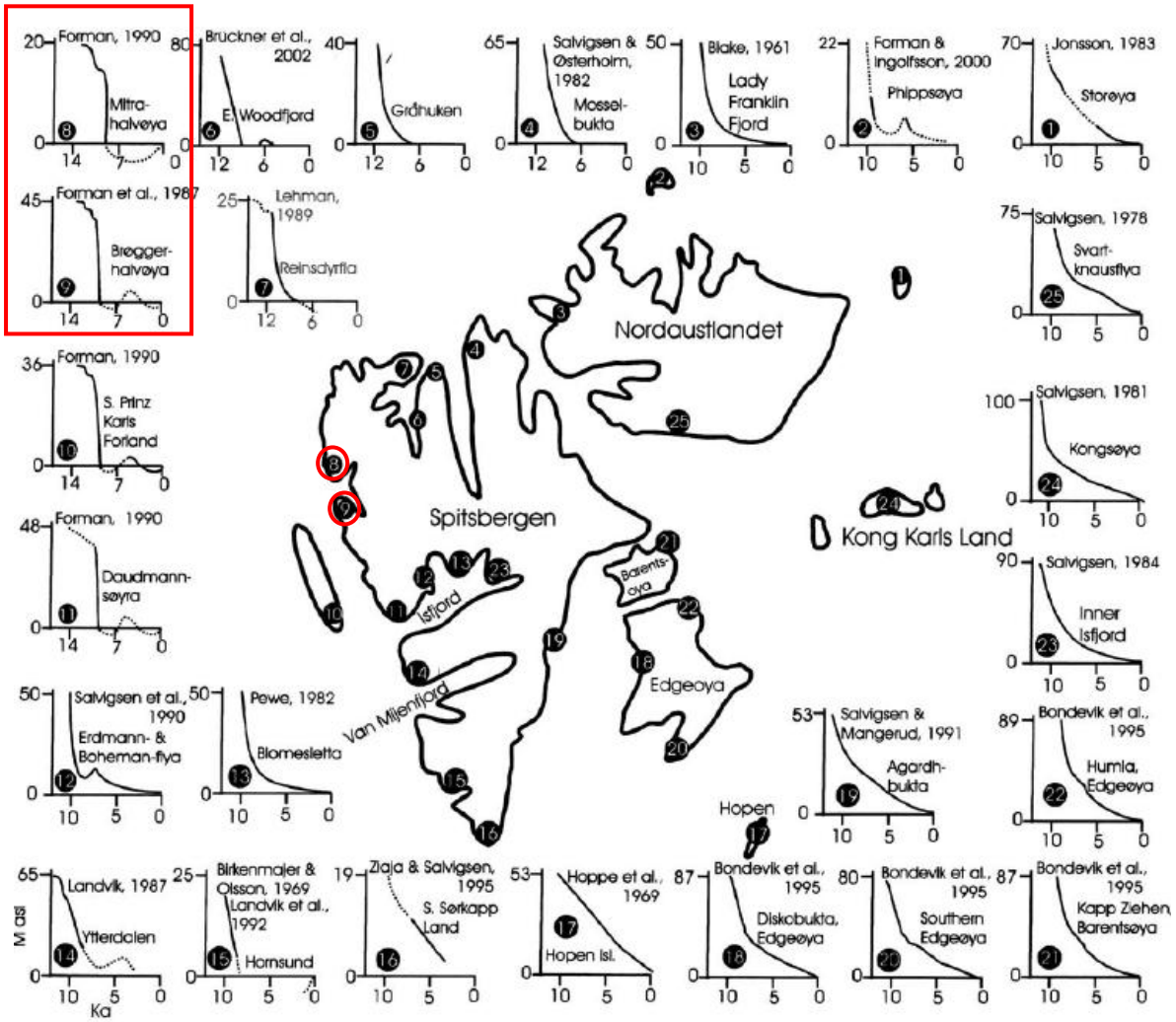

Figure 1.9: Postglacial re-emergence curves from key sites across Svalbard. Graphs have height (in m a.s.l.) on their y-axis and years (in ka) on the x-axis. The maximum recorded is on Kongsøya (number 24). The two curves near Krossfjorden are indicated by red circles and the red box. Modified from Forman *et al.* (2004).

Dowdeswell *et al.* (2010) and Landvik *et al.* (2013) suggested that the SBSIS may have been a multi-dome ice sheet and that there were periods with both warm and cold-based ice, which has repercussions for isostatic uplift. Using CRN dating of samples from bedrock and erratics Landvik *et al.* (2013) place deglaciation of the Kongsfjorden–Krossfjorden complex at 16 ka BP on the shelf and 13 ka BP for the inner fjord. The new CRN dates support this by suggesting the ice-sheet in northwest Spitsbergen, and specifically within Krossfjorden, was thinning between 25 – 16 ka with ice surfaces becoming 100 – 200 m lower (Gjermundsen *et al.*, 2013). A retreat of approximately 25 km took place from the continental shelf edge to the inner shelf west of Spitsbergen between 20.5 and 16.85 ka (Jessen *et al.*, 2010; Hormes *et al.*, submitted) and can be associated with Heinrich event 1.

Then between 15 – 14 ka there was a rapid retreat from the inner shelf to the inner fjords on the west coast (Hormes *et al.*, submitted). This is represented by both radiocarbon dates of marine cores and lithostratigraphic sections. This deglaciation date coincides with high sedimentation and IRD rates on the continental shelf (Elverhøi *et al.*, 1993; Kleiber *et al.* 2000), which reached their maximum values ca. 14.5 ka BP and is associated with meltwater pulse 1A (Dowdeswell and Elverhøi, 2002; Jessen *et al.*, 2010; Hormes *et al.*, submitted). These events are largely associated with a spike of isotopically light water which originate from meltwater plumes and accompanying laminated sediments (Jones and Keigwin, 1988; Elverhøi *et al.*, 1995), linked to an influx of warm AW (Jessen *et al.*, 2010).

Support for the retreat of the ice sheet from pinning positions on the outer coast of Spitsbergen around this time is provided by radiocarbon dates from Forman (1990) and Mangerud *et al.* (1992). Complete ice retreat from the western continental margin occurred prior to 12 ka (Elverhøi *et al.*, 1995; Svendsen *et al.*, 1996). The associated increase in influence from warm AW is evident in the lithology of deposits with an absence of IRD (Jessen *et al.*, 2010), which permitted the colonisation of the archipelago by thermophilous molluscs around 10 ka BP (Salvigsen, 2002; Brückner and Schellman, 2003).

Local glaciers may have been stable or marginally expanded in central, northern and eastern areas of Svalbard during the Younger Dryas (YD; Bondevik *et al.*, 1995; Elverhøi *et al.*, 1995; Landvik *et al.*, 1995; 1998; Forwick and Vorren, 2010; 2012; Gjermundsen *et al.*, submitted-B), including a minor re-advance noted between 12.6 – 12.4 ka BP near Isfjorden (Svendsen *et al.*, 1996). Other areas of Svalbard are not thought to have re-advanced until

Late Holocene growth during the LIA (Mangerud and Svendsen, 1990; Salvigsen and Høgvard, 2005), including in Kongsfjorden (Lehman and Forman, 1992).

The chronology indicated by the new CRN dating (Hormes *et al.*, submitted; Gjermundsen *et al.*, 2013) and multi-proxy dating of sediment cores (Jessen *et al.*, 2010) provide a chronology of deglaciation earlier than previously thought (e.g. Elverhøi *et al.*, 1993; 1995; Siegert and Dowdeswell, 1995; Andersen *et al.*, 1996; Landvik *et al.*, 1998; Mangerud *et al.*, 1998; Dowdeswell and Elverhøi, 2002) and so demonstrate that there is still more data collection and modelling necessary to try to understand this last glacial period better.

1.3 Regional bathymetry

In the present interglacial period, the continental shelves and fjords of Svalbard have lost their grounded ice and are now occupied by the ocean. This submergence has allowed the preservation of the submarine morphology which can provide evidence of the past nature of ice sheets (Ó Cofaigh *et al.*, 2005; Ottesen *et al.*, 2005). This evidence has been predominantly well preserved because the submarine environment is relatively stable below the wave-base when compared with terrestrial locations where glacial landforms have been subjected to periglacial activity and subaerial erosion (Lambeck, 1996; Ottesen and Dowdeswell, 2006).

The continental shelf off northwest Spitsbergen is around 60–85 km wide and is quite shallow, at generally <100 m (Fig. 1.9) (Elverhøi *et al.*, 1995). The swath-bathymetric data published in Ottesen *et al.* (2007) demonstrates a distinct cross-shelf trough from the mouth of Kongsfjorden to the shelf edge, known as Kongsfjordrenna (Fig 1.9B). Kongsfjordrenna is 90 km long with a shelf width of 60 km and is estimated to have drained a palaeo-ice stream with a basin of about 8000 km^2 (Batchelor and Dowdeswell, in press). There are also a large number of glacial lineations within the trough; these are interpreted as megascale glacial lineations, which indicate fast ice flow through the trough (Fig. 1.10) eroding and deforming the sedimentary substrate (Stokes and Clark, 1999; Dowdeswell *et al.*, 2004; Ottesen and Dowdeswell, 2006; Ottesen *et al.*, 2007).

Bathymetric and acoustic surveys also revealed transverse ridges. One of these is visible at the shelf edge, which has been interpreted as marking the maximum extent of ice during the

Late Weichselian. Another ridge located midway through the trough has been interpreted as a grounding-zone wedge (GZW; Fig. 1.9B, C, D). This GZW indicates that there was a stillstand of the ice-sheet at this position and therefore ice retreat through the trough was episodic, rather than rapid (Ó Cofaigh *et al.*, 2005; Ottesen *et al.*, 2007; Dowdeswell *et al.*, 2008). In contrast, Sarkar *et al.* (2011) demonstrated that the shelf to either side of the cross-shelf trough had a landform assemblage that is characteristic of a slower more gradual retreat (an inter-ice stream region; Ottesen and Dowdeswell, 2009).

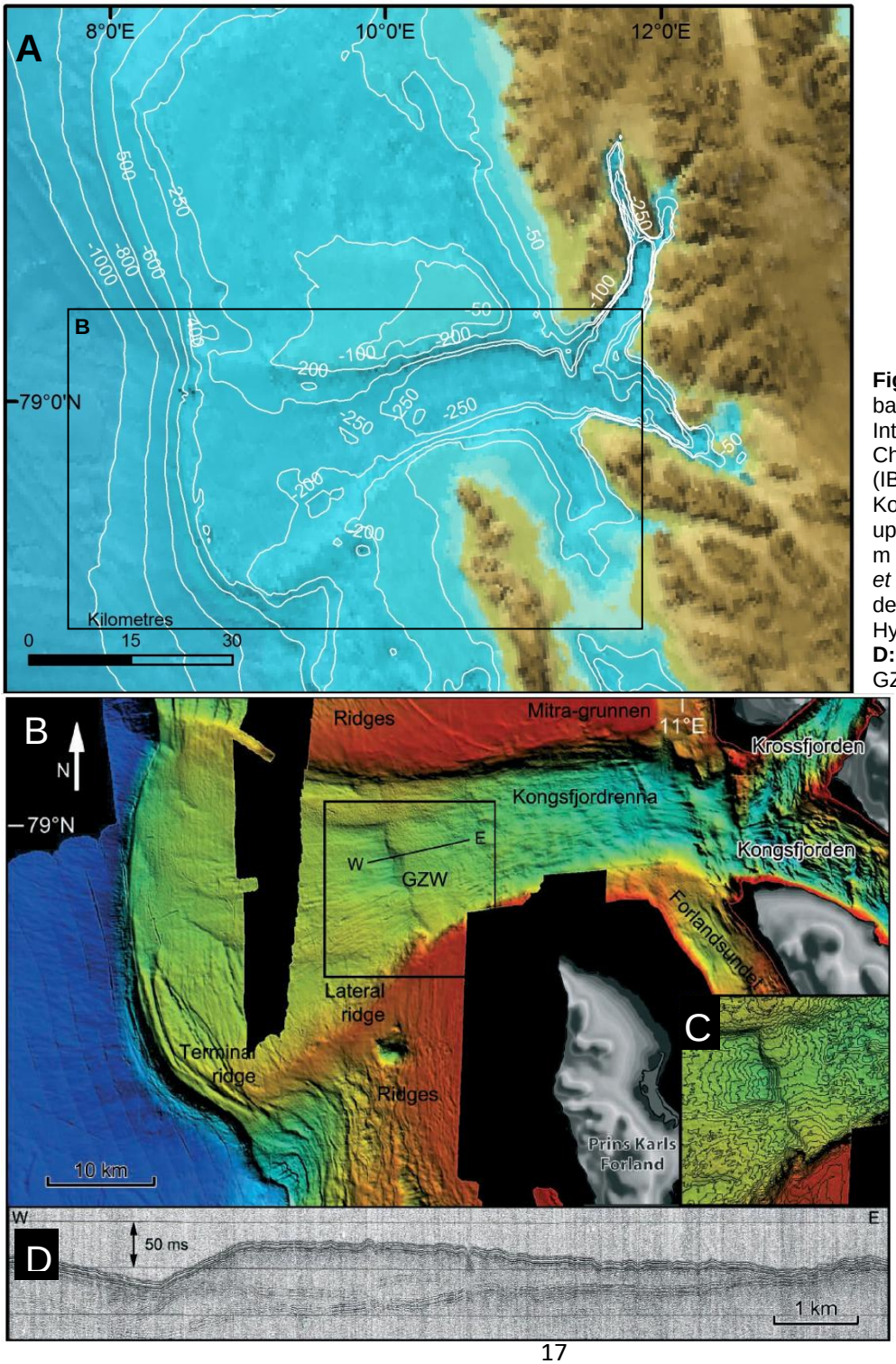

Figure 1.10: A: Regional bathymetry shown in the International Bathymetric Chart of the Arctic Ocean (IBCAO) 3. **B:** bathymetry of Kongsfjordrenna. **C:** a close-up of the approximately 50 m high GZW. From Ottesen *et al.*, 2007 but originally derived from the Norwegian Hydrographic Service. **D:** Acoustic profile of the GZW.

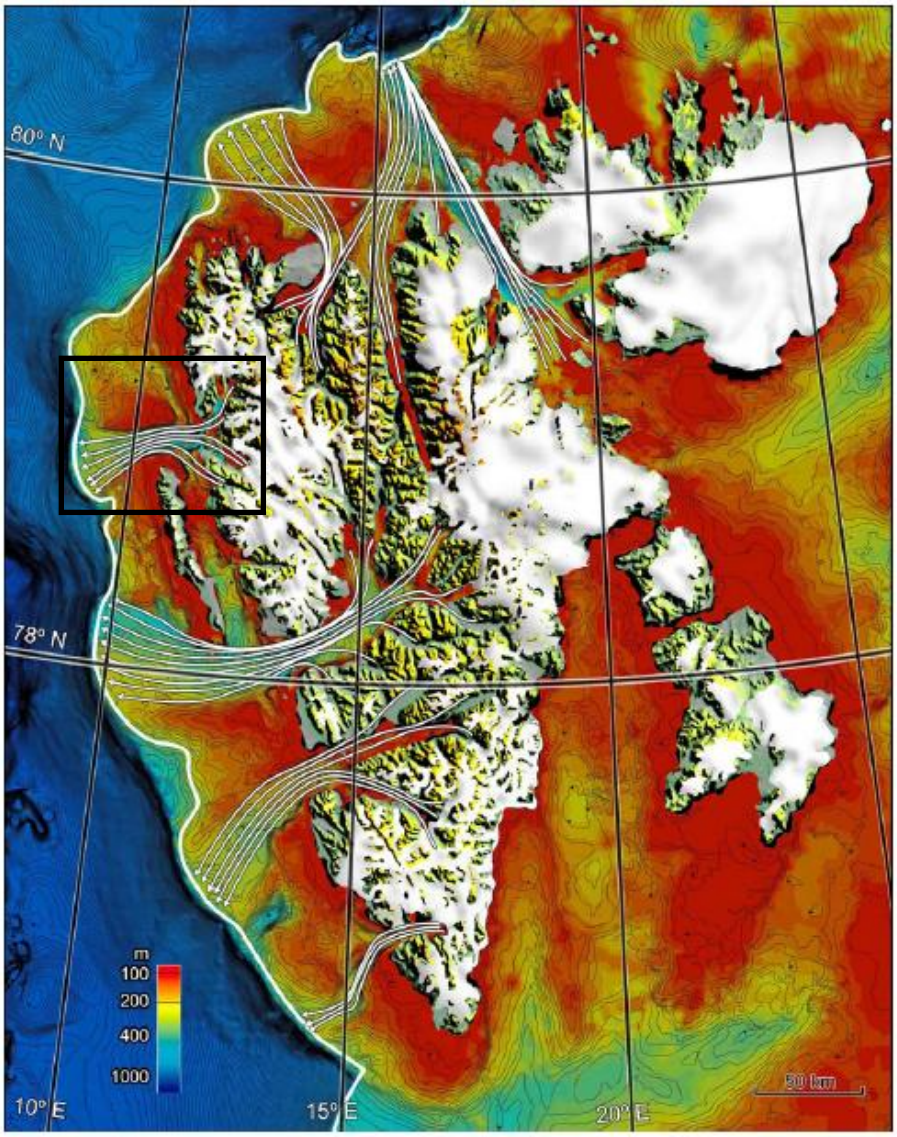

Figure 1.11: Overview of the Svalbard archipelago with ice-streams marked with arrows in the direction of ice flow. The Kongsfjorden-Krossfjorden ice-stream is marked by the black box. Modified from Ottesen *et al.* (2007).

1.4 Structure of thesis

This thesis continue in Chapter 2 with an explanation of the methods used to collect, process and analyse the swath bathymetric data, as well as briefly mention the types of data previously collected which assist in the analysis of the study fjords.

Descriptions and interpretations of the landforms and sediments in Lilliehookfjorden are set out in Chapter 3, and the sea-floor features from the Möllerfjorden system and outer Krossfjorden are discussed in Chapters 4 and 5. The findings from these fjords are then discussed in Chapter 6 in context of previous work in the study area, the history of the ice-fronts. Landsystem maps for the fjords are presented and the implications of these are then discussed further in Chapter 7, alongside models for submarine landform assemblages, before some concluding remarks are given in Chapter 8.

Chapter 2 - Methods

Several datasets were assembled and analysed to describe and interpret the seabed landforms and sediments of the Krossfjorden system. The geophysical data from the Krossfjorden system were collected by the Norwegian Hydrographic Service (NHS) during cruises which surveyed Krossfjorden in 2000 and again in 2010 to cover the Möllerfjorden system. These surveys utilised Kongsberg Maritime EM1002 and EM 3002D multi-beam echo sounders to obtain the swath-bathymetric data. TOPAS (TOpographic PArametric Sonar) sub-bottom profiler data and gravity cores from Sexton *et al.* (1992) and Howe *et al.* (2010) have also been taken into consideration for this study to assist analysis. A background mosaic of aerial photographs (from Norsk Polarinstitutt) of the land areas surrounding Krossfjorden was produced so that the marine geological data could be viewed in the context of the adjacent glaciers.

2.1 Multi-beam swath bathymetry

Multi-beam swath bathymetry measures the depth of a water body at different angles from a ship's transponder to the seabed (Fig. 2.1), using transmitters and receivers to send pings of energy through the water column to the seafloor. The beams are reflected from the seafloor and return to the hull-mounted receivers which calculate the time taken for each echo to return. Based on this time, and taking into account ship speed, water depth can be calculated (using the formula Depth = Speed x Time / 2).

The transmit beams are electronically stabilised for roll, pitch and yaw, whilst the receive beams are stabilised for roll movements through the use of gyroscopes and a motion reference unit. Sound velocity probes are also used because the speed of the sound waves through water depends on its temperature and salinity. As a result, datasets produced from these bathymetric systems have a high degree of accuracy (Dowdeswell *et al.*, 2006; Hogan *et al.*, 2010), with grid cell sizes reaching 1 m. The positions of the NHS surveys are accurately determined through the use of a GPS system.

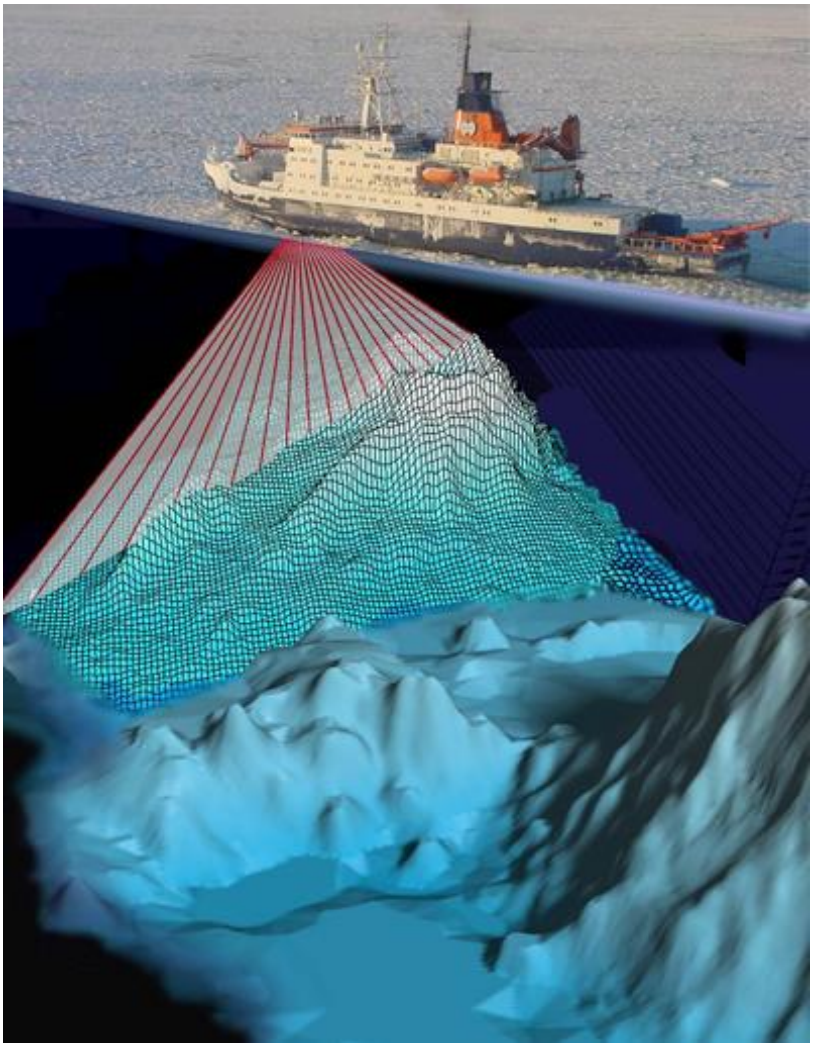

Figure 2.1: The principles of a multi-beam swath bathymetric system: the beams of a ping, shown in red, spread out from the ship and the area is represented on the seafloor, from where the beams are reflected to receivers. This technique produces a 3D image of the seafloor. Image from the Alfred Wegener Institut (2013).

The NHS conducted two missions to collect high-resolution multi-beam swath bathymetric data across the study area (Table 2.1, Fig. 2.2).

Table 2.1: Details of the two cruises conducted by the NHS and the type of bathymetric system used.

Cruise name	Date	Bathymetric system	Systems details
Sjoemaalern-4100	Summer 2000	Kongsberg Maritime EM 1002	The EM 1002 has a range which spans from shallow coastal waters to 1000 m depths. It operates at a frequency of 95 kHz and emits 111 beams per ping (Kongsberg Maritime, 2004).
Hydrograf 2010-113	Summer 2010	Kongsberg Maritime EM 3002D	The EM 3002D system has exceptionally high-resolution, with a shallow depth range from less than 1 m to around 300 m in good conditions. This system operates around the 300 kHz band and emits a maximum of 508 soundings per ping, resulting in a swath width of 10 times the water depth (Kongsberg Maritime, 2006). Therefore this system is much better suited for the inner fjords, as it allows very detailed visualisations to be produced.

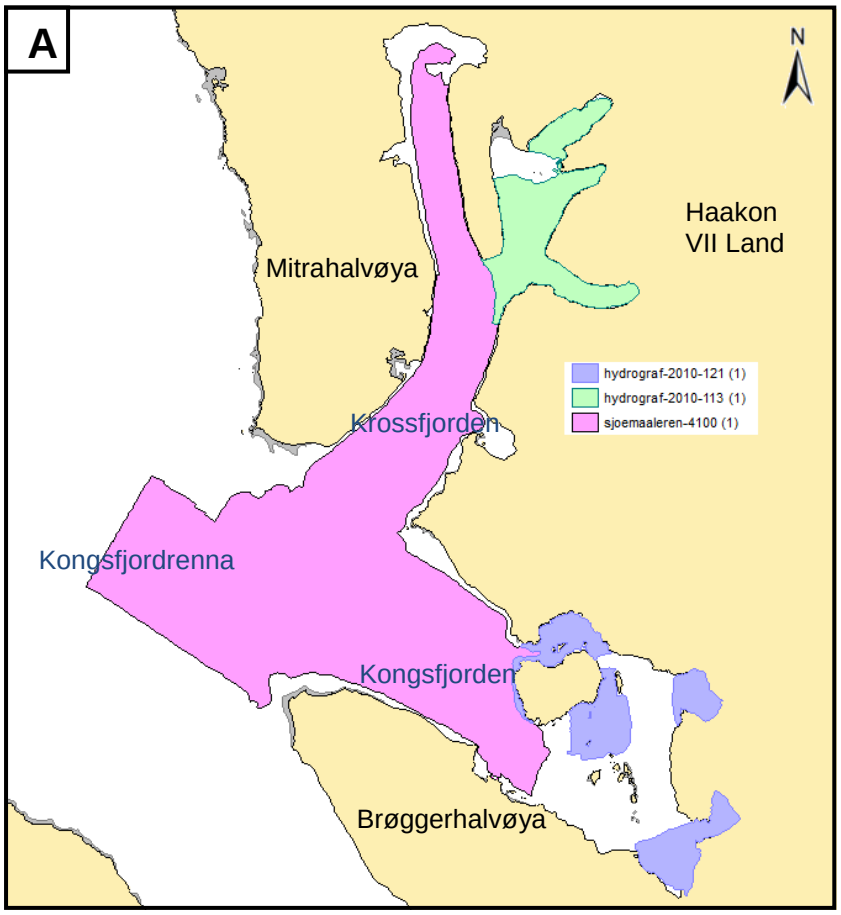

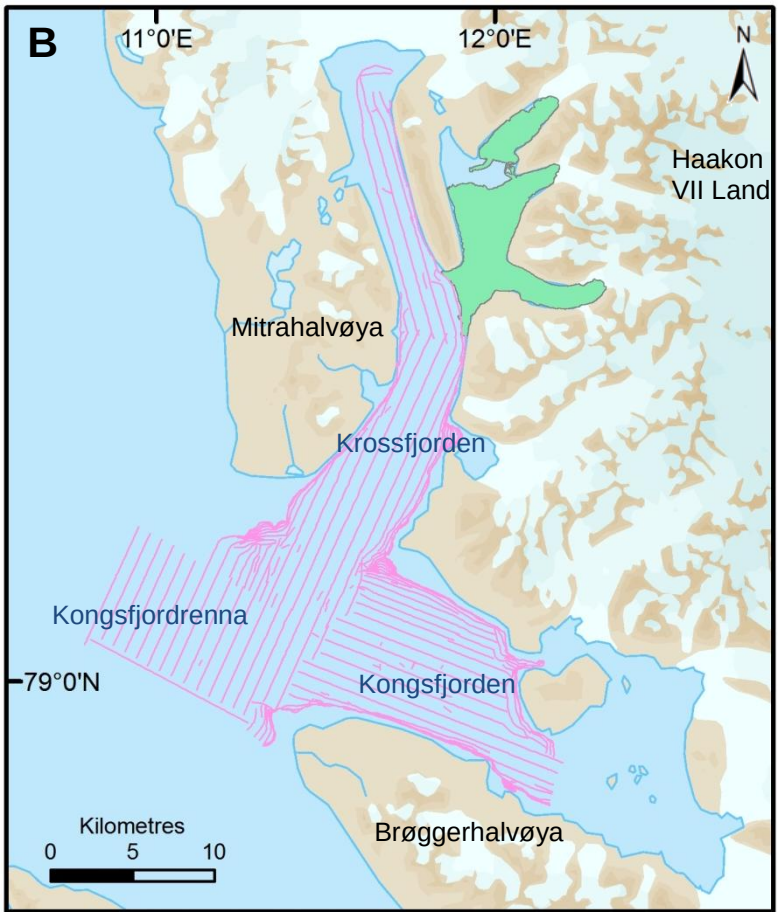

Figure 2.2: A: Map of the study area showing the two cruises of the Norwegian Hydrographic Service, rose = 2000, green = 2010. The cruise names are shown in the key. Image is courtesy of the Norwegian Hydrographic Service. **B:** Ship's tracks for the Sjoemaaleren-4100 cruise in pink and the survey area of Hydrograf-2010-113 cruise in green.

The data from the 2000 Sjoemaalern-4100 cruise had already been processed when it was obtained for this study and the ship's tracks were available (Fig. 2.2B). However, the ship's tracks for the Hydrograf 2010-113 cruise were not yet available from the NHS and required some processing. The processing procedure, which utilised a suite of IVS processing and 3-D visualisation programmes, is outlined in Table 2.2.

Table 2.2: Outline of the processing procedure.

Programme	Procedure
DMagic	PFM files were produced for sections of both cruises.
Fledermaus and 3D Editor	The PFM files were imported into Fledermaus where 3D Editor was used to remove soundings with unrealistic depths, as well as those with unrealistic longitudes and latitudes, from the data because they were interpreted as errors. The PFM files were then converted to XYZ files in Fledermaus
DMagic	XYZ files were exported back to Dmagic and were gridded with a cell size of between 1 and 2 m for the 2010 cruise and between 5 and 15 m for the cruise in 2000.This was because the earlier cruise has a lower resolution due to the constraints of the EM1002 echosounder. Interpolation was conducted on specific datasets in order to minimise artefacts and data gaps.
Fledermaus	Once gridded in DMagic it was possible to analyse images from Fledermaus, where they could be exported to ArcGIS.
ArcGIS	Bathymetric data were combined with a background map (Section 2.4) and figures were produced.

Errors can arise from presence of icebergs or sea ice disturbing the survey, or can be due to interference from strong winds or waves, and variations in the water column (Hogan, 2008). An example of an area affected by this interference and which required processing can be seen in Figure 2.3, both pre and post-processing.

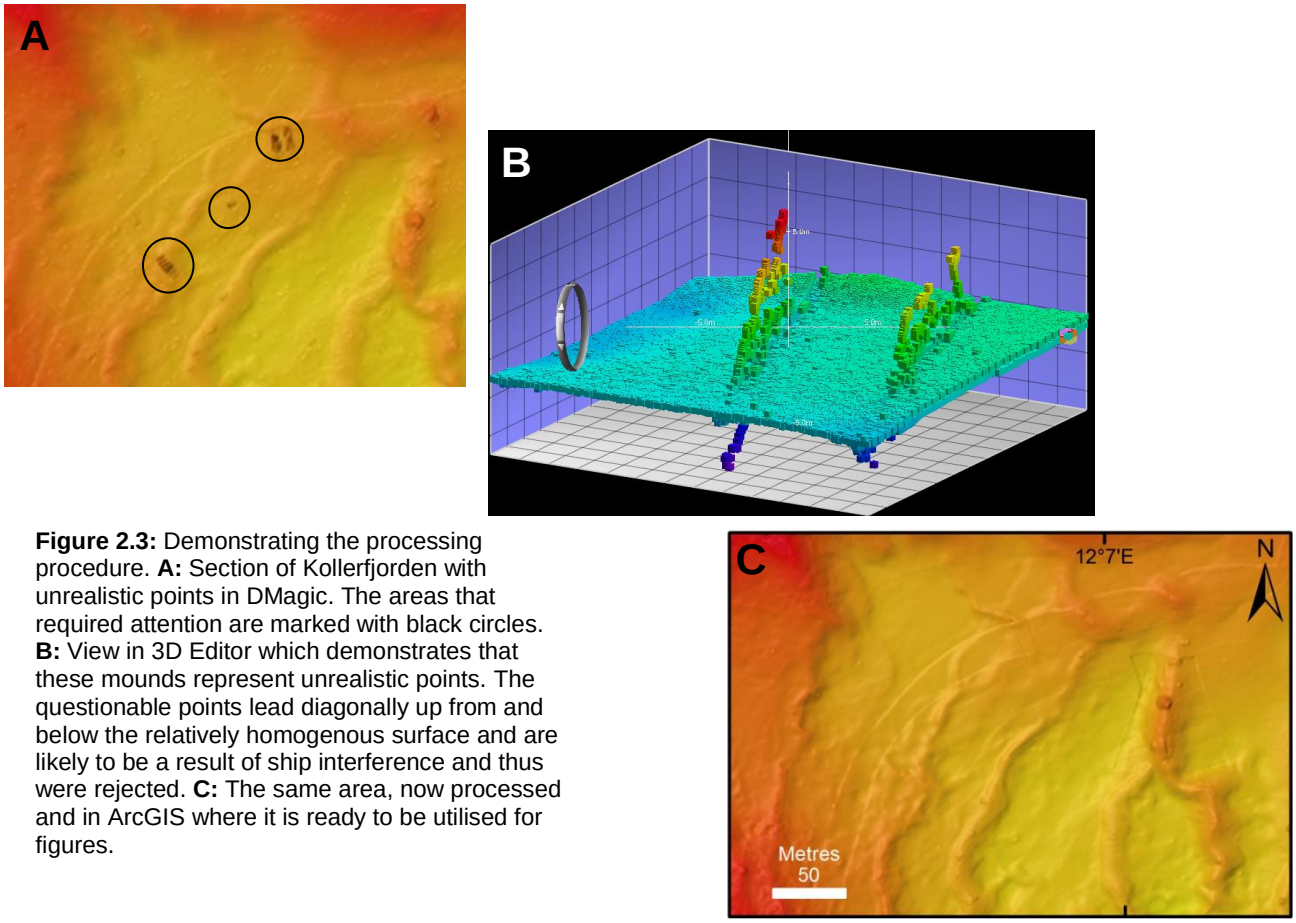

Figure 2.3: Demonstrating the processing procedure. **A:** Section of Kollerfjorden with unrealistic points in DMagic. The areas that required attention are marked with black circles. **B:** View in 3D Editor which demonstrates that these mounds represent unrealistic points. The questionable points lead diagonally up from and below the relatively homogenous surface and are likely to be a result of ship interference and thus were rejected. **C:** The same area, now processed and in ArcGIS where it is ready to be utilised for figures.

The swath bathymetric data obtained from the two Kongsberg systems provided the necessary information for mapping the geometry of the seafloor, since it allows a 3-D visualisation to be produced and the dimensions of individual landforms to be calculated (Dowdeswell *et al.*, 2008). The images of the seafloor produced consist of an assemblage of superimposed landform features which makes it possible to reconstruct the nature of past ice flow. From this superimposition a relative age is demonstrated, with the youngest features cross-cutting older landforms (Ottesen *et al.*, 2005; Ottesen and Dowdeswell, 2006). Because it makes it possible to reconstruct the nature of past ice flow, collection and analysis of multi-beam swath bathymetric data has been widely used in a number of projects within both polar regions. For example, the flow of the West Antarctic Ice Sheet through the Belgica Trough has been examined by Ó Cofaigh *et al.* (2005) and Pine Island Bay by Evans *et al.* (2006) using this technology. Numerous works in the Arctic include Ottesen *et al.* (2005) and Hogan *et al.* (2010a; 2010b), both of which investigate submarine landforms and their implications for the direction of ice flow around the Svalbard archipelago. Dowdeswell *et al.* (2008) and Ottesen and Dowdeswell (2006; 2009) demonstrate how characteristic landform assemblages allow the production of geomorphic models which may be applied to a number of similar localities.

2.2 Acoustic, seismic and sediment core datasets

Acoustic profiling data, deep penetrating seismic reflection profiles and sediment cores have also been used and re-interpreted in this project to help with the interpretation of the bathymetric data (Table 2.3).

Table 2.3: The type, sources and method of the data previously presented for Krossfjorden that are useful to consider applying with the bathymetric data in this thesis.

Data Type	Presented previously by:	Method	Application
Shallow acoustic sub-bottom profiling	Sexton et al. (1992) and Howe et al. (2003).	Shallow acoustic data were collected using TOPAS, with a frequency of 0.5 – 5 kHz, from *RRS James Clark Ross* during cruise JR127 in 2005 (Maclachlan *et al.*, 2010). The acoustic nomenclature used in the articles, which describes the relation of seismic profiles to the sediment lithology, has been based on Damuth's (1978) work on the echo character of Quaternary sedimentation in the Norwegian-Greenland Sea. Damuth's (1978) classification is based on the prolongation of the bottom echo return as well as the transmittance of the sediment. Fine-grained material is seen as acoustically transparent whilst coarser-grained material is increasingly opaque (Elverhøi, 1984).	These data have been analysed to produce a shallow acoustic stratigraphy for a number of transects in the Krossfjorden system, with a particular focus on areas close to present glacier termini. They provide a characterisation of sediments, showing the upper few metres are unconsolidated; however, they have not previously been combined with such detailed swath bathymetric data that include the heads of the study fjords.
Deep penetrating seismic records	Sexton et al. (1992).	Seismic data in Krossfjorden were gathered by a Hartley HML 3.6 kJ sparker system, which was operated from the research vessel Lance in 1987. The Hartley system has a nine electrode array and 50 element streamer (with a filter setting 100–500 Hz), and the analogue recording was via a single channel (Sexton *et al.*, 1992). Sound waves are transmitted to the seabed and the varying acoustic impedance of different sediment and rock layers reflect varying amounts of energy (Stoker et al., 1997). This reflected energy is then detected by a hydrophone and then processed, so that a survey transect is produced.	The use of boomer systems provides a high resolution for the near- surface (Stoker et al., 1997) and is therefore beneficial when looking at glacial marine geology, allowing intepretations of the seabed landforms and sediments.
Sediment cores	Sexton et al. (1992) and Cromack (1991).	The sediment cores were retrieved using the gravity coring method. Gravity corers use weights on top of the coring device to force them into the sediment below the seabed. The device consisted of a 6 m long galvanised steel tube with fins to stabilise it and thus ensure a vertical penetration. At the bottom of the core is a removable cone which provides the cutting edge to penetrate the sediments, and a core catcher which allows sediment to pass into the core, but does not allow it to be flushed out. The sediment passes into an inner plastic tube, with a diameter of 100 mm, which is protected by the outer steel. Once the core is imbedded in the sediment, a winch on the ship is used to retrieve it. At the top of the core a watertight liner prevents wash-out of the sediments. Once aboard, the core is split in half longitudinally with a circular saw and an osmotic knife, labelled and cold stored. One half is analysed whilst the other half is archived.	The sixteen cores taken in Krossfjorden were analysed for grain size distribution and a ^{210}Pb-dated core was discussed to approximately measure the sedimentation rate over the past 200 years or so (Cromack, 1991; Sexton *et al.*, 1992). They also demonstrate the variation between ice-proximal and ice-distal locations.

2.3 Background mosaic of land areas

The background mosaic (Fig. 2.5) used throughout this project is a compilation of Landsat imagery, combined with aerial photography. A digitised topographic map and an updated coastline of the study area were also used. The mosaic produced from these datasets provided a cloud- and snow-free visual aide to the interpretation of the swath bathymetric data in the context of the adjacent land areas and ice cover. More detailed information on how this map was acquired and produced is given in Table 2.4. Images were processed and cropped in ERDAS Imagine before being imported into ArcGIS.

The coastline file provided by the Norsk Polarinstitutt (NPI) was edited to match the aerial images from 2009 - 2011 to provide an up-to-date coastline for the study area (Fig. 2.4). Some tidewater margins from the NPI's coastline were delineated at their 1990 extent, which resulted in a obvious inaccuracy at these margins as the NPI's aerial images showed that glaciers in these areas have retreated significantly, especially Lilliehöökbreen (Fig. 2.4), thus some of the bathymetric data were overlapping these lines. Therefore in ArcGIS the tidewater margins of Lilliehöökbreen, Mayerbreen and Tinayrebreen were fitted to their 2009 extent and Kollerbreen to its 2011 extent obtained from the NPI's aerial photographs. Additionally, further data accessed on the Norsk Polarinstitutt's GIS server was used in the production of figures (overview maps) and analysis (topographic map within the background mosaic).

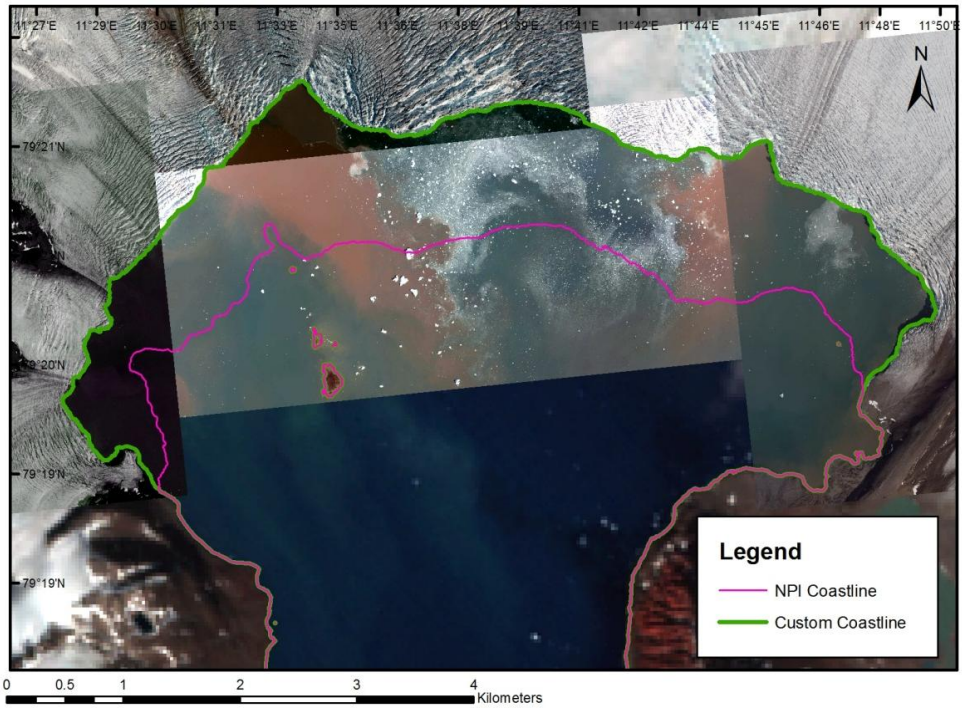

Figure 2.4: Comparison between the coastline provided by the Norsk Polarinstitutt (NPI) and their aerial photography for 2009 – 2011. In Krossfjorden the coastline still showed the extent of glaciers in 1990 (pink line).The edited coastline with the 2009 tidewater margins of Lilliehöökbreen, Mayerbreen and Tinayrebreen and 2011 margin for Kollerbreen is represented by the green line.

The Randolph Glacier Inventory (RGI 2.0), downloaded from the Global Land Ice Measurements from Space initiative (GLIMS), was used to visualise and obtain the size of the various local drainage basins of the study area. The part of this inventory which covered Svalbard was the result of a joint collaboration between the Norsk Polarinstitutt, the University of Oslo and Uppsala University (GLIMS Technical Report, 2012). The primary data sources were SPOT5-HRS DEMs and aerial photographs, but also included ASTER and Landsat images due to cloud and snow cover (König *et al.*, 2012). Data obtained in 2007-2008 accounts for 71% of Svalbard delineations; however, for areas with poor cover during this time, data from as early as 2001 were used (GLIMS Technical Report, 2012); it still vastly improves the outdated delineations in the inventory prepared by Hagen *et al.* (1993).

Table 2.4: The type, sources, identification codes and the acquisition date of the data are included in the table below for all the datasets from which the background mosaic was constructed.

Data type	Source	Identification	Acquisition Date
Landsat 7 ETM SLC-on	Earth Explorer – United States Geological Survey (USGS). Originally from NASA.	LE72180031999191SGS00	10/07/1999
Landsat 7 ETM SLC-on	Global Land Cover Facility – University of Maryland Originally from NASA.	233-280 GLS 2005 - LT52200032006200KIS00 233-269 GLS2005 - LT52160032006204KIS00 233-270 GLS2005 - LT52160032006204KIS00 233-283 GLS2005 - LT52210032006207KIS00	19/07/2006 23/07/2006 23/07/2006 26/07/2006
Aerial Photography	Norsk Polarinstitutt – TopoSvalbard online aerial photography	Forbesbreen – 13822736 Lilliehöökbreen (north-west) – 13822754 Lilliehöökbreen (east) – 13822821 Lilliehöökbreen (south) – 13822756 Kollerbreen – 251601 Mayerbreen – 138222834 Tinayrebreen (north) - 13822813 Tinayrebreen (south) – 13822811 Fjortende Julibreen - 13822770	2009 2009 2009 2009 2011 2009 2009 2009 2009
Digital TopoMap	Norsk Polarinstitutt	NP_TopoSvalbard_U33W84_WML/MapServer/WMSServer	Variable
Coastline	Norsk Polarinstitutt	Upon request, provided by Anders Skoglund of the Norsk Polarinstitutt.	Variable
Local Drainage Basins	Global Land Ice Measurements from Space (GLIMS)	Randolph Glacier Inventory 2.0	Variable – Predominantly 2007-2008

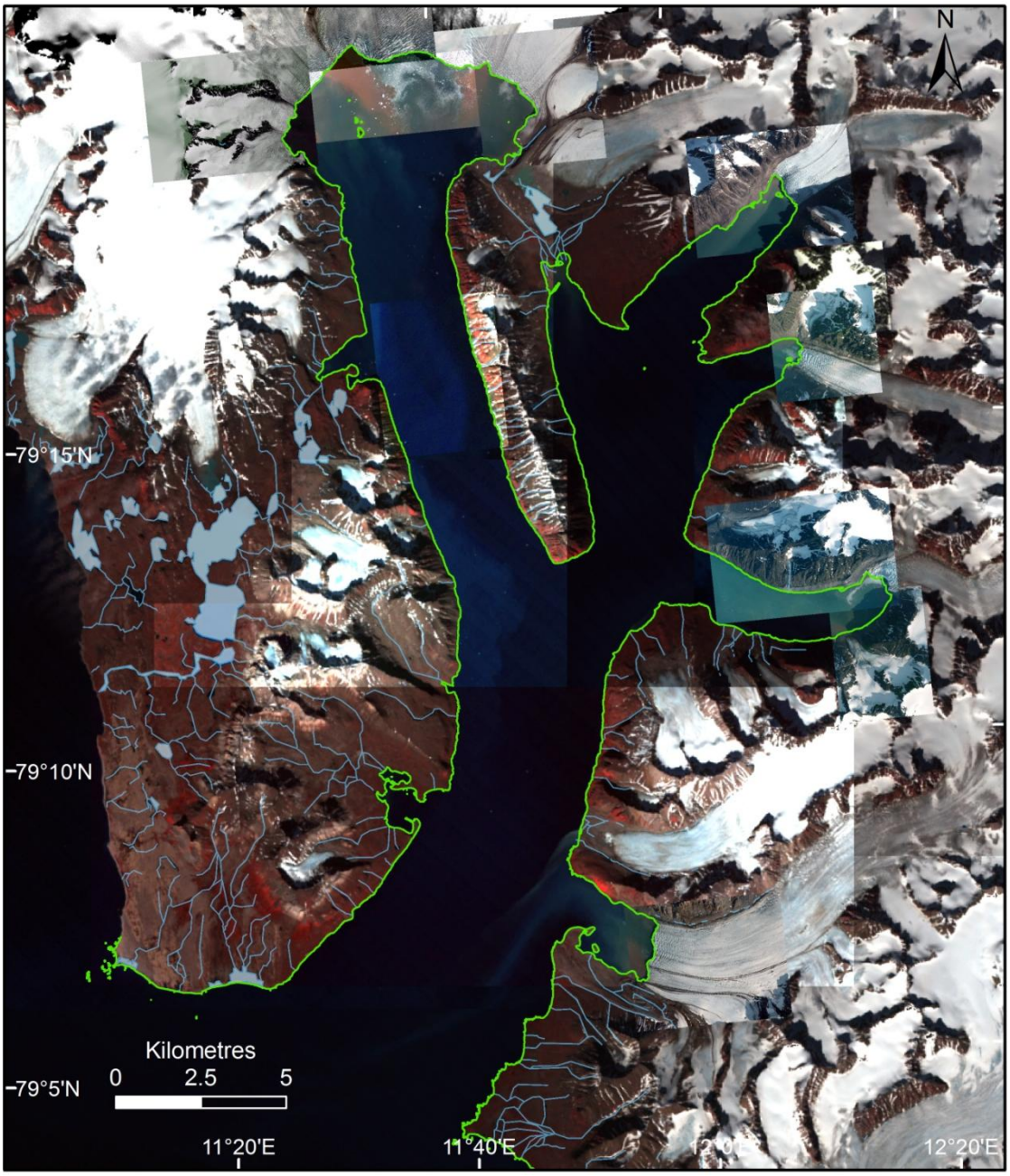

Figure 2.5: Background mosaic of the Krossfjorden system.

Chapter 3 - Submarine landforms in Lilliehöökfjorden

Lilliehöökfjorden is a 17 km long fjord in northwest Spitsbergen with a tidewater glacier at its head. High resolution swath-bathymetric data come to within 2 km of the ice front of Lilliehöökbreen. Swath data from Lilliehöökfjorden were gridded to a 5 m cell size to show the distribution of submarine landforms within the fjord (Fig. 3.1). The features vary in their mode of formation and are individually described and interpreted. These landforms have implications for the extent and dynamics of the trunk glacier and tributary glaciers that form Lilliehöökbreen (Table 1.1, Fig. 1.2).

The north-western section of the survey area is the most ice-proximal, with several small islands found approximately 1.5 km beyond the current ice front (in summer 2009) and 0.5 km from the extent of bathymetric data (Fig 3.1). Lilliehöökfjorden has a large number of subglacial features within the inner fjord with fewer in the outer fjord; thus these two areas are discussed separately (Fig. 3.1).

3.1: Inner Lilliehöökfjorden

Inner Lilliehöökfjorden refers to approximately the innermost 5 km of the fjord, where a ridge separates inner and outer part of the fjord (Fig. 3.2). The inner fjord opens into a 7.5 km wide bay surrounded by Lilliehöökbreen and its tributary glaciers (Fig. 3.2).

3.1.1 Large transverse ridges: terminal and overridden moraines

Description:

Lilliehöökbreen has a large subparallel transverse ridge at approximately 5 km from the current glacier front (Fig. 3.2A). The ridge varies in height and width across the fjord; however, typically it has a height of 30 m on its proximal (northern) side and 60-100 m on its distal side. The ridge is clearly asymmetrical in cross section, with an average slope of 9° on its proximal side compared to 13° on its distal side (Fig 3.2B). At its shallowest point the ridge is only 100 m deep.

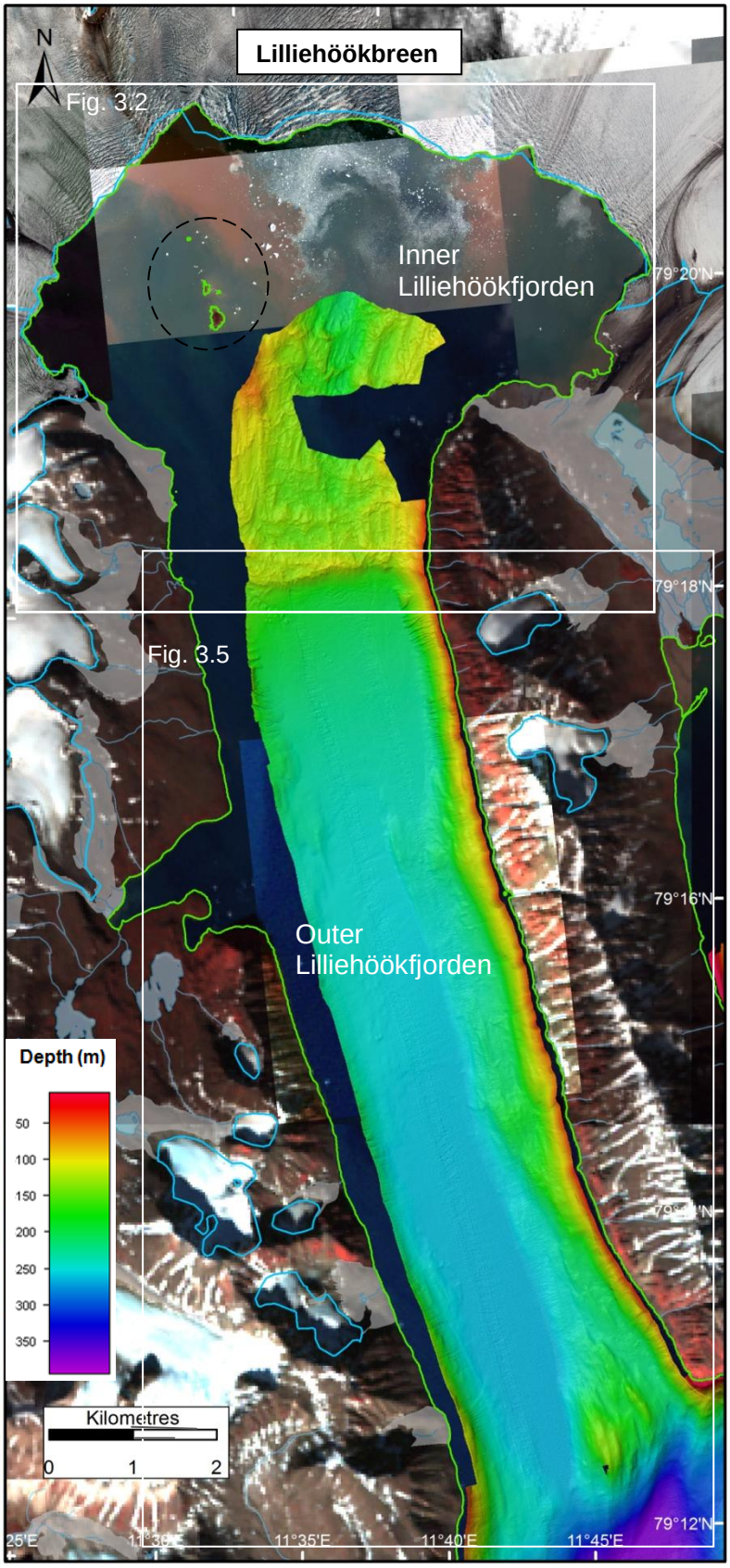

Figure 3.1: Overview map of Lilliehöökfjorden; the outer and inner fjord are labelled as well as the tidewater margin of Lilliehöökbreen. The dashed black circle highlights several small unnamed islands. Bathymetric data show the seabed topography. The bathymetric data are artificially illuminated from 315°, with an elevation above the horizon of 50° (unless stated otherwise). The water depth bar has been hypsometrically optimised for the range within each area. The background map derived from Landsat imagery and aerial photographs shows the adjacent glaciers and snow-free land.

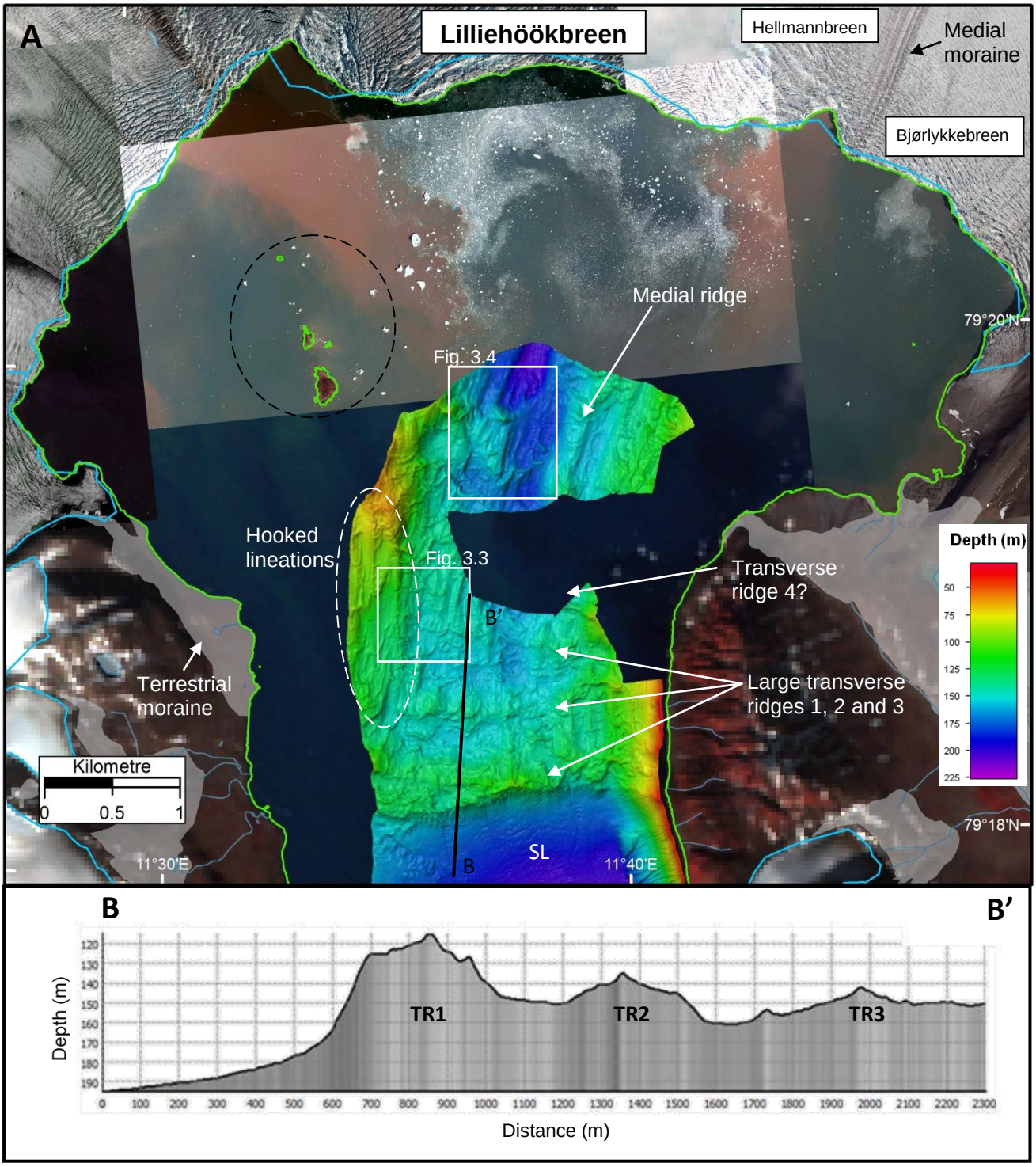

Figure 3.2: A: Inner Lilliehöökfjorden. Many of the sea-floor features described and interpreted are labelled within this figure. SL denotes small lobe-like features. Streamlined features and smaller transverse ridges are evident throughout inner Lilliehöökfjorden; additionally hooked lineations are indicated by a dashed white circle. The white labelled boxes indicate the locations of Figures 3.3 and 3.4. The green coastline is from the Norsk Polarinstitutt but has been modified to fit the aerial photography of the tidewater margins (2009). The blue line delineates glacier drainage basins within the study area, from the Randolph Glacier Inventory. The group of unnamed islands is highlighted by the dashed black circle.
B: The three large transverse ridges described are evident in this long profile as well as a few of the smaller transverse ridges. TR1, 2 and 3 denote the three large transverse ridges.

Along the base of the first transverse ridge a number of small irregular lobe-like features are evident on the ice-distal side (Fig. 3.2A). They are most clearly visible near the steepest parts of the ridge and are spaced regularly with around 20 m between them and with heights of 1.5 – 2.5 m. There also appear to be gullies leading down slope on the distal side of this ridge, which have depths of about 1 – 4 m and widths between 5 – 30 m, with V-shaped leading into U-shaped morphologies present.

On the ice-proximal side of the first large transverse ridge (TR1) there appear to be two less pronounced large transverse ridges (TR2, 3; Fig. 3.2), with possibly another in the data cover gap. The more ice-distal of these (TR2) has a width of around 350 m, a height of between 10 – 25 m and spans 1.5 km. The second, more ice-proximal ridge (TR3) is more ambiguous, but there is still a distinguishable change in the morphology and depth of the sea-floor (Fig. 3.2B). There is a narrow, transverse ridge approximately 15 m high and 80 m wide which could mark a fourth large ridge (Fig. 3.2A). However, because it extends into the gap where bathymetric data are absent an interpretation of it has not been made.

Interpretation:

The large transverse ridge is interpreted to represent the maximum extent of Lilliehöökbreen during its last significant glacial advance (Ottesen *et al.*, 2007). There is no evidence on the distal side of this ridge to suggest that past ice flow extended any further during this last advance and the ridge can therefore be described as a terminal moraine (Ottesen *et al.*, 2005). Large terminal moraines form when a glacier front remains at one place for a significant time, often decades. Soft sediment pushed by ice concentrates and extrudes at the margin, which in turn produces a depocentre and a mound that grows in size (Benn and Evans, 2010). Large terminal moraines have commonly been observed in bathymetry around Svalbard (Ottesen and Dowdeswell, 2006; 2009; Ottesen *et al.*, 2008a; Forwick and Vorren, 2010; Robinson *et al.*, 2011; Gjermundsen *et al.*, submitted-B). Terminal moraines have a characteristically steeper ice-distal side than ice-proximal side as a result of their formation by a glacier (Bennett, 2001; Dowdeswell and Vásquez, 2013) similar to those observed in Lilliehöökfjorden. However, terminal moraines with steeper ice-proximal sides have been described in Ottesen and Dowdeswell (2006) and Ottesen *et al.* (2008) around Svalbard. The likely reason for the occurrence of these uncharacteristic moraines could be because of greater slope instabilities, likely to be associated with their formation during surges, which resulted in the moraine being more susceptible to mass wastage.

The small irregular lobe-like features towards the base of the terminal moraine appear to indicate down-slope creep of debris, perhaps produced as a result of instabilities of unconsolidated material within the moraine. Similar features found in acoustic profiles have been named as slip surfaces (Sexton *et al.*, 1992; Plassen *et al.*, 2004) which demonstrate instabilities related to the shear strength and pore water pressure of the sediments (Springman *et al.*, 2003) leading to creep (Forwick and Vorren, 2007). The presence of gullies supports the interpretation that instabilities have led to some mass wastage (Forwick and Vorren 2012). It may also be possible that these gullies could have formed from dense and turbid meltwater underflow down the slope when the glacier was positioned at this location (Gales *et al.*, 2013).

Transverse ridges 2 and 3 are interpreted to be recessional or terminal moraines from previous ice advances, given that they are cross cut by several of the landforms described below. They could represent previous surges from the glacier; however, Lilliehöökbreen is not known to be a surge-type glacier and so this is not thought to be the cause (Liestøl, 1993; Sevestre *et al.*, unpublished).

3.1.2 Fjord-perpendicular ridge: medial moraine

Description:

On the north-eastern side of the data extant within the inner fjord there is a large curvilinear ridge (Fig. 3.2A). The feature is 35 m high on the western side, 15 m high on the eastern side and around 120 m wide. It is 1 km long and leads into the data gaps close to the glacier front and within the swath mosaic.

Interpretation:

This ridge is interpreted as a possible medial moraine from the north-eastern part of Lilliehöökbreen's drainage basin, similar to shear margin moraines described in Benn and Evans (2010). These moraines are formed due to the stresses between different glacier flow filaments derived from different drainage basins, usually linked to the varying velocity of ice flow. Looking at the aerial photographs and satellite imagery of the glacier, a possible source for the formation of this feature is the medial moraine and shear margin between the subsidiary glaciers of Hellmannbreen and Bjørlykkebreen (Fig. 3.2A).

3.1.3 Streamlined bedforms: glacial lineations

Description:

A large number of curvilinear features are observed running parallel with the fjord-axis (southward trending) and are present over the entire area of swath coverage between the present day glacier front and the large transverse ridge interpreted as a terminal moraine (Figs. 3.2A, 3.3A). The streamlined bedforms vary between 1 - 5 m in height, are around 50 m wide, reach over 500 m long and thus have elongation ratios (length/width) of <10:1. Some of these linear bedforms, particularly on the western-most side, have hooked distal-ends (Figs. 3.2, 3.3A, B).

Interpretation:

These streamlined bedforms are interpreted as glacial lineations and are understood to form through the movement of ice on a sedimentary substrate which frequently produces landforms that vary considerably in scale, but are all aligned parallel to ice flow (Ottesen and Dowdeswell, 2006; Dowdeswell and Vásquez, 2013) and match descriptions of flutings (Solheim *et al.*, 1990; Benn and Evans, 2010). The formation of these is similar to mega-scale glacial lineations (MSGL); however, MSGL are larger and more elongate than the formations in Lilliehöökfjorden (Clark, 1993; Stokes and Clark, 1999; King *et al.*, 2009).

The lineations with hooked distal-ends (Fig. 3.3A) are streamlined bedforms which appear to be closely associated with small transverse ridges. They are interpreted to be the result of either the way the small transverse ridges were formed (discussed below) which links them to possibly being a type of crevasse-squeezed ridge or the result of minor glacitectonic thrusting of material or both. This minor thrusting could occur if the material is not frozen to the bed of the glacier but is still formed into faint lineations with a hooked or C-shaped end. They are similar to features described in Ottesen *et al.* (2005) and Hogan (2008) but are a smaller-scale version and there is generally no depression on their stoss side.

It is likely that across inner Lilliehöökfjorden all the processes mentioned above have helped form the lineations described; however, their dimensions are variable and do not allow a clear separation and classification amongst them.

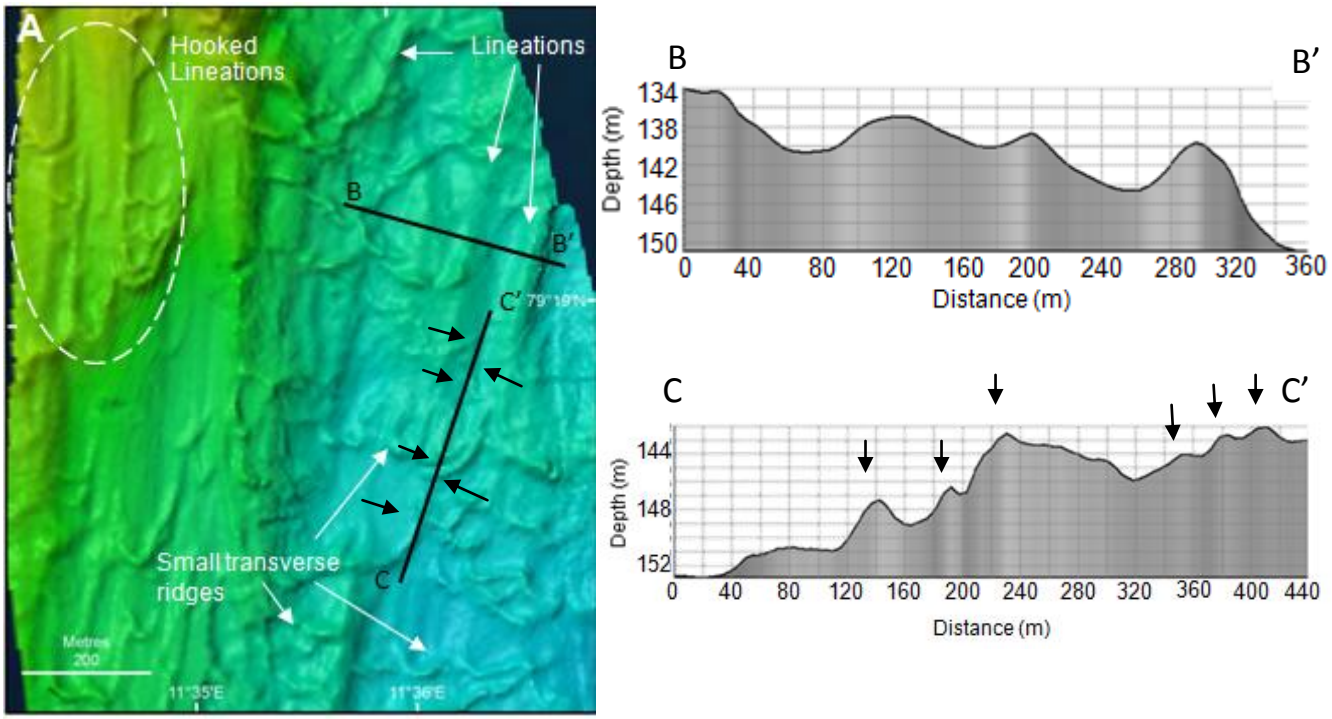

Figure 3.3: A: Western flank of inner Lilliehöökfjorden (located in Fig. 3.2A) showing greater detail of the lineations, hooked lineations and the sets of small transverse ridges. **B:** Cross-sectional profile across a set of glacial lineations. **C:** Surface long-profile demonstrating the morphology of small transverse ridges (marked with black arrows).

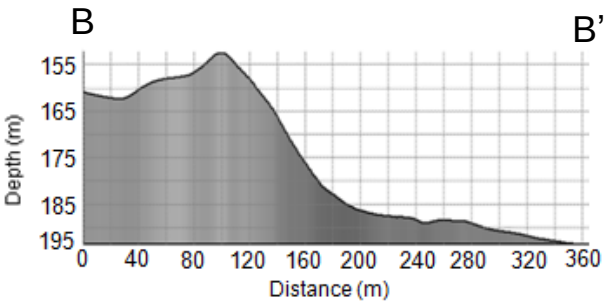

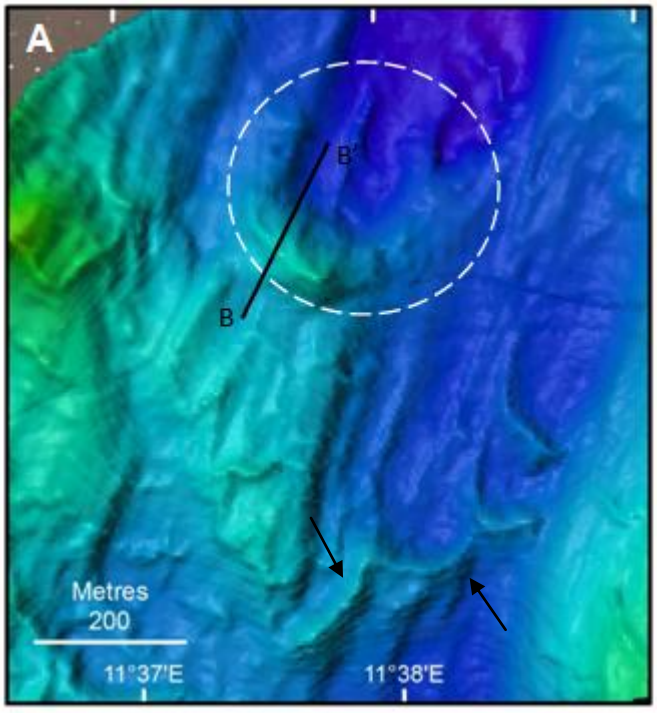

Figure 3.4: A: The C-shaped transverse ridge is highlighted by a dashed white circle (located in Fig. 3.2A). The black arrows indicate the medium sized transverse ridge. **B:** Long-profile of the C-shaped transverse ridge.

3.1.4 Small transverse ridges: recessional moraines

Description:

Within the inner part of Lilliehöökbreen a number of much smaller transverse ridges lead back towards the current glacier front and are perpendicular to ice flow (Fig 3.3A, C). These ridges have varying heights, ranging from 0.5 m – 6 m, with most between 1 – 4 m. At the ice proximal extent of the data cover, near the deepest point of 202 m, there is a distinct C-shaped ridge that is around 35 m high (Fig. 3.4A, B), with a width of 125 m and a length of only about 180 m. There are a few smaller features with a similar C-shape across inner Lilliehöökfjorden. There is also a medium-sized ridge approximately 3 km from the 2009 front of Lilliehöökbreen (Fig. 3.4A). This ridge has a height of around 10 m, but reaches about 20 m in the deep central part of the fjord, and has widths of approximately 80 m.

Interpretation:

The extensive series of small transverse ridges represent small push moraines which are interpreted as recessional moraines. It is possible that they could have been formed annually (Dowdeswell *et al.*, 2008; Ottesen and Dowdeswell, 2009), during small winter re-advances; however this is not believed to be the case here. The ridges are more complex than at other locations with regularly-spaced annual-retreat moraines, such as those described at Borebukta, Isfjorden, central Spitsbergen (Ottesen and Dowdeswell, 2006). There are a number of ridges cross-cutting others and C-shaped loops in the Lilliehöökbreen data, and so there is more uncertainty about their chronology and even their formation.

The ridges are a lot more concentric than at other tidewater margins in Svalbard. This concentric shape in plan form is similar to that described at Skálafjellsjökull, south-east Iceland (Sharp, 1984) and can be linked to be the former shape of the glacier front, indicating that the glacier was crevassed during its retreat (Bennet, 2001; Bradwell, 2004; Burki *et al.*, 2009). However, this crevassing may not have been basal because there is no clear evidence indicating a significant presence of crevasse-filled ridges, as exemplified at Borebukta (Ottesen and Dowdeswell, 2006).

The C-shaped disjointed ridges, exemplified in Figure 3.4, are likely to be the result of glacitectonic thrusting caused by stresses from glacier ice (Hambrey and Huddart, 1995; Benn and Evans, 2010). This occurs when ice freezes to the bed and removes basal debris

with it when it moves, pushing up sediment in a concentric arc shape, similar to the formation and appearance of hill-hole pairs, as described in Ottesen *et al.* (2005).

The transverse ridges described here are classified as small ones because they can still be traced to link with the smaller ridges found at the shallower sides of the inner fjord. The deeper central part has an apparent pattern of one large ridge followed by a sizeable retreat before another (Fig. 3.2A). In contrast, there are a number of small transverse ridges over the same distance of retreat on the shallower sides (Figs. 3.2, 3.3). This indicates a slower more regular retreat in the shallows with less frequent but more dramatic retreats at greater depths. This is not surprising given the links between iceberg calving, water depth and glacier retreat rates (Benn *et al.*, 2007).

A number of small, particularly arcuate transverse ridges are also closely associated with some of the low relief lineations (referred to above as hooked lineations) similar to those described by Solheim *et al.* (1990). Their formation possibly reflects the varying stresses at a palaeo-grounding line, producing C-shaped ridges. However, they could also be linked to crevasse-filled ridges or small-scale glacitectonic features.

3.2 Outer Lilliehöökfjorden

Outer Lilliehöökfjorden is about 12 km long and, in this thesis, refers to the area south of the large transverse ridge which is interpreted as a terminal moraine, to the mouth of the fjord (Figs. 3.1, 3.5A). The fjord mouth converges with the mouth of Möllerfjorden, marking the end of the tributary fjords and the start of central Krossfjorden. There are substantially fewer features evident on the sea-floor within this region and its appearance is predominantly smooth.

3.2 .1 Smooth outer fjord: sediment-filled basin

Description:

On the distal side of the largest transverse ridge (Fig. 3.2), which is interpreted as a terminal moraine, there is an approximately 11 km long, regular and relatively featureless sea-floor (Fig. 3.5A). This has an average gradient of 12° near the terminal moraine before gradually becoming an almost flat surface (with an average slope angle of 0.3°)

On the eastern side of Lilliehöökfjorden there is a decrease in depths around 3 km from the terminal moraine for an area approximately 600 m wide. Within this area, and to a lesser extent on the western side, there are a few small subtle features that are almost completely obscured (Fig. 3.5B). The features appear to be streamlined parallel to glacial ice-flow.

Interpretation:

The long, smooth outer part of Lilliehöökfjorden is interpreted to represent a sediment-filled basin. This was probably filled with sediment and debris from the rainout of suspended sediment carried in turbid meltwater plumes and from iceberg rafted debris (Dowdeswell, 1986; Powell and Molnia, 1989; Dowdeswell and Dowdeswell; 1989; Dowdeswell *et al.*, 1998). There appears to have been a considerable amount of sediment deposited which has covered, and therefore gives a smooth appearance to, most of outer Lilliehöökfjorden and any pre-existing features within it. This is particularly the case for the central and western parts of the fjord, which is likely to be linked to the Coriolis Effect on the circulation pattern of fjords in northwest Spitsbergen (Section 1.2.3; Syvitski, 1989).

The subtle features still just visible in Figure 3.5B appear to be glacially sculpted protruding bedrock which has been streamlined, possibly as drumlins or whalebacks; however, as they are partially covered by sediment it is hard to ascertain their exact form.

3.2.2 Drumlinised bedrock outcrop

Description:

The break in slope which acts as a sill is thought to be the result of bedrock and marks where the more distant glacier (Lilliehöökbreen) would have converged with ice-flow from Möllerfjorden under full-glacial conditions (Fig 3.5A). On the eastern side of the break in slope into central Krossfjorden there is a pronounced feature about 1 km wide and 2.5 km long (Fig. 3.5C, D). The proximal (northern) side is around 1.5 km long and gradually rises to145 m. It then increases rapidly in depth for 1 km, reaching 367 m (the deepest part of Krossfjorden). This feature itself comprises of a number of individual ridges, which vary in size, on its surface with a more blunt stoss side followed by a gently tapering tail in the down-fjord direction.

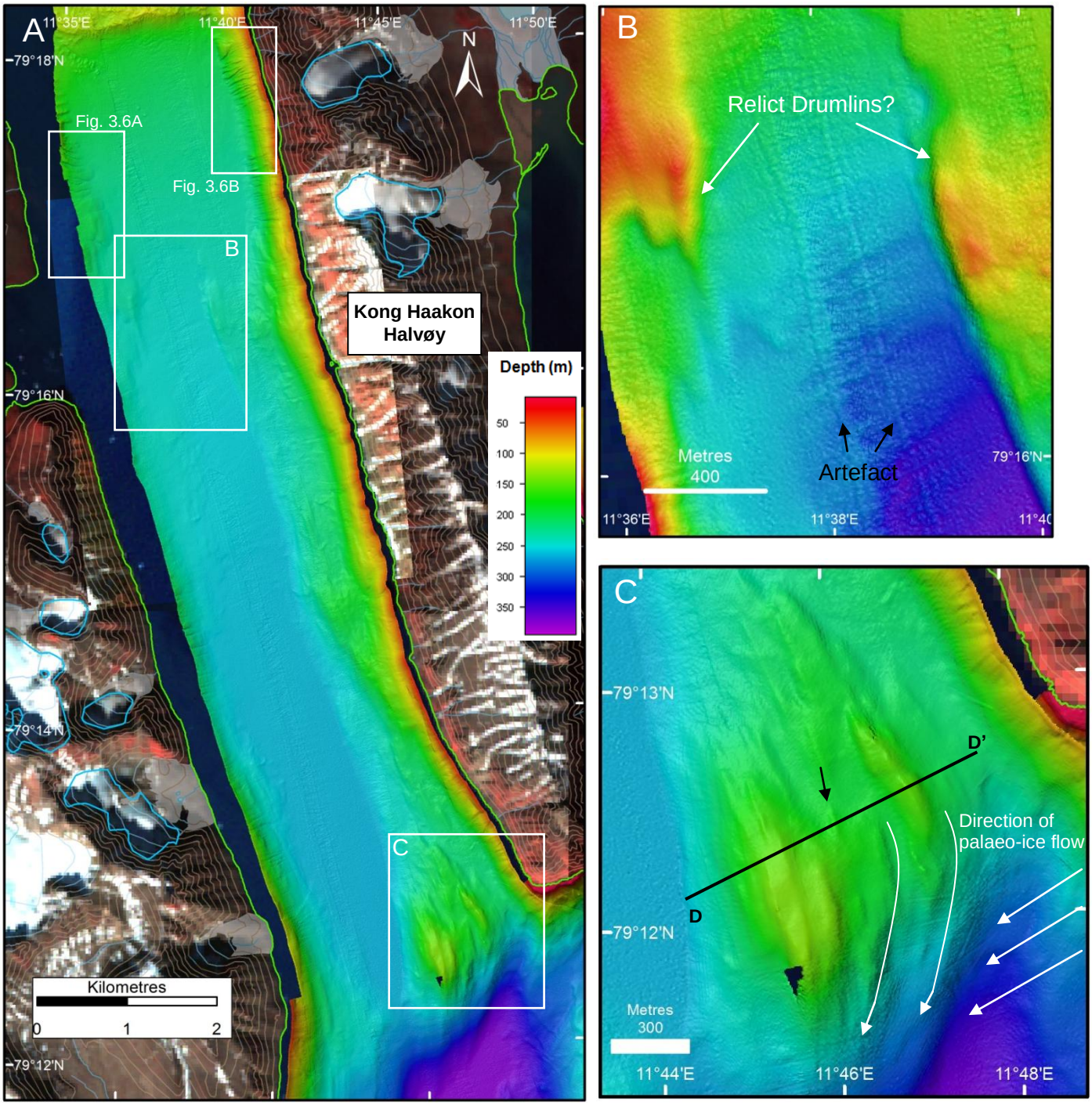

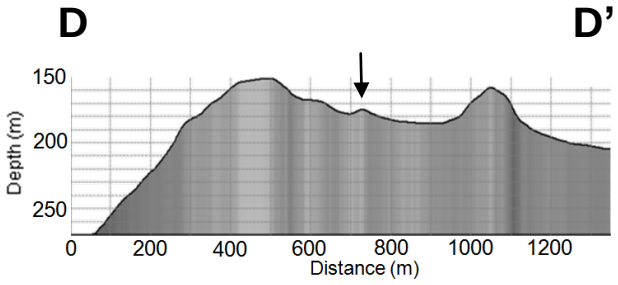

Figure 3.5: **A:** Seabed topography of outer Lilliehöökfjorden. The white boxes indicate the locations of Figure 3.6A and B. **B:** Possible relict drumlins. The area has been individually hypsometrically optimised with an artificial illumination of 45° and a sun elevation angle of 30°. Red indicates around 220 m and purple 255 m depth. The 'zipper-like' patterns are artefacts of the processing of swath imagery. **C:** Modified bedrock feature at the sill of outer Lilliehöökfjorden and the entrance to Krossfjorden. It has been influenced by palaeo-ice flow from Möllerfjorden on the lee slope – indicated by arrows. Despite being processed and interpolated there are still some artefacts on the slope at the 5 m horizontal resolution and a small gap in data on the modified bedrock feature. **D:** Cross-profile across the prominent bedrock outcrop. One of the drumlinised landforms imposed upon the bedrock is marked with a black arrow.

Interpretation:

This large feature at the end of Lilliehöökfjorden is interpreted as a large modified bedrock outcrop with a number of drumlinised features on its surface. The convergence with ice from Möllerfjorden is clearly evident because the tapering lee sides of the outcrop can be seen to curve towards the west. This curving form could be linked to the shear zone and stress gradient between two ice masses, as is thought to be the case for the lateral moraines of Kongsfjordrenna, on the shelf near Krossfjorden (Ottesen *et al.*, 2005; 2007).

3.2.3 Depositional and erosional features: debris lobes and gullies

Description:

Along the sides of outer Lilliehöökbreen there are a number of lobe-shaped deposits and gullies (Fig. 3.6). Due to the extent of the data cover being closer to the steep shore of Kong Haakon Halvøy (Fig. 3.5A) the majority of the gullies are found on the eastern side of the fjord. The most visible lobe-shaped deposits are all situated on the western side of the fjord. The lobe-shaped deposits are only just covered by the data, but they represent large mounds along the edge of the fjord (Fig. 3.6A). Widths of these features vary from 400 – 150 m with average slope angles of around 5 – 6°.

The gullies on the eastern side of the outer fjord are between 20 – 70 m wide and around 5 – 10 m deep with some bifurcating into separate channels (Fig. 3.6B). These gullies have a steep average slope of 19°. Closer to the head of the fjord, the gullies appear to look fresher compared with those nearer the fjord-mouth.

Interpretation:

The lobe-shaped deposits can be grouped together and interpreted as mass transport deposits. They appear to be the remnants of downslope debris flows originating from outside the swath coverage (Fig. 3.6A). All but one of the lobes appear smooth, thus it is interpreted that they are either very fine-grained sediments, old enough to have been covered by a layer of sediment or their appearance is a combination of both of these factors. Looking at the topographic map and Landsat images of the land area surrounding the fjord, a number of streams can be seen to enter the fjord close to many of these features (Fig. 3.6A). The lobe-shaped deposits on the western side of the fjord could be the result of slumping on glacio-

fluvial deltas (Dowdeswell and Vásquez, 2013) combined with the effects of undercutting and failure of the side-walls (Laberg *et al.*, 2007).

The gullies described are likely to have formed by down-slope mass wasting of material from the steep fjord walls (Fig. 3.6B, C) when snow melts in summer, depositing coarse grained material (such as rockfalls) whilst any fine-grained material is transported away (Mercier *et al.*, 2010). The gullies have a similar morphology to terrestrial gullies described in Kongsfjorden (Mercier *et al.*, 2010) and appear similar to, although at a much smaller-scale, to Type 1 gullies in Gales *et al.* (2013). The base of these gullies could also have been eroded from along-slope currents because they are still prominent near the base of the side-wall (Laberg *et al.*, 2007). The gullies closer to the mouth of Lilliehöökfjorden are thought to represent older inactive gullies that have been partially filled by sediment (Laberg *et al.*, 2007; Mercier *et al.*, 2010).

The difference between the two side-walls of the fjord is likely to be the result of differing physical properties of the sediments and slope characteristics (Laberg *et al.*, 2007; Gales *et al.*, 2013). The lobes represent areas with a very high delivery of fine-grained sediments, which possibly explains why they are absent on the eastern side because Kong Haakon Halvøy is only a narrow steep strip of land, rising over 600 m in 1 km, and is unlikely to act as a significant source area (Fig. 3.6B, C).

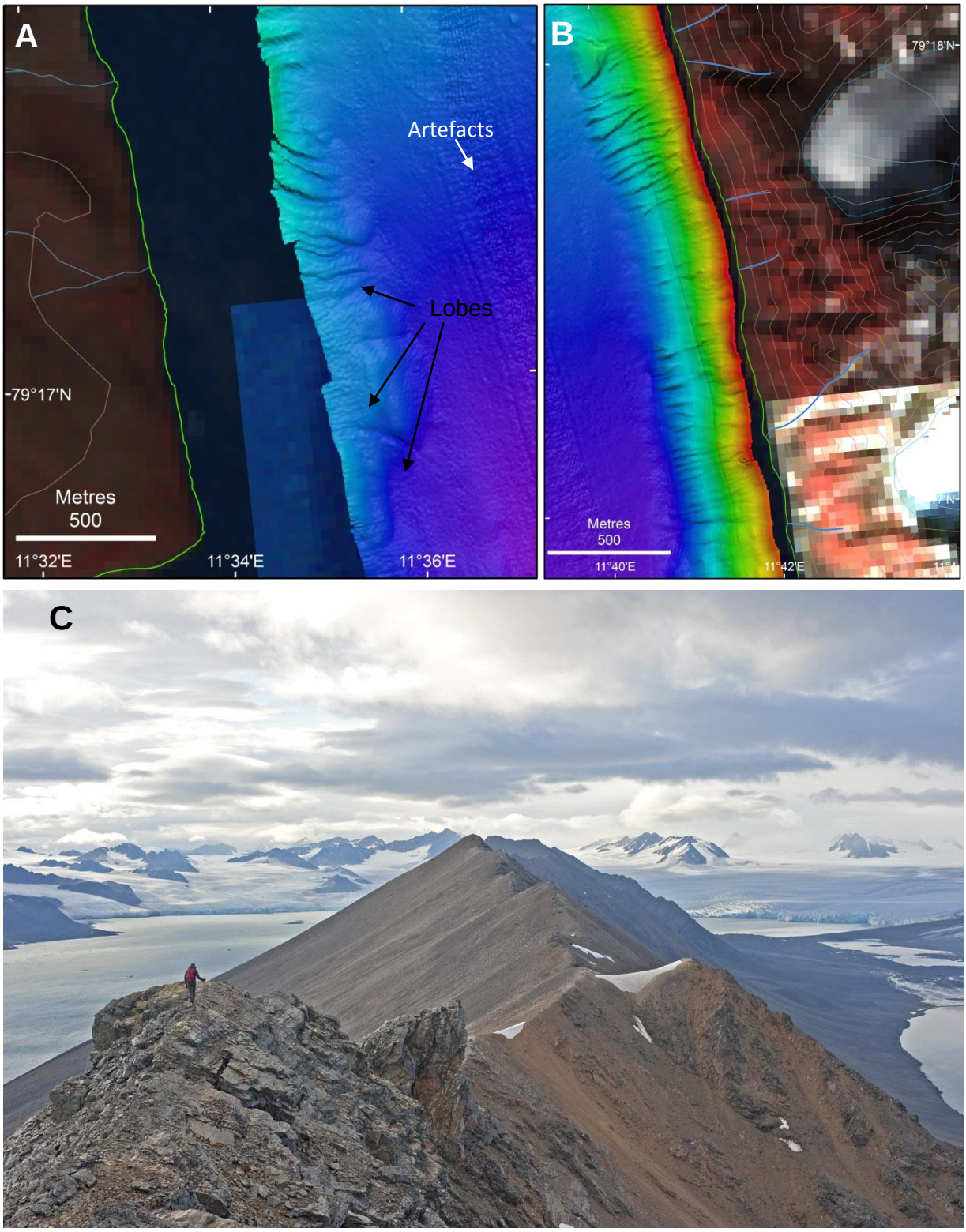

Figure 3.6: A: Lobe-shaped deposits at the base of the western side-wall of outer Lilliehöökfjorden. **B:** Gullies on the eastern side-wall. Both have been individually hypsometrically optimised and the artificial illumination on B has been changed to 45° (NE). Locations of **A** and **B** are indicated in Figure 3.5 and streams are indicated by blue lines. **C:** Photograph looking down Kong Haakon Halvøy (east side of Lilliehöökfjorden), exemplifying how the terrain is. The tidewater terminus of Lilliehöökbreen is visible in the background. Photo courtesy of Endre Før Gjermundsen.

3.3 Distribution and timing of submarine landforms in Lilliehöökfjorden

3.3.1 Geographical distribution

There are three main types of landforms within Lilliehöökfjorden; subglacial, ice-marginal, and post-glacial. Subglacial and ice-marginal landforms are both directly related to glacial activity. The geographical distribution of these features is shown in Figure 3.7 and it exemplifies the difference in distribution of the features between the outer and inner fjord.

The occurrence of identifiable submarine features decreases further away from the modern glacier front, with the outer fjord almost completely devoid of significant glacial features. The drumlinised bedrock at the mouth of the fjord and the possible relict features in outer Lilliehöökfjorden represent subglacial landforms from an extensive advance of ice across the whole fjord probably at the LGM and therefore also provide an indication that there was significant regional ice cover at that time. In the outer fjord the clearest, and therefore likely to be the most recent, post-glacial features appear closer to the present day glacier terminus with evidence of fresh features demonstrating mass-wasting decreasing the further towards the mouth of Lilliehöökfjorden (Fig. 3.7A). This would be expected because the most abundant sediment delivery to the fjord, and therefore the least stable debris would have been deposited when the glacier front was nearby (Forwick and Vorren, 2002; Mercier *et al.*, 2010; Dowdeswell and Vásquez, 2013).

The last significant glacial expansion and subsequent retreat of Lilliehöökbreen is identified within the data by a number of submarine landforms observed in the inner fjord (Fig. 3.7B). The ice-marginal features (the terminal and recessional moraines) indicate its maximum position, which delimits the inner fjord and subsequent retreat.

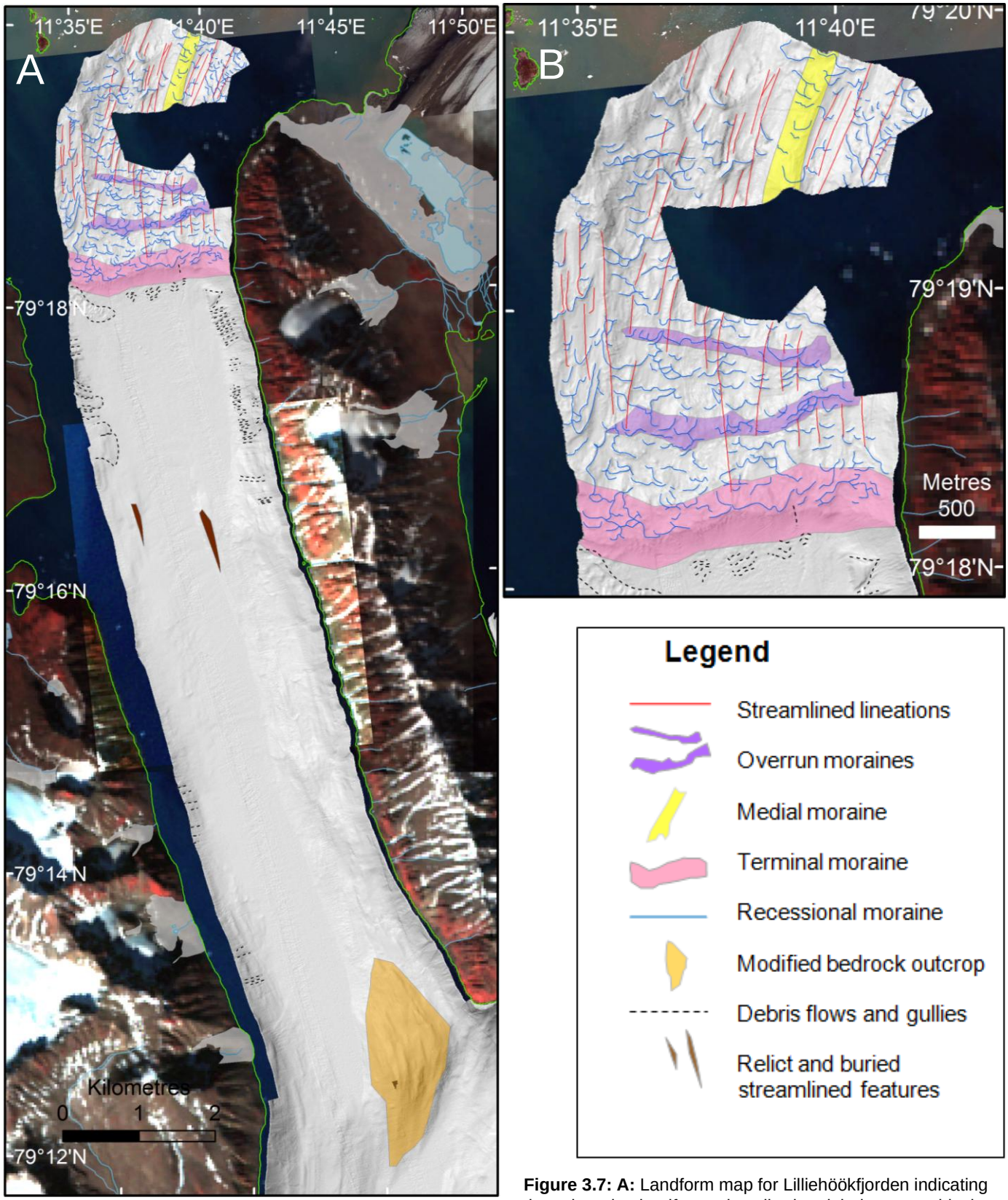

Figure 3.7: A: Landform map for Lilliehöökfjorden indicating the submarine landforms described and their geographical distribution. **B:** More detailed landform map for the area closest to the tidewater margin.

3.3.2 Timing

The cross-cutting relationships and superimposition of the features in Lilliehöökfjorden allows a reconstruction of the relative timing between the various suites of landforms to be made (Ottesen and Dowdeswell, 2006). These temporal and spatial variations are summarised in Figure 3.8. It can be seen that a significantly greater number of landforms are visible in the inner fjord than its outer part. This may be due to sedimentation over a longer period of time in the outer fjord.

The morphology of the overrun ridges (Figs. 3.2, 3.8B) is similar to those described in Ottesen and Dowdeswell (2006) for Borebukta. They appear to have been significantly modified as younger features have cross-cut them. This has resulted in their deformed and modified appearance. They are interpreted to have formed during previous advances of Lilliehöökbreen and therefore are the oldest landforms within the inner fjord (Fig. 3.8B). These ridges demonstrate that, before the terminal moraine formed, ice overran these palaeo-terminal moraines.

The glacial lineations (Fig. 3.3A) are one set of landforms which cross-cut the faint indications of the overrun moraines. This demonstrates that the lineations are of a younger age (Fig. 3.8C). The terminal moraine and medial moraine are then interpreted to have formed once the glacial advance ceased and the ice margins remained at a stable position for some time, perhaps decades, allowing the build-up of these mounds (Fig. 3.8D).

The recessional moraines leading back towards the present tidewater margin are another feature which cross-cuts the overrun moraines (Fig. 3.8E). They also modify some of the linear features and are superimposed on top of, and on the ice-proximal side of, the terminal moraine and the medial moraine. This therefore implies that they are the youngest set of landforms present.

The chronology and glacial events within the whole of the Krossfjorden system will be returned to in Chapter 7.

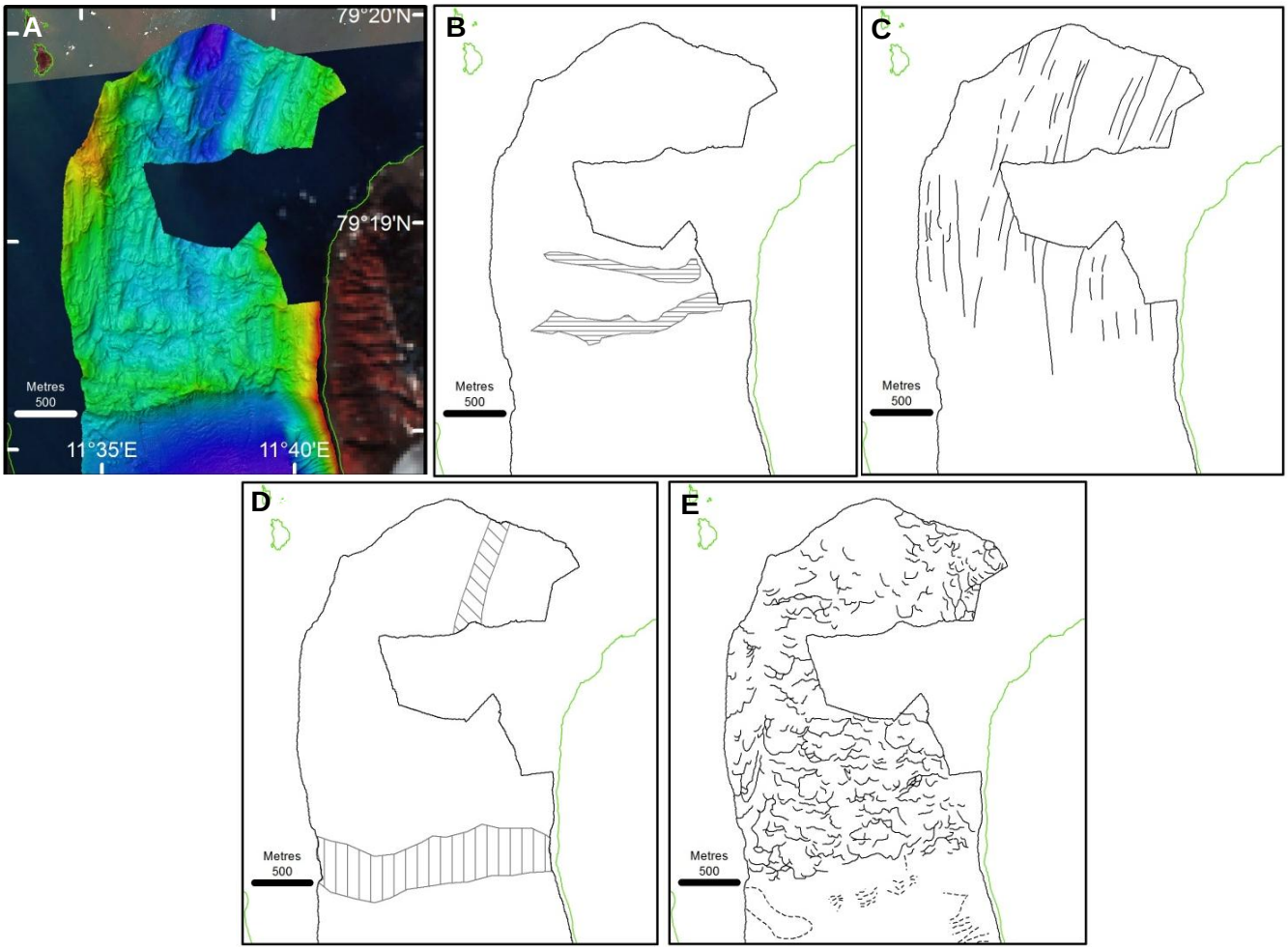

Figure 3.8: An analysis of spatial and temporal variations for individual submarine landforms, which make up the landsystem within inner Lilliehöökfjorden. The landform elements (3.8B – 3.8E) are shown in their stratigraphic order in which they are interpreted to have formed, inferred from their superposition and cross-cutting relationships, to distinguish the relative age of each set. **A:** Swath-bathymetric shaded relief image of inner Lilliehöökfjorden showing the full suite of landforms and the locations of the subsequent parts of the figure. **B:** Large overridden ridges. **C:** Streamlined bedforms. **D:** Terminal ridge and possible medial ridge. **E:** Small transverse ridges, with a number of varying morphologies, represent the youngest landforms.

4. Submarine landforms in the Möllerfjorden system

Möllerfjorden is a 9 km long inner fjord complex which leads into the bays of Tinayrebukta to the east, Mayerbukta in the northeast and Kollerfjorden at its northern limit. The areas within these bays, as well as the majority of Möllerfjorden, are all covered by the bathymetric survey data (Fig. 4.1). They all have a tidewater glacier at their head. The landforms within these fjords are individually described and interpreted below. However, there are a number of features in Möllerfjorden itself that are described and interpreted first (Fig. 4.2).

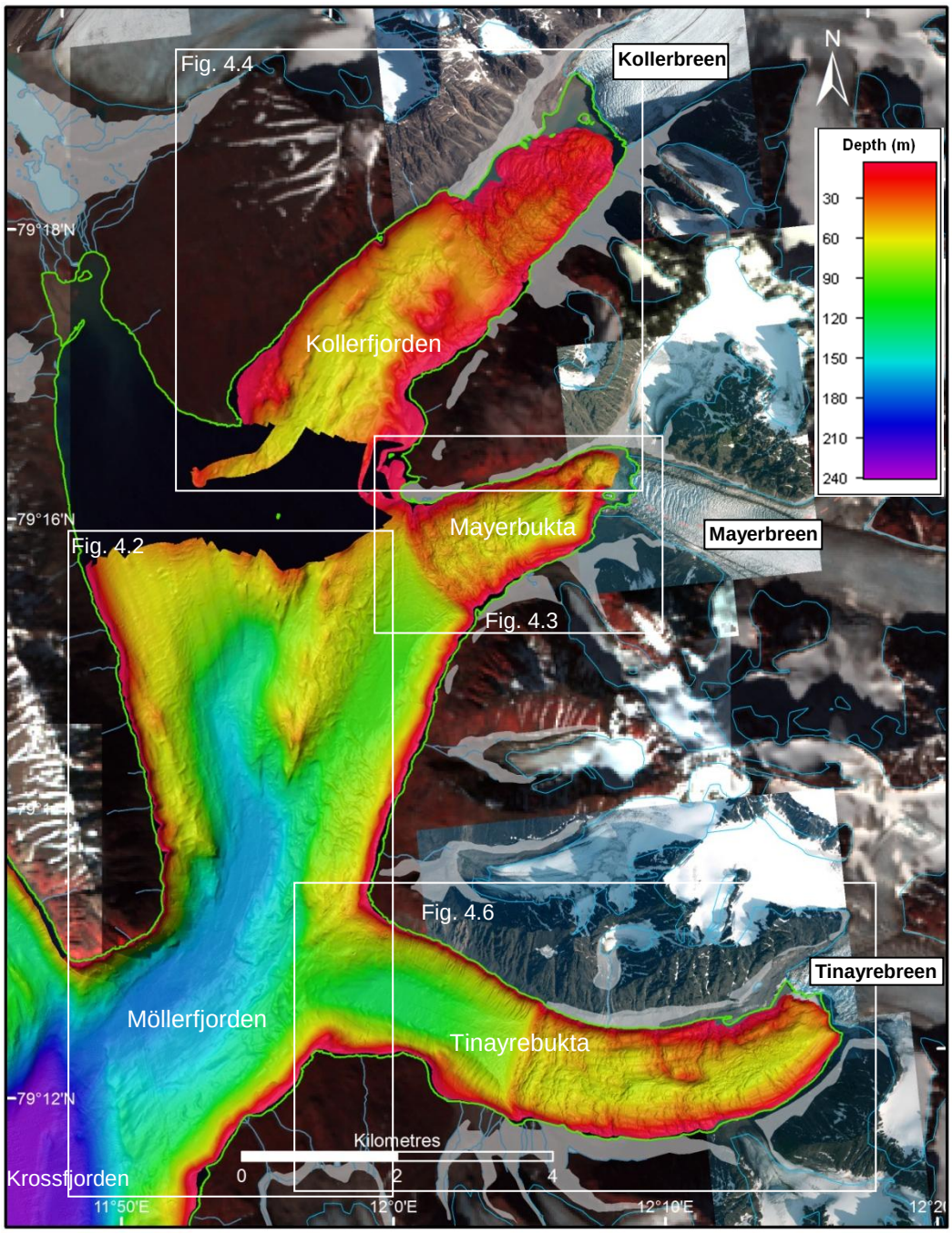

Figure 4.1: Overview map and bathymetric extent of Möllerfjorden, with the locations of Kollerfjorden, Mayerbukta and Tinayrebukta labelled. The white boxes indicate the positions of figures. The bathymetric data were gridded at 5 m grid cell sizes in this figure.

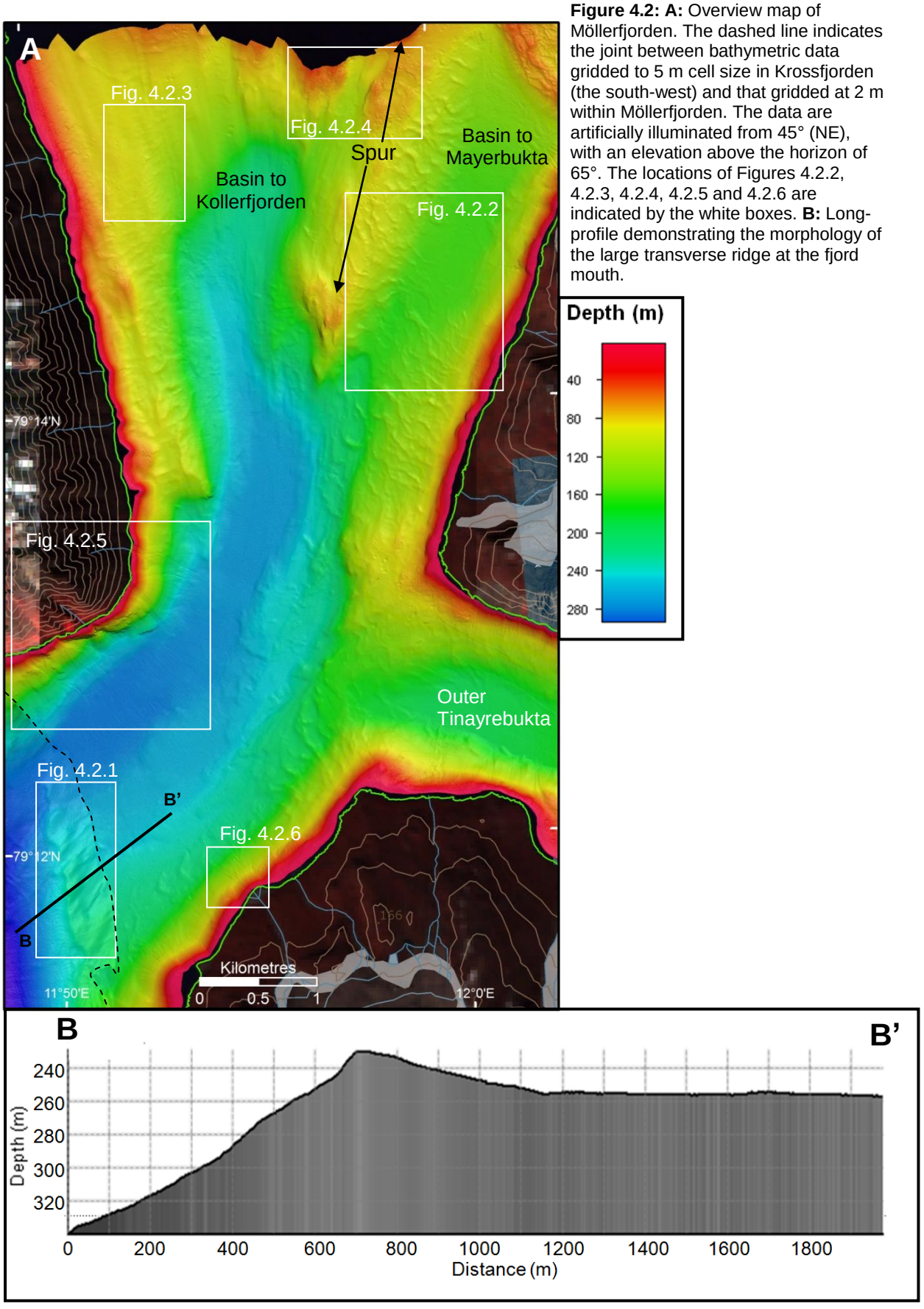

Figure 4.2: A: Overview map of Möllerfjorden. The dashed line indicates the joint between bathymetric data gridded to 5 m cell size in Krossfjorden (the south-west) and that gridded at 2 m within Möllerfjorden. The data are artificially illuminated from 45° (NE), with an elevation above the horizon of 65°. The locations of Figures 4.2.2, 4.2.3, 4.2.4, 4.2.5 and 4.2.6 are indicated by the white boxes. **B:** Long-profile demonstrating the morphology of the large transverse ridge at the fjord mouth.

4.1 Möllerfjorden

High resolution swath-bathymetric data from Möllerfjorden were gridded at 5 m (Fig. 4.2) and 2 m cell sizes and show the submarine landforms in great detail (Fig. 4.2).

4.1.1 Smooth outer: sediment-filled basin

Description:

Near the mouth of Möllerfjorden, depths reach down to 290 m. From there the outer fjord becomes smooth and gradually decreases in depth: decreasing by 10 m over a 2 km distance, with a low average slope of 0.2° (Fig. 4.2A). However, the lateral margins of Möllerfjorden are less smooth and features can be observed, including transverse ridges leading up to the mouth of Tinayrebukta, Mayerbukta and also Kollerfjorden. These features are individually described and interpreted below.

Interpretation:

The smooth appearance in the deep central parts of Möllerfjorden is very similar to that observed in outer Lilliehöökfjorden, and is interpreted to be the result of sediment and debris rainout from glacial meltwater plumes and IRD over a relatively long period of time (Powell and Molnia, 1989).

4.1.2 Large transverse ridge: palaeo-stillstand

Description:

At the mouth of Möllerfjorden there is a sill, above which a ridge is located (Figs. 4.2, 4.2.1). The ridge is around 20 m high, but reaches 30 m at its maximum. It is asymmetrical with an average slope of 4° on the ice-proximal (north-eastern) side and 13.1° on the ice-distal (south-western) side, before the distal side increases in depths into central Krossfjorden (Fig. 4.2B). There are also some linear features leading up to the ridge on the ice proximal side, which rise to heights of around 1 m.

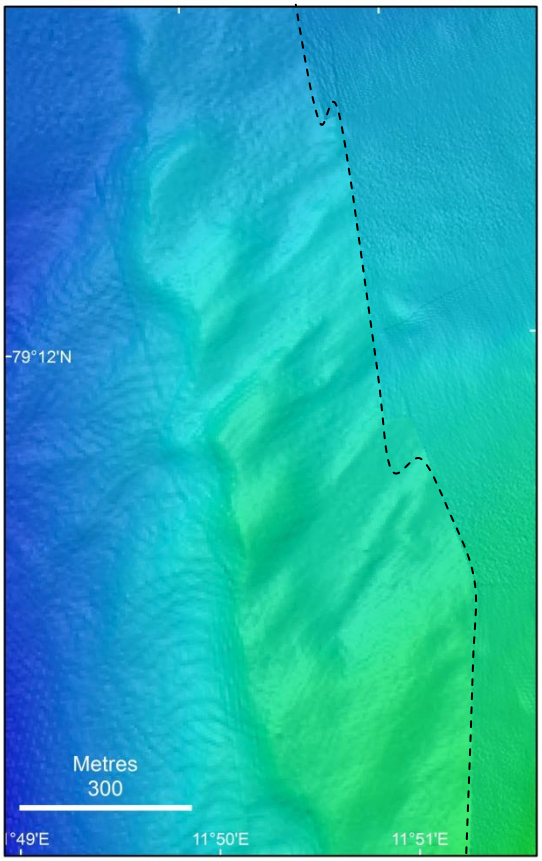

Figure 4.2.1: Detailed view of the transverse ridge at the sill of Möllerfjorden. Some linear features associated with it can also be seen. The dashed black line delineates the boundary between the two different cruises and therefore between the two different grid cell sizes – from 5 m on the left to 2 m on the right.

Interpretation:

This ridge may indicate that ice was once stable at the mouth of Möllerfjorden, which led to a terminal moraine forming at this natural pinning point (Fig. 4.2A), although the ridge's irregular morphology may suggest that it could instead be glacially sculpted bedrock outcrop, which can be traced to the fjord's side-wall (Fig. 4.2A). The preferred interpretation is a mixture: that it is a glacially sculpted bedrock feature with some glacigenic debris super-imposed upon it, indicating a brief stillstand. However, detailed acoustic data would be needed to confirm this deduction, but this feature is similar in appearance to two transverse ridges observed in Krossfjorden (Chapter 5).

4.1.3 Small transverse ridges: recessional moraines

Description:

Along the margins of the side-walls of Möllerfjorden there are number of small ridges which are orientated transverse to the fjord (Fig. 4.2). There is also a spur, around 4 km long within Möllerfjorden, which separates basins leading to Mayerbukta and Kollerfjorden (Fig. 4.2). Within these basins, and particularly within the one leading to Mayerbukta, whole sets of

transverse ridges are observed (Fig. 4.2.2). These ridges are between 2 – 5 m in heights and generally have an asymmetric plan-form near the mouth of Möllerfjorden. Closer to the mouths of Mayerbukta and Tinayrebukta, and therefore at shallower depths, these ridges increase in size reaching up to 12 m in height. In contrast, in the shallows towards Kollerfjorden, ridges rarely exceed heights of 3 m and are more regularly spaced (Fig. 4.2.3). Their appearance is, however, more obscured since they generally have heights of 0.5 m.

Interpretation:

The sets of small transverse ridges leading into the inner fjords and bays of Möllerfjorden are interpreted as recessional moraines from a previous extensive ice advance (Shipp *et al.*, 2002; Ottesen *et al.*, 2008b), likely to be linked to the LGM. Sets of ridges continue to be observed on the shallow margins, but they are absent in the deeper centre of the fjord (Fig. 4.2.2): this is interpreted to represent areas where the glacier became decoupled from the seabed in the centre of the basin and thus was no longer grounded. The glacier would therefore have had a floating central tongue; hence an unstable and faster flowing front (Benn *et al.*, 2007). It is also possible that features were obscured in the central basin due to sedimentation, as is believed to be the reason why Lilliehöökfjorden is so smooth.

The regularity of the ridges, particularly on the north-western margin of Möllerfjorden (Fig. 4.2.3), indicate a gradual retreat of ice (Ottesen and Dowdeswell, 2006; Ottesen *et al.*, 2007; Dowdeswell *et al.*, 2008). It seems possible that the smaller ridges formed annually during small winter re-advances of ice (Ottesen *et al.*, 2007; Dowdeswell *et al.*, 2008; Ottesen and Dowdeswell, 2009). However, the ridges seldom conform with the annual retreat distance of 20 m yr^{-1} put forward by Dowdeswell *et al.* (2008) for annual recessional moraines around Svalbard. But taking into account the links between calving, water depth and retreat rates of glaciers (Benn, *et al.*, 2007) and the observed instabilities of the ice front perhaps it is still a possibility for the area in Figure 4.2.3.

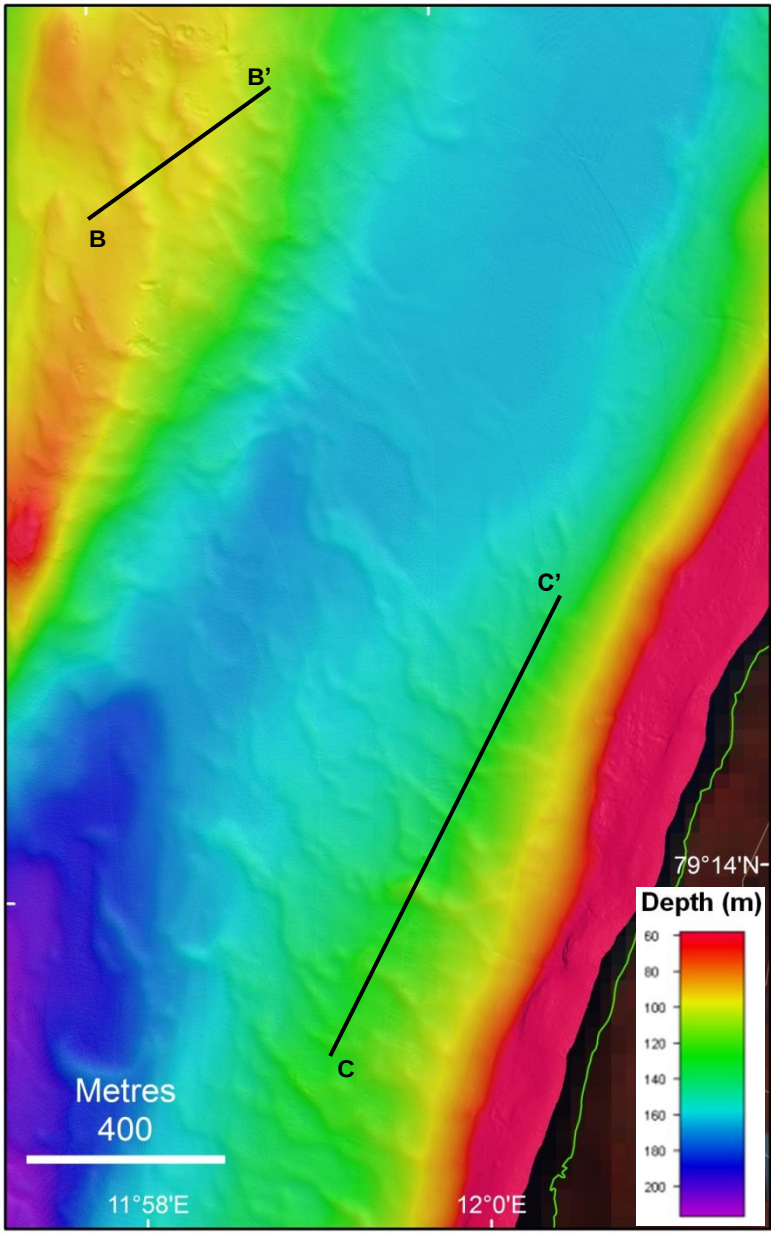

Figure 4.2.2: A: Basin leading to Mayerbukta, inner Möllerfjorden, demonstrating the small transverse ridges present and their chevron-like and discontinuous morphology in the deeper parts. Bathymetric data are gridded to 1m cell size. **B** and **C**: Fjord long-profiles showing the morphology of transverse ridges on the lateral margins of this basin.

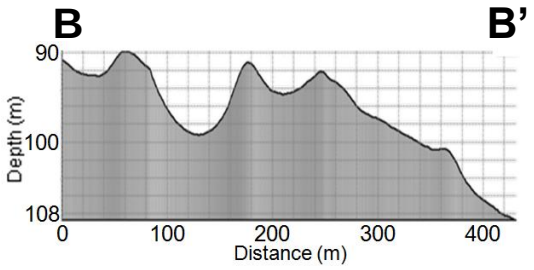

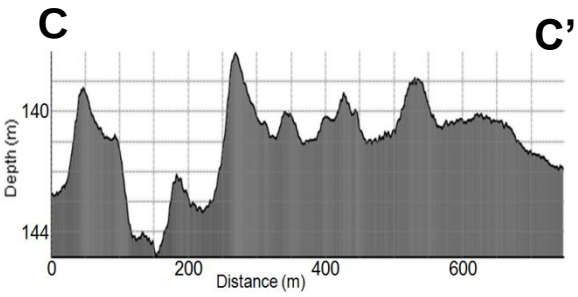

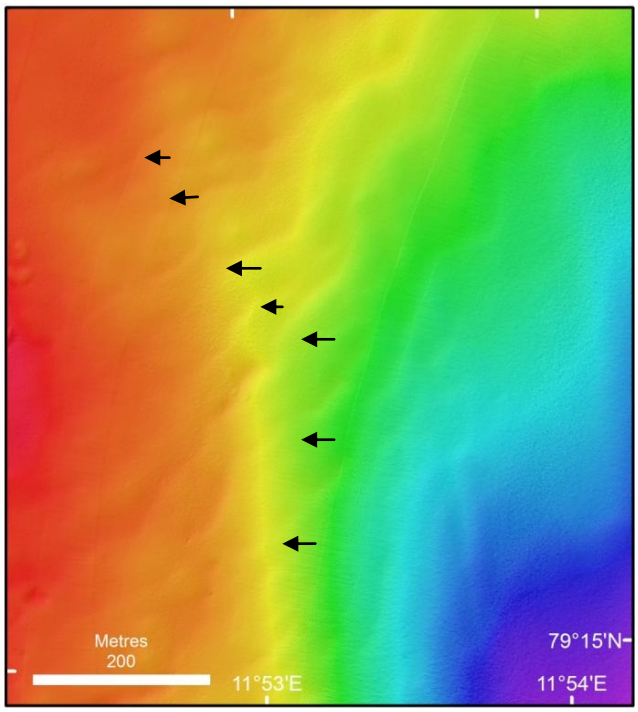

Figure 4.2.3: Small transverse ridges located on the western side of Möllerfjorden, leading towards Kollerfjorden, indicated in Figure 4.2. They are indicated with black arrows and their regular spacing can be recognised. Bathymetric data are gridded to 2m cell size, with an illumination of 135° and a sun angle of 80°.

4.1.4 Curvilinear incisions and seabed depressions: iceberg ploughmarks and pitting

Description:

There are some small curvilinear features incised into the seabed within Möllerfjorden (Fig. 4.2.4A), some of which have small berms on their sides. These incisions are observed in the shallows, between 50 – 85 m deep. They reach lengths of around 100m, but are often only 0.5 – 1m deep (Fig. 4.2.4B). These curvilinear features are often found in association with a more abundant feature, which appear as depressions on the seabed (Fig. 4.2.4A).

The depressions have varying dimensions, often with berms on their sides (Fig. 4.2.4C, D), and are found between depths of 13 m and 90 m. They are densely concentrated on topographic highs (Fig. 4.2.4A, C), which means that they cut across and merge with other depressions and curvilinear incisions. The size of individual depressions varies significantly, but is associated with the depth at which they are found. Larger depressions occur at greater depths on the slopes leading to topographic highs and are more isolated; they have the same morphology, but are around 5 m deep and 40 m wide.

Interpretation:

The small curvilinear incisions are interpreted to be iceberg ploughmarks (Fig. 4.2.4A, B), similar to those described around Svalbard in Dowdeswell *et al.* (2010), Mugford and Dowdeswell (2010), Hogan *et al.* (2010a), Batchelor *et al.* (2011) and Robinson and Dowdeswell (2011); however, they are of a significantly smaller scale. Ploughmarks occur when the keels of icebergs re-work sediments on the seabed as they drift under the influence of currents, winds and tides (Barnes and Lien, 1988).

The seabed depressions could originate from the formation of pockmarks or iceberg pitting. Pockmarks form due to migration of pore-water and the seepage gases (Hovland, 1983; Rogers *et al.*, 2006). Pockmarks have been documented to have formed due to thermogenic gas in Spitsbergen fjords over the last 11 ka BP (Forwick *et al.*, 2009) and appear relatively common. Pockmarks have a wide geographic range (Forwick *et al.*, 2009, Forwick and Vorren, 2009) with fields of pockmarks described on the outer shelf and slope near Kongsfjorden (Brünz *et al.*, 2012; Rajan *et al.* 2012). They are associated with sub-bottom geology, tectonic activity, past glacial activity and rate of sedimentation, which is linked to surging (Forwick *et al.*, 2009). Pockmarks tend not to have such pronounced berms on the

sides of the craters which are characteristic of iceberg pitting or ploughing; however, they have been described with berms (Forwick *et al.*, 2009). Detailed acoustic profiling would be required to confirm whether pockmarks are present.

Ploughmarks are generally found in areas that are also heavily incised with depressions on topographic highs and therefore it is logical that these landforms represent areas that have been heavily impacted by iceberg ploughing (Todd and Shaw, 2012). The reason for a pitted feature rather than a curvilinear ploughmark is that an iceberg may be bobbing or semi-grounded (Dowdeswell *et al.*, 1993) or it may be grounded but rotating as it melts (Barrie *et al.*, 1992; Syvitski *et al.*, 1996, 2001). Small depressions similar to this can be seen on beaches on Svalbard, before tide and wave-action remove their traces. These processes are probably part of the reason there is no evidence for these features at the shallowest depths of <5 m.

Iceberg pitting is the preferred interpretation here because of the close association with the curvilinear features interpreted as iceberg ploughmarks. Further evidence to support this interpretation is their general morphology because they appear very similar to described iceberg pitting (Todd and Shaw, 2012; Dowdeswell *et al.*, in press) and the majority of the incisions have a slight rise or berm on the sides of the pits (Fig. 4.2.4D) which is consistent with described morphologies of iceberg pits. Additionally, the shallower the depths in which the features are found, the smaller the individual depressions. This would be consistent with the idea that only smaller icebergs would reach the shallowest parts of topographic highs. There has been no trace of pockmarks in other areas, such as Smeerenburgfjorden, north-west Spitsbergen (Velle, 2012) and, most importantly, in the outer parts of Kongsfjorden-Krossfjorden (Howe *et al.*, 2003), so it is not unreasonable to suggest their absence in inner Krossfjorden. Icebergs and bergy bits are also well documented within the Kongsfjorden-Krossfjorden system (Dowdeswell and Dowdeswell, 1989; Dowdeswell and Forsberg, 1992). They are seasonally released as a pulse in May or June when shore-fast sea-ice breaks-up (Dowdeswell, 1989). The depths at which these features are found suggest icebergs and bergy bits within Möllerfjorden can have keel depths <65 m but can on occasion be larger (reaching 80 m), which is 40 m deeper than evidence of iceberg activity in Kongsfjorden today (Dowdeswell and Forsberg, 1992). This implies that icebergs in Krossfjorden are larger, or there has been an increase in their size in both fjords, or, most likely, that the high resolution bathymetric data used in this study has allowed these features to be observed.

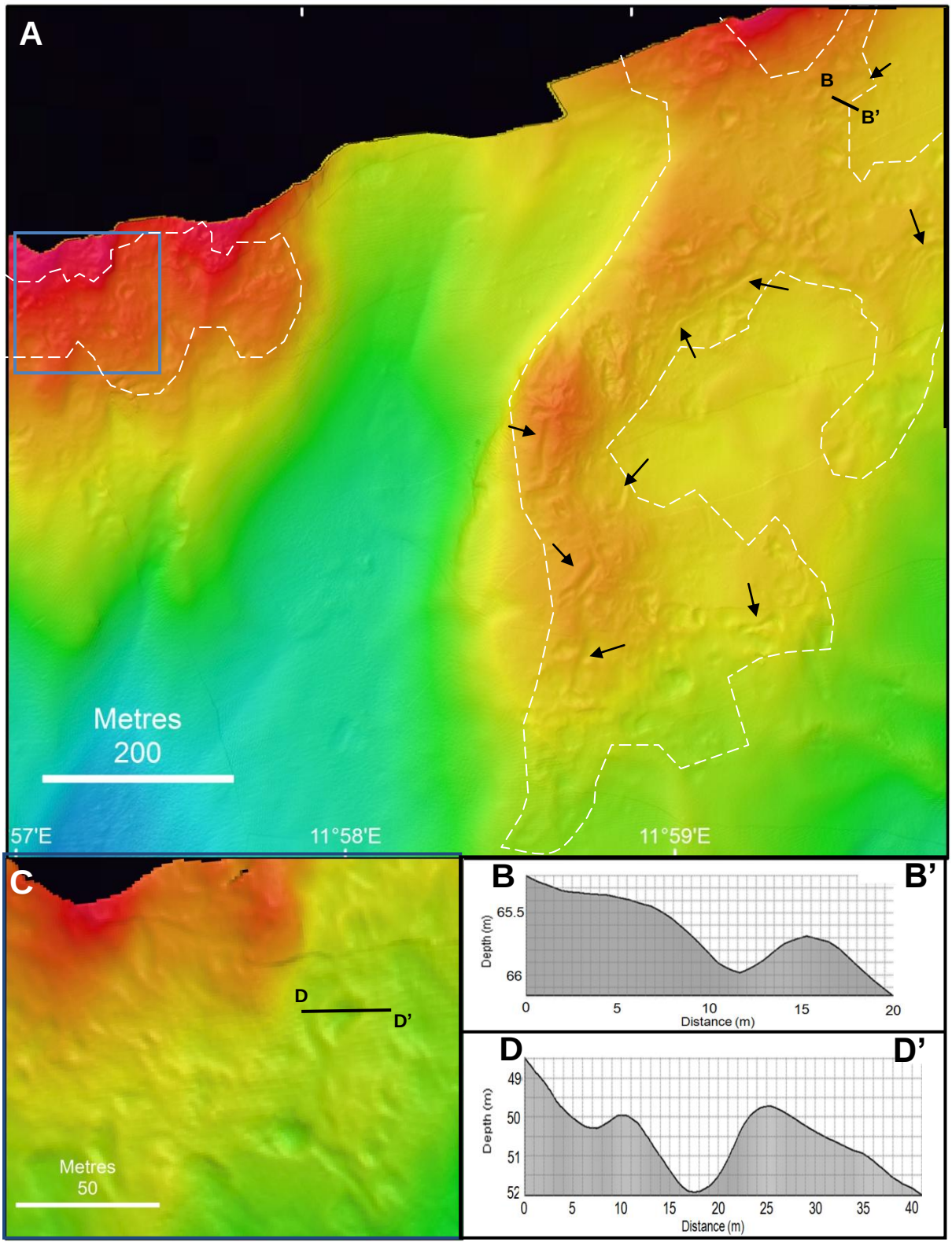

Figure 4.2.4: A: Topographic highs at the northern extent of data coverage in Möllerfjorden (location shown in Figure 4.2), which are covered in indentations and small curvilinear features. The white dashed lines denote the areas where these features are prevalent. Black arrows denote small curvilinear features. The blue box marks location of part C. **B:** Cross-profile demonstrating the morphology of the small curvilinear features. **C:** Detailed view of the indented seabed. **D:** Cross-profile demonstrating the morphology of one of these indentations. The bathymetric data in **A** and **C** are gridded at 1 m grid cell size and have an artificial illumination from 45° (NE), with an elevation above the horizon of 80°.

4.1.5 Erosional and depositional features: mass wasting and gullies

Description:

There are a number of erosional and depositional features visible along the side-walls of Möllerfjorden; Figure 4.2.5 demonstrates some clear examples of these leading down from the south side of Kong Haakon Halvøy, where it rises over 650 m a.s.l. in a 640 m distance. Two seasonal streams are indicated by the NPI topographic map and these lead into gullies. Most of the gullies have morphologies similar to Figure 4.2.5B, which clearly shows small V-shaped gullies bifurcating into larger gullies leading to the seabed of Möllerfjorden, with lengths around 500 m. At the base of some of these gullies are lobes, such as lobe 1 (L1), with a width of 200 m and height of 15 m (Fig. 4.2.5A). There is also a large, 20 m deep, V-shaped gully leading from one of the streams down the 47° slope until a sudden break in slope (Fig. 4.2.5A). At the base of this there is a steep lobe (L2) with dimensions of 175 m wide and a height of 20 m and an average slope of 33°. Additionally, on the westernmost extent of Figure 4.2.5A some blocky morphology can be observed.

At less steep localities, where glacio-fluvial rivers and meltwater streams run into Möllerfjorden, mounds of various morphologies can be observed (Fig. 4.2.6). The L1 mound in Figure 4.2.6 is around 210 m wide and 6 m high, with a slope angle of 28°. There are a number of V-shaped gullies, around 1 m deep and widths of around 20 m superimposed on them, leading down to the bottom of the fjord (Fig. 4.2.6).

Interpretation:

The gullies in Möllerfjorden are likely to have been formed by down-slope mass wasting of material from the steep fjord walls (Fig. 3.6C) when snow melts in summer, rapidly depositing coarse grained material. The particularly large V-shaped gully represents an erosive channel (Gales *et al.*, 2013) and so the large lobe at its base is not surprising (L1). The blocky morphology is interpreted to be the result of small landslides or rockfalls from the steep slopes. The clear pathways and lengths of the gullies indicate activity with a high velocity of sediment-laden water and so could be associated with turbidity-flow (Forwick and Vorren, 2012).

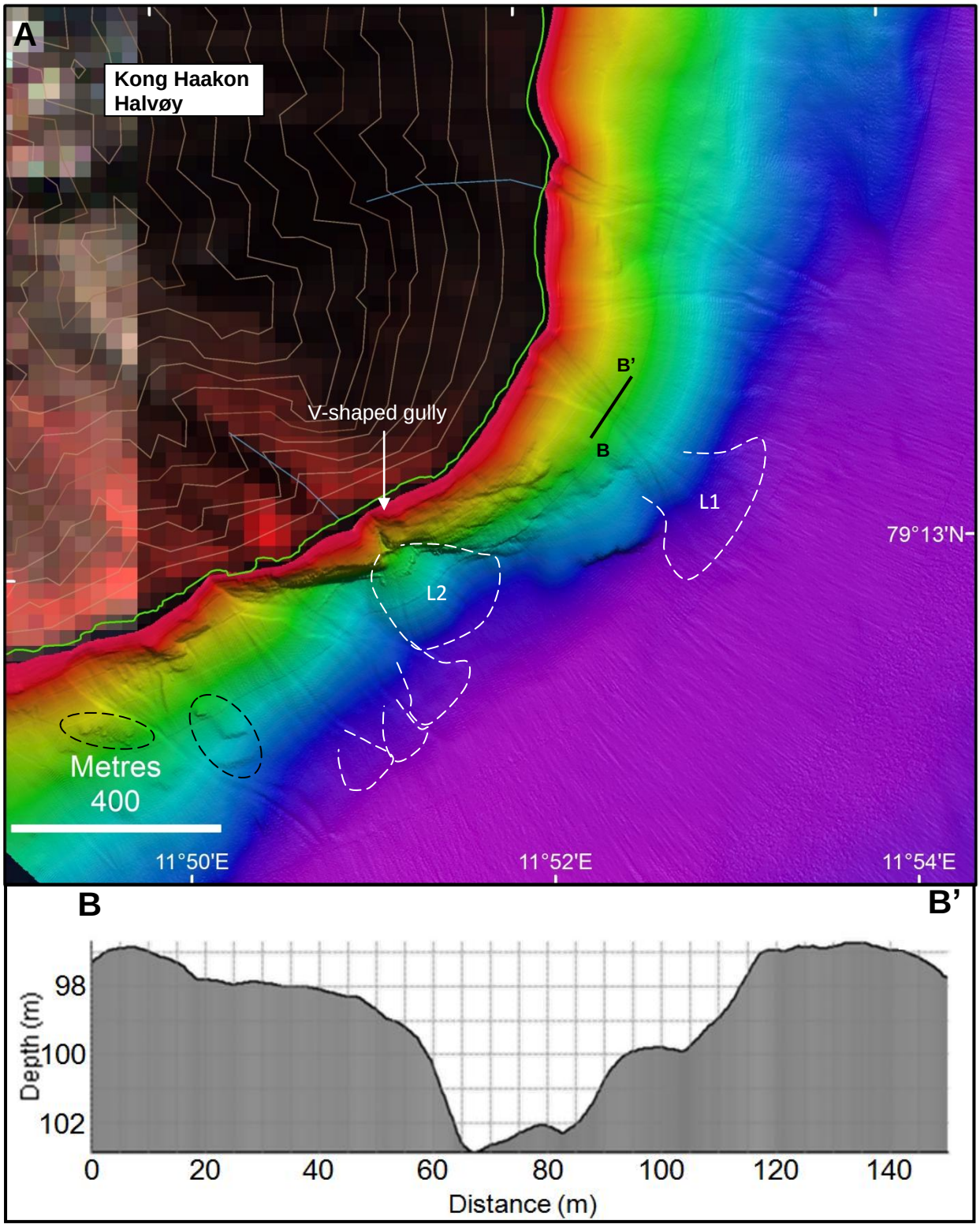

Figure 4.2.5: A: Bathymetry of Möllerfjorden by the coast of Kong Haakon Halvøy, which demonstrates the interplay between the steep slopes of the peninsula and the side-wall of the fjord. The deep V-shaped gully is labelled and L1 and L2 denote the two lobes found at the base of the side-wall. Lobes are highlighted with a dashed white line. Dashed black circles indicate areas with blocky morphology. Bathymetric data are gridded to 2m cell size. **B:** Cross-profile of one of the sets of gullies leading down the slope into the basin.

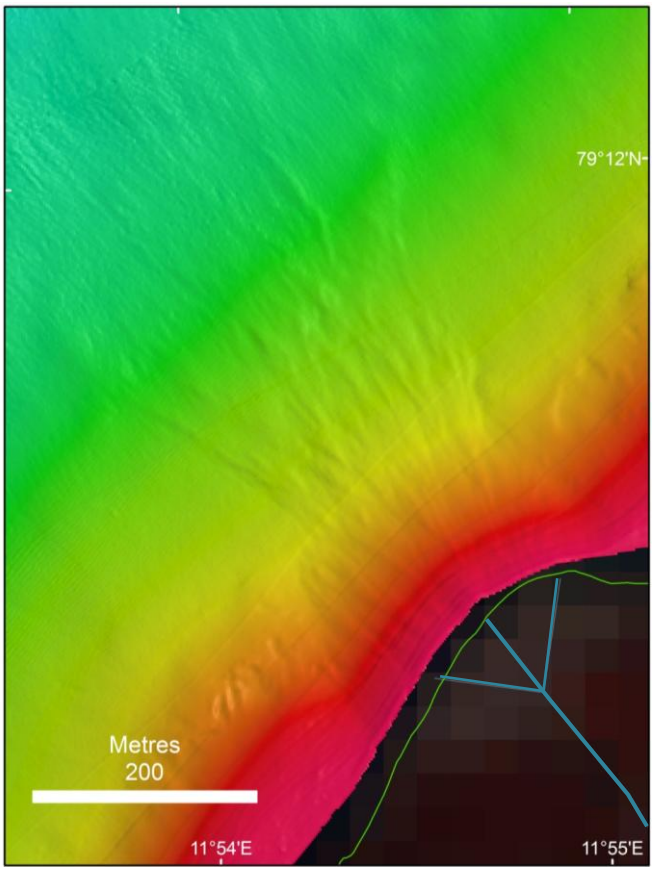

Figure 4.2.6: MTDs on the southern side-wall near the entrance to Möllerfjorden, related to inflow from the glacigenic stream. Location is shown in Figure 4.2. Bathymetric data are gridded to 2m cell size with an illumination of 315°.

The mounds observed near fluvial inflows are interpreted as fluvial MTDs. They are likely to consist of fine-grained acoustically stratified sediments, which progressively thin downslope (Forwick and Vorren, 2012). Figure 4.2.5 is associated with a small glacio-fluvial delta and is thus interpreted as a delta slope. The gullies super-imposed on them are likely to represent mass wastage and sediment reworking due to instabilities of the steep fine-grained slope with continued sediment input from the river (Zajączkowski andWłodarska-Kowalczuk, 2007). However, they could also represent chutes which act as pathways for erosive turbidity flows (Forwick and Vorren, 2012).

4.1.6: Sculpted mounds: modified bedrock

There are also smooth mounds present within the fjord, such as at the edge of the data extent towards Kollerfjorden (Fig. 4.2, 4.2.4) and at the end of the spur which separates the basins leading to Kollerfjorden and Mayerbukta (Fig. 4.2). These are interpreted as glacially sculpted bedrock. They have linear features leading down from the lee sides of the bedrock outcrops and this is interpreted as elongated sedimentary debris which was deposited subglacially in the cavity on the lee side of the outcrop, as described for crag-and-tails (Benn and Evans, 2010; Dowdeswell *et al.*, in press).

4.2 Mayerbukta

Mayerbukta is a bay about 3 km long (as of the 2009 margin of Mayerbreen) and 1.5 km wide, situated within Möllerfjorden (Fig. 4.3). At the head of the bay is the tidewater terminus of Mayerbreen, which is a glacier of about 38 km² and of possible surge-type (Table 1.1). The bathymetric data for Mayerbukta are extremely high resolution and have been gridded at 1 m cell sizes which provide great detail of the submarine landforms within the bay.

The entrance to the bay is marked by an increase in depths to around 50 m. In the central part of the bay depths increase again to 116 m before becoming much shallower near the modern tidewater margin, with depths less than 80 m.

4.2.1 Large transverse ridges: terminal moraines

Description:

At a distance of approximately 3 km from the 2009 tidewater margin of Mayerbreen there is a large, transverse ridge marking the shallow threshold to the bay. The ridge is slightly arcuate in shape, asymmetrical and covers the whole width of Mayerbukta. On the distal (western) side of this ridge, depth increases rapidly, from around 50 m to 145 m over a distance of 380 m, with an average slope angle of around 19° (Fig. 4.3). In contrast, the ice-proximal side depths only increase by an average of 5 m and the average slope angle is lower at 11°.

Like inner Lilliehöökfjorden, at the ice-distal (western) base of the first large transverse ridge there are a number of small, lobe-like features; however, they are only observed on the central and southern end of the ridge (Fig. 4.3.2). The heights of these lobes are around 3 - 5 m and their spacing varies between 20 - 40 m. There also appears to be a number of gullies located on the slope of the transverse ridge (Fig. 4.3.2).

There are also traces of three large transverse ridges (TR 2, 3 and 4) on the ice proximal side of the steep transverse ridge (Fig. 4.3B). They are slightly arcuate in their morphology and have an average spacing of 70 m. The innermost ridge is on average 219 m wide and 10 m high, with widths and heights of 150 m and 5 m respectively for the central ridge and 100 m and 10 m for the outermost ridge. Sets of smaller transverse ridges are superimposed upon all of the faint ridges; however, they are less disturbed on their lateral margins. On the southern coast of the bay the two outermost of these ridges appear to merge together.

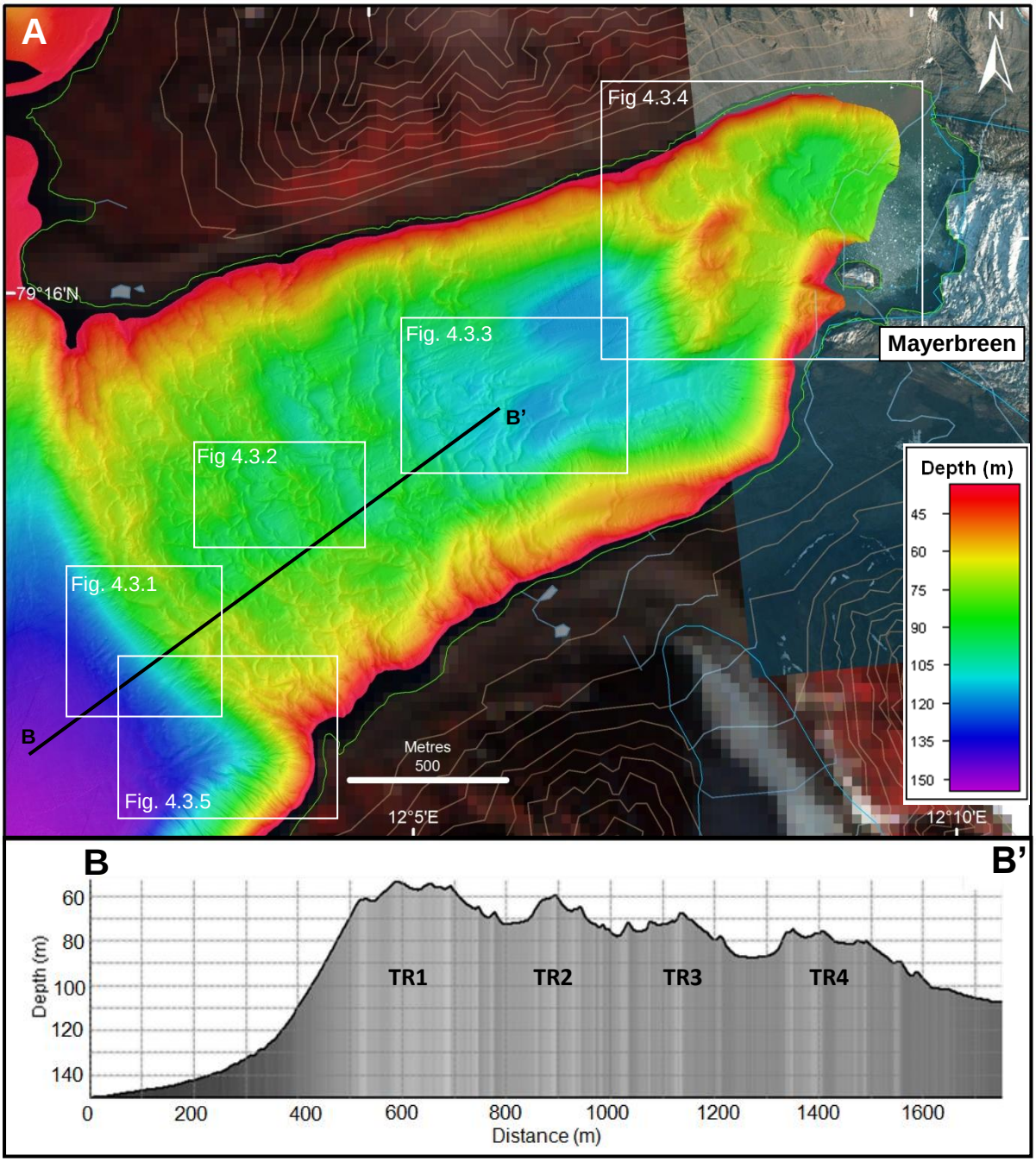

Figure 4.3: A: The seabed topography of Mayerbukta. The large arcuate ridge can be seen at the mouth of the bay, followed by the three large transverse ridges. White boxes indicate the locations of the following figures. Bathymetric data are girdded to 1 m cell size. **B:** Long profile across the four transverse ridges labelled. Additionally, a number of smaller peaks along the profile demonstrate the observed small transverse ridges. TR 1,2,3, and 4 denote these four ridges.

Interpretation:

The transverse ridge located at the entrance to the bay is interpreted as a terminal moraine marking the extent of the last significant advance of Mayerbreen. The asymmetry of the ridge

is typical for a terminal moraine with a significantly steeper ice-distal side than ice proximal (Bennett, 2001). The gullies and small lobe-like deposits are likely to represent mass wastage of the terminal moraine due to instabilities in the unconsolidated material and creep (Forwick and Vorren, 2012).

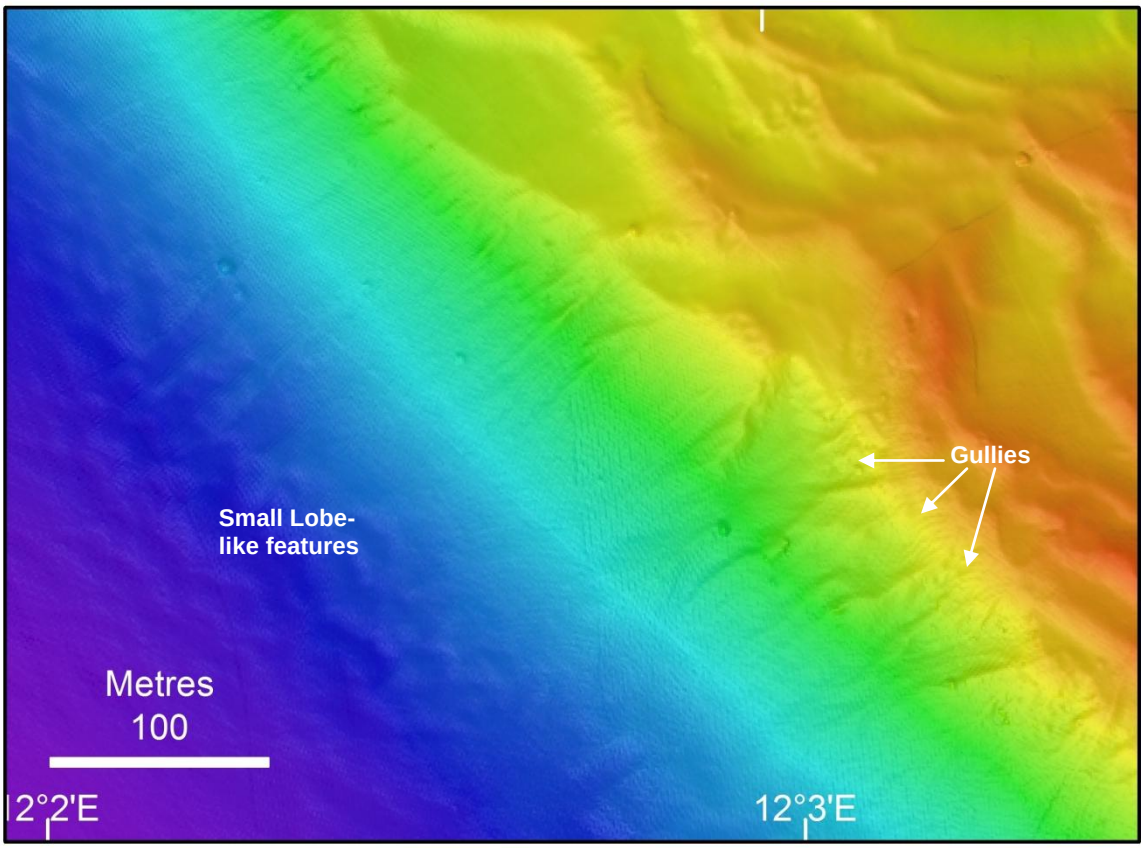

Figure 4.3.1: Large transverse ridge found at the mouth of Mayerbukta, the location of which is shown in Figure 4.3. At the base small lobe-like features are visible and on the ice-distal side of the slope gullies are also evident. Bathymetric data are gridded to 1m cell size, with an illumination of 225° and a sun angle of 80°.

The ridges within Mayerbukta (TR 2, 3 and 4) are interpreted to be examples of overrun moraines from previous glacier advances, similar to those described in Ottesen and Dowdeswell (2006). The last significant ice advance appears to have heavily modified their morphology, causing the ridge's subtle appearance, particularly in the central areas of the bay (Fig. 4.3). These ridges could represent past extent of the glacier post LGM deglaciation or could indicate surges from the glacier. Mayerbreen has not been observed to be a surge-type glacier (Liestøl, 1993; Sevestre *et al.*, unpublished), but there are indications that it could be (Błaszczyk *et al.*, 2009) and these ridges would support that.

4.2.2 Small transverse ridges: recessional moraines

Description:

Mayerbukta has a number of small transverse ridges perpendicular to palaeo-ice flow leading back towards the present glacier terminus (Figs. 4.3A, 4.3.2). The ridges vary in heights between 8 and 0.5 m, with the majority around 3 m, and are often asymmetrical with wider ice-distal sides. They are absent from the deepest part, in central Mayerbukta, but re-appear again on both sides as the fjord becomes shallower (Fig. 4.3A). Many of the ridges have 'C-shaped' morphologies and a significant number are also associated with small lineations (referred to as hooked lineations below). The ridges become more C-shaped, disjointed and have a closer association with lineations at greater depths (Figs. 4.3, 4.3.3).

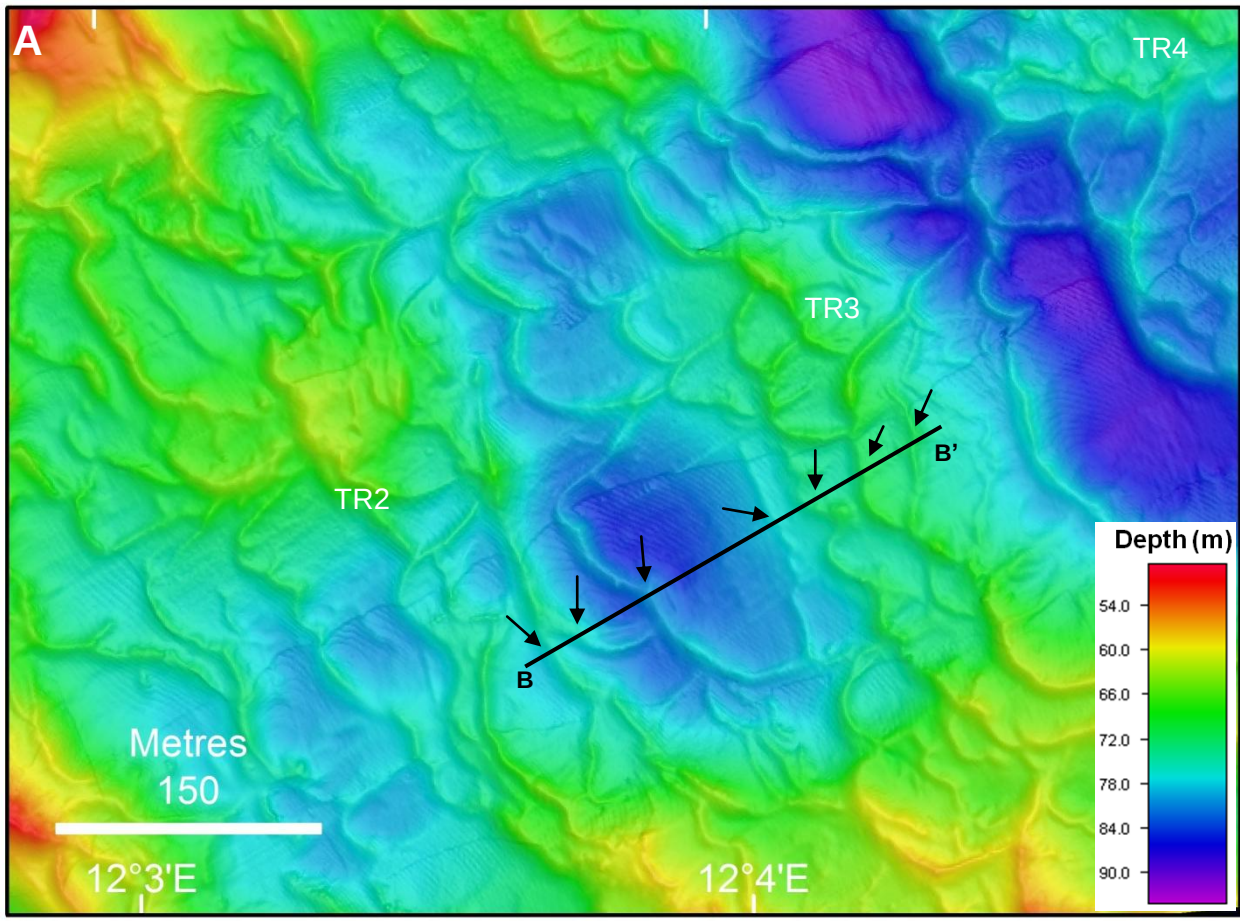

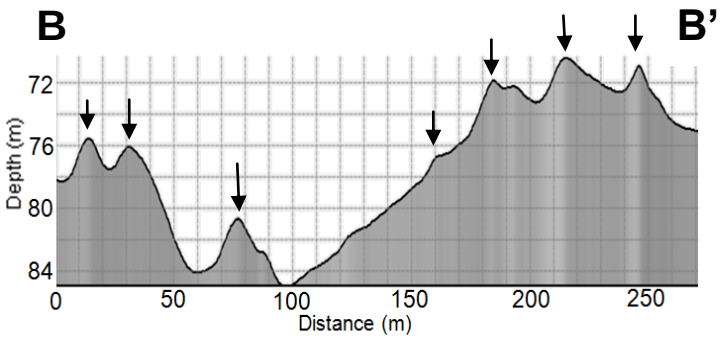

Figure 4.3.2: A: Small transverse ridges found within Mayerbukta, indicated by black arrows. They appear to be somewhat topographically controlled, with the majority found upon the large overridden transverse ridges (TR1 – 3), with fewer ridges between them. Location is shown in Figure 4.3. Bathymetric data are gridded to 1m cell size, with an illumination of 45° and a sun angle of 80°. **B:** Long profile demonstrating the morphology of small transverse ridges, indicated with black arrows within Mayerbukta.

Interpretation:

These small transverse ridges are interpreted as recessional moraines. They are likely to have formed annually at relatively shallow depths in Mayerbukta because the spacing between them is around 15 – 20 m, which conforms with the 20 m a^{-1} suggested by Dowdeswell *et al.* (2008).

The ridges observed in Mayerbukta have very complex concentric shapes but there are also more regular and longer transverse ridges present. This concentric shape has similarities to those described in Iceland and are believed to indicate a heavily crevassed retreating glacier (Sharp, 1984; Bennet, 2001; Bradwell, 2004; Burki *et al.*, 2009). There is also some evidence to suggest that crevassing was more basal within Mayerbukta with some symmetrical ridges leading away perpendicularly from the transverse ridge, which are interpreted as small, crevassed-squeezed ridges (Ottesen and Dowdeswell, 2006; Rea and Evans, 2011).

The small C-shaped disjointed ridges (Fig. 4.3.3), associated with the hooked lineations (referred to below), are interpreted to reflect the varying stresses at a palaeo-grounding line (Solheim *et al.*, 1990), or could be linked to crevasse-filled ridges or small-scale glacitectonic features.

4.2.3 Streamlined features: glacial lineations

Description:

Linear bedforms parallel to the fjord-axis (south-west trending) are present in Mayerbukta near the 2009 terminus, and in the central part of the bay (Fig. 4.3.3), in close association with transverse ridges. These are small subdued features with heights of 0.25 – 1 m and are between 5 – 15 m wide. They have a hooked or C-shaped transverse ridge at their distal-end and occasionally along their side (Fig. 4.3.3). The hooked lineations in Figure 4.3.3 are also associated with minor highs, possibly linked to buried bedrock features. Linear features are also observed on the lee side of large mounds (Fig. 4.3.4A, C) with amplitudes of 0.5 – 1 m.

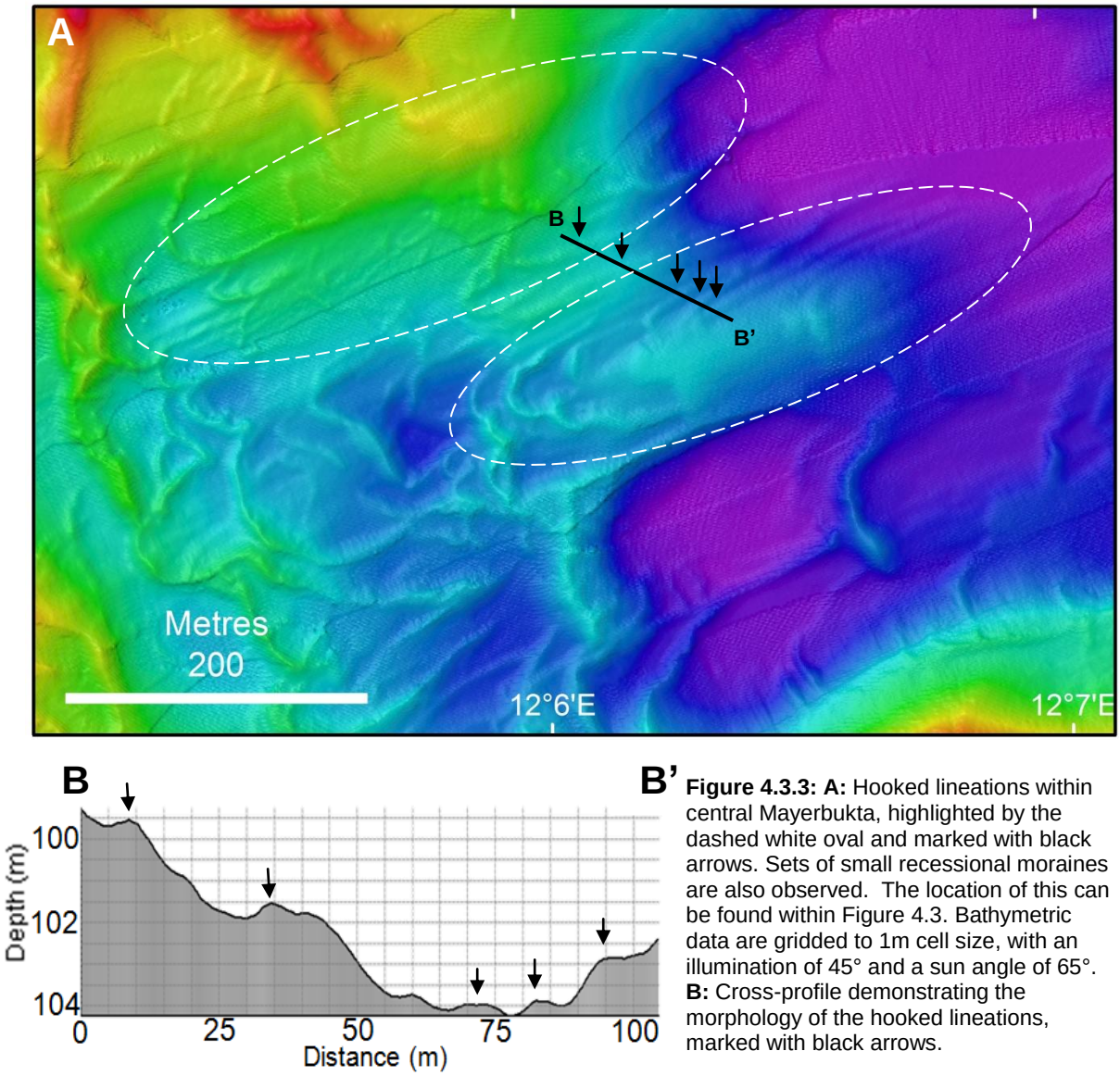

Figure 4.3.3: A: Hooked lineations within central Mayerbukta, highlighted by the dashed white oval and marked with black arrows. Sets of small recessional moraines are also observed. The location of this can be found within Figure 4.3. Bathymetric data are gridded to 1m cell size, with an illumination of 45° and a sun angle of 65°. **B:** Cross-profile demonstrating the morphology of the hooked lineations, marked with black arrows.

Interpretation:

The lineations with hooked distal-ends (Fig. 4.3.3) are streamlined bedforms closely associated with small transverse ridges. They are interpreted to be the result of either the way the small transverse ridges were formed, which suggests they are a type of crevasse-squeezed ridge, or are the result of minor glacitectonic thrusting of material. This minor thrusting could occur if the material is not frozen to the bed of the glacier but is still formed into faint lineations with a hooked or C-shaped end. They are similar to features described in Ottesen *et al.* (2005) and Hogan (2008) but constitute an even smaller-scale version to those observed in Lilliehöökfjorden. However, their association with marginally higher topography leads to the preferred interpretation of minor crevasse-squeezed ridges.

The lineations on the ice-distal side of two large mounds in Mayerbukta (Fig. 4.3.4C) are interpreted as elongated sedimentary 'tails' entrained subglacially in the cavity formed due to the presence of the large mounds (Benn and Evans, 2010; Dowdeswell *et al.*, in press).

4.2.4 Large mounds: glacially sculpted bedrock

Description:

There are two large mounds observed near the fjord terminus. The smaller mound is on the edge of the extent of bathymetric data and is approximately 100 m from the present glacier terminus (as of 2009). The second, larger mound is 600 m from the present margin and has a number of elongated lineations leading away from it on its lee side. The larger mound is around 500 m long and is almost symmetrical, with a steeper ice-proximal side than ice-distal side and average slopes of 18° and 16°, respectively. A number of transverse ridges are associated with both mounds.

Interpretation:

In the aerial photograph of Mayerbukta in 2009 the smaller mound is exposed as an island and appears to be a bedrock outcrop. The second larger mound is also interpreted as a glacially sculpted bedrock outcrop with elongated sedimentary 'tails' on its lee side, similar to those described in Möllerfjorden.

The large mound is interpreted as a large modified bedrock outcrop, which has proved more resistant than the surrounding geology during previous glacial advances, similar to descriptions of terrestrial whalebacks (Benn and Evans, 2010). The streamlined features found on the lee side of this outcrop are possibly sedimentary 'tails', which have been deposited by a glacier in the pressure shadow of the bedrock 'crag' (Benn and Evans, 2010). However, perhaps a more likely explanation is that they are sedimentary flutings, which were formed by an alteration in shape when the saturated sediment is squeezed into lee-side cavities of a basal obstruction such as a bedrock outcrop (Benn and Evans, 2010).

Both mounds have had a clear effect on the retreat of Mayerbreen, with smaller spacing and larger sizes of the adjacent transverse ridges, and show that ice-retreat was topographically controlled (Fig. 4.3.4).

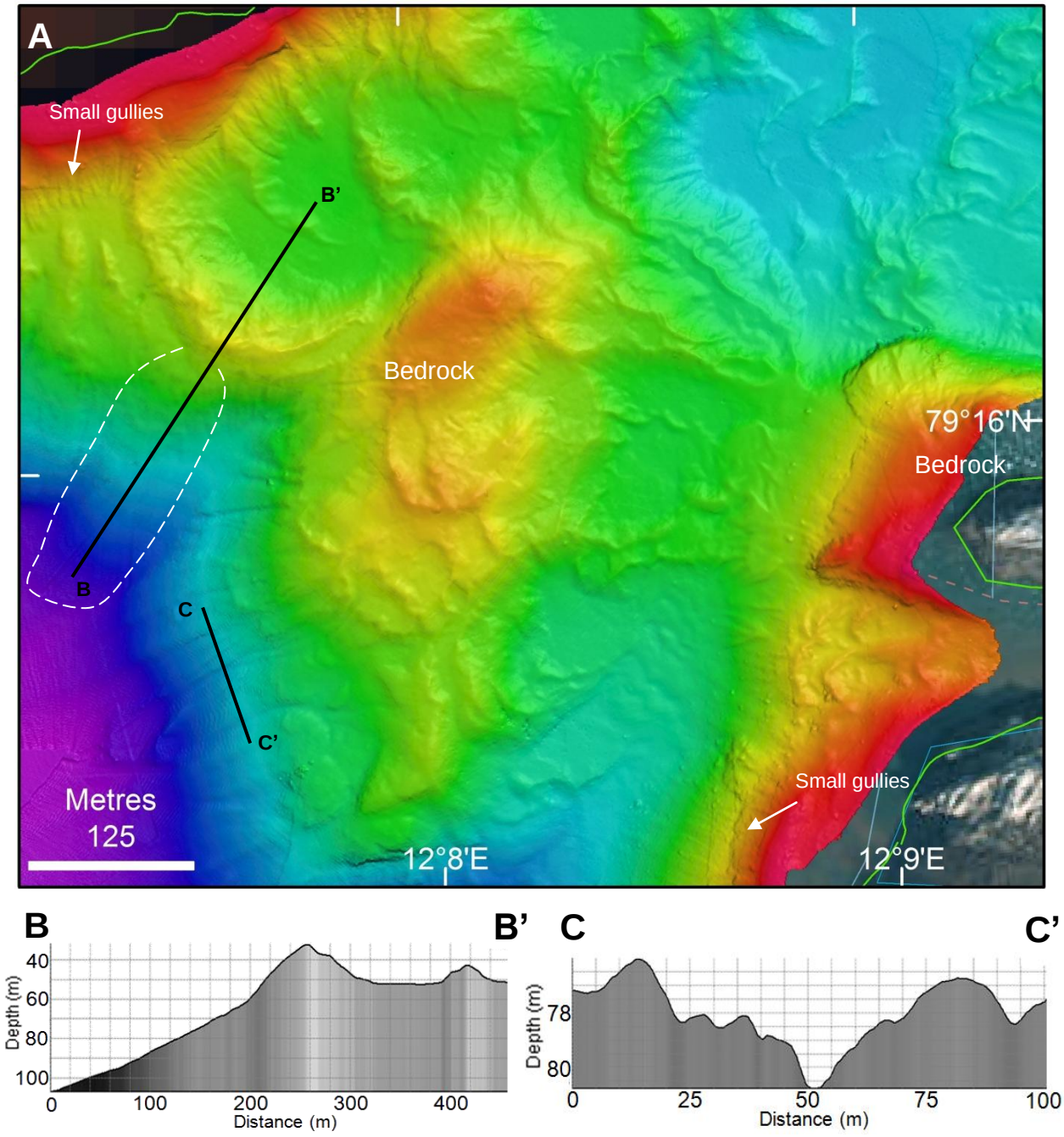

Figure 4.3.4: A: Inner Mayerbukta, proximal to the glacier terminus, the location of which is shown in Figure 4.3. The two large mounds interpreted as modified bedrock are visible, with the eastern mound protruding above the surface as an island. Their influence on the distribution of transverse ridges is evident. The white dashed line indicates the location of the lobe-shaped feature. Small gullies are also labelled. Bathymetric data are gridded at 1m grid cell size, with an illumination of 45° and a sun angle of 65° **B:** Long profile across lobe shape feature. **C:** Cross profile of the lineations on the lee side of the large mound.

4.2.5 Medium sized transverse ridge and lobe: large recessional moraine

Description:

There is a medium-sized transverse ridge located on top of the shallower part of inner Mayerbukta. The ridge has dimensions of around 15 m high and 270 m long. Its location on the topographic high in the inner fjord, interpreted to be bedrock, assists its asymmetrical shape (Fig. 4.3.4B).

Interpretation:

The ridge is interpreted as a medium-sized transverse ridge, which indicates a relatively long stillstand of ice at this position compared to the other smaller transverse ridges. The location of this ridge is clearly controlled by the mound interpreted as a bedrock outcrop, which is on its southern margin and the side-wall of the fjord, on its northern margin. It was this topographic control which probably allowed the longer stillstand at this position.

4.2.6 Lobe associated with transverse ridge: ice-contact fan

Description:

At the base of the medium-sized transverse ridge described above, a lobe-like feature is observed leading down-slope into the over-deepened basin in central Mayerbukta (Fig. 4.3.4A, C). The lobe has dimensions of 215 m long, 50 m wide and a height of 3 m near its base, with an average slope of 16°.

Interpretation:

This lobe-like feature could possibly represent an ice-contact fan. Ice-contact fans are formed from the discharge of a turbulent jet, which originated from englacial and subglacial meltwater streams, at the grounding line (Powell, 1990; Lajeunesse and Allard, 2002). The fan represents a depocentre of accumulated sediment. The fan is located at the base of a medium-sized transverse ridge. This indicates the ice-front was at a stable point long enough to produce this large ice-contact fan without deforming it (Powell, 1990). The unconsolidated fan complex has spread down-slope and so its morphology does not provide an indication of discharge rate. However, it could also be interpreted as an MTD linked to the small gullies on the side-wall of the fjord and to instabilities on the slope itself (Forwick and Vorren, 2012).

Acoustic data are required to confirm whether it is an ice-contact fan because it would show as acoustically opaque layers.

4.2.7 Erosional and depositional features: mass wasting and gullies

There are a number of gullies along the side-walls of Mayerbukta (Fig. 4.3.4) and along its terminal moraine and the southern side-wall at its mouth (Fig. 4.3.5). They are quite subtle U-shaped features on the fjord side-walls, with depths of around 0.5 m, widths of 10 m and lengths of 300 m. This morphology implies less erosive inflow of sediment compared to the more V-shaped gullies observed elsewhere in the study fjords (Gales *et al.*, 2013). From aerial photographs it appears that the gullies are associated with inflow from meltwater streams. However, at the mouth of the bay the gullies are more apparent and are around 6 m deep and 15 – 20 m wide. They are also more V-shaped and bifurcate together near their heads. They are similar to the gullies described near the terminal moraine, on the side-wall of Lilliehöökfjorden, thus imply erosive input from steep side-walls.

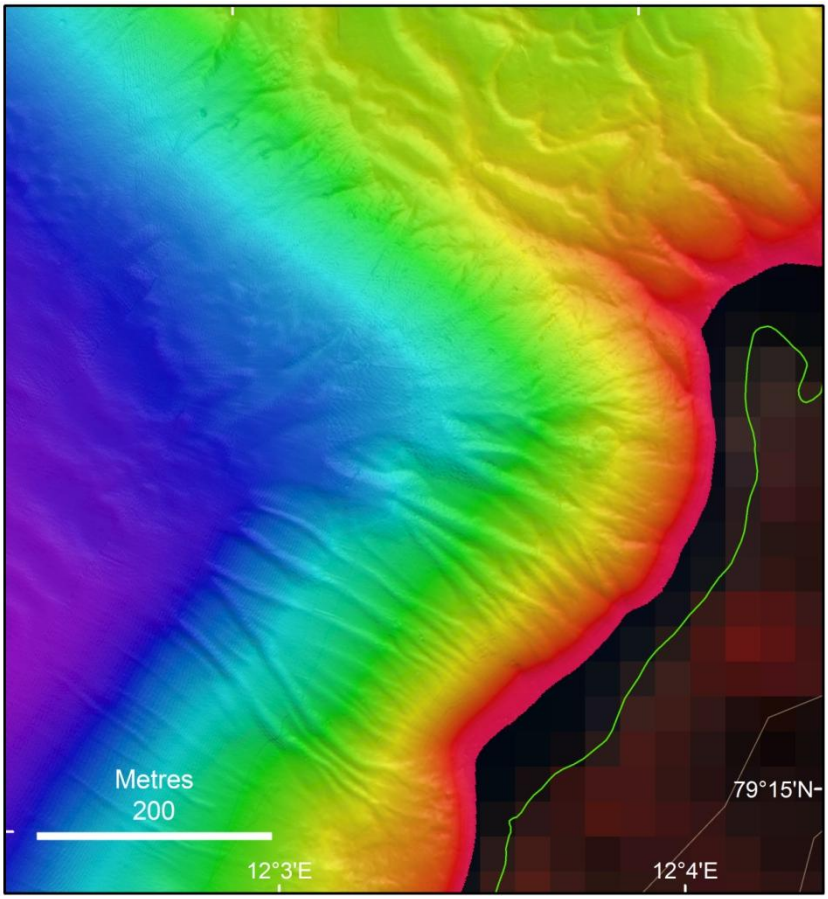

Figure 4.3.5: Gullies on the side-wall near the entrance to Mayerbukta. Location is shown in Figure 4.3. Bathymetric data are gridded to 1m cell size, with an illumination of 225° and a sun angle of 75°.

4.3 Kollerfjorden

Kollerfjorden is a fjord 5.5 km long and 1.5 km wide at the north-western extent of Möllerfjorden. At the head of the fjord is the 1 km wide terminus of Kollerbreen, which has a 28 km^2 basin (Table 1.1). The bathymetric data for Kollerfjorden are of extremely high resolution and have been gridded at 1 m cell size. Features that vary from those observed in Mayerbukta (Section 4.2) are individually described and interpreted.

The survey area runs from the mouth of the fjord to within 100 m of the modern ice front of Kollerbreen (as of summer 2011; Fig. 4.4). Kollerfjorden can clearly be separated into outer and inner fjords and features within these are discussed separately (Fig. 4.4).

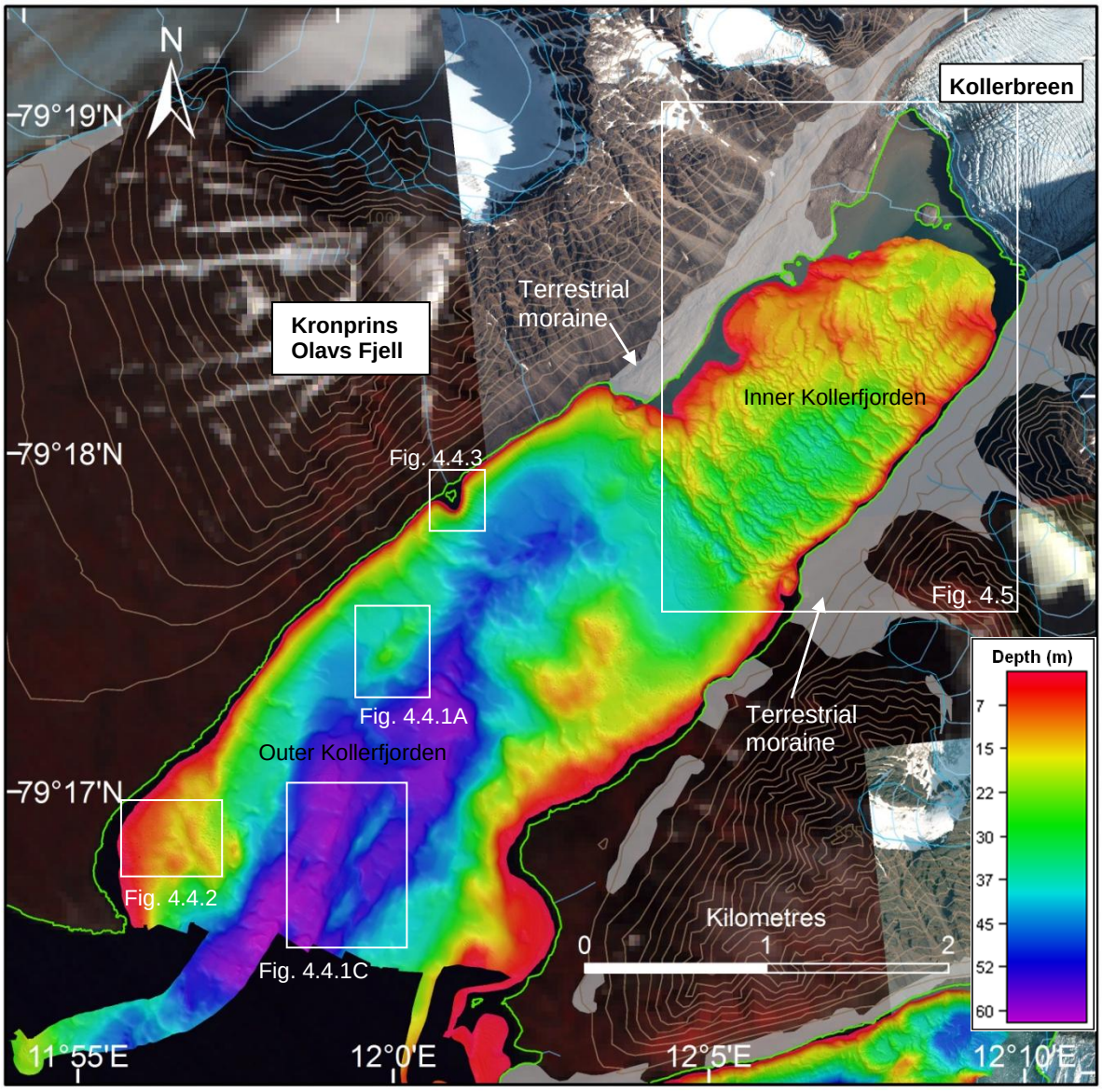

Figure 4.4: Overview map of Kollerfjorden, showing locations of figures within outer Kollerfjorden and the location of the inner Kollerfjorden figure (4.5). Bathymetric data are gridded to 1m cell size, with an illumination of 315° and a sun angle of 65°.

4.3.1 Outer Kollerfjorden

Outer Kollerfjorden refers to the area 3 km from the mouth of the fjord, where it merges with Möllerfjorden, to where the fjord narrows and continuous moraines can be observed on the shoreline (Fig.4.4).

A number of large elongated mounds are observed in outer Kollerfjorden, some of which have more rounded and others have more elongated linear morphologies (Figs. 4.4, 4.4.1).

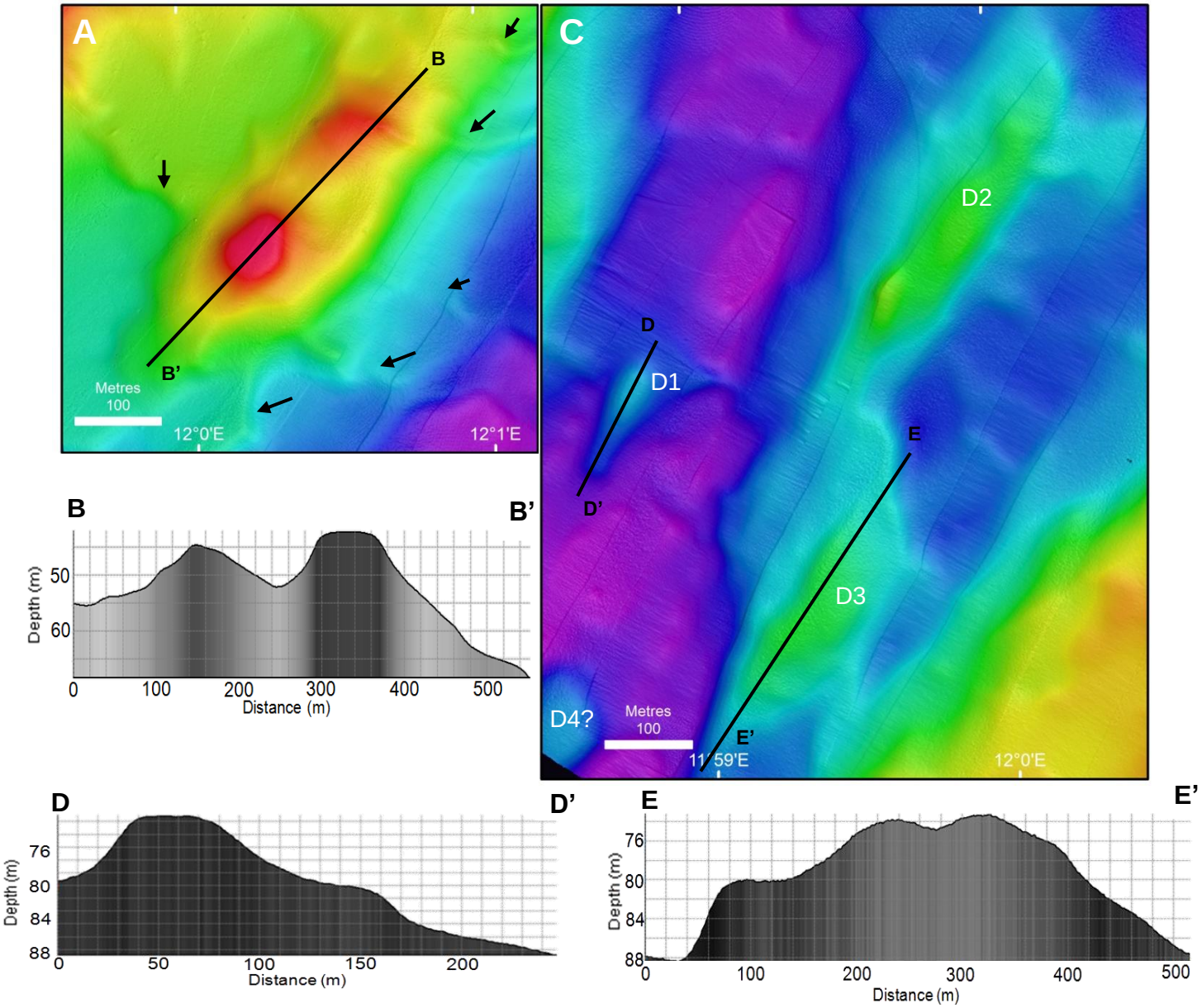

Figure 4.4.1: Features observed in outer Kollerfjorden, locations of which can be seen on Figure 4.4. **A:** Glacially sculpted feature with the appearance of whalebacks. Transverse ridges are also visible leading away from the feature and are marked with black arrows. **B:** Long profile of the features, demonstrating their drumlinised appearance. **C:** Elongated streamlined features, with similar appearances of drumlins, again their association with transverse ridges is evident. **D and E:** Long profile of features demonstrating their drumlin-like appearance. Bathymetric data in **A** and **C** are gridded to 1m cell size, withan illumination of 45° and a sun angle of 60°.

Figure 4.4.1A and B exemplify the morphology of one of the more rounded mounds. The features are slightly steeper on their stoss sides and their lee sides are slightly elongated. The features (D1–D3) in Figure 4.4.1C, D and E demonstrate the morphologies of the more elongated mounds. These elongated features clearly have blunt stoss sides and tapering lee sides, with average slope angles around 8° compared to 4°. They vary in dimensions, from around 150 m long and 60 m wide to 360 m long and 125 m wide. The outcrops also have a clear effect on the position of the transverse ridges within outer Kollerfjorden (Figs. 4.4, 4.4.1A, C). These ridges are similar to those described in Möllerfjorden and are around 10 m high and 20 m wide.

These mounds are interpreted as drumlinised glacially sculpted bedrock outcrops, which have been streamlined and elongated subglacially by ice flow to have orientations sub-parallel to the fjord axis. The more rounded mounds (Fig. 4.4.1A) are similar to descriptions of whalebacks whereas the more elongated features (Fig. 4.4.1C) fit descriptions of drumlins (Benn and Evans, 2010). Drumlins are associated with ice acceleration and ice-streams, marking their onset zones in Greenland (Wellner *et al.*, 2001; Dowdeswell *et al.*, in press) and Antarctica (Ó Cofaigh *et al.*, 2002). Therefore, they are likely to represent landforms produced during the LGM. The transverse ridges are interpreted as recessional moraines, also associated with the LGM. Their positions and frequency near the outcrops of bedrock indicate that these slight topographic highs allowed ice to rest longer over them during its retreat, compared to the deeper areas surrounding them (Fig. 4.4.1A).

Kollerbreen has a relatively small drainage basin (Table 1.1) and so the lack of observations of so many drumlinised features and such clear transverse ridges in the basins of the other bays and fjords is likely to be the result of greater sediment accumulation in these other areas.

There are a number of curvilinear incisions and depressions on the seabed of outer Kollerfjorden (Fig. 4.4.2). They are similar to those described and interpreted as iceberg ploughmarks and pitting in Möllerfjorden and are concentrated on topographic highs, including some of the shallower transverse ridges, and fjord-sides. These features do not extend deeper than 38 m, and the vast majority are concentrated between 10 and 20 m with shallow depths of around 0.25 – 0.5 m, although some of the curvilinear incisions have widths of 10 m. The fact that these features are observed at lower depths than in Möllerfjorden implies that the icebergs and bergy bits are considerably smaller than in

Möllerfjorden due to the presumed topographic high between the two, and thus have a more restricted effect on reworking of shallow sediments in Kollerfjorden.

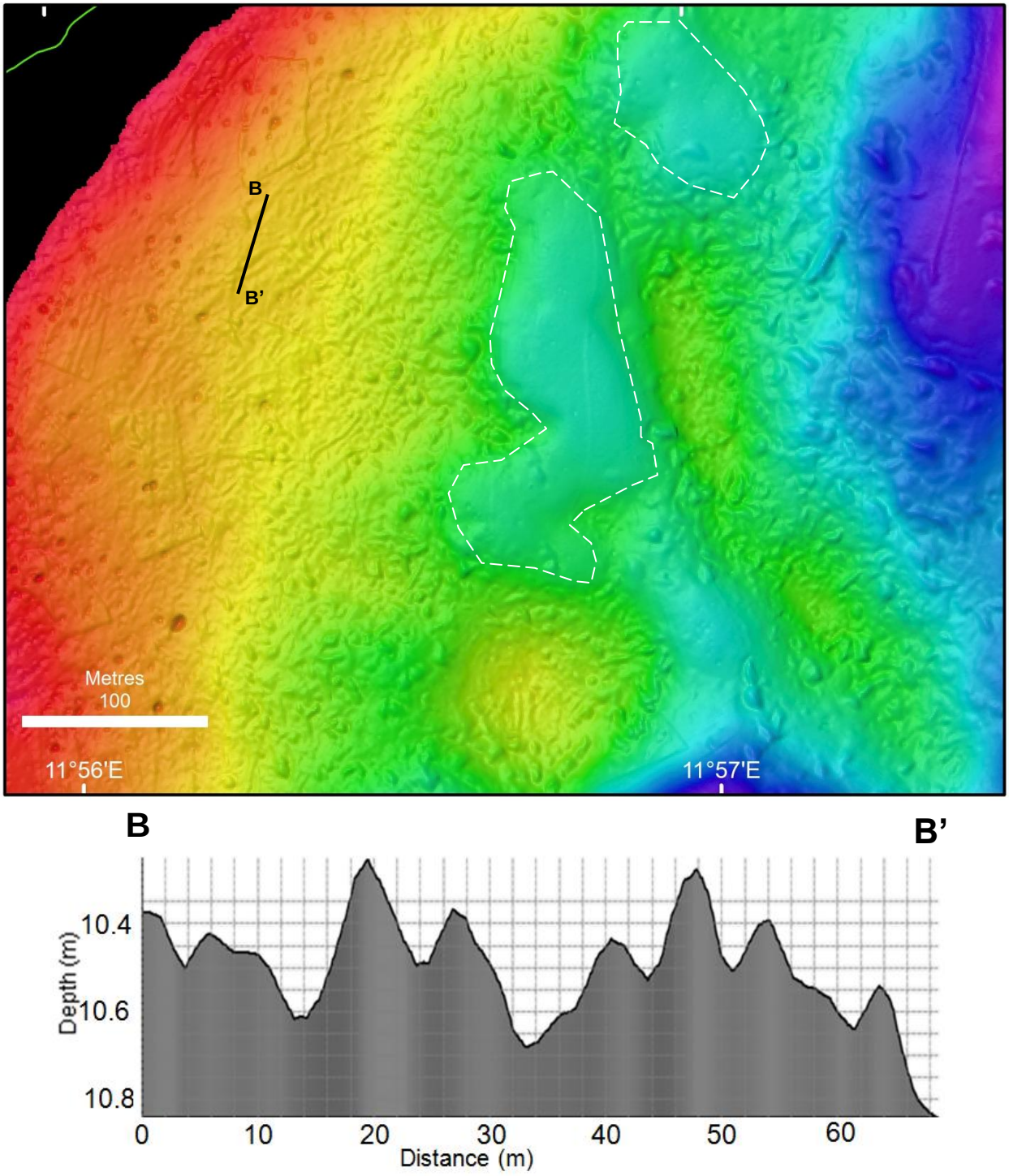

Figure 4.4.2: A: Topographic highs and the shallow side of outer Kollerfjorden with the described scouring and depressions on the seabed, location shown in Figure 4.4. The shallower ridge can be observed to protect other areas, marked with white dashed lines. Bathymetric data are gridded to 1m cell size, with an illumination of 135° and a sun angle of 60°.**B:** Cross-section of depressions and curvilinear incisions, demonstrating their morphology, with berms on the sides of many.

Gullies and fans are frequently observed along the side-walls of Kollerfjorden. Most of them are V-shaped near the surface but become U-shaped at their distal extent and occasionally bifurcate (Fig. 4.4.3). They are around 0.5 m deep, <5m wide and 130 m long.

The morphology of the gullies could imply that mass wasting from the fjord side-walls is less erosive and less significant (Gales *et al.*, 2013) for Kollerfjorden compared to other areas within the study. However, with Kronprins Olavs Fjell (Fig. 4.4) at 1006 m high and within 1.5 km of Figure 4.4.3, it is more likely that the gullies reflect older mass wasting, which does not appear as 'fresh' as in other fjords (Forwick and Vorren, 2012).

Figure 4.4.3 also shows a stream from the neighbouring mountain (Fig.4.4) leading into the fjord. The debris and sediment within this area could have accumulated on the side-wall of the fjord producing a fluvial MTD with gullies super-imposed on it, which indicates instabilities of the unconsolidated sediment (Forwick and Vorren, 2012) and is similar to that described in Möllerfjorden.

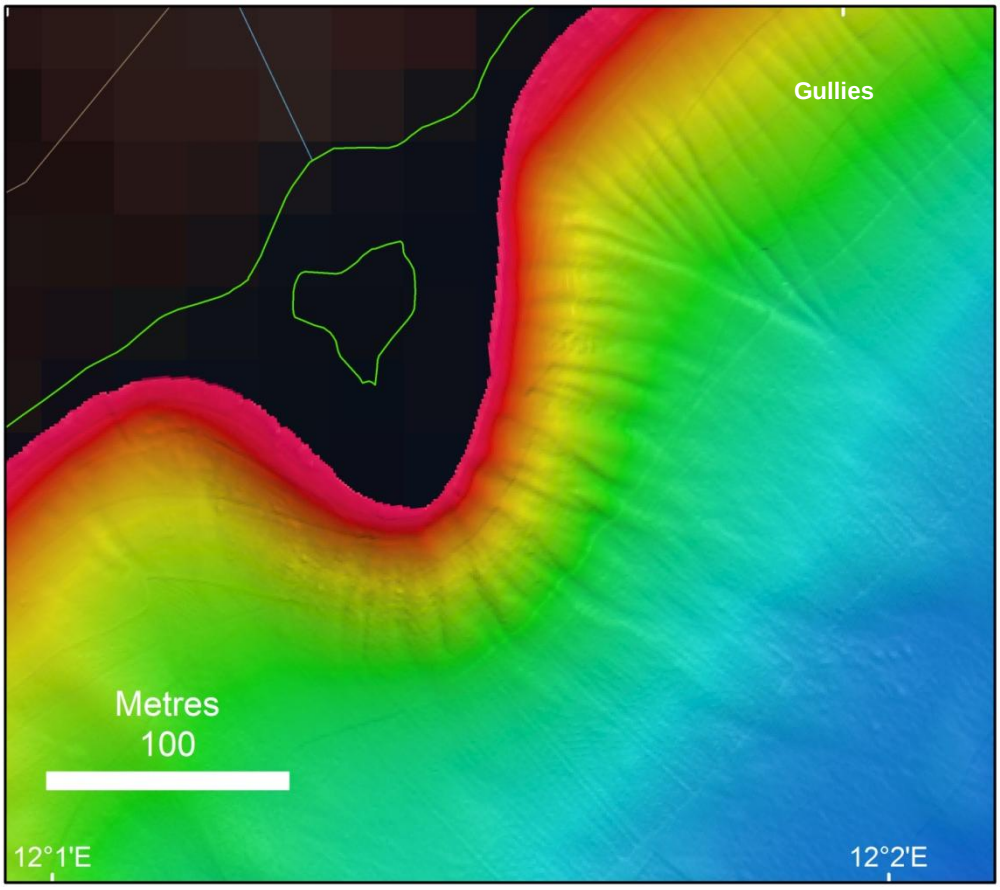

Figure 4.4.3: Possible MTD, with gullies super-imposed on it, from a fluvial stream leading into outer Kollerfjorden, location shown in Figure 4.4. Gullies on the side-wall are labelled. Bathymetric data are gridded to 1m cell size, with an illumination of 135° and a sun angle of 65°.

4.3.2 Inner Kollerfjorden

Inner Kollerfjorden refers to the 2.5 km long area, from the narrowing of the fjord to the present tidewater terminus of Kollerbreen (Fig. 4.5).

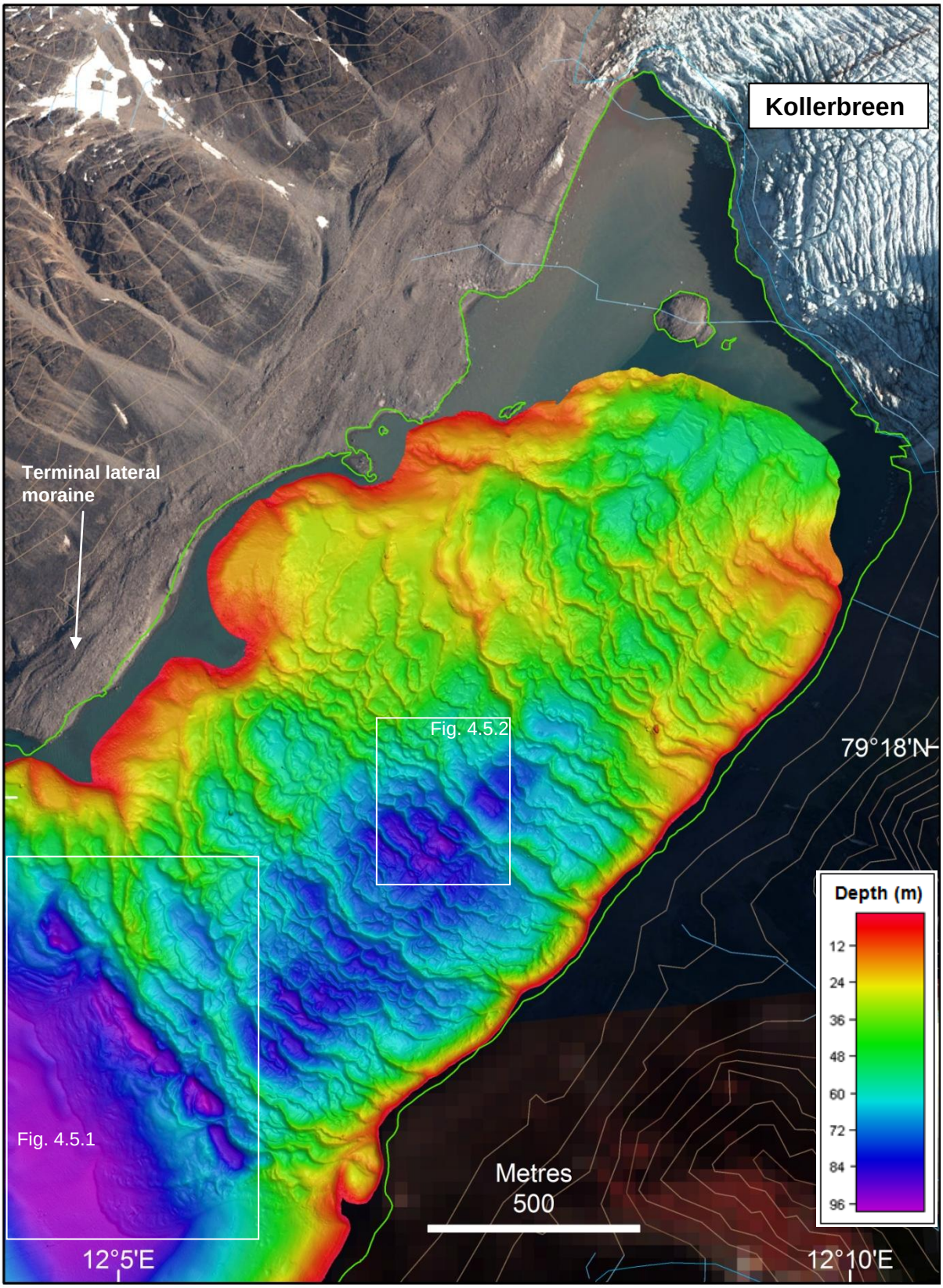

Figure 4.5: Inner Kollerfjorden and the features observed within it. The locations of Figures 4.5.1 and 4.5.2 are shown. Bathymetric data are gridded to 1m cell size, with an illumination of 45° and a sun angle of 65°.

4.3.2.1 Large transverse lobes: mobile push moraine

Description:

Compared to all the other inner fjords and bays, Kollerfjorden does not have a large transverse ridge, interpreted as a terminal moraine, at its entrance. Instead a number of large lobe landforms (Fig. 4.5.1) form a continuous feature across the width of the fjord. The lobes have lengths of 150 - 200 m, heights of 5 – 10 m and appear to consist of a number of arcuate forms. On their ice-proximal sides there are trenches between 5 – 15 m deep before the seabed rises to around 15 m, marking the beginning of the small transverse ridges leading all the way back to the present terminus of Kollerbreen.

Interpretation:

These lobe features are interpreted to represent the extrusion of subglacial deforming layers which were pushed in front of the glacier as a mobile push moraine that continuously failed (Boulton *et al.*, 1996; Bennett, 2001; Kristensen *et al.*, 2009). The glacier would have bulldozed and deformed the seabed sediment, producing a soft mass prone to failing (Boulton *et al.*, 1996) and subject to gravitational spreading (Boulton *et al.*, 1999; Kristensen *et al.*, 2009). The various layers comprising the lobes represent accumulated sediment that has been formed into compressional ridges due to ice push (Kristensen *et al.*, 2009). This deformation till implies a short-lived stillstand at this maximum extent (Boutlon *et al.*, 1996). Similar features have been observed elsewhere on Svalbard, in Van Mijenfjorden (Kristensen *et al.*, 2009) and Ekmanfjorden (Boulton *et al.*, 1996; 1999).

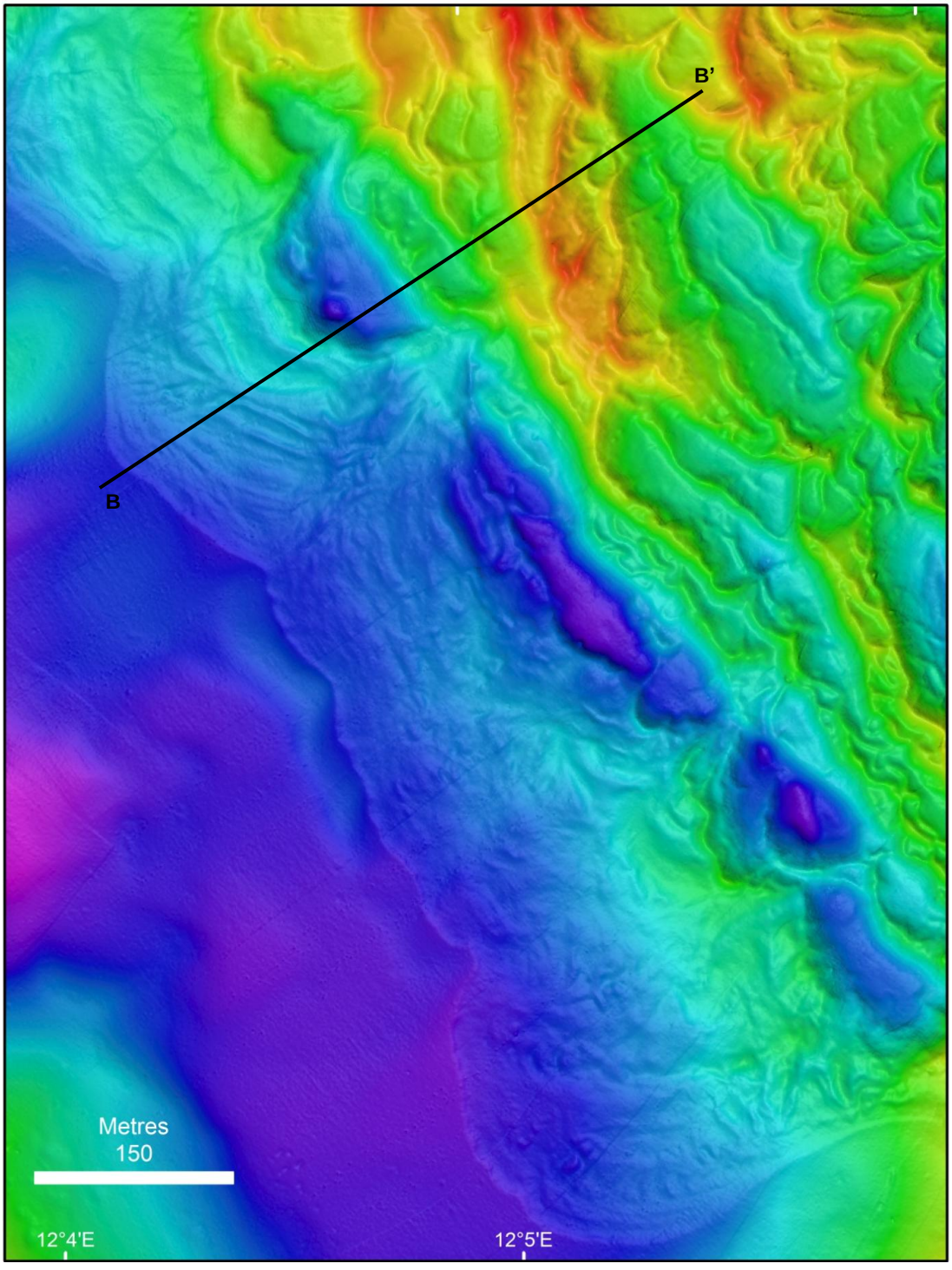

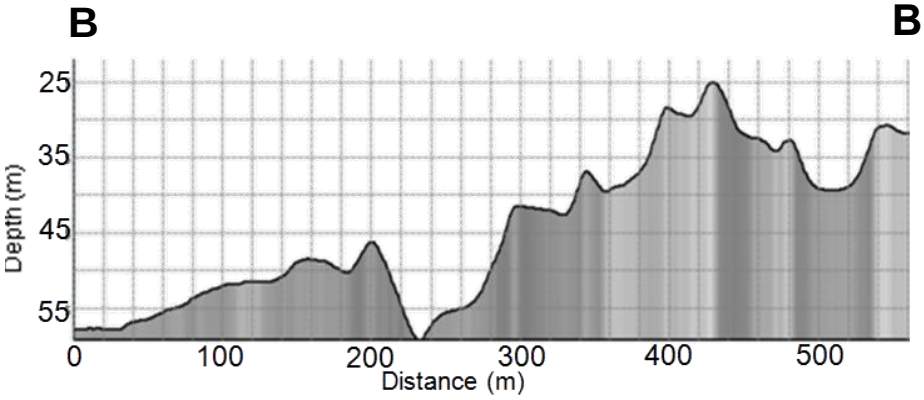

Figure 4.5.1: A: Lobe shapes at the margin between inner and outer Kollerfjorden, location is shown in Figure 4.5. Transverse ridges are also visible. Bathymetric data are gridded to 1m cell size, with an illumination of 225° and a sun angle of 60°. **B:** Long profile across a lobe and the most ice-distal transverse ridges, demonstrating their morphology.

4.3.2.2 Transverse ridges: recessional moraines

Description:

There are also a number of transverse ridges observed across the whole length of inner Kollerfjorden. They range from 1 – 10 m, 5 9– 25 m wide and are regularly spaced, with distances of around 20 m between them (4.5.2). They are generally slightly asymmetrical, with steeper ice-distal sides. There are still a few C-shaped ridges associated with lineations, but the majority are more continuous features.

Interpretation:

All the ridges are interpreted as recessional moraines. The smaller ridges are interpreted as annual retreat moraines, due to their regular spacing (Dowdeswell *et al.*, 2008). However, the larger ridges are likely to represent more than one year of build-up of glacigenic debris. Despite some obvious ice-front oscillations, their continuous form is more similar to typical recessional moraines (Ottesen and Dowdeswell, 2006). Topographic influence is also evident in their distribution, as larger ridges are found at shallower depths (Fig. 4.5).

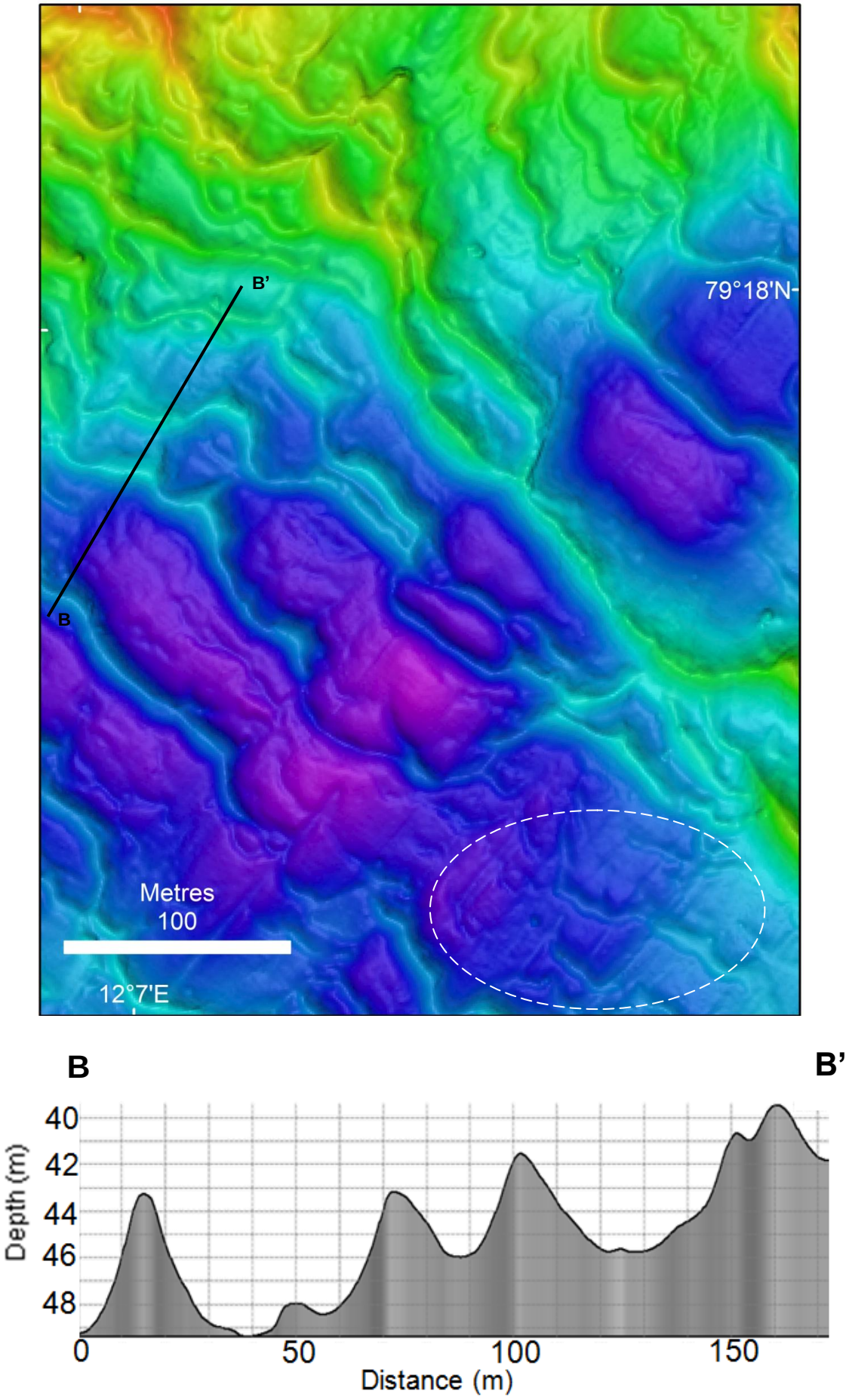

Figure 4.5.2: A: Small transverse ridges observed within inner Kollerfjorden, location is shown in Figure 4.5. Small hooked lineations are highlighted with a dashed white oval. Bathymetric data are gridded to 1m cell size, with an illumination of 225° and a sun angle of 65°.**B:** Long profile across the transverse ridges, demonstrating their morphology.

4.4 Tinayrebukta

Tinayrebukta is presently a 7 km long bay leading to the ice-front of Tinayrebreen (Figs. 4.1, 4.6). The bathymetric data within the bay were gridded at 1 m grid cell size, providing a high resolution of observed landforms. Bathymetrically, it has two clearly defined sections (Fig. 4.6).

Outer Tinayrebukta refers to the 2.5 km from the mouth of the fjord, where it converges with Möllerfjorden, to where continuous moraines are marked on the NPI's topographic map and a large transverse ridge is shown by the bathymetric data (Fig. 4.6). Like outer Lilliehöökfjorden and Möllerfjorden, outer Tinayrebreen has a smooth appearance and is thus interpreted to be a sediment-filled basin. The side-walls are also covered by bifurcating gullies 0.5 – 3 m deep with lengths of 200 m (Fig. 4.6.1), similar to those observed in the other bays and fjords within the study area. The gullies also start with a V-shape, but towards the base progress to a U-shaped morphology. They demonstrate mass wastage into the bay.

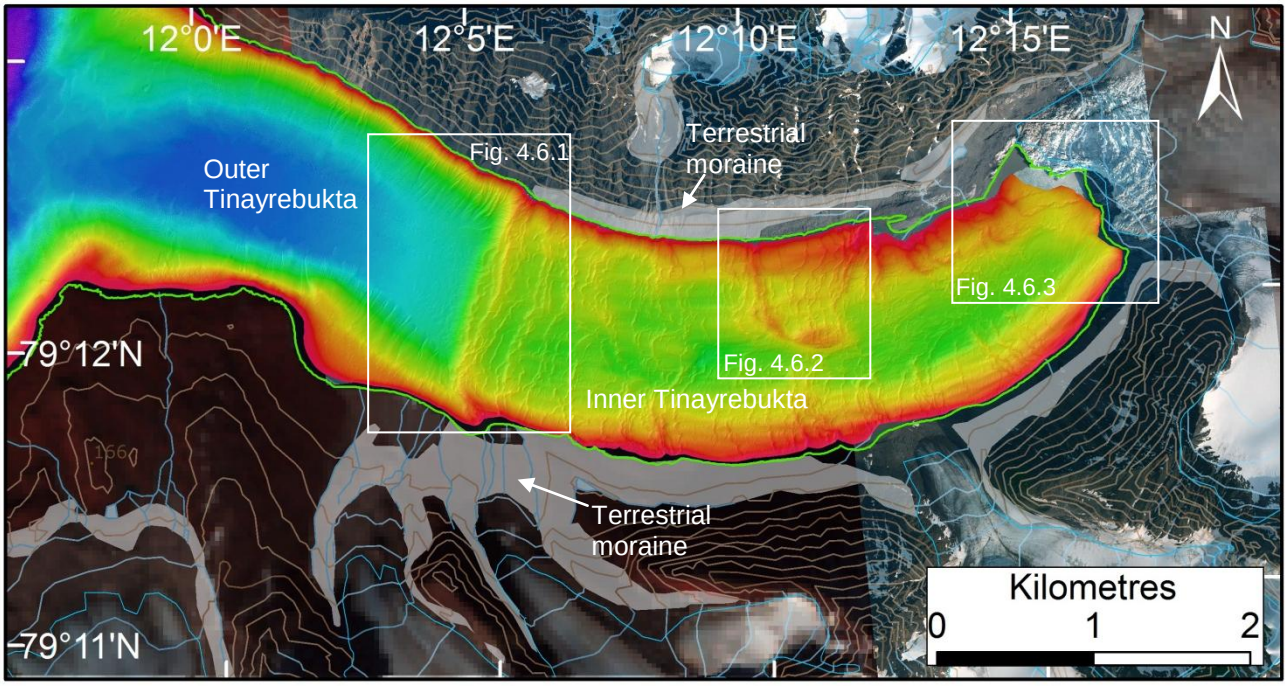

Figure 4.6: Map of Tinayrebukta, showing the bathymetry of the fjord. Locations of Figures 4.6.1 and 4.6.2 are shown. Bathymetric data are gridded to 1 m cell size, with an illumination of 315° and a sun angle of 75°.

Inner Tinayrebukta refers to the 4.5 km area from the ice-front of Tinayrebreen to the large transverse ridge (Fig. 4.6). The ridge has a height of around 60 m and is asymmetric with a steeper ice-distal (western) side. The large transverse ridge is similar in morphology to those observed in Lilliehöökfjorden and Mayerbukta (Fig. 4.6.1) and is also interpreted as a terminal moraine.

On the ice-proximal side of this ridge a large number of small transverse ridges are observed. These small asymmetric ridges vary in height, ranging from 0.5 – 8 m, and are a mixture of continuous and disjointed concentric ridges. Again, these are interpreted as recessional moraines indicating the gradual retreat of the Tinayrebreen (Dowdeswell and Ottesen, 2006). However, they are less regular and more subtle than in Mayerbukta and Kollerfjorden. Their concentric shape is similar to those observed in the other bays and fjords and this has been used to indicate a heavily crevassed ice-front as the glacier retreated (Sharp, 1984; Bennet, 2001; Bradwell, 2004; Burki et al., 2009).

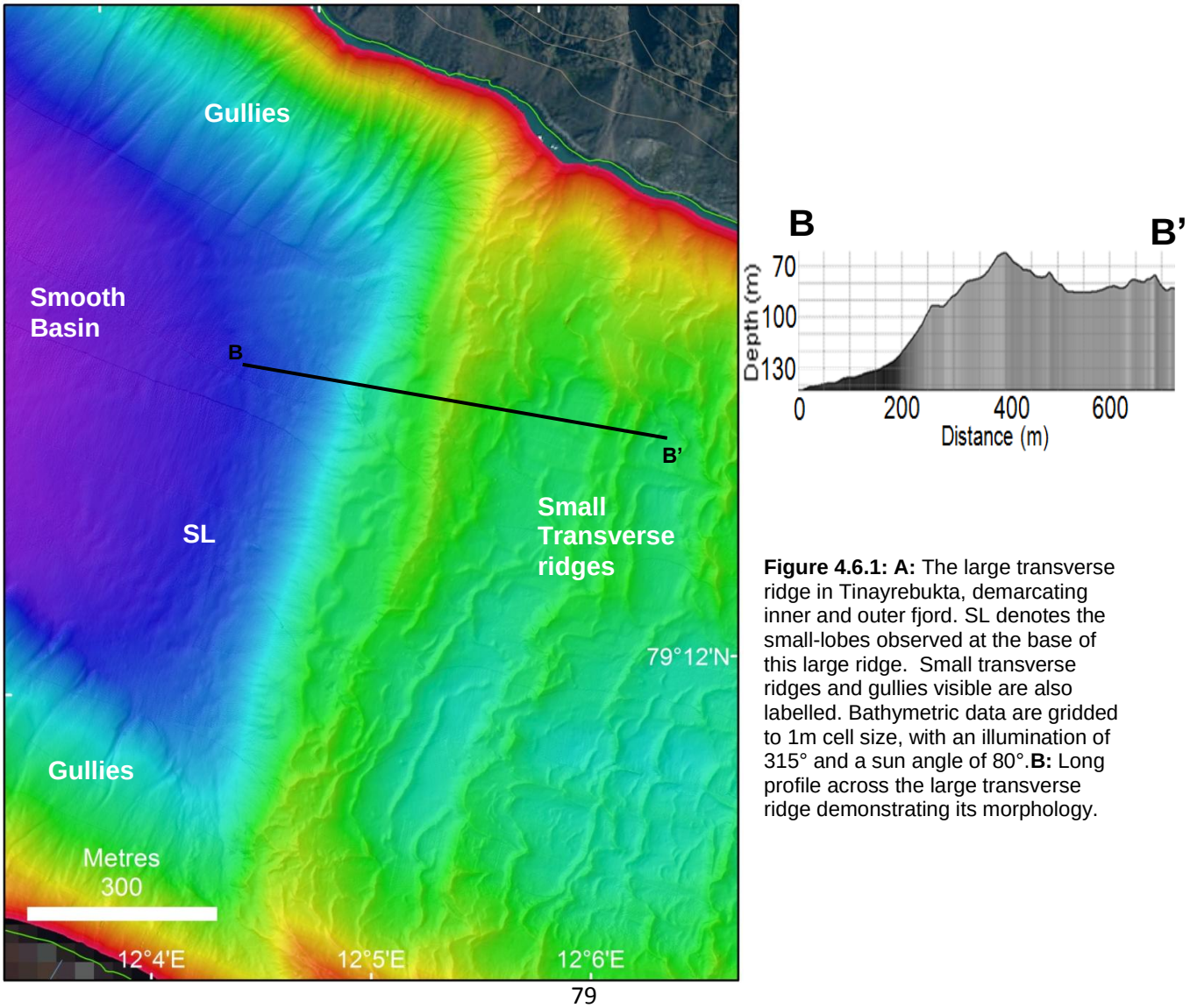

Figure 4.6.1: A: The large transverse ridge in Tinayrebukta, demarcating inner and outer fjord. SL denotes the small-lobes observed at the base of this large ridge. Small transverse ridges and gullies visible are also labelled. Bathymetric data are gridded to 1m cell size, with an illumination of 315° and a sun angle of 80°.**B:** Long profile across the large transverse ridge demonstrating its morphology.

The arcuate, medium-sized ridge shown in Figure 4.6.2 traverses half of the width of the fjord. It has heights of around 20 m on its ice-proximal side (Fig. 4.6.2B) and of 15 m on its lateral margin, in the centre of the fjord (Fig. 4.6.2C). It has a number of straight, continuous transverse ridges leading down the medium-sized ridge; these eventually join small transverse ridges from the other half of the fjord.

The arcuate mound is interpreted as a medium-sized moraine, which is probably located there due to underlying bedrock on this side of the fjord. The traces of lineations visible on the ice-distal side of this ridge are interpreted as the tails that are formed in the lee of a bedrock outcrop, similar to those found in Mayerbukta. This is also thought to be the case for the lineations observed near the ice-front of Tinayrebreen (Fig. 4.6.3). They have heights of around 0.5 m and have a maximum length of 300 m. Aerial photography from 2009 show that the glacier was receding over a bedrock outcrop (Fig. 4.6.3), which may have caused the formation of these 'tails'. The mound is not thought to represent a looped medial moraine due to the morphology of the ridge, the tails on the ice-distal side and the link between the transverse ridges on both the north and south sides of this ridge.

There are a number of lineations and low relief hooked lineations observed within Tinayrebukta (Fig. 4.6.3), as in the other inner areas (except Kollerfjorden, which only has a limited number of very small-scale hooked lineations). Most of these features tend to have a lineated mound <0.5 m wide leading back towards Tinayrebukta on both sides of a small C-shaped transverse ridge and occur in the deepest and therefore the most unstable parts of the inner fjord. However, these C-shaped ridges often form one continuous ridge, which suggests that they are linked to relatively rapid ice retreat (Fig. 3.6.3). Consequently, they are interpreted to be the result of varying stresses at a grounding line linked to minor crevasse-squeezed ridges and small-scale glacitectonic features.

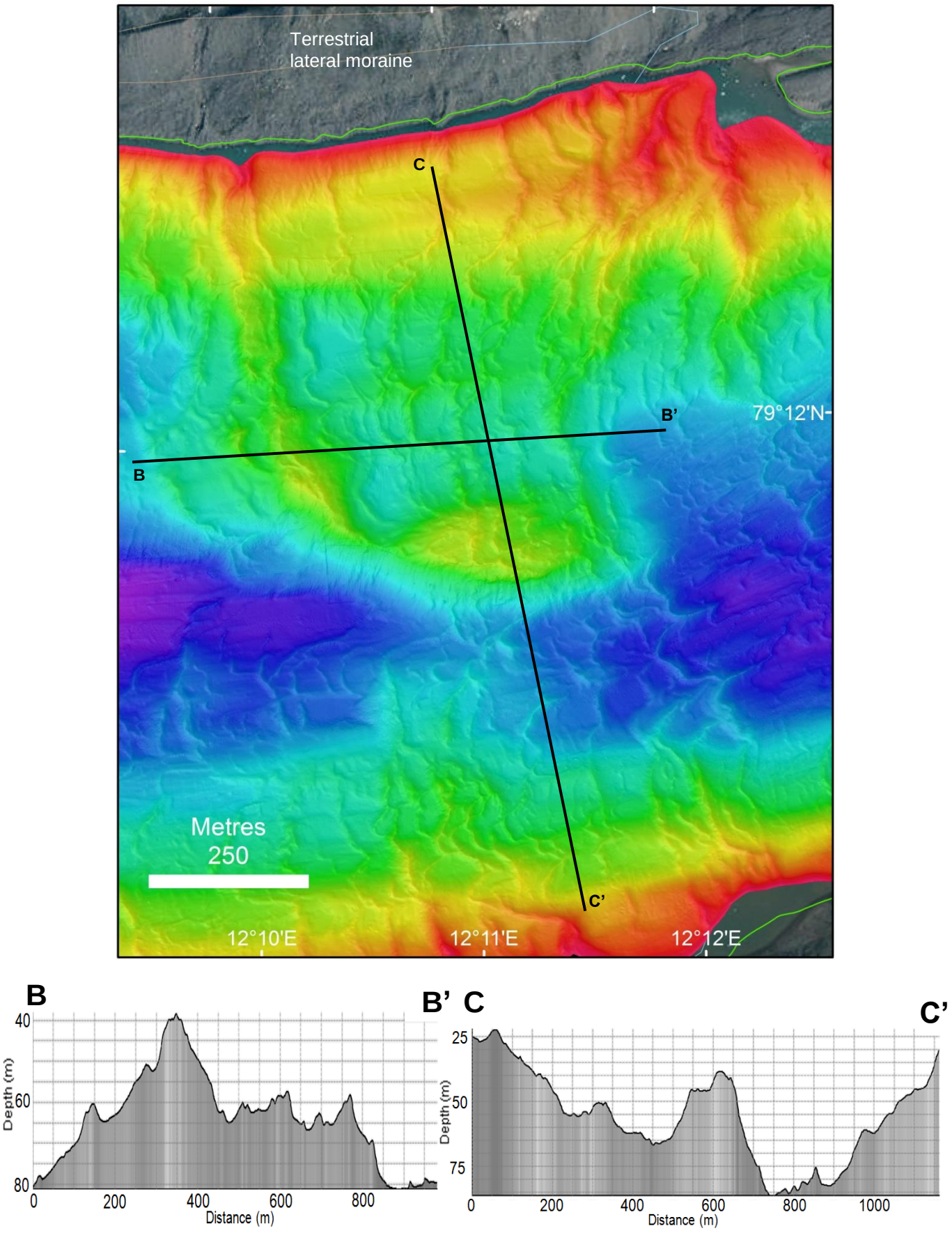

Figure 4.6.2: A: The large mound with transverse ridges imposed on it, within inner Tinayrebukta. Bathymetric data are gridded to 1m cell size, with an illumination of 225° and a sun angle of 80°. **B:** Long profile across this mound and other smaller recessional moraines. **C:** Cross-section of the area with the large mound, demonstrating the raised northern side of the fjord and deeper southern side. The large mound separates the two.

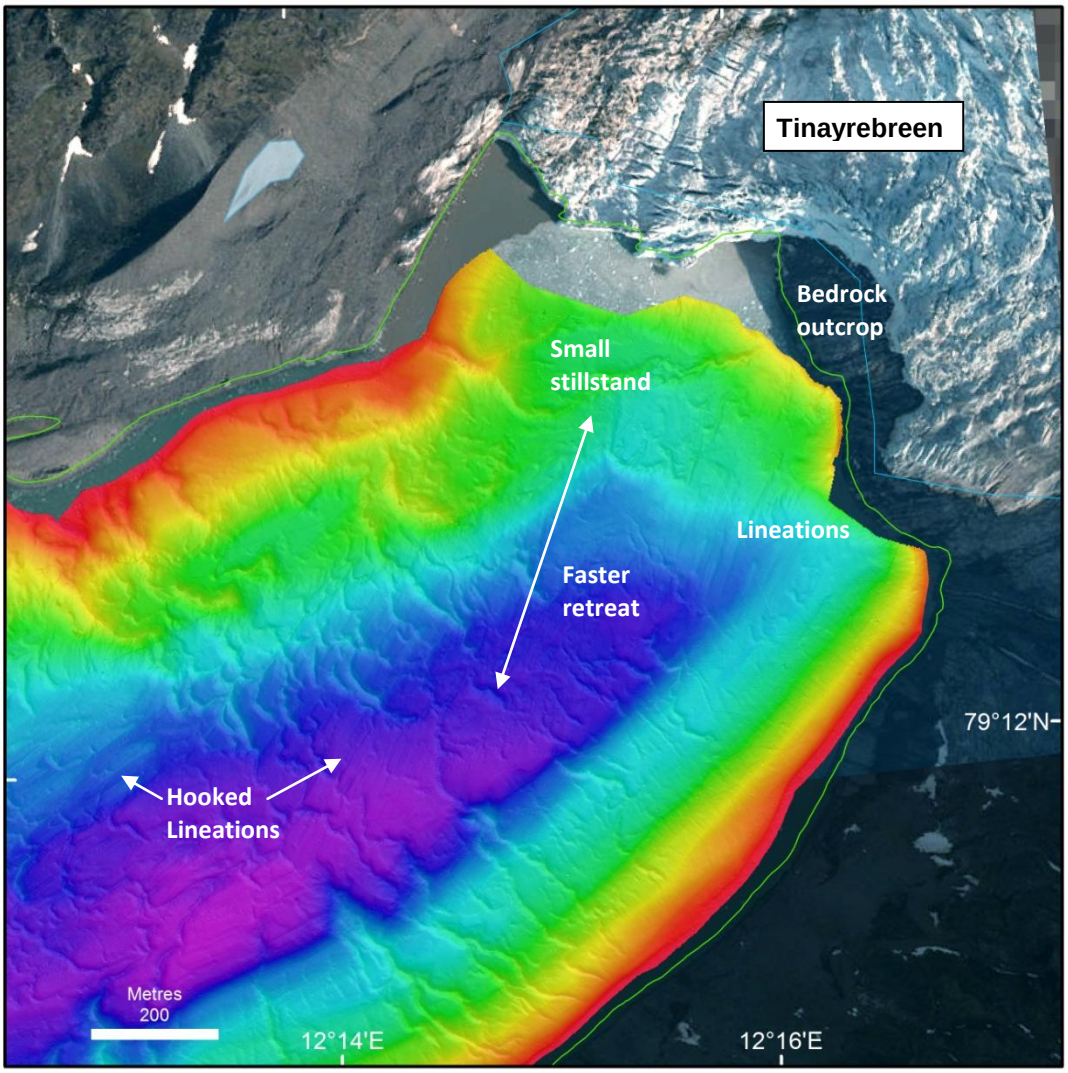

Figure 4.6.3: Area with an interpreted faster retreat, with fewer transverse ridges, is indicated, leading back to a ridge demonstrating a brief stillstand. The bedrock outcrop, associated with lineations and hooked lineations is also labelled. Bathymetric data are gridded to 1m cell size, with an illumination of 225° and a sun angle of 80°.

4.5 Distribution and timing of submarine landforms in Möllerfjorden

4.5.1 Geographical Distribution

There are three main types of landforms within Möllerfjorden; subglacial, ice-marginal, and post-glacial. Subglacial and ice-marginal landforms are both directly related to glacial activity. The geographical distribution of these features is shown in Figure 4.7, which exemplifies the disparity in distribution of the features between Möllerfjorden and its inner fjord (Kollerfjorden) and two bays (Mayerbukta and Tinayrebukta).

There are a number of features visible within Möllerfjorden, but the vast majority of landforms are located closer to the present ice-fronts. The glacially sculpted bedrock and its associated linear 'tails' and transverse ridges represent subglacial landforms produced by an extensive ice advance that reached into Krossfjorden and converged with ice flow from Lilliehöökfjorden. These features are attributed to the LGM and further support significant regional ice cover. There are also a number of post-glacial erosional and depositional features associated with the steep mountains surrounding the fjords and seasonal snow-melt. However, some of these have a 'fresher' appearance than others and are attributed to the slopes being more active closer to ice-fronts (Forwick and Vorren, 2012).

The last significant glacial expansion and subsequent retreat of Kollerfjorden, Mayerbukta and Tinayrebukta (Fig. 4.7B, C, D) is identified in the data by a number of submarine landforms observed in these innermost parts of the Krossfjorden system. The ice-marginal features (the terminal and recessional moraines) indicate maximum ice front positions, which are demarcated by the inner fjord and bays, and subsequent retreat.

Next three pages - Figure 4.7: A: Landform map of Möllerfjorden, indicating submarine landforms described and demonstrating their geographical distribution. **B:** More detailed map for the area closest to the present ice-front of Kollerbreen (inner Kollerfjorden). **C:** More detailed map for the area closest to the present ice-front of Mayerbreen (Mayerbukta). **D:** More detailed map for the area closest to the present ice-front of Tinayrebreen (Tinayrebukta). Note MTDs were not mapped due to the abundance of gullies.

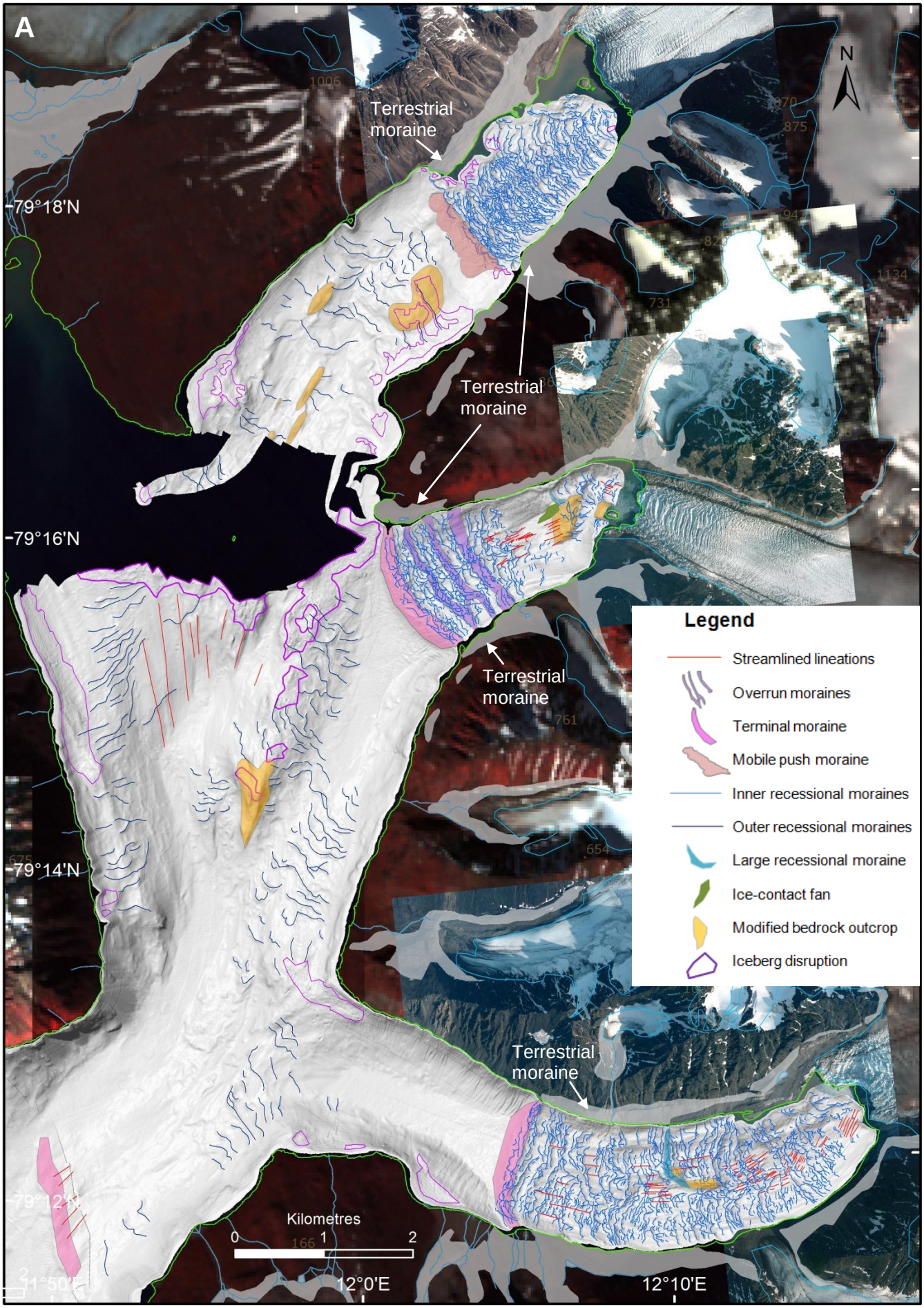
A
N
Terrestrial moraine
Terrestrial moraine
Terrestrial moraine
Terrestrial moraine
79°18'N
79°16'N
79°14'N
79°12'N
Legend
Streamlined lineations
Overrun moraines
Terminal moraine
Mobile push moraine
Inner recessional moraines
Outer recessional moraines
Large recessional moraine
Ice-contact fan
Modified bedrock outcrop
Iceberg disruption
Kilometres
0
1
2
11°50'E
12°0'E
12°10'E

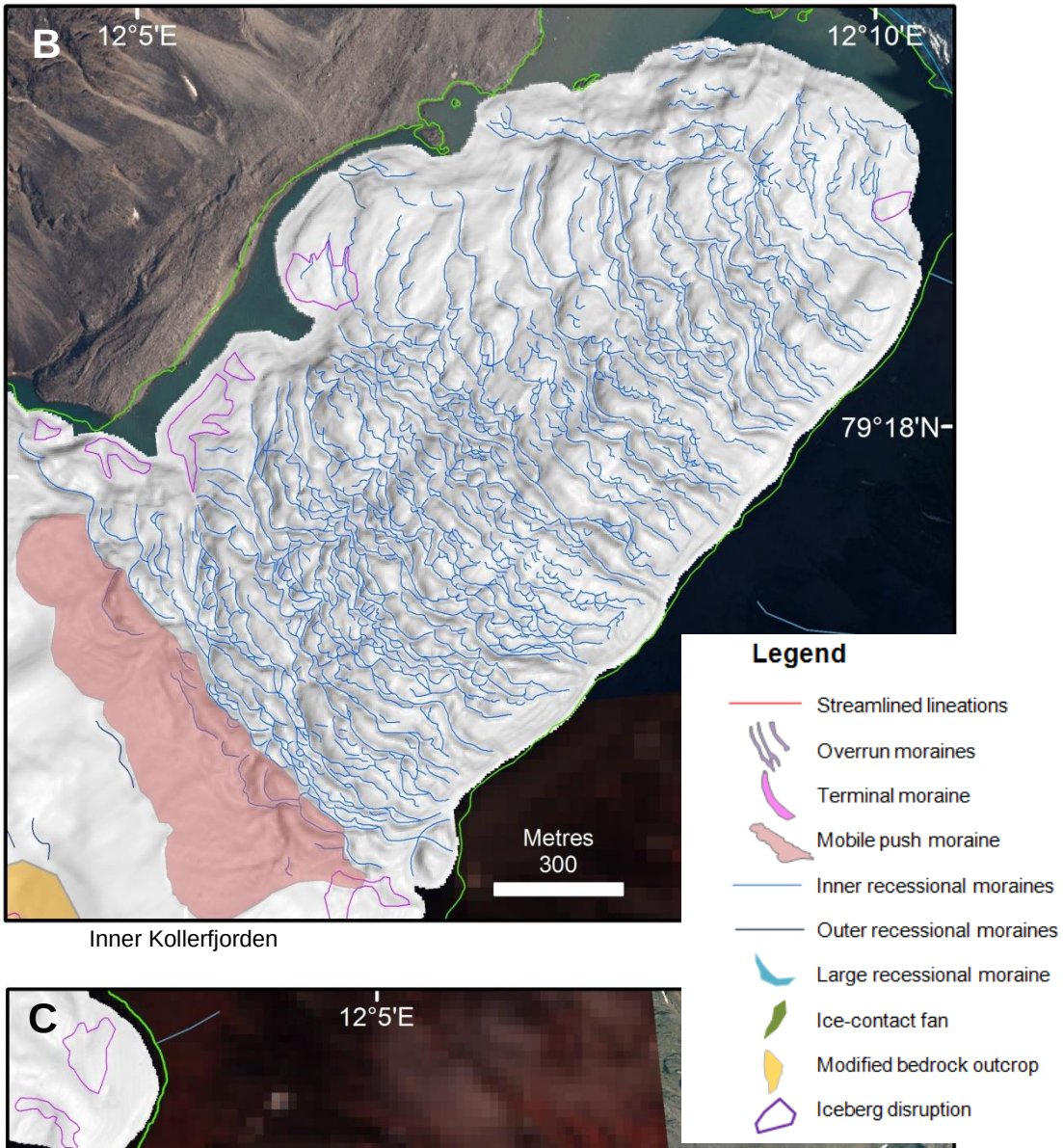

Inner Kollerfjorden

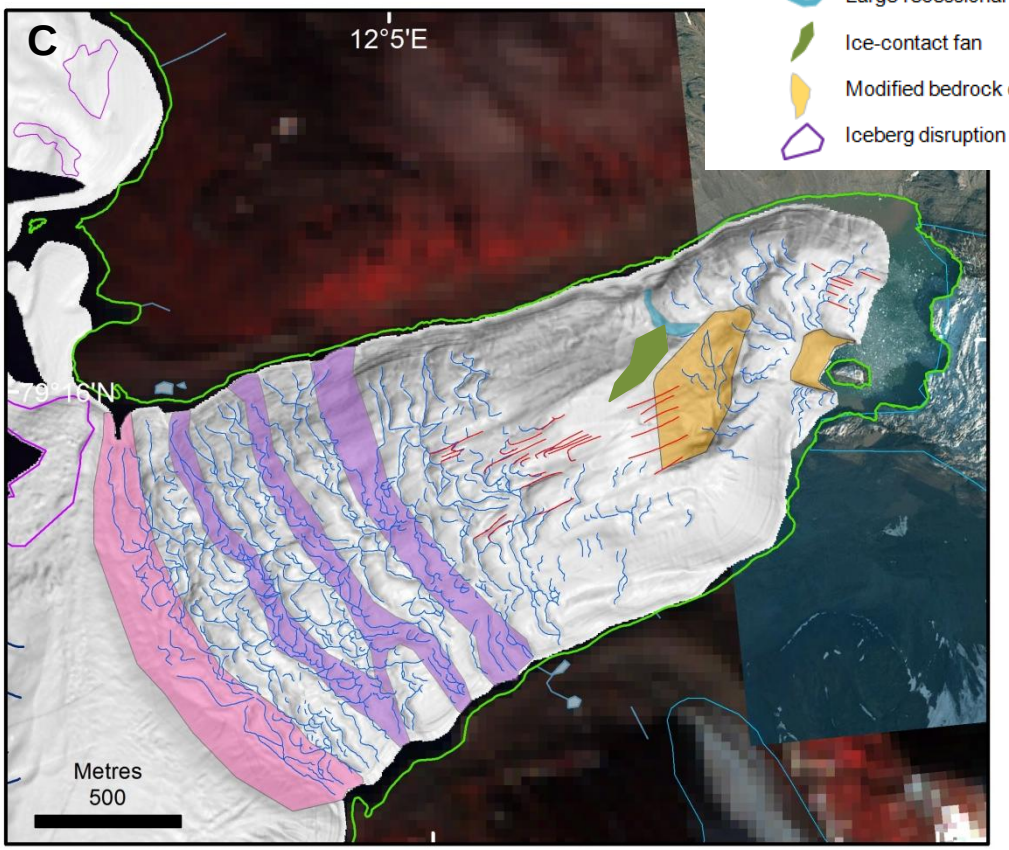

Mayerbukta

Tinayrebukta

4.5.2 Timing

The cross-cutting relationships and superimposition of the features in Möllerfjorden allows a reconstruction of the relative timing of the formation of various suites of landforms (Ottesen and Dowdeswell, 2006). These temporal and spatial variations are summarised in Figure 4.8. It can be seen that a significantly greater number of landforms are visible in the inner fjords and bays. This may be due to sedimentation over a longer period of time in the outer fjord.

Mayerbukta is the only inner area to have overrun transverse ridges (Fig 4.8B), like those found in Lilliehöökfjorden. These ridges have been significantly modified by younger features and are considered the oldest landforms observed within the inner areas, representing palaeo-terminal moraines.

The glacial lineations associated with glacially sculpted bedrock would have formed subglacially as ice advanced (Fig. 4.8C). The terminal moraine and medial moraine are then interpreted to have formed once the glacial advance ceased and the ice margins remained at a stable position for some time, perhaps decades, allowing the accumulation of these mounds (Fig. 4.8D).

The recessional moraines and hooked lineations lead back towards the present tidewater margin and overlie any other features present (Fig. 4.8E). They also modify some of the linear features and are superimposed on top of, and on the ice-proximal side of, the terminal moraine and the glacially sculpted bedrock. These characteristics imply that they are the youngest set of landforms present.

The chronology and glacial events within the whole of the Krossfjorden system will be discussed in Chapter 7.

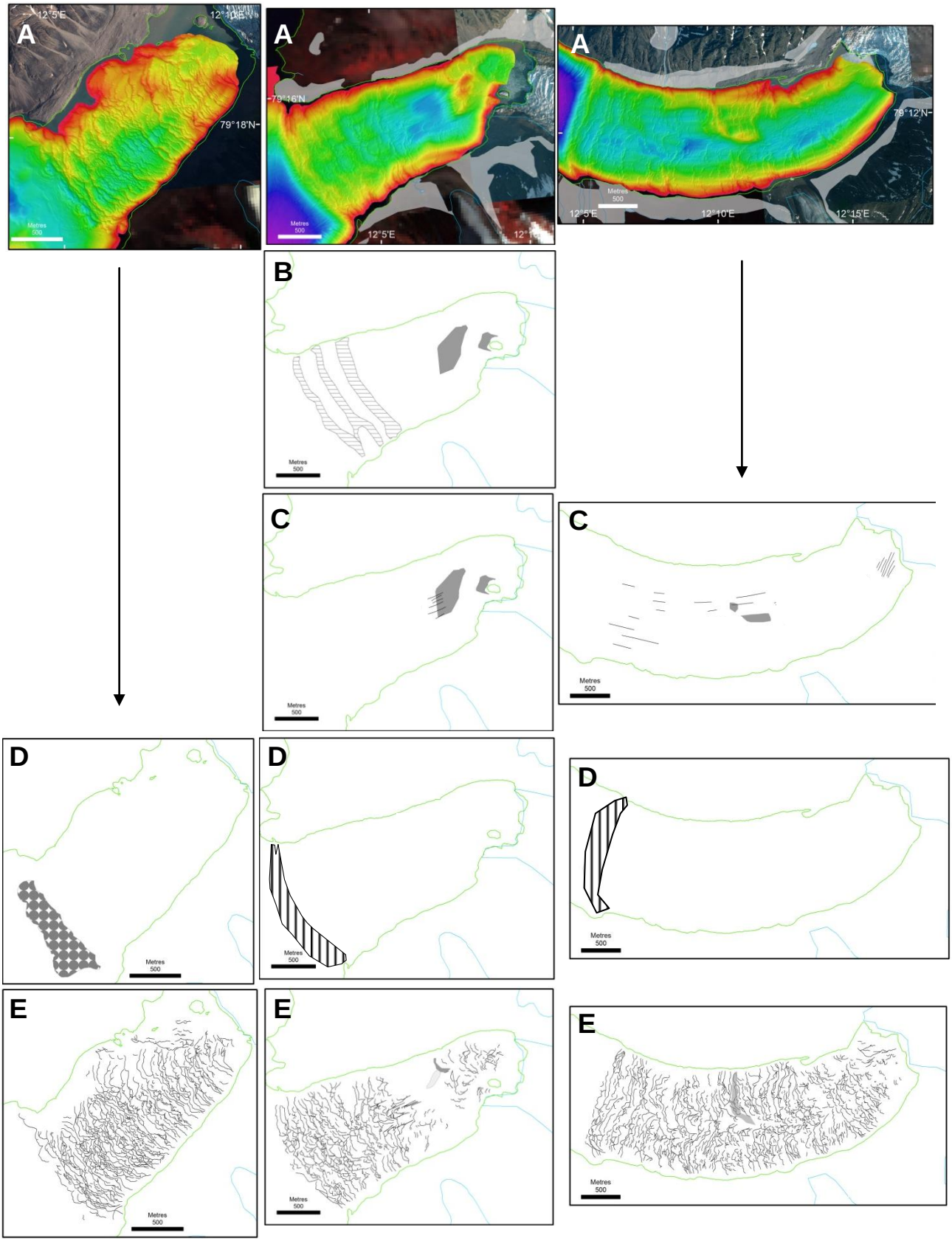

Figure 4.8: An analysis of spatial and temporal variations for individual submarine landforms, which make up the landsystem within the inner fjord and bays of Möllerfjorden. Kollerfjorden is the left-hand column, Mayerbukta the central and Tinayrebukta the right-hand column. The landform elements (4.8B – 4.8E) are shown in their stratigraphic order in which they are interpreted to have formed, inferred from their superposition and cross-cutting relationships, to distinguish the relative age of each set. Note that not all the landforms were observed in all areas and arrows are used to indicate this. **A:** Swath-bathymetric shaded relief image of Kollerfjorden, Mayerbukta and Tinayrebukta respectively. **B:** Large overridden ridges with sculpted bedrock.. **C:** Streamlined bedforms and sculpted bedrock. **D:** Mobile push moraine (Diamond-fill) and terminal moraine ridges (vertical lines). **E:** Small transverse ridges and hooked lineations, with a number of varying morphologies, represent the youngest landforms.

Chapter 5 – Krossfjorden and Fjortende Julibukta

This chapter examines the landforms observed from the bathymetric data in the outer parts of Krossfjorden, with partial coverage of Kongsfjordrenna and the small bay of Fjortende Julibukta, which leads to the ice front of Fjortende Julibreen.

5.1 Krossfjorden

The outer fjord has a smoothened appearance; however, because the majority of sedimentation has been shown to occur within the first 5 km from tidewater glacier margins (Svendsen *et al.*, 2002; Zajakowski, 2008), a large number of features can still be observed (Fig 5.1).

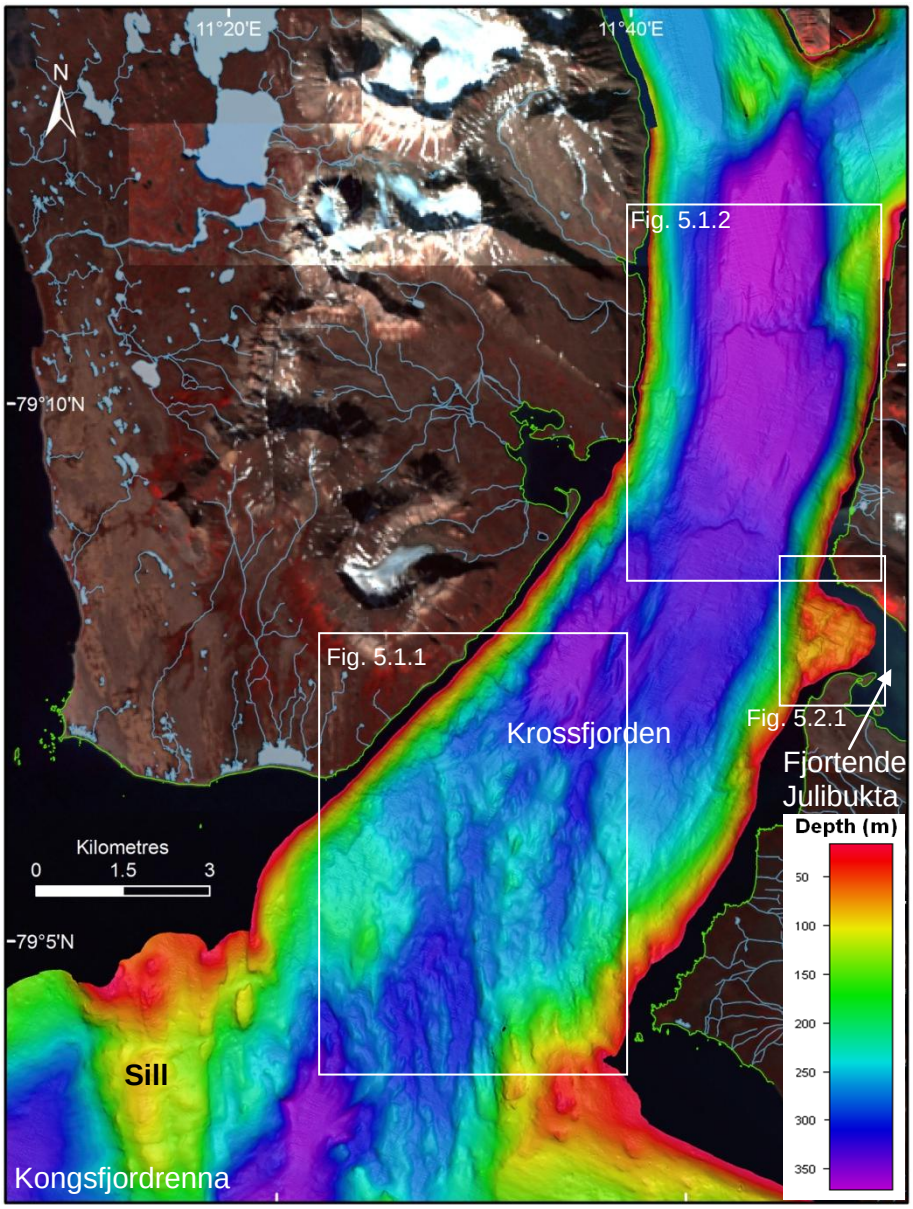

Figure 5.1: Map of the outer Krossfjorden system, comprising bathymetric data of Krossfjorden proper, Fjortende Julibukta and a part of Kongsfjordrenna. Figures are indicated by white rectangles. Bathymetric data gridded at 8 m and interpolated, illumination of 45° and sun angle of 50°.

5.1.1 Transverse morphologies: bedrock outcrops

Description:

At the mouth of the fjord a partial sill (Fig. 5.1) is observed to extend the length of the data investigated within this thesis. This feature is asymmetric, at around 200 m high and 1.5 km wide; however its widest point matches the description from Maclachlan *et al.* (2010). Additionally, the bathymetric data from the Sjoemaalern-4100 cruise extends further south, but are not shown in this study, and demonstrate that the sill decreases in heights along its length, only stretching halfway across the mouth of the Kongsfjorden-Krossfjorden system.

At the mouth of Krossfjorden proper, a complex hummocky morphology can be observed for approximately 6.5 km at a maximum height of around 200 m (Fig. 5.1.1A), again matching descriptions from Maclachlan *et al.* (2010). The general trend of the raised complex is north to south, thus roughly transverse to the fjord; however, individual features are elongated perpendicular to the fjord-axis (Fig. 5.1.1A). These vary in dimensions but average 10 m high, 130 m wide and 450 m long, but can reach 20 m high, 500 m wide and 1.2 km long. They have blunter stoss sides and tapering lee sides.

Interpretation:

Based on previous bathymetric data, gridded at 30 to 50 m, this sill has been interpreted in the past as a bedrock controlled terminal moraine bank formed during deglaciation from the LGM at a logical pinning point (Howe *et al.*, 2003; Maclachlan *et al.*, 2010). However, the higher resolution bathymetric data within this study do not provide any evidence of a glacial stillstand during deglaciation on this feature; thus it is interpreted as a glacially plucked and sculpted bedrock outcrop. This explains its asymmetric morphology, which is likely to be linked to the faults, anticlines and synclines visible in Figure 5.1.1B.

The lengthy complex of hummocky morphology was also interpreted to represent recessional moraines in Maclachlan *et al.* (2010), but again the higher resolution this study used does not reveal any evidence of ice-marginal landforms in this area. Thus it is interpreted as glacially sculpted bedrock, rather than interconnected lobate morainal segments. The interpretation that this ridge complex is bedrock controlled is supported by Figure 5.1.1B which shows a number of faults leading into the fjord at this position. Maclachlan *et al.* (2010) also state that this feature stretches across outer Kongsfjorden, thus their interpretation of features, and therefore the style of deglaciation, within Kongsfjorden is also equivocal. The morphology of

the elongate individual features matches those of descriptions of drumlins (Benn and Evans, 2010, Dowdeswell *et al.*, in press), supporting the interpretation made for some of the features by Maclachlan *et al.* (2010).

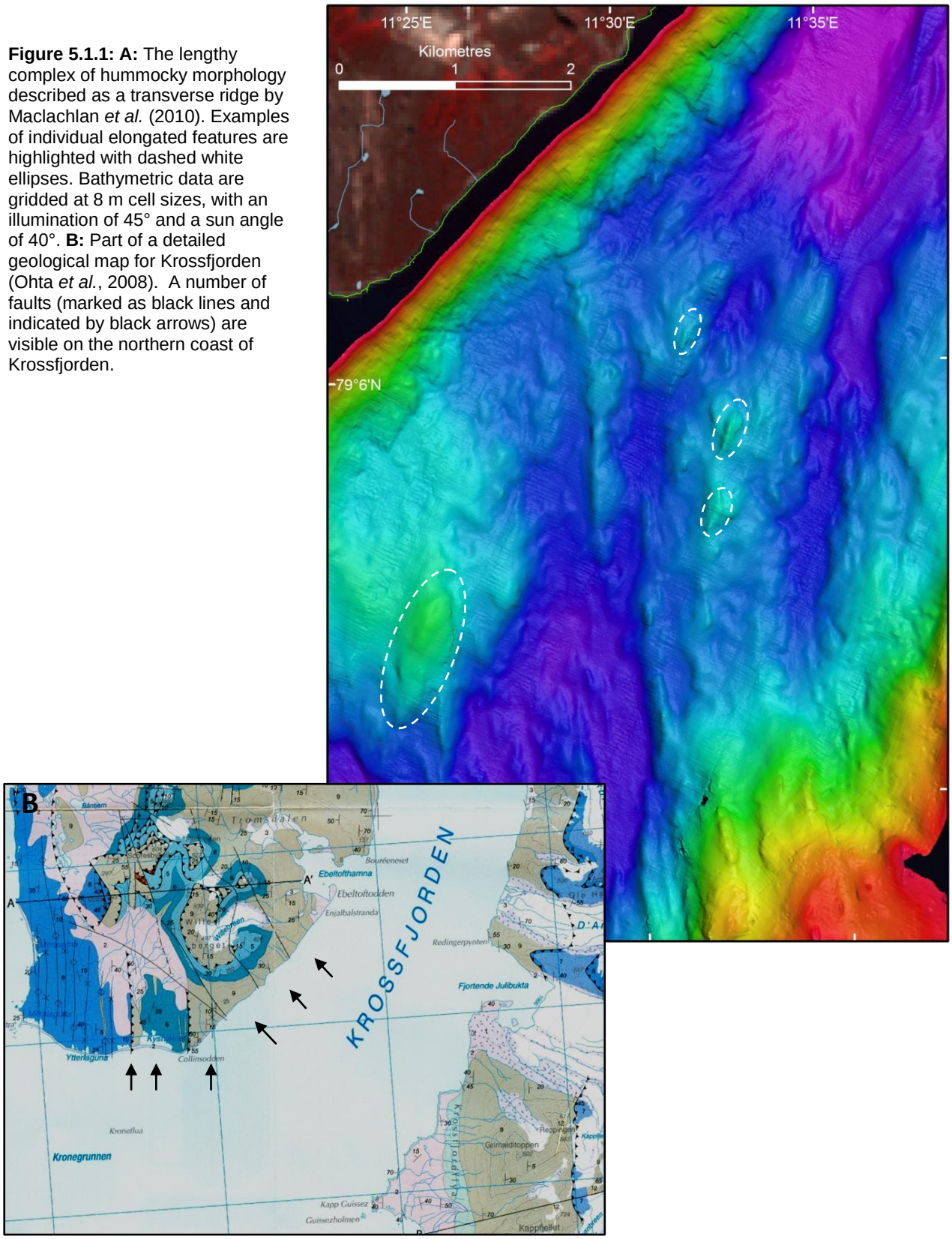

Figure 5.1.1: A: The lengthy complex of hummocky morphology described as a transverse ridge by Maclachlan *et al.* (2010). Examples of individual elongated features are highlighted with dashed white ellipses. Bathymetric data are gridded at 8 m cell sizes, with an illumination of 45° and a sun angle of 40°. **B:** Part of a detailed geological map for Krossfjorden (Ohta *et al.*, 2008). A number of faults (marked as black lines and indicated by black arrows) are visible on the northern coast of Krossfjorden.

5.1.2 Transverse ridges: recessional moraine

Description:

There are two transverse ridges (OTR1 and OTR2) visible in central Krossfjorden, which are located at a slight narrowing of the fjord (Fig. 5.1.2). The ridges have slightly steeper ice-distal slopes than ice-proximal. The outermost ridge (OTR1) is about 10 m high, between 150 m to 380 m wide and 1.8 km long, matching descriptions by Maclachlan *et al.* (2010); however, on its eastern side, height decreases to 2 m in places. OTR2 varies between heights of 1 to 5 m on the western side and 10 to 20 m on the eastern side of Krossfjorden. The ridges exhibit a peculiar morphology, similar to that described at the mouth of Möllerfjorden (Section 4.1.2), consisting of a reverse-bed slope and a number of elongated landforms on their ice-proximal side, with dimensions of around 1.5 m and widths of 60 m (Fig 5.1.2B).

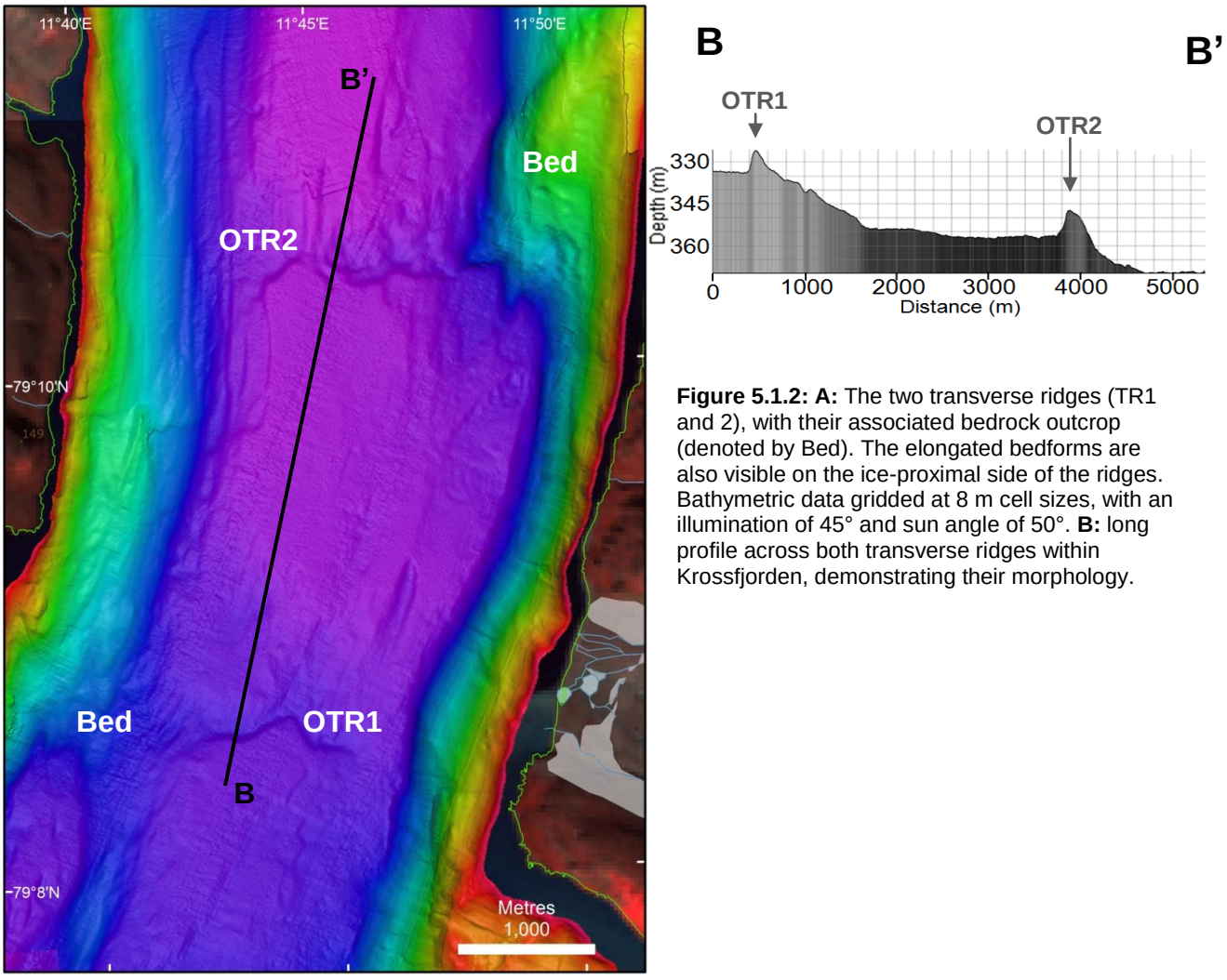

Figure 5.1.2: A: The two transverse ridges (TR1 and 2), with their associated bedrock outcrop (denoted by Bed). The elongated bedforms are also visible on the ice-proximal side of the ridges. Bathymetric data gridded at 8 m cell sizes, with an illumination of 45° and sun angle of 50°. **B:** long profile across both transverse ridges within Krossfjorden, demonstrating their morphology.

Interpretation:

These features had been interpreted to represent channels (Howe *et al.*, 2003) but due to their concave morphology this was revised to recessional moraines by Maclachlan *et al.* (2010). Bathymetric data within this thesis support the view that OTR1 and OTR2 represent stillstands during deglaciation. They are both located at natural pinning points within the fjord, where the fjord narrows or becomes shallower due to bedrock outcrops at its margins (Fig. 5.1.2). However, the bedrock outcrops for OTR1 appear to be partially covered by a glacio-fluvial MTD. The variations in height across their length are interpreted as being related to these bedrock highs and demonstrate the stabilising effect that the bedrock constrictions had on the ice. The elongate morphology on their ice-distal side could be the result of bedrock, but most probably represent glacial lineations formed subglacially where ice was grounded, whilst glacigenic debris was pushed up to form the ridge (Benn and Evans, 2010).

5.1.3 Distribution and timing of submarine landforms in Krossfjorden

The only ice-marginal features in this area of the fjord system are OTR 1 and 2, which represent small stillstands or re-advances during a period of retreat (Ottesen *et al.*, 2007; 2008a), thus indicating an even faster retreat from the shelf than that proposed by Maclachlan *et al.* (2010). The presence of large bedrock outcrops near the fjord mouth, but without ice-marginal features, indicates that ice did not rest for an extended period at these potential pinning points. The presence of drumlins and lineations indicates either rapid flow, slow flow over a long period, or corresponds to variations of the seabed characteristics and geology (Maclachlan *et al.*, 2010). However, due to large bedrock outcrops and limited streamlined lineations, the slow flow over a long period is the preferred interpretation. The chronology and glacial events within the whole of the Krossfjorden system will be analysed further in Chapter 7.

5.2 Fjortende Julibukta

Fjortende Julibukta is a small bay approximately 3.5 km long and 1.7 km wide, leading to the ice front of Fjortende Julibreen. The bathymetric data covers the outermost 1.5 km; some 2 km from the present ice front (Fig. 5.2.1B).

There are numerous bedforms perpendicular to the bay with dimensions of around 1 to 2 m high and 50 m wide (Fig. 5.2.1A). These are interpreted as streamlined glacial lineations formed by the movement of ice on a sedimentary substrate (Ottesen and Dowdeswell, 2006). Small transverse ridges are observed with dimensions approximately 1 – 5 m high and 20 m widths (Fig. 5.2.1A, C); these are interpreted as recessional moraines, indicating a gradual retreat across the bay (Dowdeswell *et al.*, 2008). There are also possible remnants of a larger ridge at the mouth of the bay, which would be a logical pinning point as a glacier retreat would have become grounded in the significantly lower water depths of the relatively shallow bay.

There is also some occurrence of iceberg pitting on topographic highs, ranging from 40 –20 m deep (Fig. 5.2.1). They vary between 2 – 25 m wide and 0.5 – 2 m deep. Small glacigenic MTDs are observed on the slope of the side-wall of Krossfjorden, but only the most recent features near the entrance to the bay are visible, with little distinguishable evidence of MTDs towards the base of the side-wall. These MTDs would have occurred due to instabilities in the unconsolidated sediments accumulating on the apex of the 20° slope and could lead to a larger slope failure (Syvitski *et al.*, 1989; Forwick and Vorren, 2009); disruption of the sediments by icebergs is also likely to be aiding this movement (Syvitksi *et al.*, 1996; Forwick and Vorren, 2009).

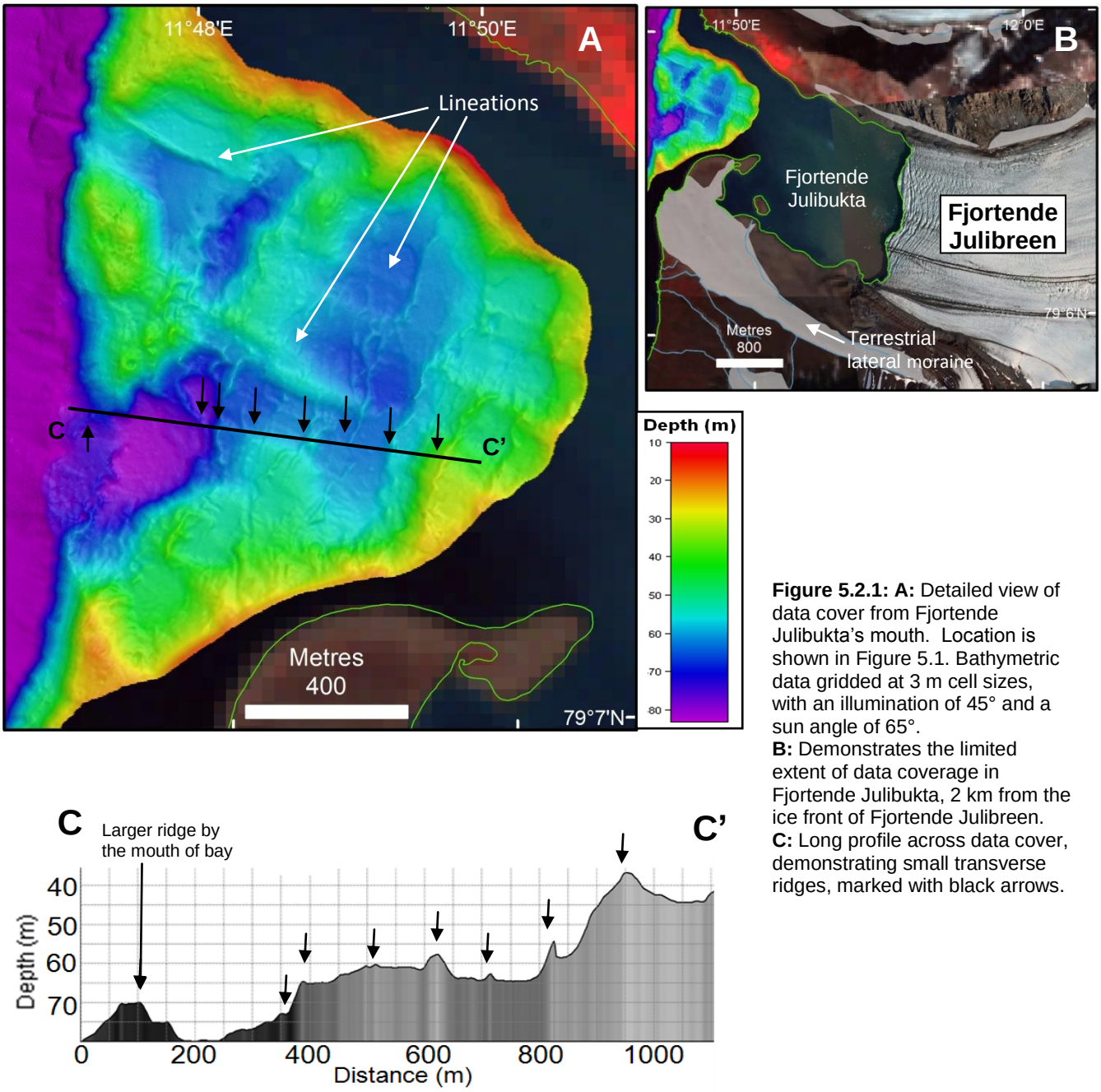

Figure 5.2.1: A: Detailed view of data cover from Fjortende Julibukta's mouth. Location is shown in Figure 5.1. Bathymetric data gridded at 3 m cell sizes, with an illumination of 45° and a sun angle of 65°.
B: Demonstrates the limited extent of data coverage in Fjortende Julibukta, 2 km from the ice front of Fjortende Julibreen.
C: Long profile across data cover, demonstrating small transverse ridges, marked with black arrows.

5.2.1 Geographical distribution

Fjortende Julibukta exhibits the same three types of landforms as observed in the other inner fjords and bays; subglacial, ice-marginal and post-glacial. The geographical distribution of these features within Fjortende Julibukta is shown in Figure 5.2.2.

The subglacial linear features show that ice covered this area and the ice-marginal features demonstrate that, during retreat of Fjortende Julibreen, a number of small stillstands or re-

advances were made within the general deglaciation of the bay. The possible remnants of a large transverse ridge at the mouth of the bay could resemble what remains of a large recessional moraine after a number of glacigenic MTDs have moved unconsolidated sediments down the fjord side-wall. The occurrence of a small ridge on the distal side of this, and the morphology of the small transverse ridge in the deep basin at the mouth of the bay, supports the concept that material is moving down the side-wall of Krossfjorden in MTDs.

It is unknown whether the landforms present at the mouth of the bay represent Fjortende Julibreen's LGM expansion into Krossfjorden and its deglaciation history or whether, because it is a known surge-type glacier, it suggests a surge since the LGM. The preferred interpretation is that these landforms are likely to represent a surge sometime between the LGM deglaciation and the LIA. This is because Fjortende Julibreen is known not to have extended this far during the LIA, at the same time the other glaciers were observed at their maximum positions, shown in Section 6.2. However, the landforms have not been covered in sediment, indicating that they are younger than the LGM deglaciation.

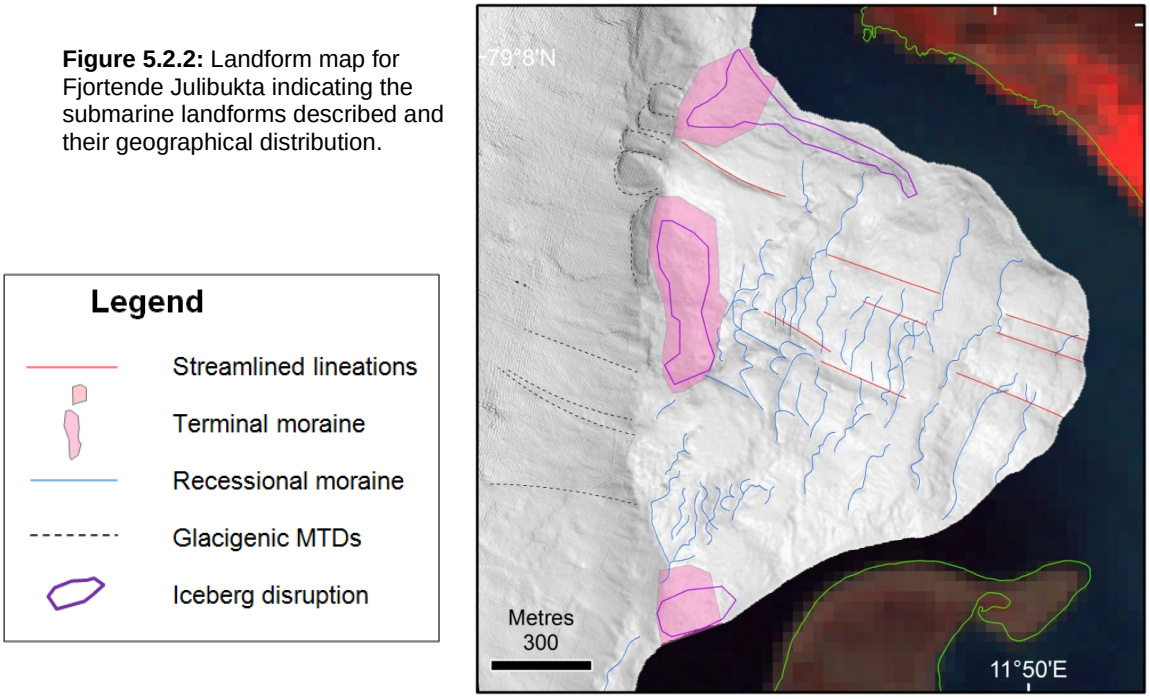

Figure 5.2.2: Landform map for Fjortende Julibukta indicating the submarine landforms described and their geographical distribution.

Chapter 6 – Acoustic, sediment cores and historical data from the Krossfjorden system

A series of acoustic survey lines and cores were taken in Krossfjorden by Sexton *et al.* (1992); these have also been discussed in Cromack (1991), Howe *et al.* (2003) and Maclachlan *et al.* (2010), and have been used to indicate how landforms developed in the fjords, the speed of ice retreat and the rate of sedimentation.

6.1 Acoustics and sediment cores

The locations of the acoustic surveys and core sites are shown with the bathymetric data from this study in Figure 6.1.

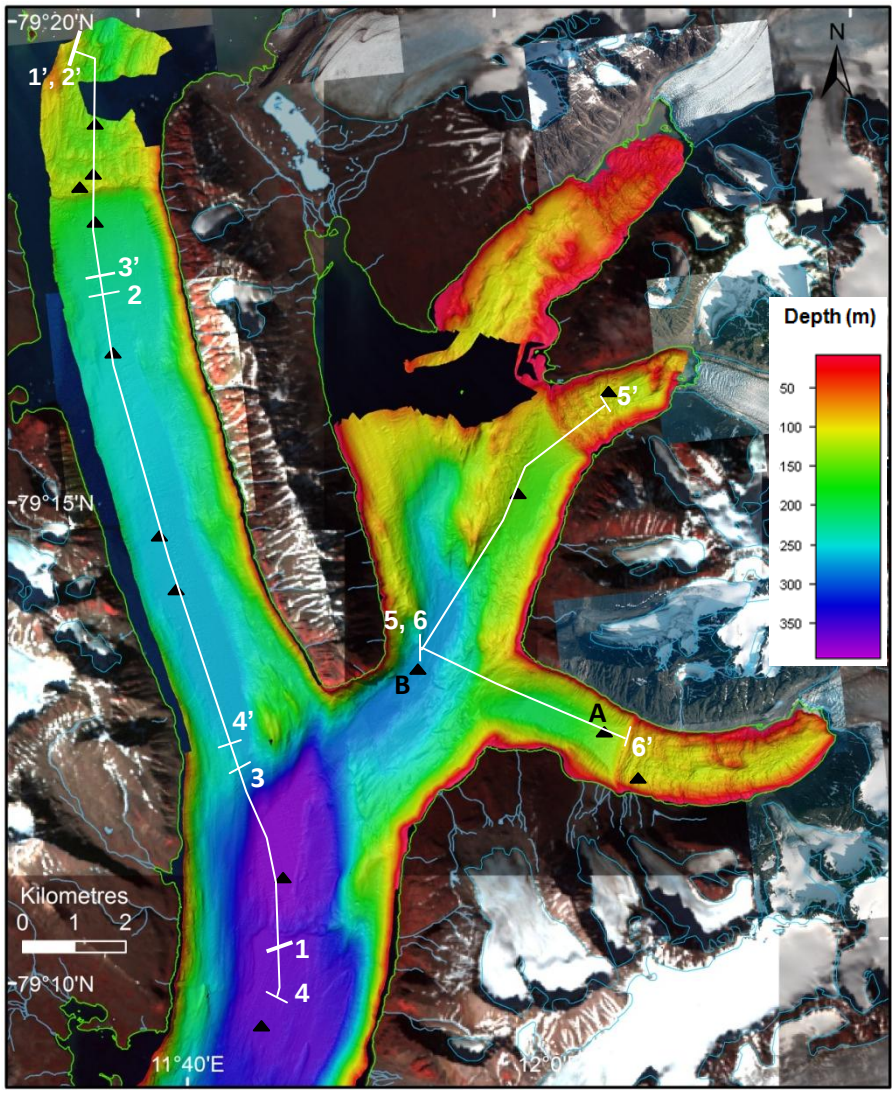

Figure 6.1: Map showing the extent of the acoustic surveys (transects **1-6**) conducted by Sexton *et al.* (1992) and the locations of gravity cores (indicated by black triangles) as well as parts A and B of Figure 6.2. Bathymetric data are gridded at a 5 m cell size with an illumination of 315°.

6.1.1 Acoustic data

The acoustic survey transects cover the majority of Lilliehöökfjorden, from the inner bay to the innermost 3 km of Krossfjorden. Additionally, two transects from Mayerbukta and Tinayrebukta were conducted, both of which lead into Möllerfjorden (Fig. 6.1). Transect 1 runs the length of Lilliehöökfjorden and the acoustic record is shown in Figure 6.1.1. The slight ridge at the mouth of the fjord is not present in the transect conducted by Howe *et al.* (2003) or in the bathymetric data, thus it is not thought to represent a significant feature.

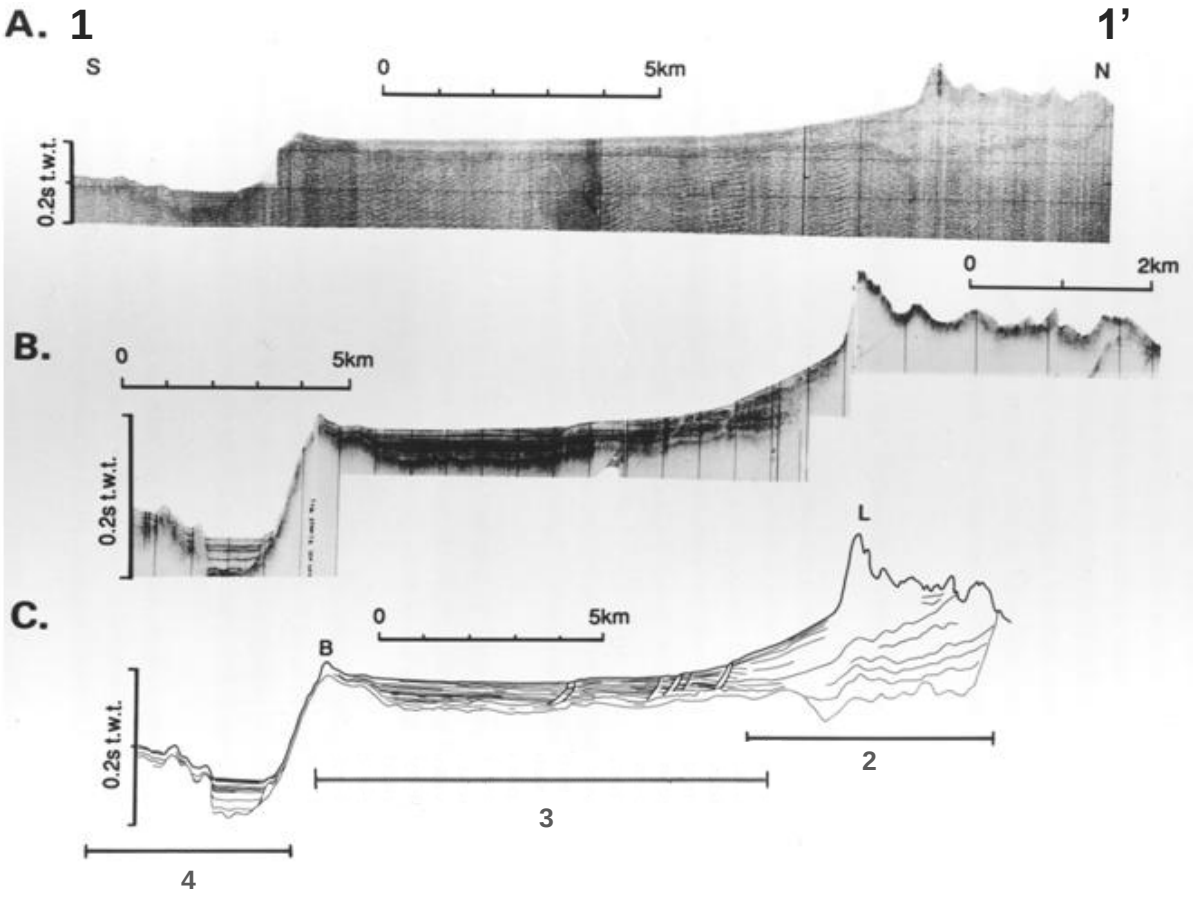

Figure 6.1.1: Acoustic profiles of sedimentary architecture in Lilliehöökfjorden. Modified from Cromack (1991). **A:** Sparker record. **B:** 3.5 kHz PDR record. **C:** Acoustic units interpreted by Sexton *et al.* (1992). B denotes the break in slope at the end of the fjord and L the large transverse ridge. The positions of the subsequent transects in Lilliehöökfjorden are given.

Transect 2 covers part of inner Lilliehöökfjorden and it is noted that, at the large transverse ridge, there is a distinct change in acoustic signature (Fig 6.1.2). Units 1 and 2 are identified within inner Lilliehöökfjorden. Unit 1 has been interpreted as representing glacimarine sediments that accumulated prior to the formation of TR1 (Fig. 6.1.2), thus correlating with unit 4 in the outer fjord; however, unit 1 was deformed by the formation of TR1 (Sexton *et*

al., 1992). Unit 2 represents a combination of reworked material from Unit 1 and glacigenic debris delivered during ice re-advance (Sexton *et al.*, 1992), implying a glacial formation. Unit 2 is covered by a thin layer of sediment accumulated after the ice front has retreated from TR1.

The presence of multiple terminal moraines in Lilliehöökfjorden has been noted by Cromack (1991), who stated that traces of two terminal moraines were identifiable on the land at the western side of the fjord. Transverse moraines can also be identified within the sparker record, which provide further supporting evidence for the ridges described as TR1, 2, 3 and 4?, from the bathymetric data (Section 3.1.1). They have around the same spacing in both the sparker record and bathymetric data. The ridges are clearly sedimentary and not composed of bedrock (Fig. 6.1.2A).

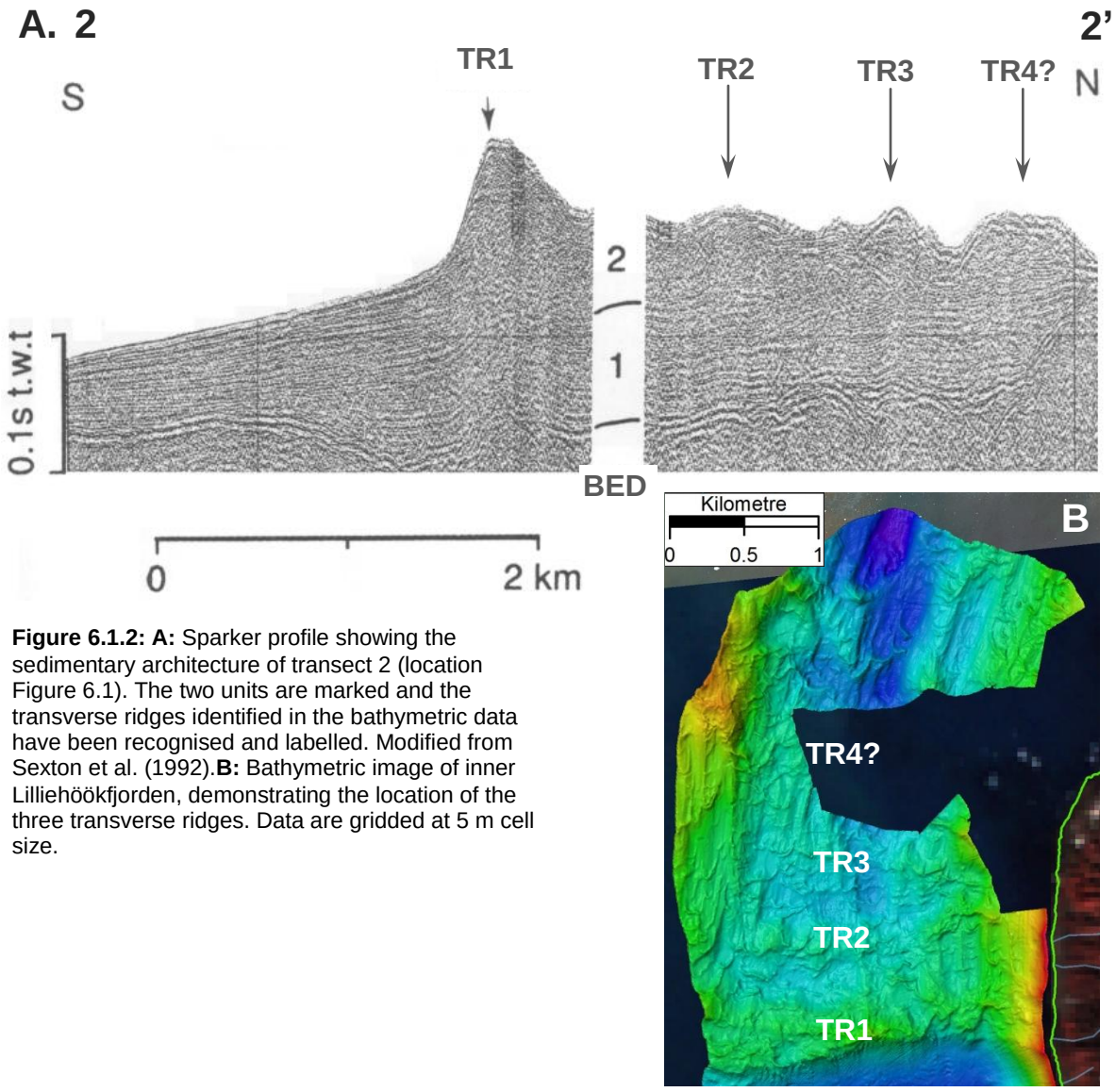

Figure 6.1.2: A: Sparker profile showing the sedimentary architecture of transect 2 (location Figure 6.1). The two units are marked and the transverse ridges identified in the bathymetric data have been recognised and labelled. Modified from Sexton et al. (1992).**B:** Bathymetric image of inner Lilliehöökfjorden, demonstrating the location of the three transverse ridges. Data are gridded at 5 m cell size.

Transect 3 of the acoustic surveys covered the ice-distal side of TR1. This record was interpreted as a sediment-filled fan complex by Sexton *et al.* (1992). Units 4a, b and 5 are identified within outer Lilliehöökfjorden (Fig. 6.1.3B); they represent sediment accumulation at differing rates, shown by acoustic laminations and thickness. However, unit 3 is interpreted as representing till, linked to an extensive ice advance and retreat (the LGM, Sexton *et al.*, 1992). This indicates that subsequent sedimentation has buried features of full-glacial origin in outer Lilliehöökfjorden, supporting the interpretation that identifying possible relict features identified in the bathymetric data here will be difficult (Section 3.2.1, Fig. 3.5B).

However, there is no evidence of a fan complex or turbidity currents, and little evidence of MTDs from the bathymetric data; thus, the outer fjord is re-interpreted as representing a smooth sediment-filled basin (Howe *et al.*, 2003), which has accumulated glacimarine sediment over a significant time (Section 3.2.1, Fig. 3.2). The packages of acoustic laminations are probably the result of rapid seasonal fluctuations in meltwater discharge (Sexton *et al.*, 1992), although each acoustic package is likely to represent a large number of annual events rather than a single year of sedimentation. The distally sloping seabed also supports this interpretation because sedimentation decreases with distance from the ice front (Zajączkowski, 2008).

Sexton *et al.* (1992) also describe slip surfaces (Fig. 6.1.3) which are interpreted to represent the small-lobe like features described by bathymetric data at the base of the large terminal moraines throughout the study fjords (Figs. 3.2, 4.6.1). This supports the interpretation of formation through movement of unconsolidated material along the shear margins of blocks of sediments.

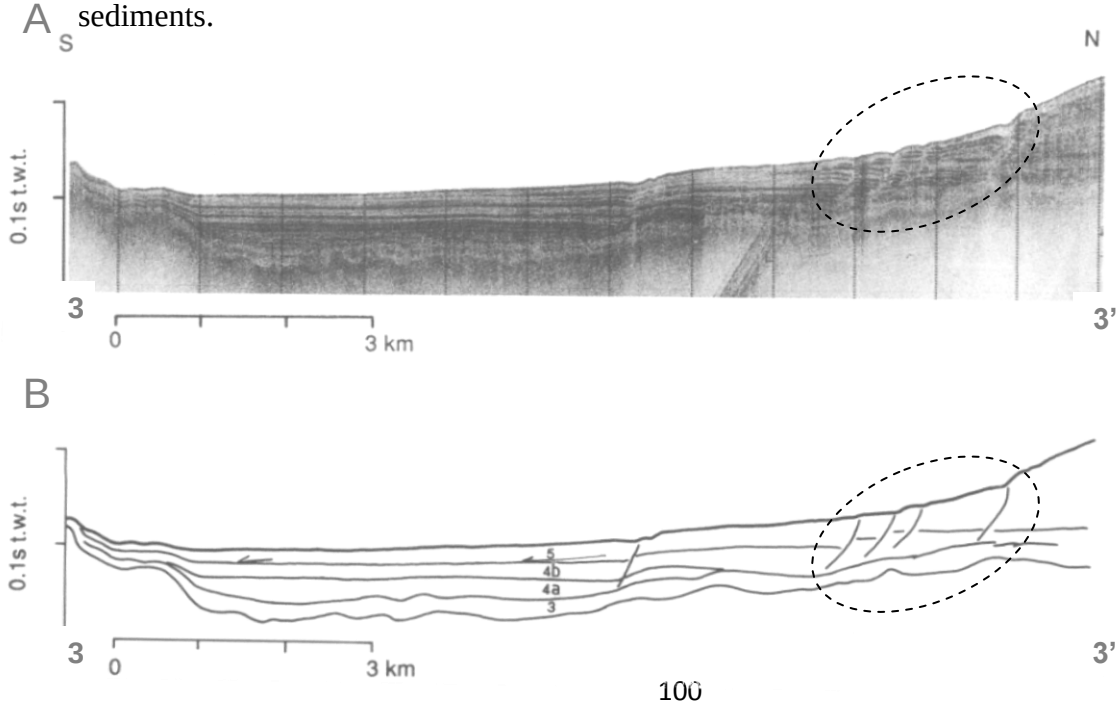

Figure 6.1.3: A: 3.5 kHz PDR record showing the sediment-filled basin. Location of transect is shown in Figure 6.1. **B:** Unit boundaries and units are labelled on the figure. Dashed black ellipses indicate the position of the small-lobe like features described along the base of TR1 in Section 3.1.1, or slip surfaces. From Sexton *et al.* (1992).

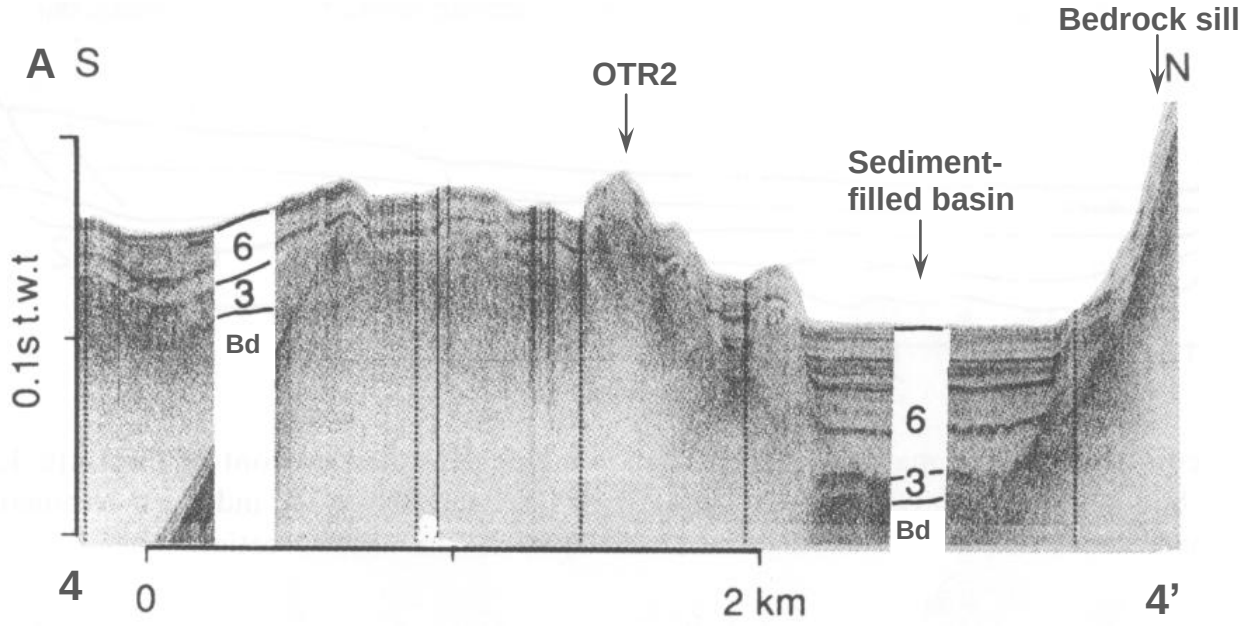

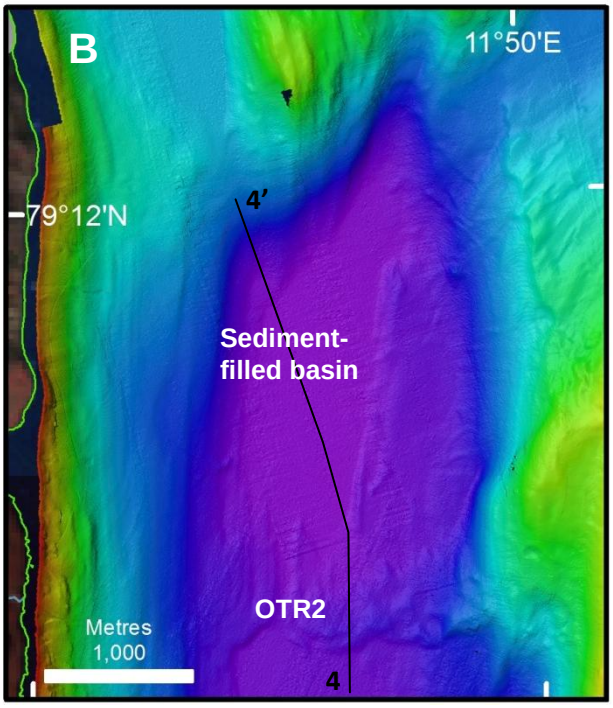

Figure 6.1.4: A: Sedimentary architecture near the cliff at the mouth of Lilliehöökfjorden. Bd denotes bedrock topography and basins and OTR2 denotes the innermost transverse ridge in Krossfjorden, described in Chapter 5. From 3.5 kHz PDR record (modified from Sexton *et al.*, 1992). **B:** Bathymetric data of the area covered by transect 4. OTR2 is again marked. The black line indicates the acoustic transect. Data are gridded at 5 m cell size.

Transect 4 extends around 3.5 km from the cliff at the mouth of Lilliehöökfjorden, interpreted as a bedrock sill, into Krossfjorden. The seismic profile in Figure 6.1.4 supports the interpretation of this sill as being composed largely of bedrock and only a thin sediment veneer. The underlying topography, including unit 3 with its glacial origin, is observed to be draped by unit 6 (Sexton *et al.*, 1992; Howe *et al.*, 2003), interpreted as sediment infilling, particularly within the deeper basins (Fig. 6.1.4A). The shallower bedrock highs have a thicker till (unit 3) above them (Sexton *et al.*, 1992) and a transverse feature is observed (Fig. 6.1.4B). This was interpreted as a fluvial channel by Howe *et al.* (2003) but on re-

examination by Maclachlan *et al.* (2010) it was interpreted as a transverse ridge, and the bathymetric data in this study support this interpretation (Section 5.1.2).

The acoustic transects in Mayerbukta and Tinayrebukta (Figs. 6.1.5, 6.1.6) exhibit very similar, although a more laterally constrained, sedimentary architecture to that observed in Lilliehöökfjorden. Before the large transverse ridges (TR1, 2, 3, 4) there is some hummocky morphology, which corresponds to the older, small transverse ridges (older STR) observed from the bathymetric data. These are attributable to older ice flow and are likely to represent deglaciation from the LGM. Both transects 5 and 6 also show a sediment-filled basin and a bedrock controlled break in slope (Sexton *et al.*, 1992). Additionally, the Mayerbukta transect (Fig. 6.1.5) also exhibits TR2, 3 and 4 (Section 4.2.1) and the hummocky morphology near the break in slope (Section 4.1.3), representing the transverse ridges described in the bathymetric data.

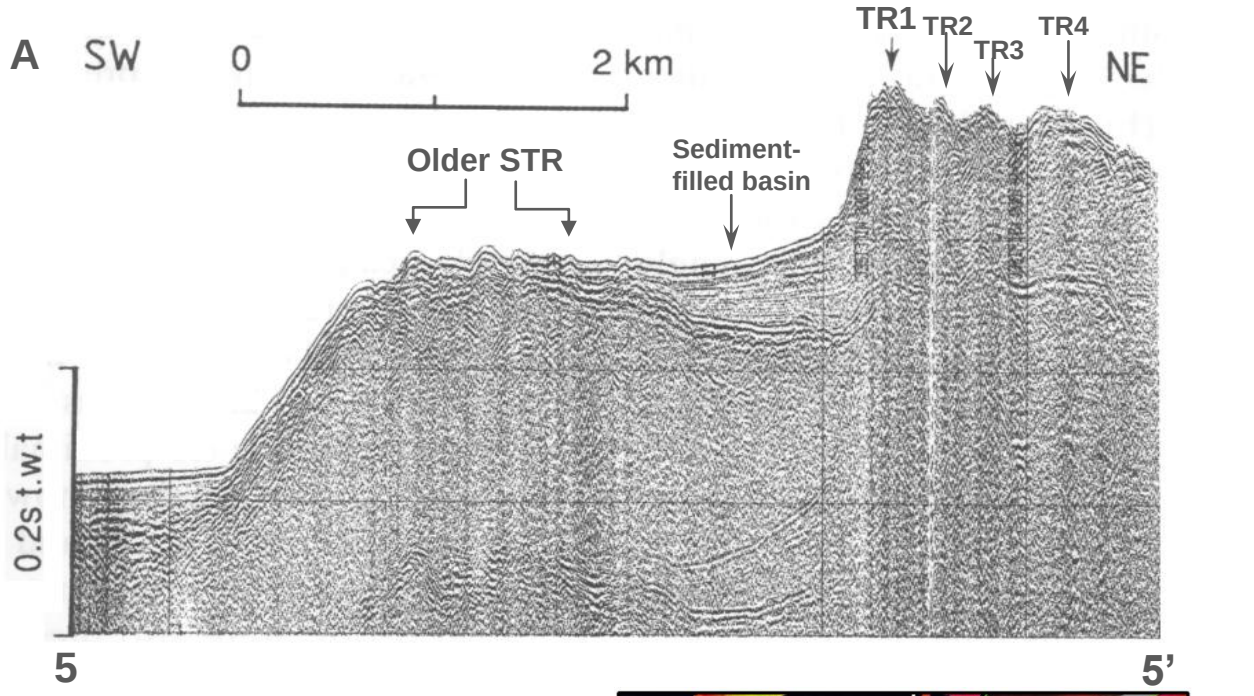

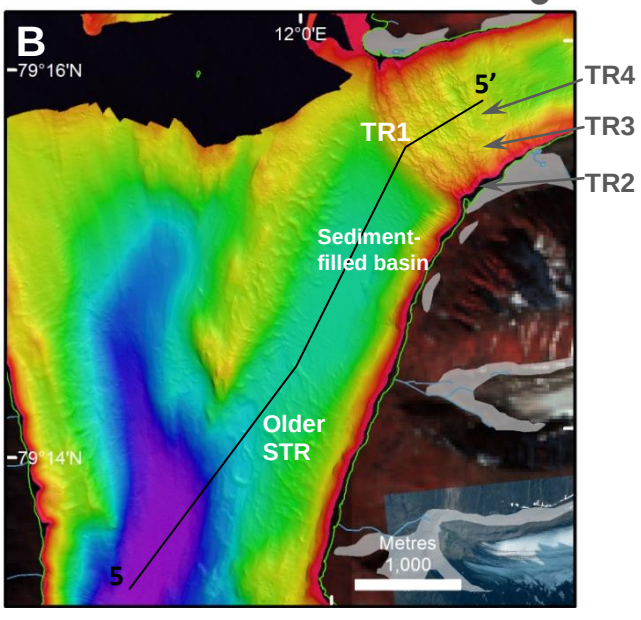

Figure 6.1.5: A: Acoustic transect 5 of Mayerbukta (Figure 6.1). TR1, 2, 3 and 4 can all be identified as well as a sediment-filled basin. STR denotes small transverse ridges. Modified from Sexton *et al.* (1992). **B:** Appearance of these features in the bathymetric data. The black line indicates the acoustic transects. Data are gridded at 2 m cell size.

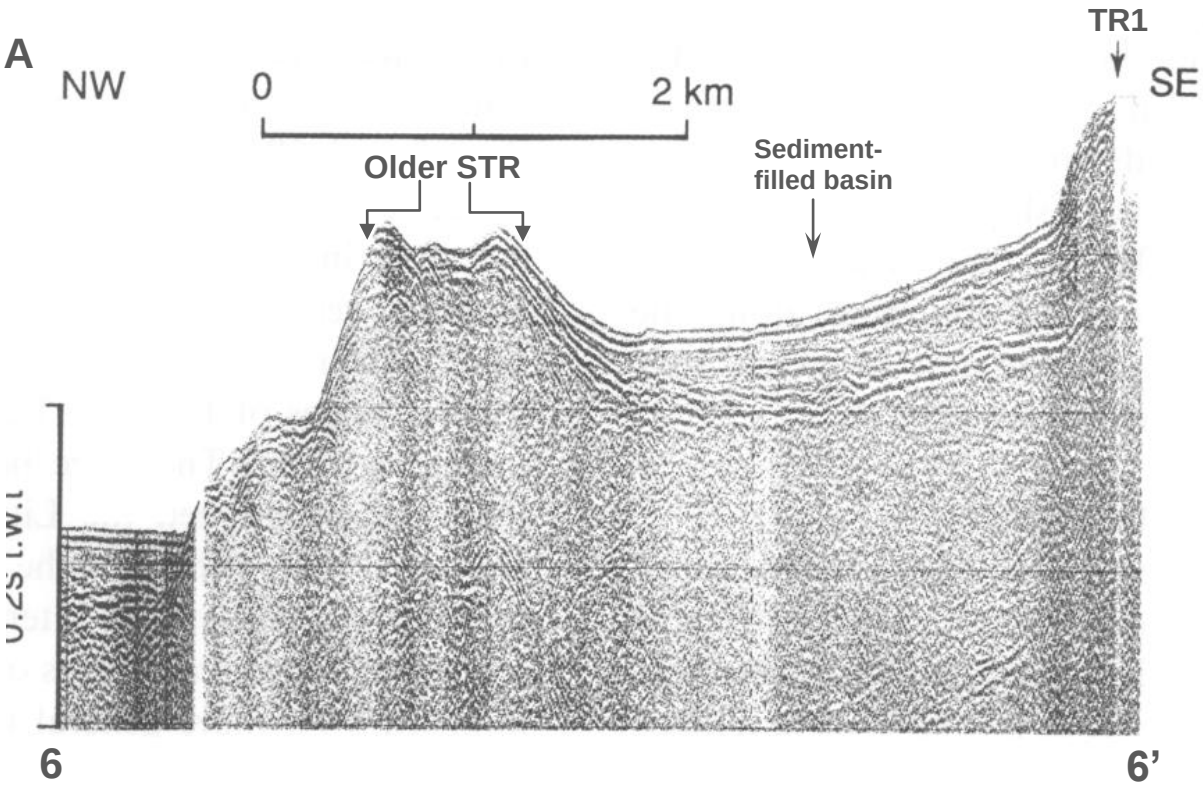

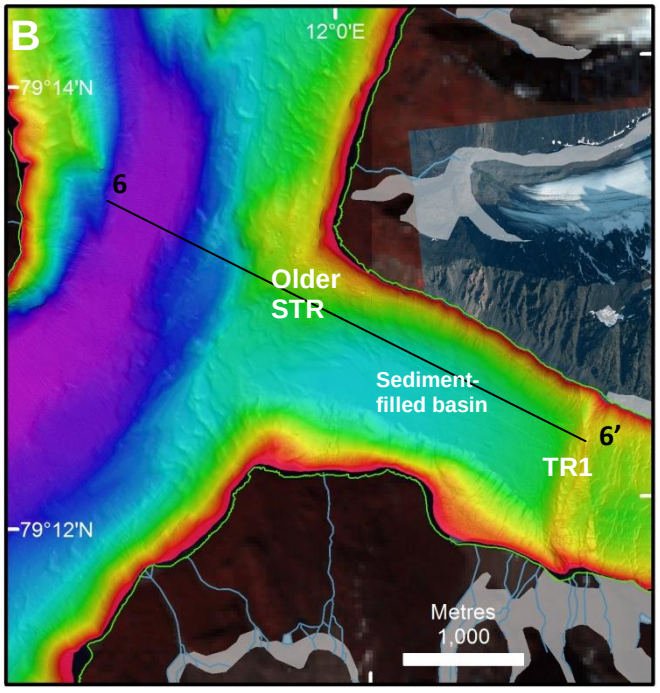

Figure 6.1.6: A: Acoustic transect 6 of Tinayrebukta (Figure 6.2). TR1 marks the boundary between the inner and outer parts of the bay. On its ice-distal side a sediment-filled basin is observed. STR denotes small transverse ridges on bedrock highs. Modified from Sexton *et al.* (1992). **B:** Appearance of these features in the bathymetric data. The black line indicates the acoustic transects. Data are gridded at 2 m cell size.

6.1.2 Gravity Cores

Logs of sediment cores presented in Sexton *et al.* (1992) and Cromack (1991) show that the inner fjords and bays of Krossfjorden consist of fine sands and clays with a large number of clasts. These clasts were interpreted as IRD and the sediment has been termed a glacimarine diamicton (Sexton *et al.*, 1992). The most ice-proximal cores in the sediment-filled basins, located in the outer fjord, are poorly sorted, silty mud (Fig. 6.2A). The sediments from these have been interpreted to be derived largely from the rainout of turbid meltwater plumes, with IRD not a significant factor (Syvitski, 1989; Cromack, 1991). Sediment cores at more ice-distal locations demonstrated increasing bioturbation and fewer sand lenses (Fig. 6.2B), indicating a smaller influence from the turbid meltwater plumes, thus a more stable environment. The sediment cores have also been calculated to have a sedimentation rate of 0.7 to 4 mm a^{-1} (Cromack, 1991).

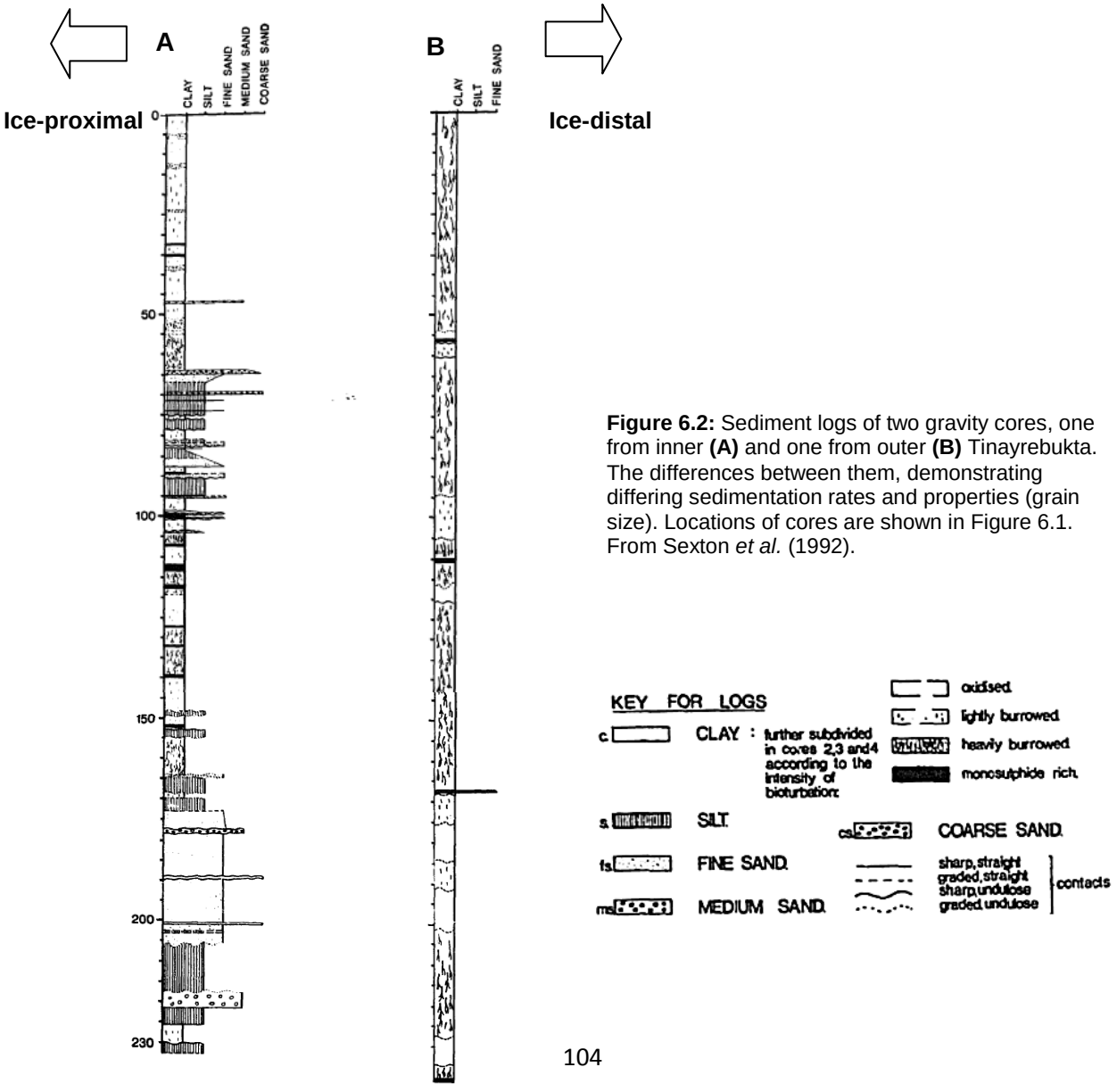

Figure 6.2: Sediment logs of two gravity cores, one from inner **(A)** and one from outer **(B)** Tinayrebukta. The differences between them, demonstrating differing sedimentation rates and properties (grain size). Locations of cores are shown in Figure 6.1. From Sexton *et al.* (1992).

6.2 Ice front positions

A painting (Fig. 1.3) and historical maps from Prince Albert I of Monaco's expedition to northwest Spitsbergen in 1906-07 and Isachsen's Norvégienne expedition in 1909-1910 (Fig. 6.3) are combined with aerial photography from the NPI's 1966 missions (Fig. 6.4) and the 1990 ice-front delineations, available on the NPI's ArcGIS server. These data give an indication of the ice fronts of the various tidewater glaciers in the Krossfjorden system in specific years, the rate of retreat of the glaciers and the variations between the fjords.

Ice front positions from 1966 photos are deemed highly accurate and have been associated with specific transverse ridges in bathymetric data. However, the delineations for the 1906-1910 period, and those of 1990, are much more subjective, with the 1990 margin clearly roughly drawn from its angular lines.

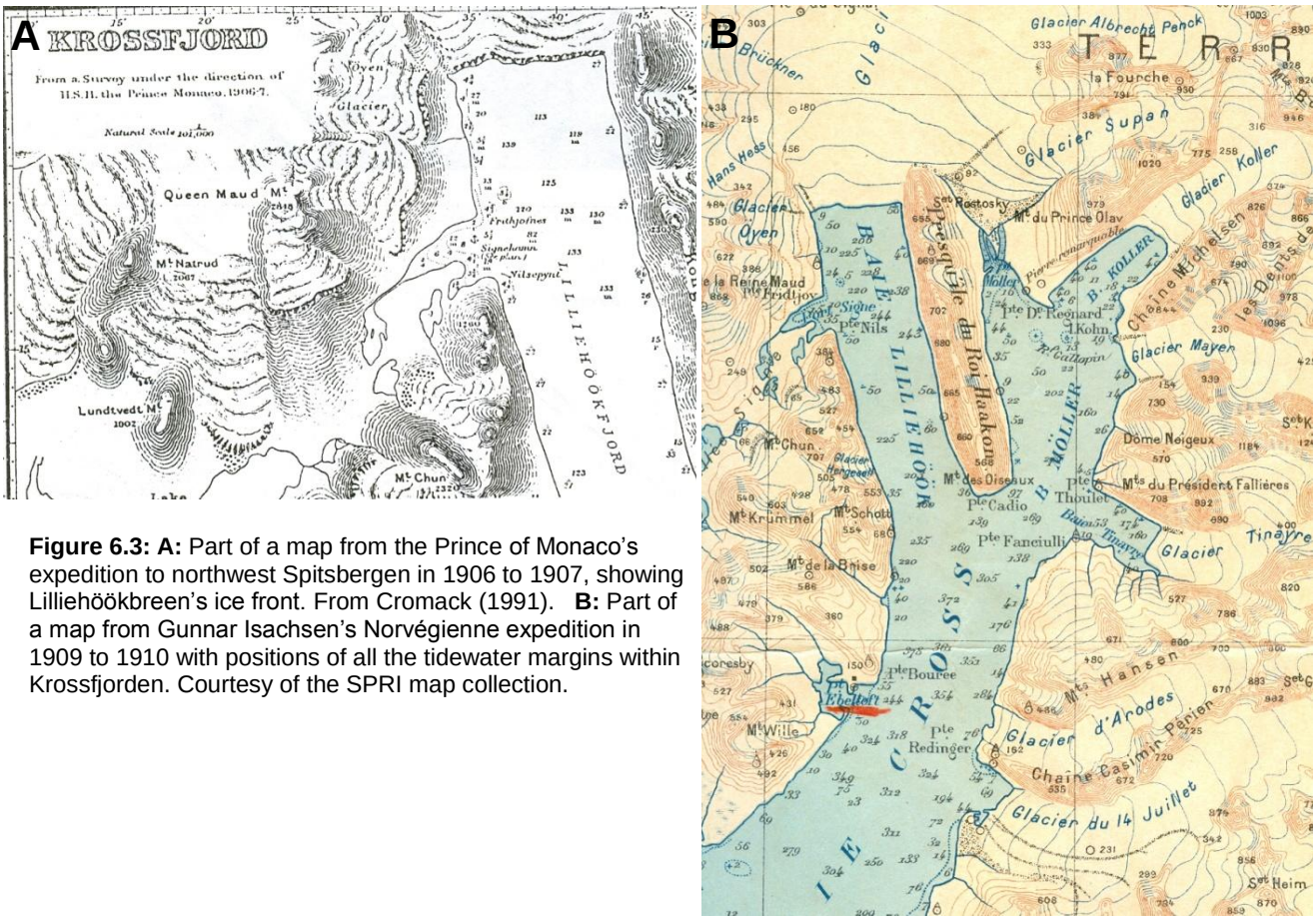

Figure 6.3: A: Part of a map from the Prince of Monaco's expedition to northwest Spitsbergen in 1906 to 1907, showing Lilliehöökbreen's ice front. From Cromack (1991). **B:** Part of a map from Gunnar Isachsen's Norvégienne expedition in 1909 to 1910 with positions of all the tidewater margins within Krossfjorden. Courtesy of the SPRI map collection.

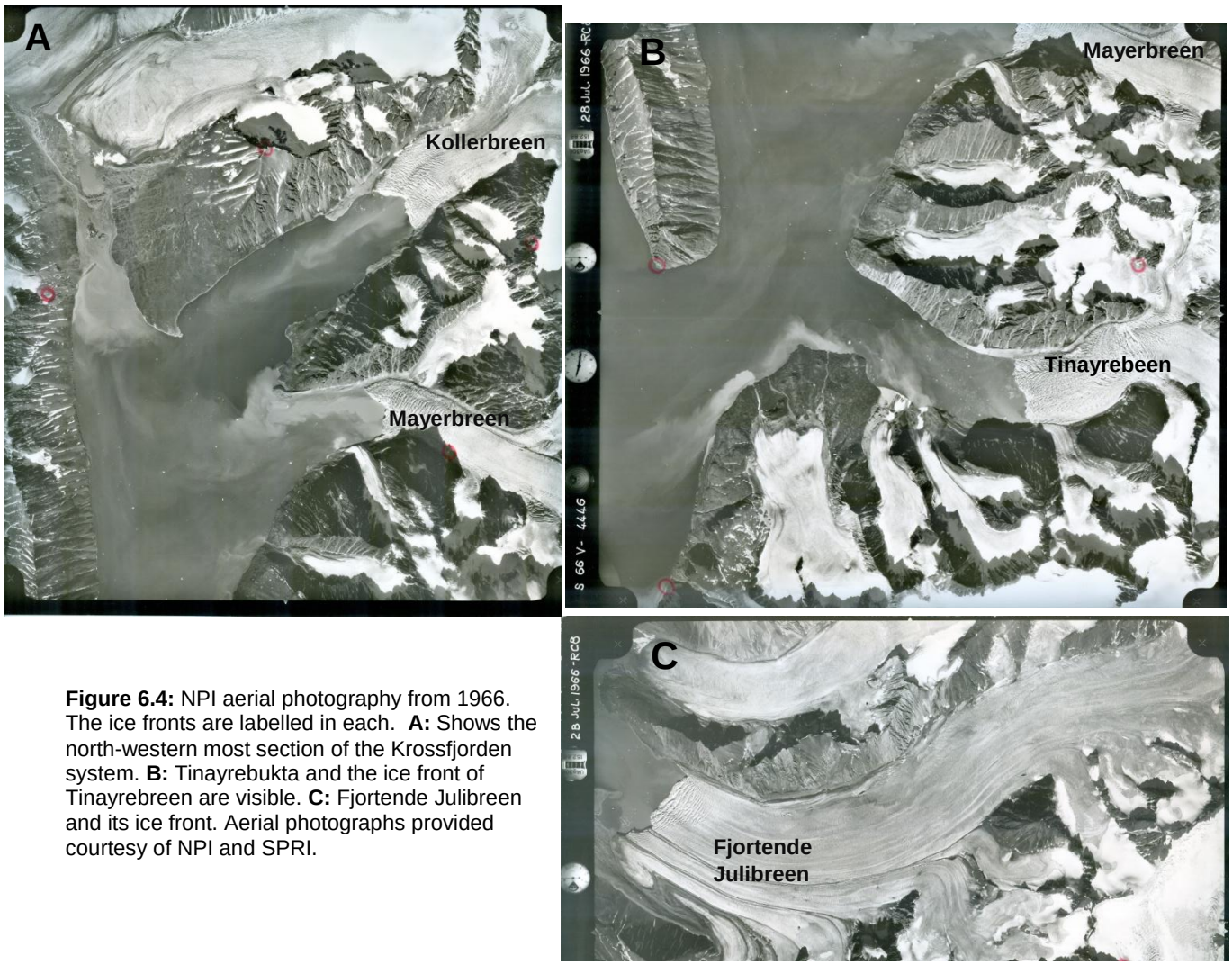

Figure 6.4: NPI aerial photography from 1966. The ice fronts are labelled in each. **A:** Shows the north-western most section of the Krossfjorden system. **B:** Tinayrebukta and the ice front of Tinayrebreen are visible. **C:** Fjortende Julibreen and its ice front. Aerial photographs provided courtesy of NPI and SPRI.

Figure 6.3 shows that the tidewater glaciers within the Krossfjorden system were all at, or proximal to, the large transverse ridges around 1907 to 1910, thus supporting the interpretation that these are terminal moraines, which had a maximum extent at this time, at the end of the LIA.

The 1966 delineation for Mayerbreen (Fig. 6.5C) shows that ice retreated faster on the southern side of the fjord but was held on the bedrock high to the north, which supports the interpretations from the bathymetric data (Sections 4.2.5, 4.2.6). Mayerbreen's subsequent retreat across the innermost shallow area has been very gradual. The 1966 photograph of Tinayrebreen (Fig. 6.5D) has a clear concave ice front which is interpreted to be a result of the bedrock outcrop resulting in lateral variations of the ice front position, with the deep central part retreating faster, but still with clear links to ridges on both the shallow northern

side and the shallows of the southern side, as interpreted from the bathymetric data (Section 4.4, Fig.4.6.3).

There are approximately 57, 37 and 79 small transverse ridges within the swath bathymetry data of Kollerfjorden, Mayerbukta and Tinayrebukta, respectively (Fig. 6.5). Given the extent of the glaciers on the earliest maps of 1906 and their positions in 1966, the majority of these must represent annual-push moraines in both Kollerfjorden and Tinayrebukta, again supporting the interpretations based on bathymetric data. The lower number of transverse ridges observed in Mayerbukta is explained by taking into consideration that retreat would have been rapid over its more featureless central part, and would have rested on the bedrock for a longer period, allowing the medium-sized ridge and ice-contact fan to form.

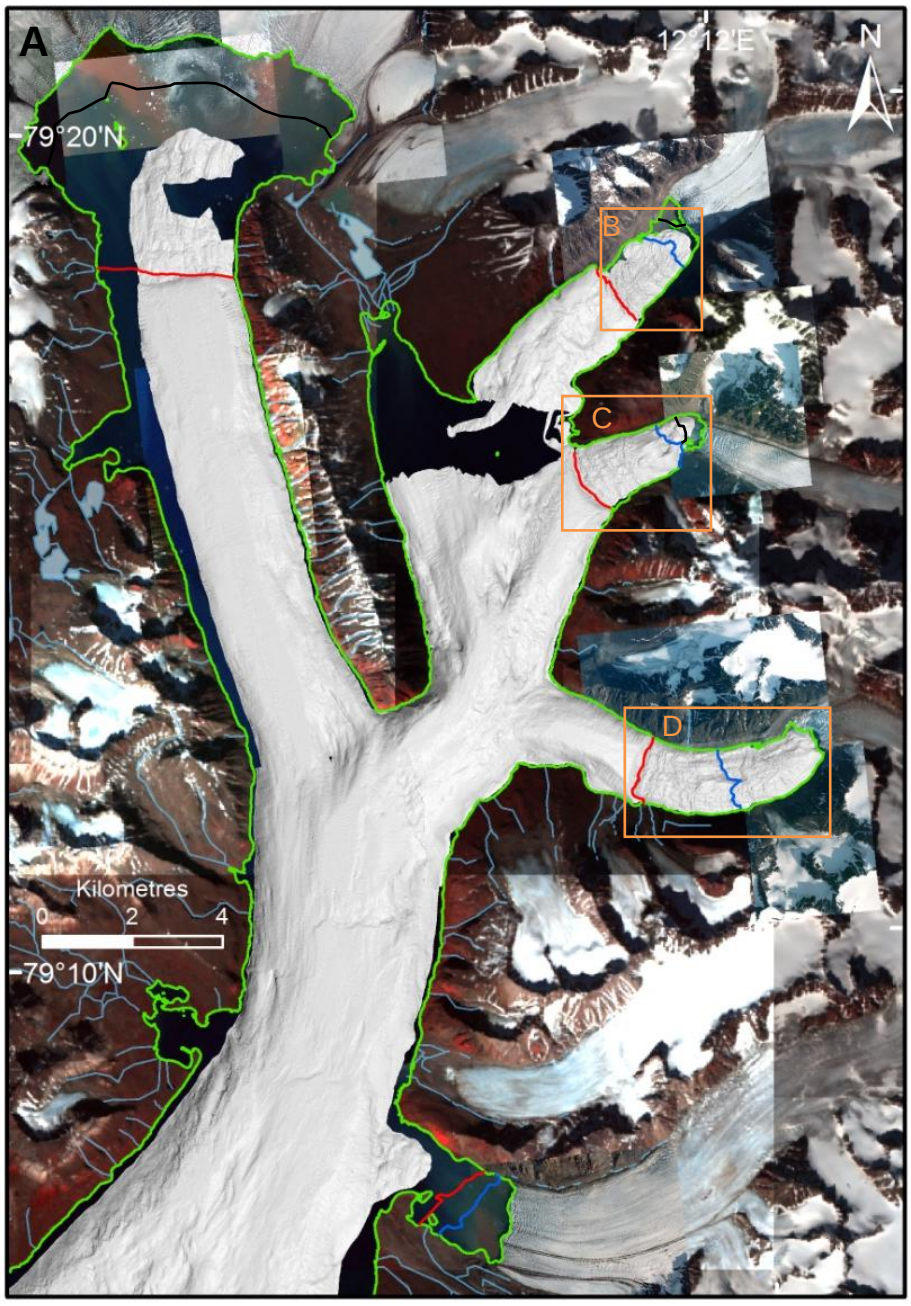

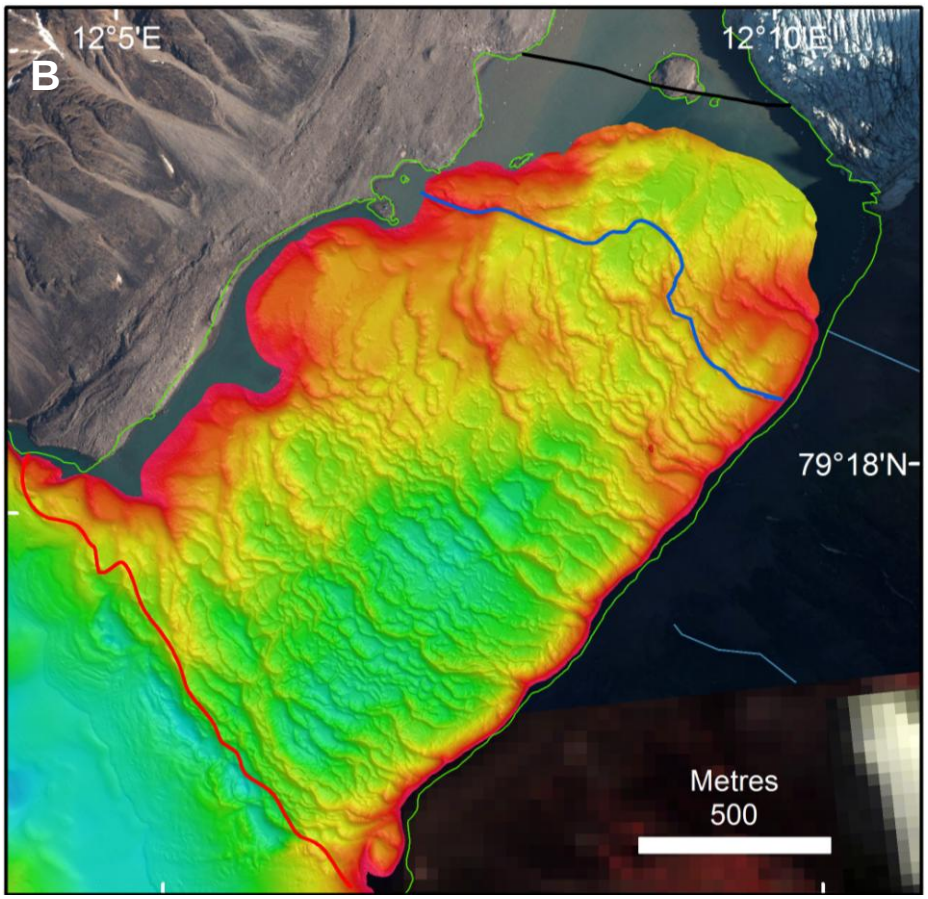

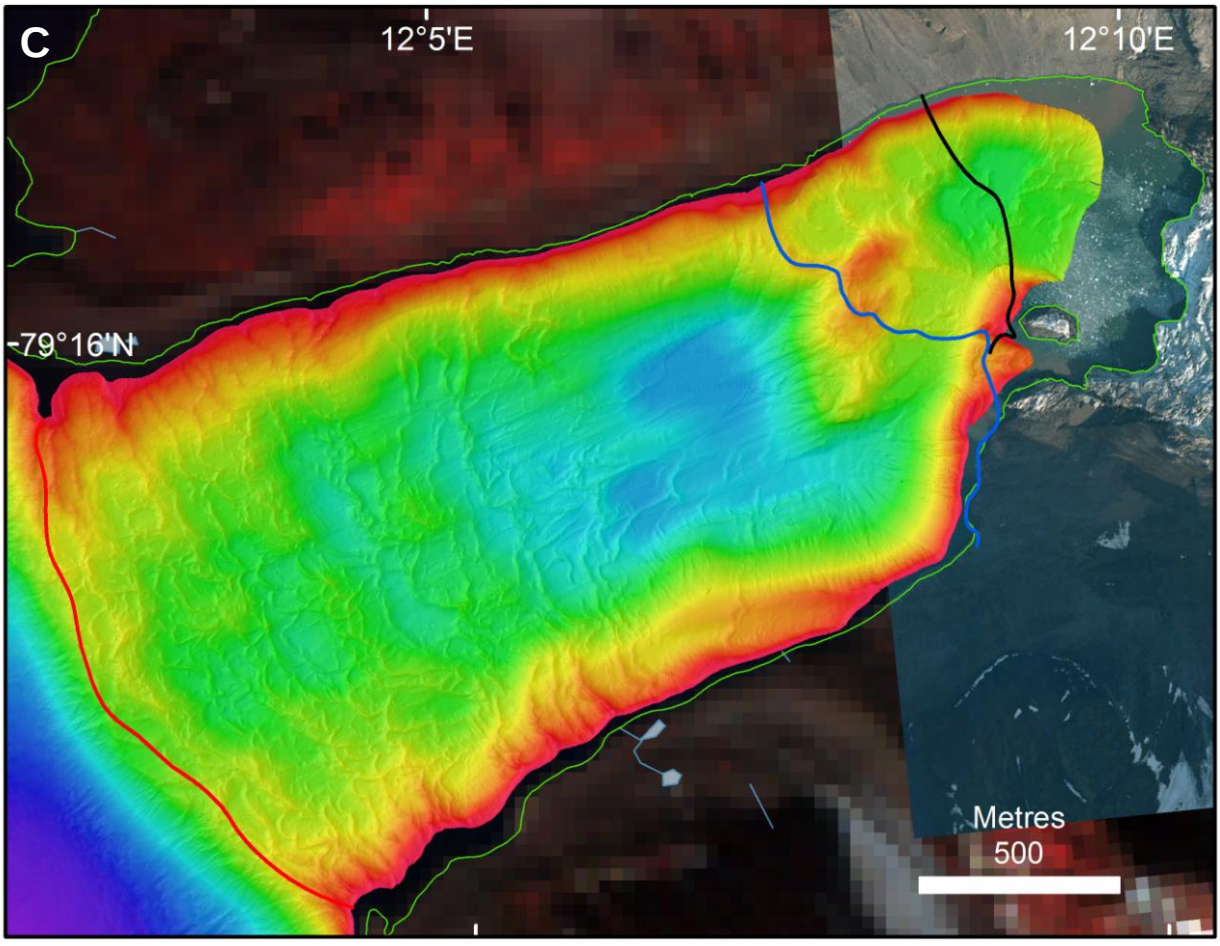

Figure 6.5: A (above): Map of study area with dated positions of the tidewater margins, where available. Red = 1906–1910, blue = 1966, black = 1990 and green is the coastline from 2009 – 2011. **B:** Detailed view of Kollerfjorden. **C:** Detailed view of Mayerbukta. **D:** Detailed view of Tinayrebukta. Bathymetric data in **B**, **C** and **D** are gridded at 1 m cell size. Note not all areas have data for each time period.

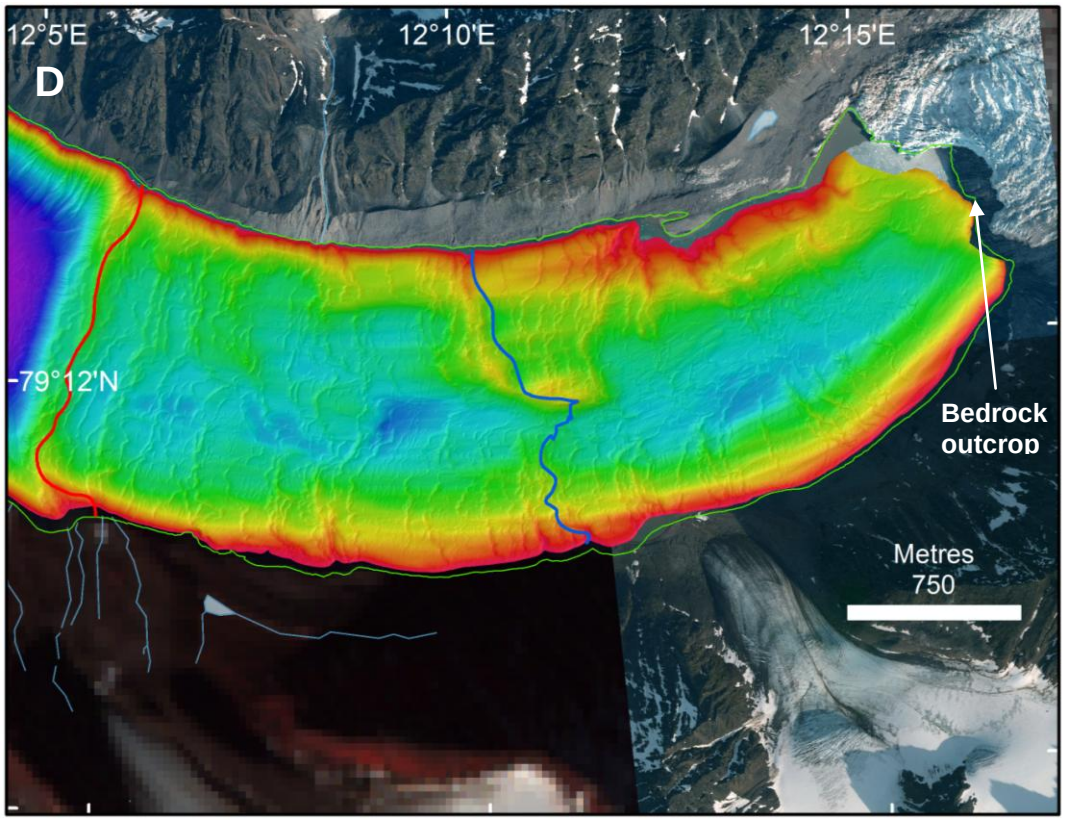

The position of the 1966 ice front shows that between 1910 and 1966 there was a retreat of 1.7 km, 2.3 km and 2.1 km for Kollerbreen, Mayerbreen and Tinayrebreen, respectively (Fig. 6.5). Subsequent to 1966 the glaciers have retreated a further 0.5 km, 0.9 km and 2 km, respectively to their present positions (Fig. 6.5). This enabled retreat rates to be calculated (Table 6.1), which indicate that ice retreat was much more rapid for the smaller glaciers of Kollerbreen and Mayerbreen in the first half of the century. In comparison Tinayrebreen's retreat rate has not declined as much over the second half of the century compared the other two glaciers. However, as Tinayrebreen can now be seen in aerial photography (Fig. 6.5D) to be partially grounded on bedrock this retreat rate is likely to be declining presently. These variations are probably the result of topographic influences linked to local geology, depth and the size of drainage basins.

Table 6.1: Calculated retreat rates for the three tidewater glaciers located within Möllerfjorden.

Date range (years)	Retreat rate (m a^{-1})		
	Kollerbreen	**Mayerbreen**	**Tinayrebreen**
1910 - 1966	30	41	37
1966 - 2009/11	11	21	46

Chapter 7 – Discussion and Conclusions

7.1 Submarine landsystems in Krossfjorden

Three landsystems have been indentified within the Krossfjorden system: subglacial, ice-marginal and post-glacial. The first, the subglacial landystem, is recognised by the presence of streamlined lineations (Fig. 3.3) and by glacially sculpted bedrock outcrops (Figs. 4.3.4, 4.4.1) which are often associated with lineations that form on their lee sides (Fig. 4.6.3). This landsystem demonstrates that ice flowed across these areas, producing and modifying landforms.

The ice-marginal landsystem refers to features formed at the ice front of a glacier. They are observed as transverse ridges (Fig. 4.6.2), which vary in scale from terminal moraines (Figs. 4.5.1, 4.6.1), to annual retreat moraines (Figs. 4.3.2, 4.5.2) depending on the length of time that the ice front is stable at a position and able to deposit sediment.

The post-glacial landsystem regards features that have formed some time after the glacier has retreated from that location. These are recognised in Krossfjorden as MTDs (Figs. 4.2.6, 4.4.3), including gullies (Figs. 4.2.5, 4.3.5), as well as iceberg ploughmarks and pitting (Figs. 4.2.4, 4.4.2).

The subglacial and ice-marginal landsystems derived from swath-bathymetric data of the Krossfjorden system can be divided into two sets: the first has features that have been interpreted to be associated with the LGM, and the second with the LIA. LGM features are recognised beyond the maximum extent of the LIA, which is clearly identifiable within the first 5 km from the four tidewater glaciers whose modern termini are located at the heads of the inner fjords. In addition, post-glacial features are frequent on and close to the side-walls of the fjords and occasionally on the relatively steep faces of moraine systems. Fortunately, the effects of these processes of sediment reworking do not significantly affect the submarine landforms associated with past glacial activity. There are notably less MTDs and gullies in Krossfjorden compared to other fjords such as the nearby Smeerenburgfjorden, northwest Spitsbergen (Ottesen and Dowdeswell, 2009; Velle, 2012); the preservation of landforms produced beneath and at the termini of former glaciers in Krossfjorden is therefore good. A partial exception is provided by the smooth sediment-filled basins of Krossfjorden and the outer parts of Lilliehöökfjorden and Möllerfjorden (Figs. 3.5. 4.2, 4.6, 5.1), where some landforms associated with the LGM at the subsequent deglaciation may have been buried and

obscured beneath the acoustically laminated sediments described in Chapter 6 (Figs. 6.1.2, 6.1.5, 6.1.6).

7.2 Past ice flow behaviour in the Krossfjorden system

The assemblages of submarine landforms within the Krossfjorden system (Figs. 3.7, 4.7) make it possible for the dynamics and style of glaciation to be inferred, both for the LGM and subsequent deglaciation and for the recent LIA advance and modern retreat of the four tidewater glaciers.

7.2.1 Implications for the ice sheet over Svalbard since the LGM

Dynamics:

The subglacial features identified between the mouths of the inner fjords and bays, marked by terminal moraines, to the limit of data extent at the mouth of Krossfjorden, are attributed to the LGM on Svalbard. Full-glacial ice filled the extensive fjord and adjacent shelf, reaching a maximum extent at the continental shelf edge west of Svalbard around 24 ka BP (Elverhøi *et al.*, 1995; Svendsen *et al.*, 2004; Jessen *et al.*, 2010) just before the onset of deglaciation in northwest Spitsbergen (Jessen *et al.*, 2010; Gjermundsen *et al.*, submitted; Hormes *et al.*, submitted). In Krossfjorden itself there are several streamlined lineations and ice sculpted bedrock features indicating the presence of an ice-stream that occupied the system at the LGM (Fig. 3.5). These glacially sculpted bedrock and sedimentary lineations demonstrate that, during the last, Late Weichselian glaciation, ice flowed through the fjords and coalesced with that in Kongsfjorden to fill the adjacent cross-shelf trough (Ottesen et al., 2005; Maclachlan et al., 2010); most such features are probably buried under the acoustically laminated sediments delivered since that time (Figs. 6.1.1, 6.1.4). There is only a limited indication, found in the submarine landform record of the Krossfjorden system, that there were two minor stillstands during ice-sheet retreat after the LGM (the transverse ridges shown in Figure 5.5.2). If there was a YD event in the area, any landforms associated with it must have been removed or buried by the LIA advance. There is no evidence for YD activity in the few seismic records we have from the area (Chapter 6).

The landform assemblage associated with the Late Weichselian glaciation observed in Krossfjorden does not seem to fit either of the schematic models for ice-stream or inter-ice-

stream landform assemblages put forward by Ottesen and Dowdeswell (2009). The Krossfjorden-Kongsfjorden system is widely interpreted to have been filled by an ice-stream at the LGM (e.g. Ottesen et al., 2005, 2007), but streamlined landforms associated with this highly dynamic ice are likely to have been buried by subsequent sedimentation in Krossfjorden.

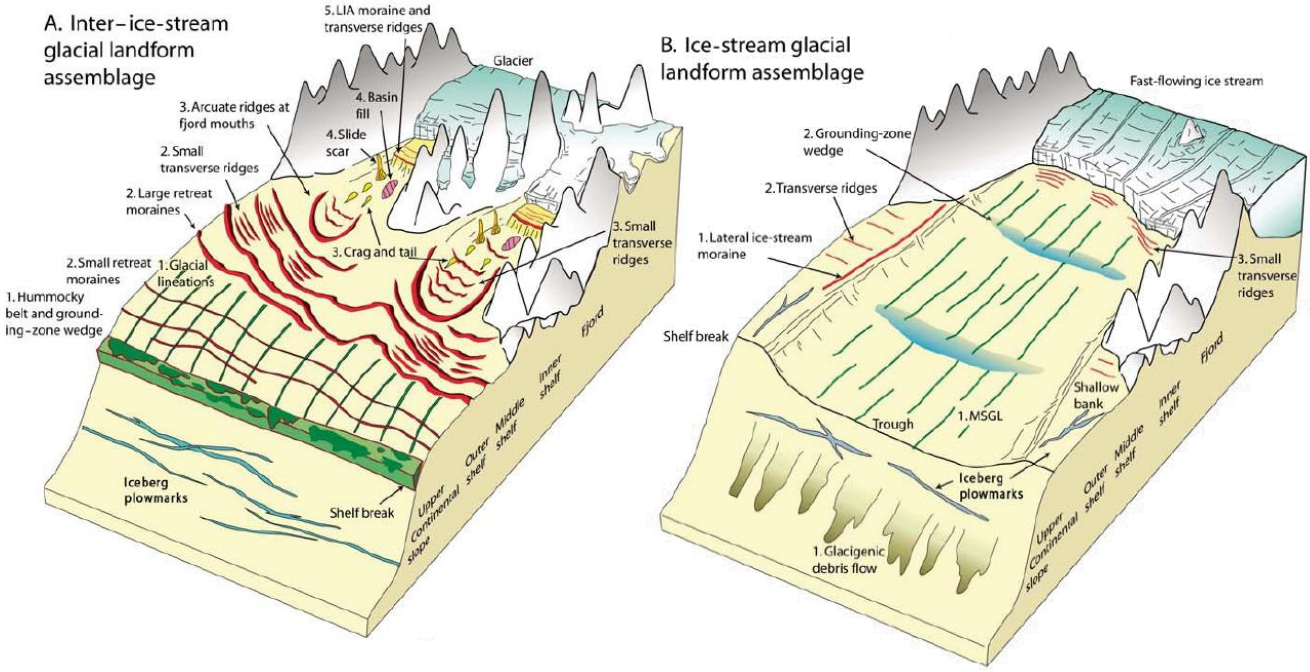

Figure 7.1: Models for inter-ice-stream (**A**) or ice-stream (**B**) landform assemblages. Features from both models have been observed in the Krossfjorden system. From Ottesen and Dowdeswell (2009).

Style of deglaciation:

The higher resolution data for Krossfjorden has made it possible for the two outermost transverse ridges, which were presented by Howe *et al.* (2003) and Maclachlan *et al.* (2010) as terminal moraines (Fig. 5.1.1), to be re-interpreted as glacially sculpted bedrock outcrops linked to the local geology and faults (Section 5). This new interpretation supports evidence for a rapid deglaciation of the outer fjord, originally put forward by Lehman and Forman (1992), but strengthened by Jessen *et al.* (2010), Gjermundsen *et al.* (2013) and Hormes *et al.* (submitted). A stillstand is likely to have occurred on the inner continental shelf, somewhere between 20.5 – 16.85 ka BP (Hormes *et al.*, submitted) and may be represented by the GZW or recessional moraine identified by Ottesen *et al.* (2007) in Kongsfjordrenna. The retreat from the inner shelf to central Krossfjorden is likely to have occurred around 15 – 14 ka BP (Hormes *et al.*, submitted). These major phases of ice-sheet retreat are likely to have been

rapid with ice thinning and decoupling from the bed, given the lack of depocentres indicative of still stands (Maclachlan *et al.*, 2010).

The first ice-marginal landforms observed are located in central Krossfjorden: these are small features indicating a relatively short stillstand at natural pinning points (Fig. 5.1.2). Their reverse-bed slope implies that the ice-front would have easily been destabilised. Ice would then have retreated to the inner fjords at the mouth of Möllerfjorden, possibly followed by a brief stillstand marked by another transverse ridge at its head, with similar morphologies to those observed in Krossfjorden. However, no strong evidence is found to indicate this in Lilliehöökfjorden, thus this stillstand is questionable and may just represent glacially sculpted bedrock at the mouth of Möllerfjorden.

The retreat within the inner fjords appears very different to the outer fjords; there is no evidence of ice-marginal features within the 12 km of outer Lilliehöökfjorden. This absence of recessional features is likely to be the result of approximately 30 m of sediment which has accumulated in the basin over the Holocene (Sexton *et al.*, 1992; Howe *et al.*, 2003). In contrast, Möllerfjorden exhibits a number of transverse ridges leading back towards the inner fjords and bays (Fig. 4.2.2). These ridges demonstrate a gradual retreat of ice (Dowdeswell *et al.*, 2008) within the shallower inner fjord system, which would have limited calving (Benn *et al.*, 2007; Gjermundsen *et al.*, submitted-B). Therefore they are likely to represent a retreat of decades to hundreds of years. However, it does appear that the central part of the ice front was floating at times in the deeper part of the fjord and this would have increased the rate of the retreat (Benn *et al.*, 2007).

7.2.2 Implications for Little Ice Age advance

The LIA age advance is identified within the submarine bathymetry – with a maximum extent which matches direct historical observations of the study tidewater glaciers at the beginning of the 20th Century, between 1906 to 1910 (Section 6.2). There are also a number of similar large terminal moraines identified on terrestrial sites and traced underwater with bathymetry across Svalbard which support this (Ottesen and Dowdeswell, 2006; 2009; Ottesen *et al.*, 2007). Some of these moraines have been lichenometrically dated and yielded ages of around 120 years (Werner, 1993) and are linked to further historical observations (Liestøl, 1988).

LIA advances of the tidewater glaciers at the heads of the Krossfjorden system varied from 2.3 km for Kollerbreen, to 5 km for Lilliehöökbreen (Fig. 6.5). Variations in distance of the

advances are likely to be linked to the size of each glaciers drainage basin, with Kollerfjorden having the smallest and Lilliehöökbreen the largest (Table 1.1). Retreat rates in Möllerfjorden varied from 30 to 41 m a^{-1} from 1910 to 1966 and 11 to 46 m a^{-1} from 1966 to the present. The speed and style of retreat appears to have been heavily affected by the depth of the fjord or bay and the presence of bedrock outcrops as well as the dimensions of the parent drainage basins (Table 1.1). Shallower areas and bedrock outcrops assist longer or more regular stillstands or even small re-advances and are probably a major reason for Mayerbukta's slower retreat rate between 1966 and 2009.

The two or three overrun transverse ridges in inner Lilliehöökfjorden and Mayerbukta may be related to possible stillstands during LIA advance to the maximum position marked by the most distal terminal moraine of each fjord. These ridges have been associated with post-LIA activity by Cromack (1991) but their submarine geomorphology indicates that they have in fact been overrun, cross-cut and modified by LIA features and therefore an older relative age is proposed. However, acoustic records show that these must only have been formed slightly earlier than the LIA terminal moraine because they consist of the same acoustic structure (Sexton *et al.*, 1992).

The reason for the occurrence of overrun transverse moraines in inner Lilliehöökfjorden and Mayerbukta is not clear. The landform assemblages of the two areas are somewhat similar to landform models produced for surging tidewater glaciers by Ottesen and Dowdeswell (2006) because of these ridges (Fig. 7.1). This supports the proposal put forward by Błaszczyk *et al.* (2009) that Mayerbreen could be a surge-type glacier and suggests Lilliehöökbreen, or subsidiaries of it, may also be of surge-type. However, crevasse-squeezed ridges are not clearly identifiable within the data, and these are believed to be an important feature used to indicate glacier surges (Evans and Rea, 2011; Fig. 7.1A). Hooked lineations could represent minor crevasse-squeezed ridges but they are located further away from the LIA maximum extent than would be expected; crevasse-squeezed ridges are associated with surge stagnation near the terminal moraine (Evans and Rea, 2011). These ridges have been observed to be poorly developed from known surge-type landform assemblages in Van Keulenfjorden and Van Mijenfjorden, southern Spitsbergen (Ottesen *et al.*, 2008b); however they remained identifiable in these other fjords.

Additionally, there is no indication of large debris lobes on the distal-slope of the LIA terminal moraines or of extensive lineations produced during the advance of a surging

glacier, both of which are associated with surge-type glaciers on Svalbard (Fig. 7.1; Ottesen & Dowdeswell, 2006; Ottesen *et al.*, 2008b). None of the glacier inventories include Mayerbreen (except Błaszczyk *et al.*, 2009) or Lilliehöökbreen (Section 1.2.1) and the majority of the landforms present would be expected from a regular LIA advance. Therefore, it seems unlikely that the overridden moraines represent previous surges. The preferred explanation is that they represent multiple small advances which were stable for some time before further advancing, until reaching the LIA maximum extent.

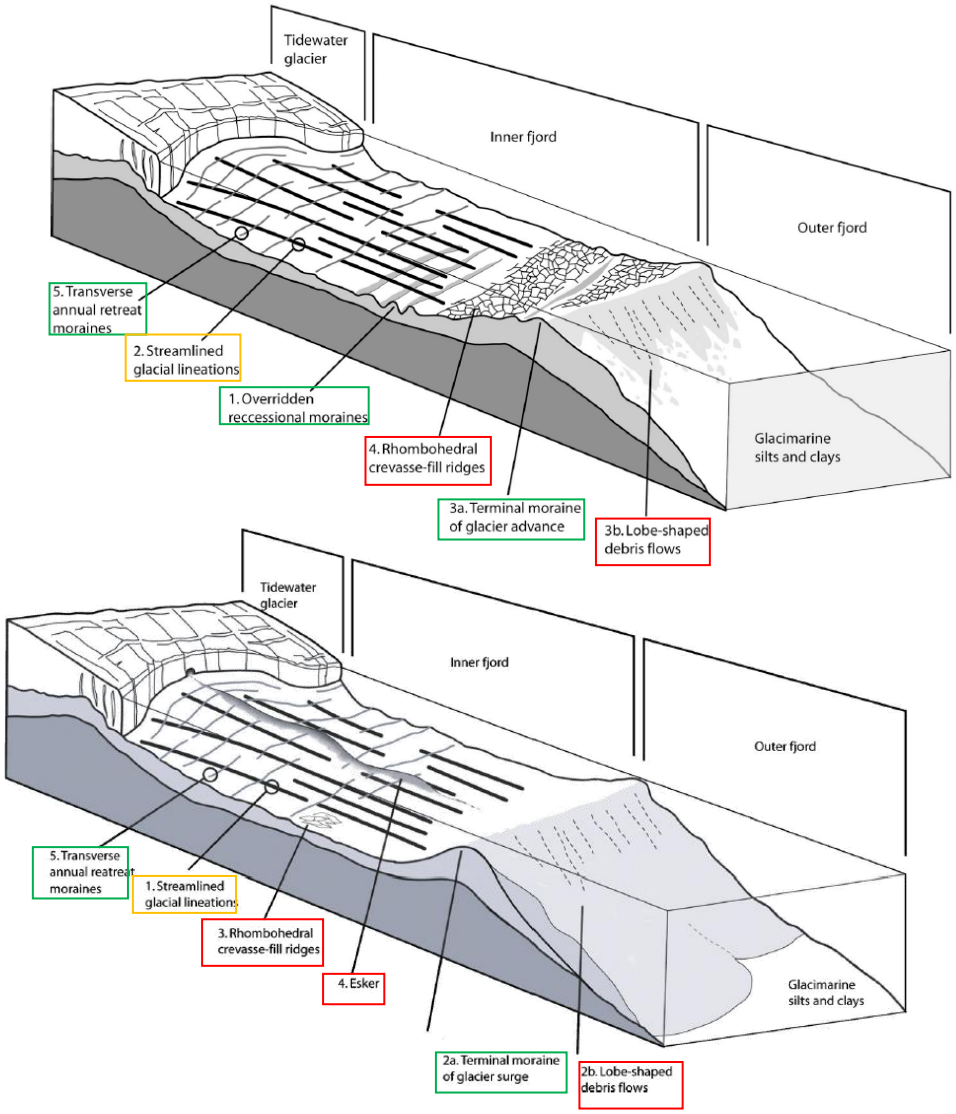

Figure 7.2: The two models put forward for surge-type tidewater glaciers on Svalbard. **A** is from Ottesen and Dowdeswell (2006) and **B** is from Ottesen *et al.* (2008b). Green indicates features observed at both Lilliehöökfjorden and Mayerbukta, amber indicates features that were observed but were not as prevalent as described for surging glaciers and red indicates features that were not observed within the study fjords.

7.3 Concluding summary

The bathymetric data within this thesis reveal that the Krossfjorden system exhibits subglacial, ice-marginal and post-glacial landform assemblages. These assemblages are summarized for each of the component fjords of the Krossfjorden system in Figures 3.7 and 4.7.

Ice flow dynamics within the fjord during the LGM are likely to have included the presence of a fast-flowing ice-stream that filled both the fjord and the adjacent cross-shelf trough. Ice in Krossfjorden probably retreated relatively rapidly from the continental shelf to the central fjord where there were two small stillstands (5.1.2), with an ice-stream which was likely to have been decoupled from the bed between these pauses. This rapid retreat is likely to have occurred around 15 – 14 ka BP. It was followed by another relatively rapid retreat to the inner fjord areas. The inner fjords appear to have had a more gradual retreat; however, there is no evidence to support this in Lilliehöökfjorden. The glaciers are likely to have been decoupled frequently from the bed at the central deepest parts of these inner fjords. Bedrock highs are frequently observed to have had a control on recessional moraines and are in some cases streamlined.

The LIA maximum extent is clearly identifiable through the presence of large transverse-to-flow terminal moraines, and provides high levels of detail for a recent ice-advance and subsequent retreat (Figs. 3.7, 4.7). This has allowed individual landform features to be visualised at exceptional resolutions (1 m horizontally at best), leading to the identification and descriptions of low-relief features, such as hooked lineations (Figs. 3.3, 4.3.3). The formation of these hooked lineations is currently unknown; however, it is thought that they may represent crevasse-squeezed ridges or minor glacitectonic thrusting.

Tidewater glacier advances varied from 2.3 to 5 km with retreat rates of 30 – 41 m a^{-1} from 1910 to 1966 and 11 – 46 m a^{-1} from 1966 to the present. The pattern of their retreat has been attributed to drainage basin size, fjord depth and the presence of bedrock outcrops as pinning points.

The landform features observed in Fjortende Julibukta also demonstrates that Fjortende Julibreen must have surged, reaching the side-wall of Krossfjorden at some point in the Holocene, post LGM and pre-LIA. There is limited evidence that all or part of

Lilliehöökbreen and perhaps Mayerbreen may also be of surge-type, but there is only limited overlap with the landforms assemblage model of Ottesen and Dowdeswell (2006).

7.4 Further research

This thesis provides a comprehensive analysis of the submarine landforms identified within the Krossfjorden system in northwest Svalbard. Swath-bathymetric data of a similarly high resolution are available for parts of the adjacent Kongsfjorden. Given more time, it would be useful to undertake a similar analysis of the submarine landforms in this nearby fjord, to test whether the landform assemblages in this area are similar or otherwise to those in Krossfjorden.

The acquisition and analysis of further acoustic data from the Krossfjorden system would also be useful in setting the submarine landforms discussed in this thesis in a stronger stratigraphic perspective.

A greater number of sediment cores from the fjord system should also provide material that could be radiocarbon dated, providing a more constrained absolute chronology for Krossfjorden. This would provide a stronger link between dates from marine cores and the terrestrial ages provided by CRN and radiocarbon dating (Hormes *et al.*, submitted), contributing to a more constrained chronology for land-sea interactions in the whole region.

8. Bibliography

Alfred Wegener Institut (2013). *Polarstern's multibeam system*. URL: http://www.awi.de/fileadmin/user_upload/News/2013_2/IBCSO/Polarstern_bathy_ping_w.jpg [12/04/2013].

Andersen, E.S., Dokken, T.M., Elverhøi, A. Solheim, A. and Fossen, I. (1996): Late Quaternary sedimentation and glacial history of the western Svalbard continental margin. *Marine Geology*, v. **133**, p. 123-156.

Barnes, P.W. and Lien, R. (1988). Icebergs rework shelf sediments to 500m off Antarctica. *Geology*, v. **16**, p. 1130-1133

Barrie, J.V., Lewis, C.F.M., Parrot, D.R. and Collins, W.T. (1992). Submersible observations of an Iceberg Pit and Scour on the Grand Banks of Newfoundland. *Geo-Marine Letters*, v. **12**, p. 1-6.

Batchelor, C.L., Dowdeswell, J.A. and Hogan, K.A. (2011). Late Quaternary ice flow and sediment delivery through Hinlopen Trough, Northern Svalbard margin: Submarine landforms and despositional fan. *Marine Geology*, v. **284**, p.13-27.

Batchelor, C.L. and Dowdeswell, J.A. (in press). The physiography of high Arctic cross-shelf troughs. *Quaternary Science Reviews*.

Bergh, S.G., Maher, H.D. and Braathen, A. (2000). Tertiary divergent thrust directions from partitioned trasnpression, Brøggerhalvøya, Spitsbergen. *Nor. Geo. Tidsskr.*, v. 80, p. 63-82.

Benn, D.I., Warren, C.R. and Mottram, R.H. (2007). Calving processes and the dynamics of calving glaciers. Earth-Science Reviews, v. 82, p. 143-179.

Benn, D.I. and Evans, D.J.A. (2010). Sediment-Landform Associations. In: *Glaciers and Glaciation*. 2nd Ed. Chennai, India: Hodder Education.

Bennett, R.M. (2001). The morphology, structural evolution and significance of push moraines. *Earth-Science Reviews*, v. **53**, p. 197-236.

Bennett, M. R. (2003). "Ice streams as the arteries of an ice sheet: their mechanics, stability and significance." *Earth-Science Reviews*, v. **61** (3-4), p. 309-339.

Bondevik, S., Mangerud, J., Ronnert, L. and Salvigsen, O. (1995): Postglacial sea-level history of Edgeøya and Barentsøya, eastern Svalbard. *Polar Research*, v. **14** (2), p. 153-180.

Boulton, G.S., van der Meer, J.J.M., Hart, J., Beets, D., Ruegg, G.H.J., van der Wateren, F.M. and Jarvis, J. (1996). Till and moraine emplacement in a deforming bed surge – an example from a marine environment. *Quaternary Science Reviews*, v. **15**, p. 961-987.

Boulton, G.S., van der Meer, J.J.M., Beets, D.J., Hart, J.K. and Ruegg, G.H.J. (1999). The sedimentary and structural evolution of a recent push moraine complex: Holmstrømbreen, Spitsbergen. *Quaternary Science Reviews*, v. **18**, p. 339-371.

Bradwell, T. (2004). Annual moraines and summer temperatures at Lambatungnajökull, Iceland. *Arctic, Antarctic and Alpine Research*, v. **36** (4), p. 502-508.

Brückner, H. and Schellmann, G. (2003): Late Pleisocene and Holocene shorelines of Andréeland, Spitsbergen (Svalbard) – geomorphological evidence and palaeo-oceanographic significance. *Journal of Coastal Research*, v. **19** (4), p, 971-982.

Burki, V., Larsen, E., Fredin, O. and Margreth, A. (2009). The formation of sawtooth moraine ridges in Bødalen, western Norway. *Geomorphology*, v. **105**, p. 182-192.

Clark, C.D. (1993). Mega-scale glacial lineations and cross-cutting ice-flow landforms. *Earth Surface Processes and Landforms*, v. **18**, p. 1-19.

Cottier, F., Tverberg, V., Inall, M., Svendsen, H., Nilsen, F. and Griffiths, C. (2005). Water mass modification in an Arctic fjord through cross-shelf exchange: the seasonal hydrography of Kongsfjorden, Svalbard. *Journal of Geophysical Research*, v. **110**. doi: 10.1029/2004JC002752

Cottier, F.R., Nilsen, F., Inall, M.E., Gerland, S., Tverberg, V. and Svendsen, H. (2007). Wintertime warming of an Arctic shelf in response to large-scale atmospheric circulation. *Geophysical Research Letters*, v. **34**. doi: 10.1029/2007GL029948

Cottier, F.R., Nilsen, F., Skogseth, R., Tverberg, V., Skarðhamar, J. and Svendsen, H., (2010). Arctic fjords: a review of the oceanographic environment and dominant physical processes. In: Howe, J.A., Austin, W.E.N., Forwick, M. and Paetzel, M. (eds.): *Fjord systems and archives*. Geological Society, London, Special Publications (eds.), v. **344**, p. 35 - 50, doi: 10.1144/SP344.4

Cromack, M. (1991). A Glacial Sedimentary System in Northwest Spitsbergen. Unpublished *PhD thesis,* University of Cambridge, p. 1-225.

Damuth, J.E. (1978) Echo character of the Norwegian-Greenland Sea: relationship to Quaternary sedimentation. *Marine Geology*, v. **28**, p. 1-36.

Dokken, T.M. and Hald, M. (1996). Rapid climatic shifts during the isotope stages 2-4 in the Polar North Atlantic. *Geology*, v. **24** (7), p. 599–602.

Dowdeswell, J.A. (1986). The distribution and character of sediments in a tidewater glacier, southern Baffin Island, N.W.T., Canada. *Arctic and Alpine Research*, v. **18**, p. 45-56.

Dowdeswell, J.A. (1989). On the nature of Svalbard icebergs. *Journal of Glaciology*, v. **35** (120), p. 224-234.

Dowdeswell, J.A. and Dowdeswell, E.K. (1989). Debris in icebergs and rates of glacimarine sedimentation: observations from Spitsbergen and a simple model. *Journal of Geology*, v. **97**, p. 221-231.

Dowdeswell, J.A., Hamilton, G.S. and Hagen, J.O. (1991). The duration of the active phase on surge-type glaciers: contrasts between Svalbard and other regions. *Journal of Glaciology*, v. **37** (127), p. 388-400.

Dowdeswell, J.A. and Forsberg, C.F. (1992). The size and frequency of icebergs and bergy bits derived from tidewater glaciers in Kongsfjorden, northwest Spitsbergen. Polar Research, v. **11** (2), p. 81-91.

Dowdeswell, J.A., Villinger, H., Whittington, R.J. and Marienfeld, P. (1993). Iceberg scouring in Scoresby Sund and on the East Greenland continental shelf. *Marine Geology*, v. **111**, p. 37-53.

Dowdeswell, J.A., Elverhøi, A. and Spielhagen, R. (1998). Glacimarine sedimentary processes and facies on the Polar North Atlantic margins. *Quaternary Science Reviews*, v. **17**, p. 243-272.

Dowdeswell, J.A. and Siegert, M.J. (1999): Ice-sheet numerical modeling and marine geophysical measurements of glacier-derived sedimentation on the Eurasian Arctic continental margins. *GSA Bulletin*, v. **111** (7), p. 1080-1097.

Dowdeswell, J.A. and Elverhøi, A. (2002): The timing of initiation off fast-flowing ice streams during a glacial cycle inferred from glacimarine sedimentation. *Marine Geology*, v. **188**, p. 3-14.

Dowdeswell, J.A. and Benham, T.J. (2003). A surge of Perseibreen, Svalbard, examined using aerial photography and ASTER high resolution satellite imagery. *Polar Research*, v. **22** (2), p.373-283.

Dowdeswell, J.A., Ó Cofaigh, C. and Pudsey, C.J. (2004). Thickness and extent of the subglacial till layer beneath an Antarctic paleo-ice stream. *Geology*, v. **32**, p. 13-16.

Dowdeswell, J.A., Ottesen, D. and Rise, L. (2006). Flow switching and large-scale deposition by ice streams draining former ice sheets. *Geology*, v. **34**, p. 313 - 316.

Dowdeswell, J.A., Ottesen, D., Evans, J., Ó Cofaigh, C. and Anderson, J.B. (2008). Submarine glacial landforms and rates of ice-stream collapse. *Geology*, v. **36**, p. 819-822.

Dowdeswell, J.A., Jakobsson, M., Hogan, K.A., O'Regan, M., Backman, J., Evans, J., Hell, B., Lowemark, L., Marcussen, C., Noormets, R., Sellen, E. and Solvsten, M. (2010). High-resolution geophysical observations of the Yermak Plateau and northern Svalbard margin: implications for ice-sheet grounding and deep-keeled icebergs. *Quaternary Science Reviews*, v. **29**, p. 3518-3531.

Dowdeswell, J.A. and Vásquez, M. (2013). Submarine landforms in the fjords of southern Chile: implications for glacimarine processes and sedimentation in a mild glacier-influenced environment. *Quaternary Science Reviews*, v. **64**, p. 1-19.

Dowdeswell, J.A., Hogan, K.A., Ó Cofaigh, C., Fugelli, E.M., Evans, J. and Noormets, R. (in press). Late Quaternary ice flow in a West Greenland fjord and cross-shelf trough system: submarine landforms from Rink Isbrae to Uummannaq shelf and slope. Quaternary *Science Reviews*.

Ebbesen, H., Hald, M. and Eplet, E.H. (2007). Lateglacial and early Holocene climatic oscillations on the western Svalbard margin, European Arctic. *Quaternary Science reviews*, v. **26**, p. 1999 – 2011.

Elverhøi, A. (1984). Glacigenic and associated marine sediments in the Weddell Sea, fjords of northwest Spitsbergen and the Barents Sea: a review. *Marine Geology*, v. **57**, p. 53-88.

Elverhøi, A., Fjeldskaar, W., Solheim, S., Nyland-Berg, M. and Russwurm, L. (1993): The Barents Sea Ice Sheet – a model of its growth and decay during the last ice maximum. *Quaternary Science Reviews*, v. **12**, p. 863-873.

Elverhøi, A., Andersen. E.S., Dokken, T., Hebbeln, D., Spielhagen, R., Svendsen, J.I., Sørflaten, M., Rørnes, A., Hald, M. and Forsberg, C.F. (1995) The growth and decay of the Late Weichselian Ice Sheet in Western Svalbard and adjacent areas based on provenance studies of marine sediments. *Quaternary Research*, v. **44**, p. 303-316.

Elverhøi, A., Dowdeswell, J.A., Funder, S., Mangerud, J. and Stein, R. (1998): Glacial and oceanic history of the polar north Atlantic margins: an overview. *Quaternary Science Reviews*, **17**, p. 1-10.

Evans, J., Dowdeswell, J.A., Ó Cofaigh, C., Benham, T.J. and Anderson, J.B. (2006). Extent and dynamics of the West Antarctic Ice Sheet on the outer continental shelf of Pine Island Bay during the last glaciation. *Marine Geology*, v. **230**, p. 53-72.

Forman, S.L. (1990): Post-glacial relative sea-level history of northwestern Spitsbergen, Svalbard. *Geological Society of America Bulletin*, v. **102** (11), p. 1580-1590.

Forman, S.L., Lubinski, D.J., Ingólfsson, Ó., Zeeberg, J.J., Snyder, J.A., Siegert, M.J. and Matishov, G.G. (2004): A review of postglacial emergence on Svalbard, Franz Josef Land and Novaya Zemlya, northern Eurasia. *Quaternary Science Reviews*, v. **23**, p. 1391-1434.

Forwick, M. and Vorren, T.O. (2002).Deglaciation history and post-glacial mass movements in Balsfjord, northern Norway. *Polar Research*, v. **21** (2), p. 259-266.

Forwick, M. and Vorren, T.O. (2007). Holocene mass-transport activity and climate in outer Isfjorden, Spitsbergen: marine and subsurface evidence. *The Holocene*, v. **17** (6), p. 707-716.

Forwick, M., Baeten, N.J. and Vorren, T.O. (2009). Pockmarks in Spitsbergen fjords. *Norwegian Journal of Geology*, v. **89**, p. 65-77.

Forwick, M. and Vorren, T.O. (2009). Late Weichselian and Holocene sedimentary environments and ice rafting in Isfjorden, Spitsbergen. *Palaeogeography, Palaeoclimatology, Palaeoecology*, v. **280**, p. 258–274.

Forwick, M. and Vorren, T.O. (2010). Stratigraphy and deglaciation of the Isfjorden area, Spitsbergen. *Norwegian Journal of Geology*, v. **90**, p. 163-179.

Forwick, M., Vorren, T.O., Hald, M., Korsun, S., Roh, Y., Vogt, C. and Yoo, K-C. (2010). Spatial and temporal influence of glaciers and rivers on the sedimentary environment in Sassendfjorden and Tempelfjorden, Spitsbergen. In: Howe, J.A., Austin, W.E.N, Forwick, M. & Paetzel, M. (eds.): *Fjord Systems and Archives*. Geological Society, London, Special Publication, v. **344**, p. 163-193.

Forwick, M., and Vorren, T.O. (2012). Mass wasting in Isfjorden, Spitsbergen. In: Yamada, Y., Kawamura, K., Ikehara, K., Ogawa, Y., Urgeles, R., Mosher, D., Chaytor, J. & Strasser, M. (eds.): *Submarine Mass Movements and Their Consequences*. Advances in Natural and Technological Hazards Research, v. **31**, p. 711-722.

Gales, J.A., Larter, R.D., Mitchell, N.C. and Dowdeswell, J.A. (2013). Geomorphic signature of Antarctic submarine gullies: Implications for continental slopes processes. *Marine Geology*, v. **337**, p. 112-124.

Gammelsrød, T. and Rudels, B. (1983). Hydrographic and current measurements in the Fram Strait, August 1981. *Polar Research*, v. **1** (2), p. 115 – 126.

Gjermundsen, E.F., Briner, J.P., Akçar, N., Salvigsen, O., Kubik, P., Gantert, N. and Hormes, A. (2013). Late Weichselian local ice dome configuration and chronology in Northwestern Svalbard, - early thinning, late retreat. *Quaternary Science Reviews*, v. **72**, p. 112-127.

Gjermundsen, E.F., Briner, J.P., Akçar, N., Foros, J., Kubik, P.W., Salvigsen, O. and Hormes, A. (Submitted-A). Arctic alpine topography minimally carved during repeated Quaternary glaciation. Reviewed by *Nature Geoscience*.

Gjermundsen, E.F., Forwick, M., Briner, J.P., Janson, M., Akçar, N., Kubik, P. and Hormes, A. (Submitted-B). Slow deglaciation of north Spitsbergen fjords. Submitted to *Geology*.

GLIMS Technical Report (2012). *Randolph Glacier Inventory: A Dataset of Global Glacier Outlines, Version 2.0.* URL: http://www.glims.org/RGI/RGI_Tech_Report_V2.0.pdf [29/03/2013].

Hagen, J.O. (1988). Glacier surge in Svalbard with examples from Usherbreen. *Norsk geogr. Tidsskr.*, v. **42**, p. 203-213.

Hagen, J. O., Liestøl, O., Roland, E. and Jørgensen, T. (1993). Glacier Atlas of Svalbard and Jan Mayen. *Norsk Polarinstitutt Meddelelser*, Nr. **129**, Oslo.

Hambrey, M.J. and Huddart, D. (1995). Englacial and proglacial glaciotectonic processes at the snout of a thermally complex glacier in Svalbard. *Journal of Quaternary Science*, v. **10** (4), p. 313-326.

Harms, A.A.P., Tverberg, V. and Svendsen, H. (2007). Physical qualification and quantification of the water masses in the Kongsfjorden-Krossfjorden system cross section. *OCEANS 2007 – Europe*. doi: 10.1109/OCEANSE.2007.4302332

Hogan, K.A. (2008). The geomorphic and sedimentary record of glaciation on high-latitude continental margins with particular reference to the Northeastern Svalbard margin. *Unpublished Ph.D. Thesis*, University of Cambridge, 227 p.

Hogan, K.A., Dowdeswell, J.A., Noormets, R., Evans, J. and Cofaigh, C.Ó. (2010a). Evidence for full-glacial flow and retreat of the Late Weichselian Ice Sheet from the waters around Kong Karls Land, eastern Svalbard. *Quaternary Science Reviews*, v. **29**, p. 3563 - 3582.

Hogan, K.A., Dowdeswell, J.A., Noormets, R., Evans, J., Cofaigh, Ó. and Jakobsson, M. (2010b). Submarine landforms and ice-sheet flow in Kvitøya Trough, northwestern Barents Sea. *Quaternary Science Reviews*, v. **29**, p. 3545 - 3562.

Hormes, A., Gjermundsen, E.F. and Rasmussen, T.L. (Submitted). From mountain top to the deep sea - deglaciation in 4D of the northwestern Barents Sea Ice sheet. Submitted to *Quaternary Science Reviews*.

Hovland, M. (1983). Elongated depressions associated with pockmarks in the western slope of the Norwegian trench. *Marine Geology*, v. **51**, p. 35-46.

Israelson, C., Buchardt, B., Funder, S. and Hubberten, H.W. (1994). Oxygen and carbon isotope composition of Quaternary bivalve shells as a water mass indicator: Last interglacial and Holocene, East Greenland. *Palaeogeography, Palaeoclimatology, Palaeoecology*. v. **111**, p. 119–134.

Jakobsson, M., Mayer, L.A., Coakley, B., Dowdeswell, J.A., Forbes, S., Fridman, B., Hodnesdal, H., Noormets, R., Pedersen, R., Rebesco, M., Schenke, H.-W., Zarayskaya, Y. Accettella, A.D., Armstrong, A., Anderson, R.M., Bienhoff, P., Camerlenghi, A., Church, I., Edwards, M., Gardner, J.V., Hall, J.K., Hell, B., Hestvik, O.B., Kristoffersen, Y., Marcussen, C., Mohammad, R., Mosher, D., Nghiem, S.V., Pedrosa, M.T., Travaglini, P.G., and

Weatherall, P. (2012). The International Bathymetric Chart of the Arctic Ocean (IBCAO) Version 3.0, *Geophysical Research Letters*, doi: *10.1029/2012GL052219*.

Jessen, S.P., Rasmussen, T.L., Nielsen, T. and Solheim, A. (2010). A new Late Weichselian and Holocene marine chronology for the western Svalbard slope 30,000 – 0 cal years BP. *Quaternary Science Reviews*, v. **29**, p. 1301-1313.

Jiskoot, H., Boyle, P. and Murray, T. (1998). The incidence of glacier surging in Svalbard: evidence from multivariate statistics. *Computers & Geosciences*, v. **24** (4), p. 387-399.

Jiskoot, H., Murray, T. and Boyle, P. (2000). Controls on the distribution of surge-type glaciers in Svalbard. Journal of Glaciology, v. **45** (5), p. 412-422.

Jones, G.A. and Keigwin, L.D. (1988). Evidence from Fram Strait (78° N) for early deglaciation. *Nature*, v. **336**, p. 56-59.

King, E.C., Hindmarsh, R.C.A. and Stokes, C.R. (2009). Formation of mega-scale glacial lineations observed beneath a West Antarctic ice stream. *Nature Geoscience*, v. **2**, p. 585-588.

Kleiber, H.P., Knies, J. and Niessen, F. (2000). The Late Weichselian glaciation of the Franz Victoria Trough, northern Barents Sea: ice-sheet extent and timing. *Marine Geology*, v. **168**, p. 25–44.

Klekowski, R.Z., Weslawski, J.M. and Tomaz, H. ed. (1990). *Atlas of the Marine Fauna of Southern Spitsbergen*. v. **1**. Gdansk, Poland: Institute of Oceanography.

Kongsberg Maritime (2004). *EM1002 multibeam echo sounder product specification*. URL: http://www.tdi-bi.com/downloads/EM1002_Product_specification.pdf [29/03/2013].

Kongsberg Maritime (2006). *EM3002 multibeam echo sounder product specification*. URL: http://www.km.kongsberg.com/ks/web/nokbg0397.nsf/AllWeb/7C8510CFA3CD21ABC1256CF00052DD1C/$file/164771ae_EM3002_Product_spec_lr.pdf [29/03/2013].

König, M., Nuth, C., Kohler, J., Moholdt, G. and Pettersen, R. (2012). A digital glacier database for Svalbard. URL: http://public.data.npolar.no/cryoclim/GLIMS_Svalbard.pdf [29/03/2013].

Kristensen, L., Benn, D.I., Hormes, A. and Ottesen, D. (2009) Mud aprons in front of Svalbard surge moraines: evidence of subglacial deforming layers or proglacial glaciotectonics? *Geomorphology*, v. **111**, p. 206-221.

Kristensen, L. and Benn, D.I. (2012). A surge of the glaciers Skobreen-Paulabreen, Svalbard, observed by time-lapse photographs and remote sensing data. *Polar Research*, v. **31**, 11106, http://dx.doi.org/10.3402/polar.v31i0.11106

Kwasniewski, S., Walkusz, W., Cottier, F.R. and Leu, E. (2013). Meszooplankton dynamics in relation to food availability during spring and early summer in a high latitude glaciated fjord (Kongsfjorden), with focus on Calanus. *Journal of Marine Systems*, v. **111**, p. 83–96.

Laberg, J.S., Guidard, S., Mienert, J., Vorren, T.O., Halfidason, H. and Nygård, A. (2007). Morphology and morphogenesis of a high-latitude canyon; the Andøya canyon, Norwegian Sea. Marine Geology, v. **246**, p. 68-85.

Lajeunesse, P. and Allard, M. (2002). Sedimentology of an ice-contact glaciomarine fan complex, Nastapoka Hills, eastern Hudson Bay, northern Québec. *Sedimentary Geology*, v. **152**, p. 201-220.

Lambeck, K. (1996). Limits on the areal extent of the Barents Sea ice sheet in Late Weichselian time. *Global and Planetary Change*, v. **12**, p. 41-51.

Landvik, J.Y., Mangerud, J. and Salvigsen, O. (1987). The Late Weichselian and Holocene shoreline displacement on the west-central coast of Svalbard. *Polar Research*, v. **5**, p. 29-44.

Landvik, J.Y., Hjort, C., Mangerud, J., Möller and Salvigsen, O. (1995). The Quaternary record of eastern Svalbard – an overview. *Polar Research*, v. **14** (2), p. 95-103.

Landvik, J.Y., Bondevik, S., Elverhøi, A., Fjeldskaar, W., Mangerud, J., Salvigsen, O., Siegert, M.J., Svendsen, J-I. and Vorren, T.O. (1998). The last glacial maximum of Svalbard and the Barents Sea area: ice sheet extent and configuration. *Quaternary Science Reviews*, v. **17**, p. 43-75.

Landvik, J.Y., Brook, E.J., Gualtieri, L., Raisbeck, G., Salvigsen, O. and Yiou, F. (2003). Northwest Svalbard during the last glaciation: Ice-fee areas existed. *Geology*, v. **31** (10), p. 905-908.

Landvik, J.Y., Ingólfsson, Ó., Mienert, J., Lehman, S.J., Solheim, A., Elverhøi, A. and Ottesen, D. (2005): Rethinking Late Weichselian ice-sheet dynamics in coastal NW Svalbard. *Boreas*, v. **34** (18), p. 7-24.

Landvik, J.Y., Brook, E.J., Gualtieri, L., Linge, H., Raisbeck, G., Salvigsen, O. and Yiou, F. (2013): ^{10}Be exposure age constraints on the Late Weichselian ice-sheet geometry and dynamics in inter-ice-stream areas, western Svalbard. *Boreas*, v. **42**, p. 43–56. Doi:10.1111/j.1502-3885.2012.00282.x.

Lehman, S.J. and Forman, S.L. (1992). Late Weichselian glacier retreat in Kongsfjorden, west Spitsbergen, Svalbard. *Quaternary Research*, v. **37**, p. 139-154.

Liestøl, O. (1993). Glaciers of Svalbard, Norway. In: Satellite *Image Atlas of Glaciers of the World* (Williams, R. S. J. and Ferrigno, J. G. eds.). *Norsk Geografisk Tidsskrift – Norwegian Journal of Geography*, v. **56**, 271–272. Oslo. Glaciers of Europe. U.*S. Geological Survey Professional Paper 1386-E*, 127–152.

Liestøl, O. (1988). The glaciers in the Kongsfjorden area, Spitsbergen. *Norsk geogr. Tidsskr.*, v. **42**, p. 231-238.

Maclachlan, S.E., Howe, J.A. and Vardy, M.E. (2010). Morphodynamic evolution of Kongsfjorden-Krossfjorden, Svalbard, during the Late Weichselian and Holocene. *Geological Society, London, Special Publications***,** v. **344**, p. 195-205.

Mangerud, J. and Svendsen, J.I. (1990). Deglaciation chronology inferred from marine sediments in a proglacial lake basin, western Spitsbergen, Svalbard. *Boreas*, v. **19** (3), p. 249-272.

Mangerud, J. and Svendsen, J.I. (1992). The last interglacial-glacial period on Spitsbergen, Svalbard. *Quaternary Science Reviews*, v. **11**, p. 633-664.

Mangerud, J., Bolstad, M., Elgersma, A., Helliksen, D., Landvik, J.Y., Lønne, I., Lycke, A.K., Salvigsen, O., Sandahl, H. and Svendsen, J.I. (1992). The last glacial maximum on Spitsbergen, Svalbard. *Quaternary Research*, v. **38** (1), p. 1-31.

Mangerud, J., Dokken, T., Hebbeln, D., Heggen, B., Ingólfsson, Ó., Landvik, J.Y., Mejdahl, V., Svendsen, J.I. and Vorren, T.O. (1998). Fluctuations of the Svalbard-Barents sea ice sheet during the last 150,000 years. *Quaternary Science Reviews*, v. **17**, p. 11-42.

Meier, M.F. and Post, A. (1969). What are glacier surges? *Canadian Journal of Earth Sciences,* v. **6**, p. 807-817.

Mercier, D., Étienne, S., Seller, D. and André, M-F. (2010). Paraglacial gullying of sediment-mantled slopes: a case study of Colletthøgda, Kongsfjorden area, west Spitsbergen (Svalbard). *Earth Surface Processes and Landforms,* v. **34**, p. 1772-1789.

Mugford, R.I. and Dowdeswell, J.A. (2010). Modeling iceberg-rafted sedimentation in high-latitude fjord environments. *Journal of Geophysical Research,* v. **115**, p. 1-21.

Nilsen, F., Cottier, F., Skogseth, R. and Mattsson, S. (2008). Fjord-shelf exchanges controlled by ice and brine production: The interannual variation of Atlantic Water in Isfjorden, Svalbard. *Continental Shelf Research,* v. **28**, p. 1838 – 1853. doi: 10.1016/j.csr.2008.04.015

Ó Cofaigh, C., Pudsey C.J., Dowdeswell., J.A. and Morris, P. (2002). Evolution of subglacial bedforms along a paleo-ice stream, Antarctic Peninsula continental shelf. *Geophys. Res. Lett.*, v. **29** (8), 1199. doi:10.1029/2001GL014488.

Ó Cofaigh, C., Larter, R.D., Dowdeswell, J.A., Hillenbrand C-D., Pudsey, C.J., Evans, J. and Morris, P. (2005). Flow of West Antarctic Ice Sheet on the continental margin of the Bellingshausen Sea at the Last Glacial Maximum. *Journal of Geophysical Research,* v. **110**, B11103, doi: 10.1029/2005JB003619.

Ohta, Y., Piepjohn, K., Dallmann, W.K. and Elvevold, S. (eds.) (2008). Geological map Svalbard 1:100 000, sheet A6G, Krossfjorden. *Norsk Polarinstitutt Temakart nr. 42*.

Ottesen, D., Dowdeswell, J.A. and Rise, L. (2005). Submarine landforms and the reconstruction of fast-flowing ice streams within a large Quaternary ice sheet: The 2500-km-long Norwegian-Svalbard margin (57 degrees-80 degrees N). *Geological Society of America Bulletin,* v. **117**, p. 1033-1050.

Ottesen, D. and Dowdeswell, J.A. (2006). Assemblages of submarine landforms produced by tidewater glaciers in Svalbard. *Journal of Geophysical Research-Earth Surface,* v. **111**, p. 1-16: DOI: 10.1029/2005JF000330

Ottesen, D., Dowdeswell, J.A., Landvik, J.Y. and Mienert, J. (2007). Dynamics of the Late Weichselian ice sheet on Svalbard inferred from high-resolution sea-floor morphology. *Boreas,* v. **36**, p. 286-306.

Ottesen, D., Stokes, C.R., Rise, L. and Olsen, L. (2008a). Ice-sheet dynamics and ice streaming along the coastal parts of northern Norway. *Quaternary Science Reviews*, v. **27**, p. 922-940.

Ottesen, D., Dowdeswell, J.A., Benn, D.I., Kristensen, L., Christiansen, H.H., Christensen, O., Hansen, L., Lebesbye, E., Forwick, M. and Vorren, T.O. (2008b). Submarine landforms characteristic of glacier surges in two Spitsbergen fjords. *Quaternary Science Reviews*, v. **27**, p. 1583-1599.

Ottesen, D. and Dowdeswell, J.A. (2009). An Inter-ice stream glaciated margin: Submarine landforms and a geomorphic model based on marine-geophysical data from Svalbard. *Geological Society of America Bulletin*, v. **121**, p. 1647-1665: DOI: 10.1130/B26467.1

Pavlov, A.K., Tverberg, V., Ivanov, B.V., Nilsen, F., Falk-Petersen, S. and Granskog, M.A. (2013). Warming of Atlantic Water in two west Spitsbergen fjords over the last century (1912-2009). *Polar Research*, v. **32**, 11206. Available at: http://dx.doi.org/10.3402/polar.v32i0.11206

Plassen, L., Vorren, T.O. and Forwick, M. (2004). Integrated acoustic and coring investigations of glacigenic deposits in Spitsbergen fjords. *Polar Research*, v. **23** (1), p. 89-110.

Powell R.D. and Molnia, F.D. (1989). Glacimarine sedimentary processes, facies and morphology of the south-southeast Alaska shelf and fjords. *Marine Geology*, v. **85**, p. 359-390.

Powell, R.D. (1990). Glaciomarine processes at grounding-line fans and their growth to ice-contact deltas. In: Dowdeswell, J.A. and Scourse, J.D. (eds.). *Glacimarine environments: Processes and Sediments*. Geological Society Special Publication, v. **53**, p. 53-73.

Rasmussen, T.L., Thomsen, E., Ślubowska, M.A., Jessen, S., Solheim, A. and Koç, N., (2007). Paleoceanographic evolution of the SW Svalbard margin (76°N) since 20,000 14C yr BP. *Quaternary Research*, v. **67**, p. 100 – 114. doi: 10.1016/j.yqres.2006.07.002

Rea, B.R. and Evans, D.J.A. (2011). An assessment of surge-induced crevassing and the formation of crevasse squeeze ridges. *Journal of Geophysical Research: Earth Science (2003-2012)*, v. **116** (F4). DOI: 10.1029/2011JF001970

Rhamstorf, S. (2002). Ocean circulation and climate during the past 120,000 years. *Nature*, v. **419**, p. 207 – 214.

Robinson, P. and Dowdeswell, J.A. (2011). Submarine landforms and the behaviour of a surging ice cap since the last glacial maximum: The open-marine system of eastern Austfonna, Svalbard. *Marine Geology*, v. **286**, p. 82-94.

Rogers, J.N., Kelley, J.T., Belknap, D.F., Gontz, A. and Barnhardt, W.A. (2006). Shallow-water pockmark formation in temperate estuaries: a consideration of origins in the western gulf of Maine with special focus on Belfast Bay. *Marine Geology*, v. **225**, p. 45-62.

Saloranta, T.M. and Svendsen, H. (2001). Across the Arctic front west of Spitsbergen: high-resolution CTD sections from 1998-2000. *Polar Research*, v. **20** (2), p. 177 – 184.

Salvigsen, O. (2002). Radiocarbon dated Mytilus edulis and Modiolus modiolus from northern Svalbard: climatic implications. *Norsk Geografisk Tidsskrift–Norwegian Journal of Geography*, v. **56** (2), p. 56–61.

Salvigsen, O. and Høgvard, K. (2005). Glacial history, Holocene shoreline displacement and palaeoclimate based on radiocarbon ages in the area of Bockfjorden, north-western Spitsbergen, Svalbard. *Polar Research*, v. **25** (1), p. 15-24.

Sarkar, S., Berndt, C., Chabert, A., Masson, D.G., Minshull, T.A. and Westbrook, G.K. (2011). Switching of paleo-ice stream in northwest Svalbard. *Quaternary Science Reviews*, v. **30**, p. 1710-1725.

Sevestre, H., Benn, D.I. and Hagen, J.O. (unpublished). *Inventory of surge-type glaciers on Svalbard*.

Sexton, D.J., Dowdeswell, J.A., Solheim, A. and Elverhøi, A. (1992). Seismic architecture and sedimentation in northwest Spitsbergen fjords. *Marine Geology*, v. **103**, p. 53-68.

Sharp, M. (1984). Annual moraine ridges at Skálafjellsjökull, south-east Iceland. Journal of *Glaciology*, v. **30** (104), p. 82-93.

Shipp, S.S., Wellner, J.S. and Andersen , J.B. (2002). Retreat signature of a polar ice stream: sub-glacial geomorphic features and sediments from the Ross Sea, Antarctica. In: Dowdeswell, J.A. & Ó Cofaigh, C. (eds.): *Glacier-influenced Sedimentation on High-*

Latitude Continental Margins. Geological Society, London, Special Publications, v. **203**, p. 277-304.

Siegert, M.J. and Dowdeswell, J.A. (1995): Numerical modelling of the Late Weichselian Svalbard-Barents Sea Ice Sheet. *Quaternary Research*, v. **43**, p. 1-13.

Siegert, M.J. and Dowdeswell, J.A. (2002). Late Weichselian iceberg, surface-melt and sediment production from the Eurasian Ice Sheet: results from numerical ice-sheet modelling. *Marine Geology*, v. **118**, p. 109-127.

Skarðhamar, J. and Svendsen, H. (2010). Short-term hydrographic variability in a stratified Arctic fjord. *In:* Howe, J.A., Austin, W.E.N., Forwick, M. and Paetzel, M. (eds.): *Fjord systems and archives*. Geological Society, London, Special Publications, v. **344**, p. 51-60, doi: 10.1144/SP344.5

Skogseth, R., Haugan, P.M. and Jakobsson, M. (2005). Watermass transformations in Storfjorden. *Continental Shelf Research*, v. **25**, p. 667–695, doi: 10.1016/j.csr.2004.10.005

Ślubowska-Woldengen, M., Rasmussen, T.L., Koç, N., Klitgaard-Kristensen, D., Nilsen, F. and Solheim, A. (2007). Advection of Atlantic Water to the western and northern Svalbard shelf since 17,500 cal yr BP. *Quaternary Science Reviews*, v. **26**, p. 463-478, doi: 10.1016/j.quascirev.2006.09.009

Solheim, A., Russwurm, L., Elverhøi and Nyland Berg, M. (1990). Glacial geomorphic features in the northern Barents Sea: direct evidence for grounded ice and implications for the pattern of deglaciation and late glacial sedimentation. In: Dowdeswell, J.A. and Scourse, J.D. (eds.): *Glacimarine Environments: Processes and Sediments*, Geological Society of London, Special Publication No. **53**, p. 121-137.

Springman, S.M., Jommi, C. and Teysseire, P. (2003). Instabilities on moraine slopes induced by loss of suction: a case history. *Géotechnique*, v. **53** (1), p. 3-10.

Stoker, M.S., Pheasant, J.B. and Josenhams, H. (1997).Seismic methods and interpretation. In: Davies, T.A., Bell, T., Cooper, A.K., Josenhans, H., Polyak, L., Solheim, A., Stoker, M.S. and Stravers, J.A (eds.) *Glaciated continental margins: an atlas of acoustic images*. Chapman and Hall: London.

Stokes, C.R. and Clark, C.D. (1999). Geomorphological criteria for identifying Pleistocene ice streams. *Annals of Glaciology*, v. **28**, p. 67-74.

Svendsen, J.I. and Mangerud, J. (1992). Paleoclimatic inferences from glacial fluctuations on Svalbard during and the last 20,000 years*. *Climate Dynamics*, v. **6**, p. 213-220.

Svendsen, J.I., Elverhøi, A. and Mangerud, J. (1996). The retreat of the Barents Sea Ice Sheet on the western Svalbard margin. *Boreas*, v. **25** (4), p. 244-256.

Svendsen, H., Beszczynska-Møller, A., Hagen, J.O., Lefauconnier, B., Tverberg, V., Gerland, S., Ørbæk, J.B., Bischof, K., Papucci, C., Zajaczkowski, M., Azzolini, R., Bruland, O., Wiencke, C., Winther, J.-G. and Dallmann, W. (2002). The physical environment of Kongsfjorden-Krossfjorden, an Arctic fjord system in Svalbard. *Polar Research*, v. **21**(1), p. 133–166.

Svendsen, J.I., Alexanderson, H., Astakhov, V.I., Demidov, I., Dowdeswell, J.A., Funder, S., Gataullin, V., Henriksen, M., Hjort, C., Houmark-Nielsen, M., Hubberton, H.W., Ingólfsson, O., Jakobsson, M., Kjær, K.H., Larsen, E., Lokrantz, H., Lunkka, J.P., Lysså, A., Magerud, J., Matiouchkov, A., Murray, A., Möller, P. Niessen, F., Nikolskaya, O., Polyak, L., Saarnisto, M., Siegert, C., Siegert, M.J., Spielhagen, R.F. and Stein, R. (2004). Late Quaternary ice sheet history of northern Eurasia. *Quaternary Science Reviews*, v. **23**, p. 1229-1271.

Syvitski, J.P.M. (1989). On the deposition of sediment within glacier-influenced fjords: oceanographic controls. *Marine Geology*, v. **85**, p. 301-329.

Syvitski, J.P.M., Lewis, M.C.F. and Piper, D.J.W. (1996). Palaeoceanographic information derived from acoustic surveys of glaciated continental margin: examples from eastern Canada. In: Andrews, J.T, Austin, W.E.N., Bergsten, H. and Jennings, A.E. (eds.): *Late Quaternary Palaeoceanography of the North Atlantic Margins*, Geological Society Special Publication, v. **111**, p. 51-76.

Syvitski, J.P.M., Stein, A.B. and Andrews, J.T. (2001). Icebergs and the sea floor of the East Greenland (Kangerlussuaq) Continental Margin. *Arctic, Antarctic, and Alpine Research*, v. **33** (1), p. 52-61.

Todd, B.J. and Shaw, J. (2012). Laurentide Ice Sheet dynamics in the Bay of Fundy, Canada, revealed through mutlibeam sonar mapping of glacial landsystems. *Quaternary Science Reviews*, v. **58**, p. 83-103.

Velle, J.H. (2012). Holocene sedimentary environments in Smeerenburgfjorden, Spitsbergen. *Master's thesis*, University of Tromsø, p. 1-127.

Walkusz, W., Kwasniewski, S., Falk-Petersen, S., Hop, H., Tverberg, V., Wieczorek, P. and Weslawski, J.M. (2009). Seasonal and spatial changes in the zooplankton community of Kongsfjorden, Svalbard. *Polar Research*, v. **28**, p. 254–281.

Wellner, J.S., Lowe, A.L., Shipp, S.S. and Anderson, J.B. (2001). Distribution of glacial geomorphic features on the Antarctic continental shelf and correlation with substrate: implications for ice behavior. *Journal of Glaciology*, v. **47**, p. 397-411.

Werner, A. (1993). Holocene moraine chronology, Spitsbergen, Svalbard: lichenometric evidence for multiple Neoglacial advances in the Arctic. *The Holocene*, v. **3**, p. 128-137.

Zajączkowski, M. (2008). Sediment supply fluxes in glacial outwash fjords, Kongsfjorden and Adventfjorden, Svalbard. *Polish Polar Research*, v. **29** (1), p. 59 – 72.

Zajączkowski, M. and Włodarska-Kowalczuk, M. (2007). Dynamic sedimentary environments of an Arctic glacier-fed river estuary (Adventfjorden, Svalbard). I. Flux, deposition and sediment dynamics. *Estuarine, Coastal and Shelf Science*, v. **74**, p. 285-296.